Experimental Investigation and ANN Modelling of the Behavior of Asphalt Binders Modified with Novel Geopolymers

by

Abdulrahman Hamid

A thesis
presented to the University of Waterloo
in fulfillment of the
thesis requirement for the degree of
Doctor of Philosophy
in
Civil Engineering

Waterloo, Ontario, Canada, 2022

Examining Committee Membership

The following served on the Examining Committee for this thesis. The decision of the Examining Committee is by majority vote.

External Examiner:	Ahmed Shalaby Professor, Department of Civil Engineering University of Manitoba
Supervisor(s):	Hassan Baaj Professor, Department of Civil & Environmental Engineering University of Waterloo
Supervisor(s):	Mohab El-Hakim Professor, Department of Civil & Environmental Engineering Manhattan College
Internal Member:	Susan Tighe Professor, Department of Civil & Environmental Engineering University of Waterloo
Internal Member:	Adil Al-Mayah Professor, Department of Civil & Environmental Engineering University of Waterloo

Internal-External Member: Kaan Anal
Professor, Department of Mechanical & Mechatronics Engineering
University of Waterloo

Author's Declaration

I hereby declare that I am the sole author of this thesis. This is a true copy of the thesis, including any required final revisions, as accepted by my examiners.

I understand that my thesis may be made electronically available to the public.

Abstract

The design of asphalt pavement has an impact on a country's economic and environmental development. The main factors limiting the service life of flexible pavements are severe weather and increasing traffic volumes. Rutting and cracking of flexible pavement are two common types of distress that affect the serviceability and quality of the world's transportation network. This subject has been studied extensively for decades, and it has evolved into a serious challenge that has yet to be fully resolved. Multiple research efforts have been undertaken around the world to increase pavement service life to fulfil future demand for economic expansion and community development. Multiple options for developing sustainable and cost-effective asphalt mixes with extended service life are being investigated. Although improving the characteristics of the asphalt binder has been shown to be a promising strategy.

Geopolymer research is gaining a lot of attention these years because it can be employed in a variety of applications, such as geopolymer concrete and mortar, soil stabilization, and pavement construction. The geopolymer is formed when the aluminosilicate source, such as fly ash, reacts with the alkaline solution. Geopolymers are environmentally friendly materials that emit minimal CO_2 during manufacture and can be used to eliminate waste and by-product materials like fly ash. It has also demonstrated its potential to rapidly acquire mechanical properties, improve fire resistance, and reduce energy use and greenhouse emissions. Despite, the use of geopolymer materials as a modifier for asphalt binder and mixture has gotten minimal attention, which could be due to the lack of research linking the effect of temperature and curing time on geopolymer performance and asphalt binder rheological behavior. Thus, considering these effects could motivate scientists to employ various types of geopolymers using by-products and waste materials, which would have significant financial and environmental benefits.

This research aimed to evaluate the effects of geopolymers on the rheological and performance of asphalt binder, considering the impact of temperatures, frequencies, and stresses. The rheological and performance properties of neat and modified asphalt binder were investigated using Dynamic Shear Rheometer (DSR), Bending Beam Rheometer (BBR), and Environmental Scanning Electron Microscopy (ESEM) imaging devices. Also, the Viscoelastic Continuum Damage (VECD) model with the Linear Amplitude Sweep (LAS) was utilized to evaluate the fatigue behavior of the asphalt binder. Moreover, the Multiple Stress Creep Recovery (MSCR) test was conducted at various temperatures and stresses to calculate the non-recoverable creep compliance (J_{nr}) and the percent strain recovery (R). Furthermore, the Hamburg Wheel Rut Test (HWRT), dynamic/complex modulus,

and moisture damage evaluation tests were conducted to evaluate the effect of additives on the performance of asphalt mixes.

On the other hand, the interactive effects of geopolymer content and temperature on non-recoverable creep compliance (J_{nr}) and creep recovery percentage (R) of geopolymer modified asphalt binders were investigated and predictive mathematical models were developed using the Response Surface Method (RSM) and regression method. Also, the Artificial Neural Networks (ANNs) model was developed to predict the recovery and non-recovery performance of asphalt binders using five input parameters (temperature, frequency, storage modulus, loss modulus, and viscosity) and one hidden layer with five neurons. To implement a backpropagation learning process in a feed-forward neural network, Scaled Conjugate Gradient (SCG), Levenberg-Marquardt (LM), and Bayesian Regularization (BR) training algorithms were performed.

The results showed that fly ash and glass powder could be used as an aluminosilicate source during the preparation of geopolymer as an asphalt modifier, which has an essential influence on the rheological and performance of asphalt binder. While increasing the percentage of the geopolymer does not seem to affect the microstructure of the asphalt binder. The geopolymer has a significant impact on the binder's sensitivity to temperature, whereby the temperature sensitivity for both unaged and RTFO modified asphalt binders decreases. While adding the geopolymer to SBS enhances the binder's ability to withstand extremely heavy traffic under high stress and temperature, the permanent deformation of the asphalt mix decreases by 82% compared with using the neat asphalt binder. Therefore, the combination of geopolymer and SBS could be used to improve the rutting resistance capability of asphalt concrete in hot climate countries. Furthermore, it was noted that the ANNs model is appropriate to predict the percent recovery and non-recovery compliance of modified asphalt binder using unaged or aged binders at different temperatures.

Acknowledgements

I want to express my sincerest gratitude to my supervisors, Professor Hassan Baaj and Professor Mohab El-Hakim, for their guidance, encouragement, and support throughout my Ph.D. research. I am grateful to the members of the Examining Committee who graciously consented to read and comment on this thesis: Professor Susan Tighe, Professor Adil Al-Mayah, and Professor Kaan Anal.

I truly appreciate all my CPATT colleagues' help, valuable discussions, and friendship. I would like to thank technical staff members at the Department of Civil and Environmental Engineering, Mr. Richard Morrison and Mr. Peter Volcic, for their assistance with many of the laboratory tests detailed in this thesis. I'm also grateful to Yellowline Asphalt Products Ltd., Steed and Evans, and the Centre for Pavement and Transportation Technology (CPATT) for providing materials and testing equipment. In addition, I'd like to express my gratitude to the Hadhramout Foundation for supporting my graduate studies financially. I also want to thank Canada, its people, and its government; you have my admiration and love.

Finally, I would like to thank my mother (Muneera), my wife (Ehsan), and my children (Muneera, Mohammed, Maryam, and Muaath) for their love, understanding, and support during the years of my graduate studies. I am also indebted to my brothers and other members of my family for their continuing support during my academic years.

Dedication

To my dear mother and siblings, my beloved wife, and my children

Table of Contents

List of Figures

List of Tables

List of Abbreviations

AASHTO: American Association of State Highway and Transportation Officials

AC: Asphalt Concrete

ANNs: Artificial Neural Networks

ASTM: American Society for Testing and Material

BBR: Bending Beam Rheometer

BRD: Bulk Relative Density

CPATT: Centre for Pavement and Transportation Technology

DSR: Dynamic Shear Rheometer

ESEM: Environmental Scanning Electron Microscope

FTIR: Fourier Transform Infrared

GHG: Greenhouse Gas

HMA: Hot Mix Asphalt

HWTT: Hamburg Wheel-Track Tester

LAS: Linear Amplitude Sweep

LVE: Linear Viscoelastic

MEPDG: Mechanistic-Empirical Pavement Design Guide

MSCR: Multiple Stress Creep Recovery

MTO: Ministry of Transportation Ontario

MTS: Material Testing Systems

PAV: Pressure Aging Vessel

PG: Performance Grading

PMA: Polymer Modified Asphalt

RAP: Reclaimed Asphalt Pavement

RSM: Response Surface Method

RTFO: Rolling Thin Film Oven

RV: Rotational Viscometer

SARA: Saturates, Aromatics, Resins, and Asphaltene

SBS: Styrene-Butadiene-Styrene

SFE: Surface Free Energy

SGC: Superpave Gyratory Compactor

SMA: Stone Mastic (Matrix) Asphalt

TTS: Time-Temperature Superposition

Va: Air Voids

VECD: Viscoelastic Continuum Damage

VFA: Voids Filled with Asphalt

VMA: Voids in Mineral Aggregate

WLF: William-Landel-Ferry

WMA: Warm Mix Asphalt

XRD: X-Ray Diffraction analysis

Chapter 1

Introduction

1.1 Preface

This thesis includes two journal articles and three unpublished journal articles, in addition to a general introduction, literature review, methodology, and general conclusion. The first manuscript, which is published in the Advances in Materials Science and Engineering journal, investigates the possibility of preparing a suitable geopolymer as a modifier for asphalt binder, considering the effect of temperature, additive content, and curing time on the rheological properties of asphalt binder. The effect of geopolymer particles on the microstructure of asphalt binder was also evaluated. The second manuscript, which is published in the Polymers journal, presents the influences of temperature, stresses, polymer[1] type, and modification rate on the rutting behavior of the asphalt binder modified with fly ash-based geopolymer (GF), Styrene Butadiene Styrene (SBS) polymer, and a combination of SBS and GF. In addition, additive effects on the rutting resistance of asphalt mixtures were investigated. It was found that using geopolymers as an asphalt binder modifier proved to be an effective way to improve rutting performance. Furthermore, the findings of the article might help asphalt pavement designers choose appropriate modifiers based on local temperature, stress, and traffic volume.

In the third manuscript, temperature and aging effects on the rheological and performance of asphalt binder and mixture were investigated. Also, the influence of additives on moisture damage and cracking resistance was studied. The fourth article investigates the effects of temperature and additive content on the performance of asphalt binder modified

[1] A macromolecule with a defined size and molecular weight is referred to as a polymer [68]

with glass powder and fly ash-based geopolymer. While predictive mathematical models were developed using the response surface method (RSM) and regression method. It was noted that the RSM is an effective method to predict the recovery and non-recovery performance of geopolymer modified asphalt binder. The fifth manuscript predicts the recovery and non-recovery performance of asphalt binders using the Artificial Neural Networks (ANNs) model and considering the mechanical test parameters (temperature and frequency) and asphalt binder properties (storage modulus, loss modulus, and viscosity) as inputs. The optimal ANN architecture was chosen and the Levenberg-Marquardt (LM) algorithm was used to train the ANN model. It was found that the model performed better in estimating the recovery and non-recovery performance of asphalt binders. Furthermore, aged input variables have a higher level of predictability when it comes to the non-recovery performance.

1.2 Research Significance

Asphalt binder is the most widely used pavement material in the world. The production of asphalt binder requires a significant amount of energy and results in CO_2 emissions into the atmosphere. Meanwhile, greenhouse gas (GHG) emissions must be reduced by 50 to 80 percent by 2050 to keep global warming below 2 °C, which is considered a difficult goal to attain [125]. The production stage of raw materials and the mixing process of asphalt concrete should be focused on lowering (GHG) emissions from the construction of asphalt pavement [144], whereby reducing the amount of asphalt binder used and the amount of energy consumed during the production of hot mix asphalt could have the potential to save the environment. Modifiers in asphalt binder would lower the optimum asphalt content while enhancing stability by increasing the bond between the asphalt binder and the aggregates [49].

On the other hand, there is a global trend toward reducing waste materials and then lowering pollution. Therefore, governments set aside a significant budget to develop ways to incorporate these materials with the raw materials used in many fields. The amount of waste products such as fly ash and glass powder has increased worldwide because of increasing human activity, which has resulted in more landfill space being utilized to dispose of these wastes. Furthermore, the construction industry's use of natural aggregates and asphalt binders during the construction and rehabilitation of asphalt pavement has been shown to be environmentally deteriorating and unsustainable over time. So, using waste materials to reduce the use of asphalt binder during the construction of flexible pavement would have significant economic and environmental benefits by reducing emissions and fuel

consumption due to the extraction and transport of asphalt binders.

1.3 Research Objectives

Three primary objectives are defined for this research: a) evaluate the influence of geopolymer on the rheological and performance of asphalt binder, b) generate sufficient experimental data, to develop new proper models for predicted recovery and non-recovery behavior of asphalt binder; considering the effect of temperature, stresses and asphalt modifiers on the rheological properties of asphalt binder, and c) evaluate the effects of additives on the rutting, cracking, and moisture resistance of asphalt mixture. A detailed breakdown of the objectives includes:

1. **Develop** a suitable geopolymer as an asphalt modifier, considering the effect of temperature and curing time on the rheological and performance of the asphalt binder.
2. **Investigate** the potential usage of geopolymer-based on fly ash and glass powder on the rheological and performance of asphalt binder.
3. **Evaluate** the effects of temperature, additive content, and stresses on the creep recovery and non-recovery behavior of asphalt binder.
4. **Develop** new models considering the effects of the three variables that significantly impact the performance of asphalt binder: a) additive content; b) temperature; and c) asphalt binder properties. A sensitivity analysis will be conducted to evaluate the influence of each variable, individually and in combination, to assess the effect of asphalt modifiers on the recovery and non-recovery performance.
5. **Investigate** the influence of geopolymer additives on the performance of asphalt mixtures.

1.4 Dissertation Outline

This manuscript-based thesis is divided into nine chapters:

Chapter 1: Introduction - This chapter explains the research's general scope and overall objectives.

Chapter 2: Literature Review - This chapter contains a comprehensive literature review that covers a variety of subjects relating to this study, including:

- Flexible pavements
- Asphalt pavement distresses
- Viscoelastic behavior
- Artificial Neural Networks (ANNs)
- Geopolymer material

Chapter 3: Methodology - This chapter describes the research methods used to meet the study's objectives. There is also a description of the materials utilized in this study, as well as laboratory testing and analysis methods.

Chapter 4: Evaluating Fly Ash-Based Geopolymers as a Modifier for Asphalt Binders -This chapter investigates the rheological and microstructural properties of the neat and modified asphalt binders were investigated using an experimental matrix of laboratory testing with various amounts of geopolymer using a Rotational Viscometer, a Dynamic Shear Rheometer (DSR), and an Environmental Scanning Electron Microscopy (ESEM) imaging instrument. The influence of geopolymer curing time on rheological properties has also been studied.

Chapter 5: Rutting Behavior of Geopolymer and Styrene Butadiene Styrene-Modified Asphalt Binder - This chapter evaluates the effects of temperature, stress, polymer type, and modification rate on the rutting behavior of asphalt binder modified with fly ash-based geopolymer (GF), Styrene Butadiene Styrene (SBS), and a mix of SBS and GF. The frequency sweep test was used to study the rheological properties of asphalt binders at various temperatures. The Multiple Stress Creep Recovery (MSCR) test was also carried out at various temperatures and stresses to determine the non-recoverable creep compliance (J_{nr}) and percent strain recovery (R). The Hamburg wheel rut test was used to determine the asphalt mixture's rutting resistance (HWRT).

Chapter 6: Temperature and Aging Effects on the Rheological Properties and Performance of Geopolymer-Modified Asphalt Binder and Mixture - This chapter evaluates the influence of geopolymer and geopolymer combined with SBS polymer on the rheological and performance of asphalt binder and mixture at low and intermediate temperatures. Using Dynamic Shear Rheometer (DSR) and Bending Beam Rheometer (BBR) instruments, the rheological and performance of neat and modified asphalt binder were examined. In addition, the Viscoelastic Continuum Damage (VECD) model with

the Linear Amplitude Sweep (LAS) was used to assess the asphalt binder's fatigue behavior. The effect of additives on the performance of asphalt mixtures was evaluated using dynamic/complex modulus and moisture damage evaluation tests.

Chapter 7: Evaluating the Effect of Glass Powder/Fly Ash-Based Geopolymer on the Rheological and Performance of Asphalt Binder - This chapter investigates the effects of temperature and additive content on the performance of the asphalt binder modified with glass powder/fly ash-based geopolymer (GFG). A dynamic shear rheometer was used to test the performance of the asphalt binder with various amounts of GFG. The Multiple Stress Creep Recovery test was used to investigate the rutting capabilities of asphalt samples that were tested at various temperatures. The interaction of geopolymer content and temperature on non-recoverable creep compliance (J_{nr}) and creep recovery percentage (R) of geopolymer modified asphalt binders was explored, and prediction mathematical models employing the response surface method (RSM) and regression technique were developed.

Chapter 8: Predicting the Recovery and Non-Recovery Performance of Asphalt Binders Using Artificial Neural Networks - This chapter employs the artificial neural networks (ANNs) to predict the recovery and non-recovery performance of asphalt binders using mechanical test parameters and binder properties. The study includes the manufacture of 11 laboratory-blended asphalt binders with a total of 880 data points, as well as rheological testing of asphalt binders using a dynamic shear rheometer (DSR). The recovery and non-recovery properties of asphalt binders were also evaluated using Multiple Stress Creep Recovery (MSCR). Five input parameters (temperature, frequency, storage modulus, loss modulus, and viscosity) and one hidden layer with five neurons were used to develop the ANN model.

Chapter 9: Conclusions and Recommendations - This chapter includes a broad conclusion as well as an overview of the research's significant findings. This chapter also includes recommendations for future work.

Chapter 2

Literature Review

2.1 Flexible Pavements

Flexible pavement is a structure that consists of multiple layers of materials that can resist the traffic loads under different environmental conditions for a specific minimum lifespan. It is expected to withstand different types of distresses such as rutting, fatigue cracking, and thermal cracking. The flexible pavement is typically constructed in different ways, conventional, full depth, deep strength, or perpetual asphalt pavements [109]. The primary objectives of this research are to investigate the geopolymer effects on the performance of asphalt concrete. Therefore, in this section, brief information regarding the conventional asphalt pavement and its components will be discussed.

The traditional flexible pavement, as shown in Figure 2.1, usually constructed using hot mix asphalt (a mixture of aggregate, fillers, and asphalt binder). Then a layer of aggregate that has less asphalt content is directly applied to the surface layer and called the course cement. While the base layer is located directly underneath the course cement. Below the base layer, there is the subbase, which typically consists of granular materials. Finally, the subgrade, or natural soil, is the foundation on which the road is constructed. In the conventional asphalt pavement, each layer has a function, such as distress resistance, enhancing the strength of the pavement, or drainage system [78]. The conventional asphalt pavement mainly consists of the following layers:

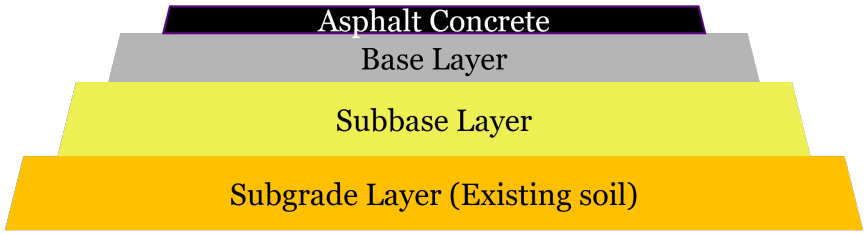

Figure 2.1: Flexible Pavement

2.1.1 Wearing Surface Layer

The surface layer is relatively thin HMA surface courses that is directly exposed to the traffic loading and severe weather. This layer contains the highest quality materials and acts to provide a smooth riding and waterproof surface to prevent the spread of surface water to the underneath layer [91, 109].

2.1.2 Intermediate Layer

The Intermediate layer is a thick aggregate layer which sometimes called cement course and essentially consisted of one or more lifts. The main function of this layer is to distribute the loading of traffic on the base layer [91, 109].

2.1.3 Base Layer

HMA or high-quality granular material is used to design the base layer [91], which be located below the intermediate course layer. The main function of this layer is to resist the stresses due to the cycles of freeze-thaw and promote the drainage in the pavement. In Ontario, Canada, the granular material is widely used, which called "Granular A" [78].

2.1.4 Subbase Layer

The granular material is used to construct the subbase layer which called "Granular B" regarding some references and textbooks [78]. The main purpose of this layer is enhancing the drainage, minimizing the freeze-thaw influences, and acting as a proper stand for the upper layers. The material quality of the subbase layer should be better than subgrade

material whereby this layer is not essential in all pavement constructions and could be constructed depending on the material properties of the subgrade layer.

2.2 Asphalt Pavement Distresses

Rutting and Cracking of flexible pavement is a widely noticeable modes of distresses impacting the serviceability and the quality of the roadway network in the world. This problem has been intensively investigated for decades whereby it is becoming a critical challenge, but not fully solved until now. Numerous additives and solutions were developed to improve the performance of paving materials by enhancing its properties, optimizing aggregate gradation, improving the quality of aggregates, and using additives to enhance the quality of asphalt binder [247].

The asphalt binder is a viscoelastic material that exhibits both viscous and elastic properties when deformed. The asphalt binder is suitable for most environmental conditions that lie between the extremes of hot and cold climates. Because of this variety of behavior, asphalt binder is an appropriate adhesive substance for paving. However, due to its complexity, it is a difficult material to understand and describe [109]. While the production of asphalt binder requires a substantial quantity of energy, resulting in the emission of CO_2. Therefore, lowering the amount of asphalt binder and energy utilized in the production of hot mix asphalt could be beneficial.

Governments provide significant budgets to improve their road infrastructure, as this is critical for the growth of the country's economy. In this regard, it is worth noting that countries spend a significant amount of money each year on road infrastructure maintenance due to severe weather and high traffic loads that cause pavement deterioration. Modifiers that have a significant effect on the performance of asphalt binders could be used to reduce pavement distress such as rutting and cracking [19, 107]. Consequently, the potential development of modifier materials could reduce maintenance and rehabilitation costs.

2.2.1 Permanent Deformation (Rutting)

The surface depression in the wheel path is known as permanent deformation or rutting, as depicted in Figure 2.2, which usually appears when the wheel routes are filled with water during the rainy seasons [116]. Pavement rutting is caused by increased loads, continuous traffic loads, soil volume changes, compressive material under the pavement system, and

climate changes [192]. Rutting can be caused by the asphalt mix's plastic deformation in hot weather or by poor compaction during construction [116], as depicted in Figure 2.3. Asphalt mixture properties have a significant influence on the rutting behavior of asphalt pavement [207, 86, 117]. Tarefder et al. (2003) [207] noted that binder content, temperatures, aggregate gradation, moisture condition (wet or dry), and the content of asphalt binder significantly affect the rutting performance of asphalt mixes. Temperature and material qualities, according to Feyissa (2009) [86], have a major impact on the development of rutting distress. While Hussan et al. (2017) [117] noted that rut depth has a direct link with aggregate flakiness index, bitumen penetration, and temperature, while rut depth has an inverse relationship with percent coarse aggregates.

Figure 2.2: Permanent deformation (rutting) - The pictures were taken by Abimbola Grace Oyeyi

2.2.2 Fatigue and Thermal Cracking

Cracking is one of the crucial problems in asphalt concrete pavement, which occurs due to heavy traffic, harsh environmental conditions, and construction deficiencies. It leads to pavement failure in its later stages. Cracking appears at the top of the pavement layer in different shapes such as longitudinal, alligator, transverse, and reflective cracks.

Fatigue cracking is considered the main mode of pavement failure, which occurs when the pavement has been stressed for a long time by repeated load applications [109]. The fatigue life measures the resistance of the asphalt concrete to fatigue cracking and is defined as the number of cycles to which the material can be subjected before failing. Tensile

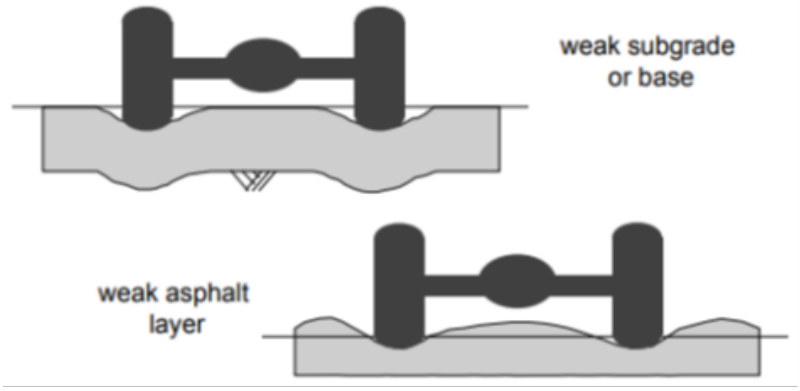

Figure 2.3: Pavement layers effect on the rutting performance [89]

stresses occur as repeated traffic loading acts on the pavement surface after the pavement has been in service [109]. There are two types of fatigue cracking, alligator or bottom-up cracking, as shown in Figure 2.4(a) and longitudinal or top-down cracking as depicted in Figure 2.4(b). Alligator cracking occurs when cracks initiate at the bottom of the asphalt layer and then propagate to the surface of the pavement under repeated load applications. Whereas longitudinal cracking occurs when cracks initiate at the pavement surface and propagate downwards under repeated load applications. Fatigue cracks in asphalt pavement are influenced by different external factors such as compaction level and method, time of asphalt placement, and poor subgrade drainage [109]. Also, temperature, air voids, and amount and type of asphalt binder are affected the fatigue life [179]. The best ways to avoid fatigue cracking are to design for the expected traffic loads during the service life; keep the subgrade dry; use thicker pavements; use paving materials that can resist moisture; and use resilient paving materials that can endure normal deflections [89].

Thermal cracking in asphalt pavement is a critical problem in the cold regions. Thermal cracking occurs as a result of gradual tensile stress that builds up in the asphalt layer due to the temperature drops [36]. When these stresses exceeded the capacity of the material to relieve stress through deformation, cracks form on the surface perpendicular to the road direction, as depicted in the Figure 2.5. With time, thermal cracking leads to water infiltration, loss of smoothness [36], and finally structural failure of the asphalt pavement. There are many factors influence the rate at which thermal cracks occur, such as decreases in temperature, the properties of the asphalt binder and aggregate, the asphalt rheological properties, and other environmental factors [222]. Yin et al. (2010) [232] indicated that thermal cracking could be reduced by using asphalt concrete mixture with a higher ductility for the surface layer. The asphalt binder is crucial in low temperature cracking, which is

Figure 2.4: Fatigue cracks in asphalt pavement, (a) alligator cracking, (b) longitudinal cracking

more common in hard and aged asphalt binders than in soft asphalt binders [89]. Therefore, the designers must choose a soft binder that can resist ageing during the service life to prevent low temperature cracking.

Figure 2.5: Low-temperature (thermal) cracking

2.3 Viscoelastic Behavior

The asphalt binder exhibits the characteristics of both viscous liquids and elastic solids depending on the temperature and rate of loading. When heated, asphalt acts as a lubricant, allowing the aggregate to be mixed, coated, and tightly compacted. Because of this range of behavior, the asphalt binder is termed viscoelastic [109].

Figure 2.6 demonstrates the Visco-Elastic behavior of asphalt binder. For one hour at 60 °C or ten hours at 25 °C, the flow behavior of asphalt binder could be the same. Asphalt binder behaves like a viscous liquid and flows at high temperatures, which is sometimes referred to as plastic because it does not return to its original position (non-recovery). As a result, wheel path ruts develop. However, aggregate quality influences rutting in asphalt pavements during hot weather, so it's probably more accurate to say the asphalt mixture behaves like a plastic.

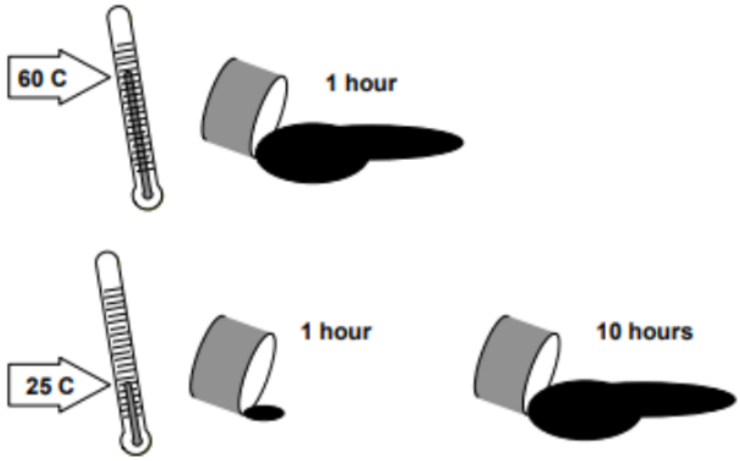

Figure 2.6: Viscoelastic behavior of asphalt binder [89]

Figure 2.7 and Table 2.1 show the Superpave tests that are used to characterise asphalt binder at various temperatures and ages. Superpave classifies them based on the real pavement temperatures as well as the times when asphalt distress is most likely to occur [89].

Viscoelastic materials can be classified into two groups: viscoelastic solids, when the phase angle value lies between 0° and 45°, and viscoelastic fluids, when the phase angle value lies between 45° and 90°. While the materials behave ideally elastic if the phase angle is equal to 0°, whereby there is no time lag between the stress and the strain, as shown

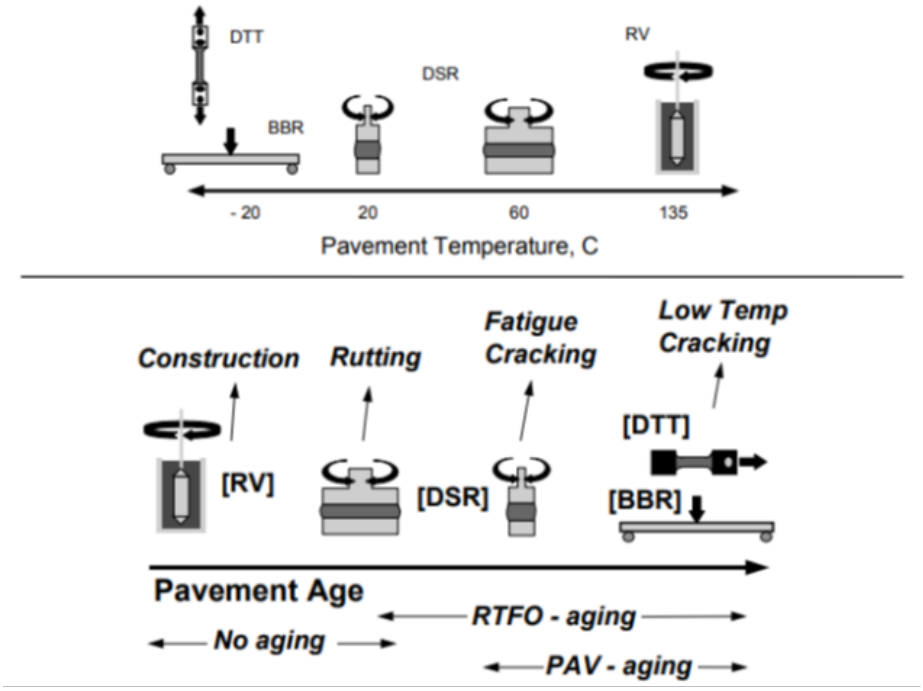

Figure 2.7: Viscoelastic behavior of asphalt binder [89]

Table 2.1: Superpave asphalt binder tests [89]

Superpave Binder Test	**Purpose**
Dynamic Shear Rheometer (DSR)	Measure properties at high and intermediate temperatures
Rotational Viscometer (RV)	Measure properties at high temperatures
Bending Beam Rheometer (BBR) Direct Tension Tester (DTT)	Measure properties at low temperatures
Rolling Thin Film Oven (RTFO) Pressure Aging Vessel (PAV)	Simulate hardening (durability) characteristics

in Figure 2.8. On the other hand, the materials behave ideally viscous when the phase angle value is 90°. Figure 2.8 shows a typical viscoelastic response of asphalt mixture. The stress can be expressed by Equation 2.1:

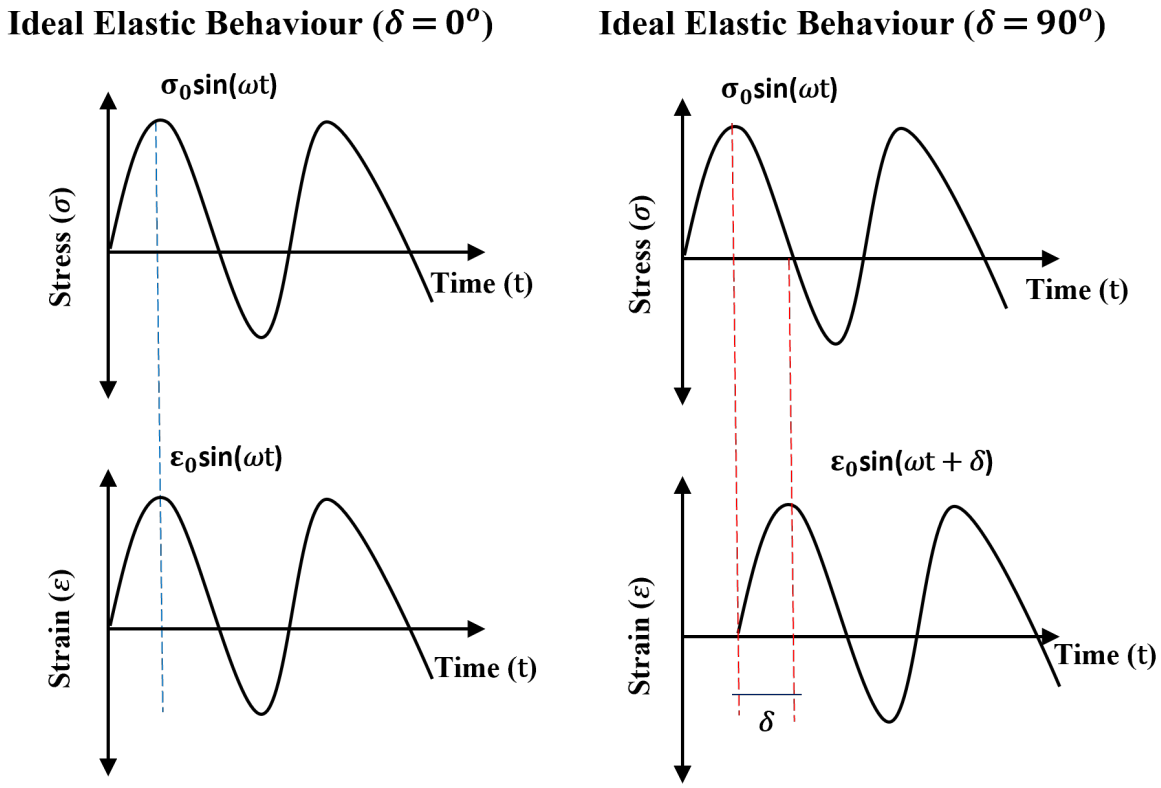

Figure 2.8: Graphical explanation of dynamic modulus parameters

$$\sigma = \sigma_0 \sin \omega t \tag{2.1}$$

Where σ_0 is stress amplitude, ω is related to frequency (f), $\omega = 2\pi$f, and t is the time (seconds). The strain can be expressed by Equation 2.2:

$$\varepsilon = \varepsilon_0 \sin(\omega t + \delta) \tag{2.2}$$

where ε_0 is strain aplitude, δ is phase angle. The complex modulus is expressed by Equation 2.3:

$$E^*(i\omega) = \frac{\sigma^*}{\varepsilon^*} = \frac{\sigma_0}{\varepsilon_0} \times e^{i\delta} = E^{'} + iE^{''} \tag{2.3}$$

$E^{'}$ is the storage modulus and $E^{''}$ is the loss modulus (see Figure 2.9), which are calculated using equations 2.4 and 2.5 respectively.

$$E^{'} = \frac{\sigma_0 \cos(\delta)}{\varepsilon_0} \tag{2.4}$$

$$E^{''} = \frac{\sigma_0 \sin(\delta)}{\varepsilon_0} \tag{2.5}$$

The complex modulus value is expressed by Equation 2.6.

$$|E^*| = \frac{\sigma_0}{\varepsilon_0} \tag{2.6}$$

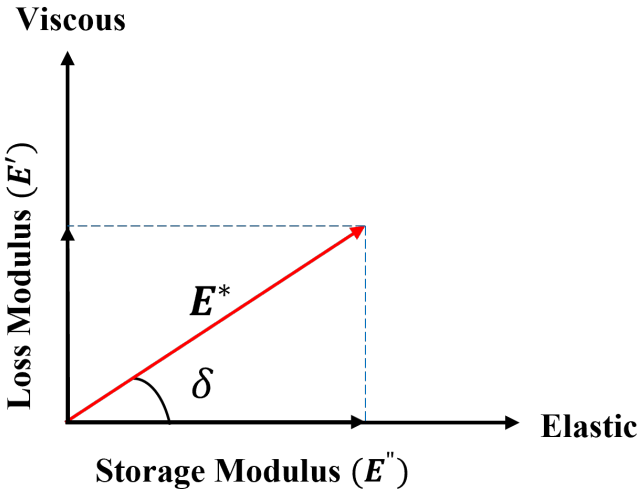

Figure 2.9: Relationship between storage modulus and loss modulus

Dynamic/complex modulus test data analysis contains constructing master curves; whereby the generation of the master curve helps to perform a comparison of the stiffness of asphalt mixture over different ranges of temperatures and frequencies. The master curve was constructed using a shift factor to the E* values to normalize them to a reference temperature. The master curve can be developed using a randomly specified reference temperature and applying a relationship between complex modulus and frequency [57].

Numerous models have been used to describe the relationship between shift factor (a_t) and temperature (T) for viscoelastic materials, such as the Williams-Landel-Ferry (WLF)

equation (Equation 2.7) [227], modified Kaelble equation (Equation 2.8) [182], Arrhenius equation (Equation 2.9), and log-linear equation (Equation 2.10) [234].

$$Log\ a_t = \frac{-C_1(T - T_{ref})}{C_2 + (T - T_{ref})} \tag{2.7}$$

$$Log\ a_t = \frac{-C_1(T - T_{ref})}{C_2 + \mid T - T_{ref} \mid} \tag{2.8}$$

Where T_{ref} is the reference temperature, and C_1 and C_2 are constants to reduce the difference between actual and predicted data [234]. The WLF equation has been shown to be suitable for asphalt binders and mixes [90, 135].

$$Log\ a_t = C\ (\frac{1}{T} - \frac{1}{T_{ref}}) = \frac{0.434E_a}{R}\ (\frac{1}{T} - \frac{1}{T_{ref}}) \tag{2.9}$$

Where T and T_{ref} are test and reference temperatures in kelvins, R is the common gas constant (8.314 J/mol.K), and E_a is the activation energy[1] (J/mol).

$$Log\ a_t[\frac{T}{T_{ref}}] = \beta\ (T - T_{ref}) \tag{2.10}$$

Where β is the straight-line slope of the temperature - Log a_t correlation [162]. The log-linear equation has been shown to be suitable for asphalt mixtures [90]. Figure 2.9 shows a master curve that was constructed using a shift factor to the E^* values to normalize them to a reference temperature.

Modifying asphalt binders is an effective method of improving the viscoelastic properties of asphalt binders such as their resistance to rutting, fatigue, and fracture issues [220]. Application of modifiers in asphalt binder would result in a reduction of optimum asphalt binder content, increasing stability, increasing the bond between asphalt binder and aggregates, and improving density [49]. Also, modifiers would minimize the environmental impact on roads, such as traffic noise and the total expenditure for repair and maintenance of road structures. However, because modification changes the behavior of binders, substantial laboratory testing is required before field application to determine the best mixtures, which means substantial time and cost.

[1]The minimum amount of energy required before any intermolecular movement may take place [234]

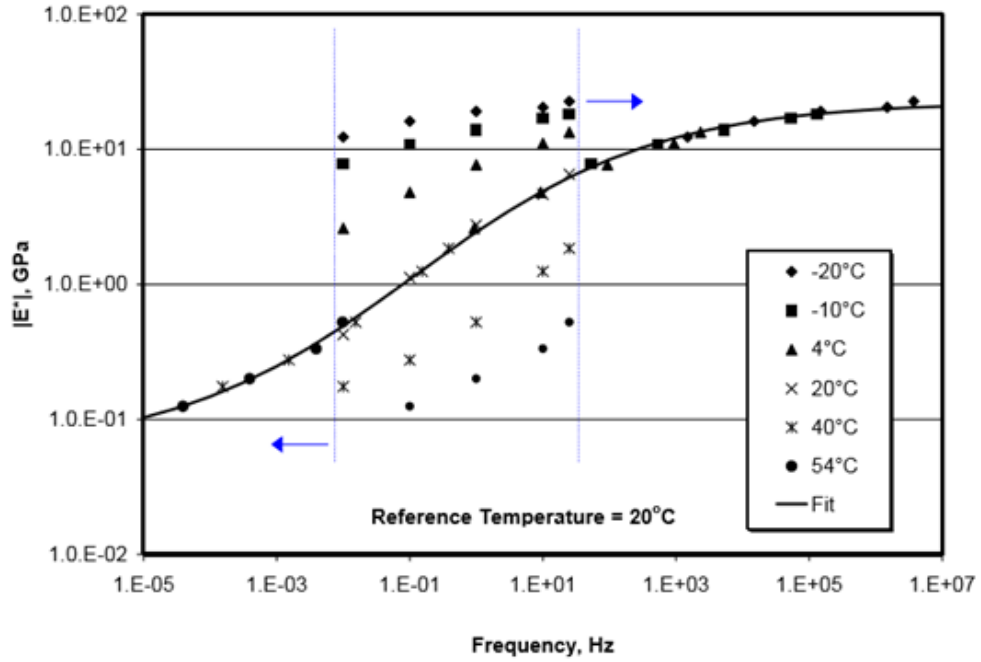

Figure 2.10: Example of a complex modulus master curve [57]

2.4 Artificial Neural Networks (ANNs)

The ANNs is a mathematical model made up of many interconnected neurons, with three groups of rules in this model: multiplication, summation, and activation [170]. The link between input parameters and targets is learned using a training data set. The principal work of an artificial neuron is demonstrated in Figure 2.11 and Equation 2.11.

Several studies have recently used various methods to predict the rheological and performance of asphalt binders and mixes, such as regression models, the Response Surface Method (RSM), and artificial neural networks (ANNs), which could have a significant impact on reducing the time and cost of experimental work. The ANNs has been used in a variety of pavement applications, such as designing the airfield pavement [53, 52, 176, 126], predicting the rutting performance [26, 71] and the indirect tensile strength [130] of flexible pavement. Also, the ANNs model was used to predict the performance of asphalt mixture modified with recycled asphalt shingles [140], fiber [208], nano-silica [87], SBS [39], glass fiber [214], crushed Boron Waste [127]. Table 2.2 summarizes the ANNs models that were used to predict the performance of asphalt mixtures.

Moreover, the ANNs model was used to predict the rheological and performance of asphalt binder modified with rubber [220, 241], SBS [131, 216], geopolymer [22], filler [231], and waste engine oil [230]. Table 2.3 summarizes the ANNs models that were used to predict the rheological and performance of asphalt binder. It was noted that the ANNs model is an effective tool to predict the rheological and performance of modified asphalt binder with high accuracy.

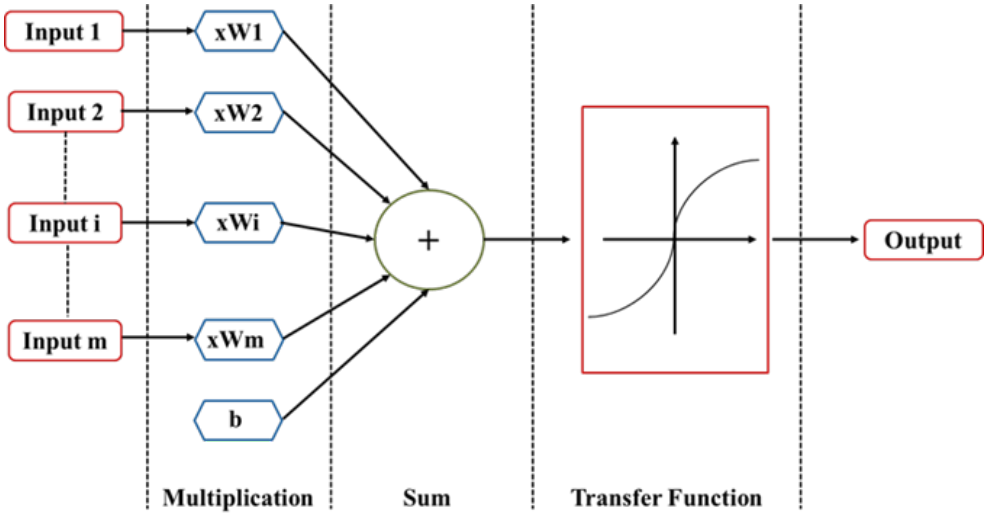

Figure 2.11: The principal work of an artificial neuron

$$y_i(k) = f(\sum_{i=0}^{m} w_i(k) \times x_i(k) + b) \tag{2.11}$$

y_i(k): Output value

f: Transfer function

w_i(k): Weight value

x_i(k): Input value

b: The bias

Table 2.2: Predicting the performance of asphalt mixtures Using ANNs model

Ref.	Predicted parameter	ANNs model	Train Algorithm	Main Comments
[208]	FT and FS	Four inputs, one hidden layer with four neurons, and 73 data points were used.	LM	The asphalt mixture's FT and FS may be predicted using the ANNs model.
[140]	E*	Nine inputs, two hidden layers with 15-15 neurons, and 1701 data points were used.	BPNN	The ANNs model is an effective tool to predict the E* of the asphalt mixture.
[87]	TS	Five inputs, one hidden layer with four neurons, and 48 data points were used.	LM	A more accurate model is provided by the ANNs model.
[39]	ITSM, MS, and MQ	6 inputs, 1 and 3 hidden layers with 8 neurons in each layer for MQ and ITSM and MS. 129 data points were used.	-	Using the ANNs model during the design phase of asphalt mixtures can be extremely beneficial.
[127]	Flow and stability	Seven inputs, two hidden layers with 20 and 15 neurons were used.	LM	The ANNs model can be used to predict the stability and flow of asphalt mixtures.
[214]	MS	Five inputs, one hidden layer with six neurons, and 128 data points were used.	BPNN	The ANNs model can accurately predict the MS of asphalt concrete reinforced with glass fibre.

Note: BPNN: back-propagation neural network, FT: Fracture Temperature, FS: Fracture Strength, TS: Temperature Sensitivity, ITSM: Stiffness modulus, MS: Marshall stability, MQ: Marshall quotient

2.5 Geopolymer Material

Geopolymer is an inorganic polymer that incorporates the properties of polymers and cements by combining the silica and alumina using high alkaline solution. Historically, the

Table 2.3: Predicting the rheological and performance of asphalt binder Using ANNs model

Ref.	Predicted parameter	ANNs model	Train Algorithm	Main Comments
[231]	G*	Three inputs, two hidden layers with five or four neurons, and 201 data points were used.	LM, CPG, SCG	The ANNs model is a powerful tool for accurately predicting G*.
[220]	η, G*/sinδ, and tanδ	Eight inputs, two hidden layers with seven and three neurons, and 2,200 data points were used.	SCG	The ANNs model could be well used in predicting asphalt binder performance.
[22]	G*, G$'$, G$''$, and δ	Three inputs, one hidden layer with eight or five neurons, and 252 data points were used.	LM, CPG, SCG	The highest performing model was the G* model using the LM algorithm and 1-5-1 network structure.
[216]	G*/sinδ and G*.sinδ	16 inputs, one hidden layer with twelve neurons, 1980 and 1668 data points for rutting and fatigue parameters.	-	ANNs model can be used to predict rutting and fatigue parameters with $R^2 >$ 0.95.
[230]	G* and δ	Three inputs, one hidden layer with twelve neurons.	LM	The ANNs model can predict the rheological characteristics of asphalt binders with high accuracy.
[241]	Viscosity	Eight inputs, one hidden layer with five and three neurons, 90 data points.	-	The training data for an ANN network model should involve a variety of indicators and be as practical as possible.

Note: SCG: Scaled Conjugate Gradient, LM: Levenberg-Marquardt, and CPG: Polak-Ribiere conjugate gradient

Cheops Pyramid in Gaza was built using formed in-situ blocks made of alkali activated aluminosilicate minerals, according to Demortier (2004) [70]. Geopolymer belongs to the

alkali activated cementitious materials group, which has a low calcium concentration [221], as shown in Figure 2.12. Davidovits (1989) [65] reported that geopolymer, like zeolites [2] and feldspathoids[3], can adsorb harmful chemical contaminants. It operates as a binder to turn semi-solid waste into an adhesive solid and bind toxic elemental waste inside the geopolymer framework. Hazardous components in waste materials blended with geopolymer compounds are retained in the geopolymer matrix's three-dimensional framework. Geopolymer research is gaining a lot of attention these years because it can be employed in a variety of applications, such as geopolymer concrete and mortar, soil stabilization, and pavement construction.

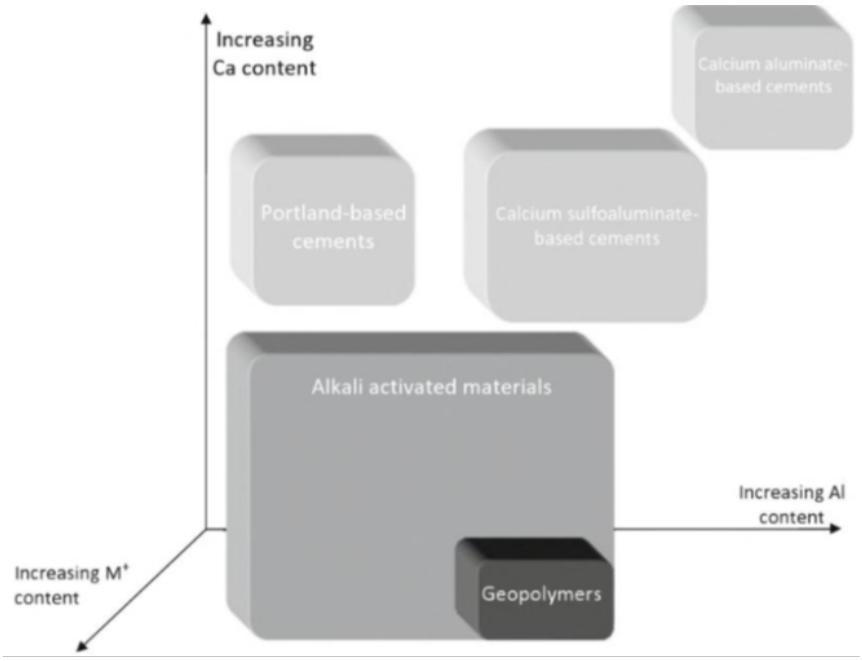

Figure 2.12: Classification of Geopolymer as a part of alkali activated materials [172]

2.5.1 Chemical Reaction

The geopolymer is formed when the aluminosilicate source, such as fly ash, reacts with the alkaline solution, as summarized in Figure 2.13. This reaction was summarized into the

[2] "A class of hydrated aluminosilicates of highly crystalline alkaline and alkaline earth metals with pores smaller than 2.0 nm" [136]

[3] "Feldspars are more closed than zeolites [136]"

following steps [76]: (a) hydroxyl ions (OH^-) in the highly concentrated alkaline solution cause the dissolution of fly ash minerals such as alumina and silica. (b) diffusion of the silica and alumina monomers, which interact to form dimers, trimers, tetramers, and so on. (c) condensation with sodium cations (Na^+) to form the N-A-S-H gel with time, as shown in Figure 2.13(a). This gel changes with time [59], whereby the initial gel 1 consists of high alumina ions in the early stages of the reaction because the Al-O bond is weaker than the Si-O bond. The second gel 2 is formed due to increasing the Si-O with time, which raises the silicon concentration in the N-A-S-H gel, as illustrated in Figure 2.14. (d) The last step is crystallization to hardening, whereby the tetrahedral silica (SiO_4) and alumina (AlO_4) are joined by oxygen (O_2) in the three-dimensional chain networks that are called geopolymers. Equation 2.12 and 2.13 describe the chemical reactions during the geopolymerisation process [229].

$$\mathrm{n(Si_2O_5,Al_2O_2)+2nSiO_2+4nH_2O+}NaOH \rightarrow Na^+ + n(OH)_3 - Si - O - Al^-(OH)_2 - O - Si^-(OH)_3 \tag{2.12}$$

$$\mathrm{n(OH)_3\text{-}Si\text{-}O\text{-}Al^-(OH)_2\text{-}O\text{-}Si\text{-}(OH)_3+}NaOH \rightarrow Na^+ - (Si - O - Al^- - O - Si - O-) + 4nH_2O \tag{2.13}$$

Figure 2.16 demonstrates the developed model by Fernandez-Jimenez et al. (2005) for fly ash-based geopolymer using a high alkaline activator (8 molar of NaOH). Figure 2.16 (a,b) and Figure 2.15(a) depict the initial chemical attack on a particle's surface, which eventually expands into a larger hole, as shown in Figure 2.16(b). As a result, reaction products are formed both inside and outside the sphere's shell until the ash particle is consumed completely or nearly completely, whereby dissolution is the mechanism in play at this point, as depicted in Figure 2.16(c). As a result of reaction product precipitation, a coating of reaction products covers portions of the smaller fly ash spheres, as shown in Figure 2.16(e) and Figure 2.15(b). This cover keeps the alkaline activating solution out. As the alkaline activation process continues, the unreacted fly ash hidden behind the precipitates may be unaffected by the high pH of the activating solution, resulting in a decrease in reaction rate. As shown in Figure 2.16(d), diffusion currently controls activation at this stage.

2.5.2 Application of Geopolymer

Geopolymer has many applications in the field of construction materials such as concrete construction, soil stabilization, asphalt materials enhancement. Geopolymers are environmentally friendly materials whereby there are minimal CO_2 emissions during production,

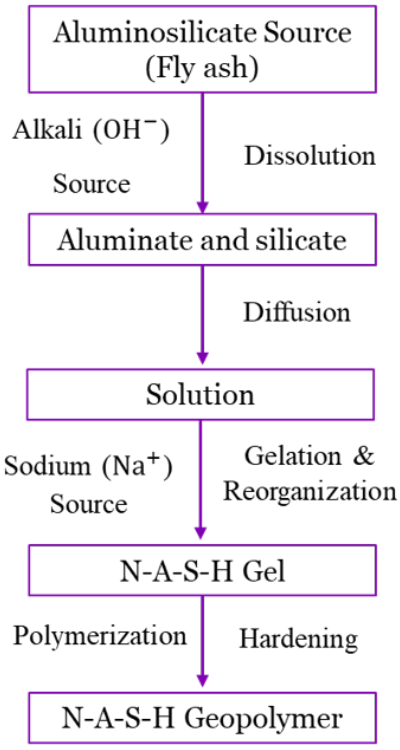

Figure 2.13: Chemical reaction steps during the geopolymerisation process [92]

and it has ability to reduce the waste and by-product materials such as fly ash and slag. Geopolymer has also demonstrated its capacity to improve mechanical characteristics, increase fire resistance, and reduce energy use and greenhouse emissions [67, 99, 223, 107]. Geopolymer is used in a variety of industries, including aerospace and automotive, metallurgy and nonferrous foundries, civil engineering, and the plastics industry [68]. Because of their propensity to absorb harmful chemical wastes, geopolymer materials are used in toxic waste management [68].

Geopolymer Concrete

During the past two decades, geopolymers were widely used as an environmentally friendly additive to Cementous construction materials, because of its ability to reduce the CO_2 emissions [79]. One tonne of kaolin-based geopolymer generates 0.180 tonnes of CO_2 which is six times less than Portland cement production. Meanwhile, producing fly ash-based geopolymer emits up to nine times less CO_2 than Portland cement [68]. For instance,

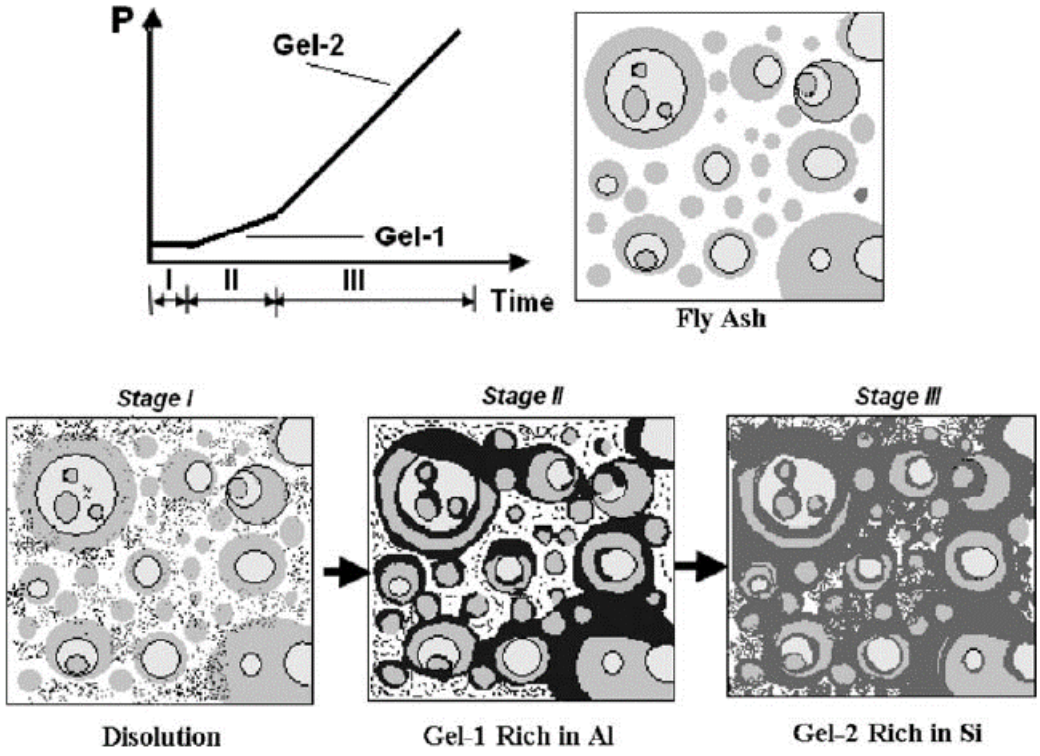

Figure 2.14: A diagram depicting the progression of mechanical performance over time [85]

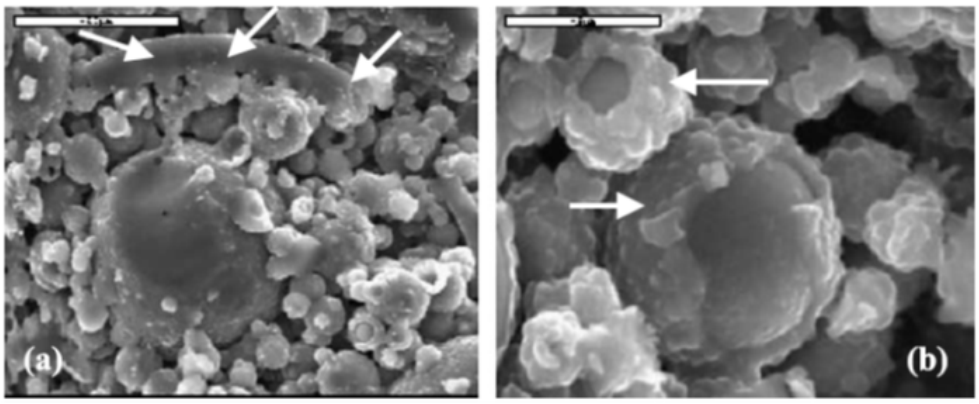

Figure 2.15: SEM images of fly ash based geopolymer, (a) a big sphere's reaction process, (b) the response of a few tiny spheres [84]

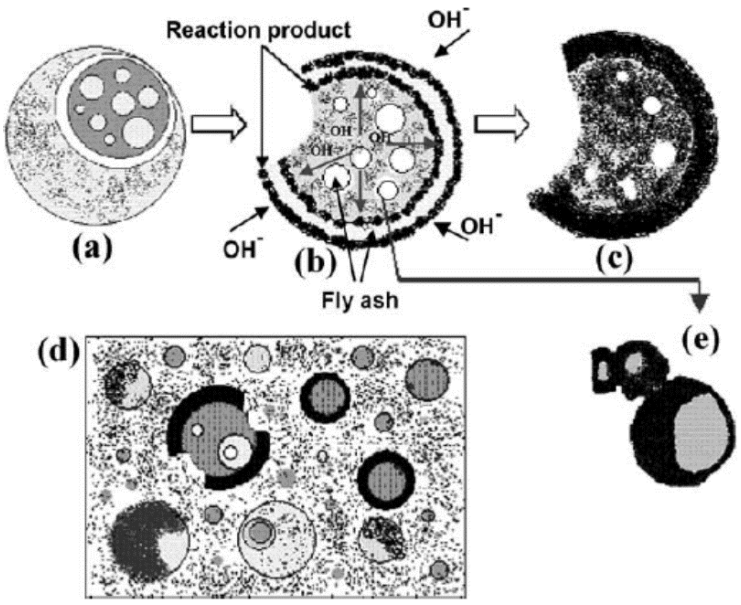

Figure 2.16: Fly ash alkali activation: a descriptive model [84]

it is mixed with concrete for casting structural elements [99, 199]. Nmiri et al. (2017) [157] investigated the possibility of using the kaolinitic clay material as an aluminosilicate source to produce geopolymer concrete. The clay was heated to a temperature between 550 and 1100 °C and NaOH and KOH solutions at concentrations of 5, 8, 10, 13, 15, or 18 molar were used to activate the calcined clay. X-ray diffraction, infrared spectroscopy, and thermal analysis were used to characterize the mineral and chemical composition of clay and geopolymer. Compressive strength, porosity, and water absorption were used to characterise the physicochemical characteristics of samples. According to the findings, a temperature of around 700 °C and an alkaline concentration of 13 molar are required to develop a metakaolin with the highest degree of reactivity, whereby the various physical characteristics reach their optimal levels. Whereas at greater temperatures and concentrations, these values declined.

Hadi et al. (2017) [102] used slag as an aluminosilicate source and sodium hydroxide and sodium silicate as alkaline activators to produce the geopolymer, while the Taguchi method has been used to design optimum mix proportions. The effects of binder content, alkaline activator to binder content (Al/Bi) ratio, sodium silicate to sodium hydroxide (SS/SH) ratio, and sodium hydroxide (SH) concentration were studied. The results showed that the specimens with the maximum 7-day compressive strength (60.4 MPa) had a binder content

of 450 kg/m3, an Al/Bi ratio of 0.35, an SS/SH ratio of 2.5, and an SH concentration of 14 molar. On the other hand, fly ash (FA), metakaolin[4] (MK), and silica fume (SF) were utilized to enhance the setting time of geopolymer concrete by partial replacements for slag in various amounts.

Soil Stabilization

Geopolymer was used to enhance soil properties. Geopolymer has a significant effect on the clayed soil properties and it can also be used as an effective alternative binder to ordinary Portland cement (OPC) in soil stabilization [12, 93]. Abdullah, et al. (2017) [12] investigated the potential usage of slag and fly ash geopolymers for stabilizing clayed soil. It was noted that replacement of fly ash using slag in the geopolymer-clay mixture induces a significant increase in soil strength. Ghadir and Ranjbar (2018) [93] stabilized clayed soil using geopolymer and OPC and compared the mechanical performance, whereby the impact of curing time and conditions, volcanic ash/clay ratio, and alkali activator was investigated. The results showed that alkali activator has a significant effect on the compressive strength of the geopolymer treated soil and soil stabilized by OPC has less ductility compared by geopolymer treated soil.

Table 2.4 summarizes the types of geopolymer that were utilized to stabilized different types of soil. Phummiphan et al. (2018) [167] used high calcium fly ash geopolymer to stabilize silty clayed sand; whereas slag was utilized as a replacement material in the soil. Three factors, slag content, curing time, and Na_2SiO_3/NaOH ratio, were used to investigate the effect of stabilizers on the soil properties. The results indicated that the soaked 7-day UCS of stabilized soil with different ratios of Na_2SiO_3/NaOH met the strength for both high and low volume roads, and 10% of slag is recommended at high Na_2SiO_3/NaOH ratios ($>$ 80:20).

Sore et al. (2018) [195] studied the feasibility of using geopolymer to stabilize compressed earth blocks (CEBs). The geopolymer was formed using metakaolin as an aluminosilicate source and sodium hydroxide with a concentration of 12 molar as an alkaline activator. Different percentages of geopolymer were utilized to stabilize the CEBs, and their physical, mechanical, and thermal properties were compared to CEBs and CEBs with 8% Portland cement. The results indicated that using geopolymer with CEBs greatly improved their mechanical performance and provided them with thermal properties that were quite close to those of CEBs without geopolymer. While stabilizing the CEBs with

[4]Metakaolin is a highly reactive pozzolana made by calcining kaolin clay at temperatures between 700 °C and 900 °C [96]

15% of geopolymer achieved properties like Portland cement stabilized CEBs, particularly in terms of water resilience.

Asphalt Pavement Construction

Mohammadinia et al. (2016) [151] investigated how geopolymer stabilized recycled construction and demolition (CD)[5] materials behaved. The geopolymers were developed by combining various percentages of fly ash (FA) and slag (S) (4% FA, 2% FA+ 2% S, or 4% S) as an aluminosilicate source and NaOH and Na_2SiO_3 as alkaline activators. The geotechnical engineering and strength parameters of these materials were tested to determine their performance for pavement base and subbase applications. For unconfined compression and repeated load triaxial testing, the effect of curing duration on the strength of CD materials was investigated. The results showed that using the geopolymer enhanced the resilient modulus and compressive strength, which were increased. When compared to fly ash-based geopolymer stabilization, slag-based geopolymer stabilization attained a higher compressive strength. While using geopolymer as a RAP stabilizer is a realistic and long-term solution for future pavement bases and subbases.

Hoy et al. (2016) [114] conducted the environmental evaluation of geopolymer stabilized RAP. High calcium fly ash is used as an aluminosilicate source and NaOH and Na_2SiO_3 as alkaline activators. XRD and SEM techniques were used to investigate microstructural development. The Unconfined Compressive Strength (UCS) of RAP-FA blends and RAP-FA geopolymers was compared to the requirements of road authorities. Toxicity Characteristic Leaching Procedure (TCLP) is used to determine the heavy metals' leachability and compare it to international standards. The findings showed that utilizing geopolymer with RAP in pavement construction has no environmental hazard, as the geopolymer binder lowers heavy metal leaching in the RAP-FA mixture.

Dayal and Nagan (2018) [69] explored the potential of employing geopolymer as a coating for aggregates and its impact on asphalt mixture properties. The geopolymer was formed using fly ash as an aluminosilicate source and NaOH and Na_2SiO_3 as alkaline activators. Aggregate testing, SEM analysis of fly ash and fly ash-based geopolymer, Marshall mix design, indirect tension tests, and repetitive load tests on asphalt mixtures were conducted during this study to evaluate the effect of geopolymer. The results revealed that the geopolymer based on fly ash can be utilized to coat natural aggregate to improve its physical and mechanical properties. Furthermore, using geopolymer to coat aggregates

[5]Crushed brick (CB), recycled crushed aggregate (RCA), and reclaimed asphalt pavement (RAP) are examples of construction and demolition materials

Table 2.4: Using geopolymers as an effective stabilizer for soil

Ref.	**Soil Type**	**Geopolymer**		**Main Comments**
		Activator	Pozzolanic	
[239]	Clay	NaOH+ Na_2SiO_3	MK	Metakaolin-geopolymer can be used as a soil stabilizer for clayey soils.
[187]	Silty sand	NaOH+ Na_2SiO_3	FA+S+ RG	Improving the strength and durability of soil.
[198]	Silty clay	NaOH+ Na_2SiO_3	FA	Improving the compressive strength of soil.
[60]	Sandy clay	NaOH+ Na_2SiO_3	FA	Reducing activator/ash ratio has a significant effect on the strength.
[165]	Silty clay	Na_2SiO_3+ CCR+ water	FA	CCR can be used as an alternative alkaline activator to produce geopolymer.
[164]	Silt, sand, and clay	NaOH+ Na_2SiO_3	FA+ CCR	FA-geopolymer enhanced the strength and considered as an effective green soil stabilizer.
[75]	Clay	Na_2SiO_3+ CCR	S	Improving water absorption, permeability, and strength.
[12]	Clay	NaOH	FA+S	Improving the compressive strength of soil.
[134]	Silt, sand, clay, and gravel	NaOH (or KOH)+ Na_2SiO_3	FA	Increasing the compressive strength as the ratio of FA/ soil increases.

Note: MK: Metakaolin; FA: Fly Ash; S: Slag; RG: Red Gypsum; CCR: Calcium Carbide Residue

Table 2.5: Using geopolymers as a modifier for asphalt binder

Ref.	**Asphalt Type**	**Form of Additive**	**Geopolymer**		**Main Comments**
			Activator	Pozzolanic	
[118]	80/100	Gel	NaOH+ Na_2SiO_3	FA (F)	Asphalt binder modified with geopolymer could remain stable at high storage temperature.
[204]	AH-90	Dry	NaOH+ Na_2SiO_3	MK+S+SF	Geopolymer is a suitable additive for developing high-performing WMA.
[181]	80/100	Gel	NaOH+ Na_2SiO_3	FA (F)	Structural chain mobility properties and storage stability of geopolymer modified asphalt are enhanced.
[205]	AH-90	Dry	NaOH+ Na_2SiO_3	MK+S+SF	The potential of geopolymer to absorb bitumen VOCs and PM emissions is relatively high.

Note: MK: Metakaolin; FA: Fly Ash; S: Slag; SF: Silica fume; VOCs: volatile organic compounds

in asphalt mixtures will improve the mixture's stability and service life, and can thus be used as a corrective method for fly ash disposal.

Recently, geopolymer was used as a modifier for asphalt binder, as summarized in Table 2.5. Tang et al. (2018) [204] investigated geopolymer uses in warm mix asphalt. As an activator for aluminosilicate in metakaolin, slag, and silica fume, sodium hydroxide and sodium silicate were utilized at various concentrations. The findings revealed that geopolymer has excellent performance and numerous advantages, such as lowering the mixing temperature and minimizing the cost.

Rosyidi et al. (2020) [181] investigated the geopolymer effect on the chemical properties of asphalt binder using the Fourier Transform Infrared Spectroscopy (FTIR). The geopolymer were prepared using fly ash (class F) and alkline activator (NaOH and Na_2SiO_3). The

results showed that the addition of geopolymer had no significant effect on the FTIR spectra, showing that the asphalt binder's functional group has not changed, as shown in Figure 2.17. This could be due to the addition of a small amount of geopolymer (less than 10%), which had no major impact on the geometry of the modified asphalt binder's FTIR spectrum. Physically, but not chemically, the reaction that occurs throughout the modified asphalt binder process was observed. Beside using geopolymer as a modifier increased the asphalt binder's bonding workability, and the high work cohesion[6] value indicates that the cracking resistance of the asphalt binder is enhanced as shown in Figure 2.18.

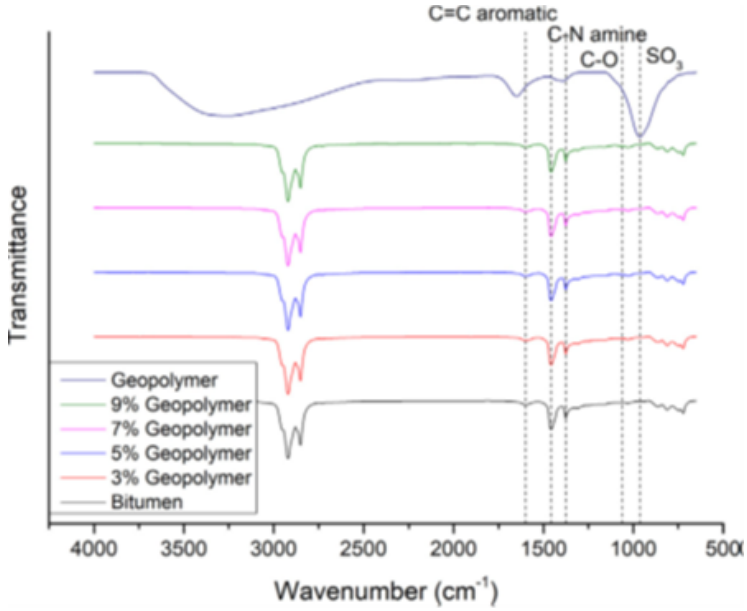

Figure 2.17: Base bitumen, geopolymer, and GMBs FTIR spectra [181]

Moreover, Rosyidi et al. (2020) [181] used Surface Free Energy (SFE) test to evaluate the effect of geopolymer on the adhesion properties between asphalt binder and two types of aggregate (limestone and granite). The results showed that the work of adhesion of samples with geopolymer modified asphalt binder was higher than that for the control sample, with the exception of 5% of geopolymer modified asphalt binder which showed a slightly lower work of adhesion[7] compared to the control asphalt binder, as shown in Figure 2.19.

[6]The energy that separates asphalt binder from one unit of an area into two new surfaces is known as asphalt binder cohesion work[181]

[7]The energy required to remove the asphalt binder bond from the aggregate interface is known as adhesion work [181]

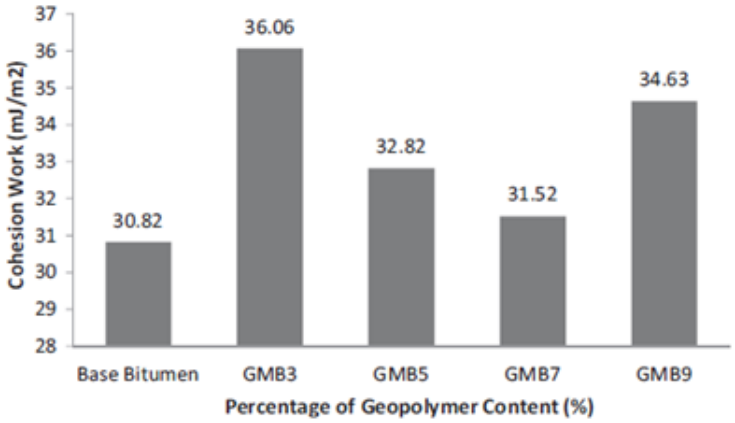

Figure 2.18: Effect of geopolymer on cohesion work [181]

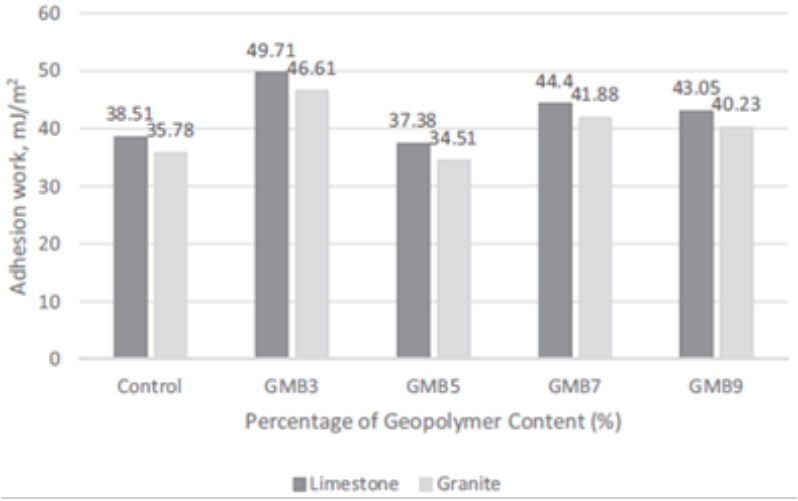

Figure 2.19: Effect of geopolymer on adhesion work [181]

Tang et al. (2020) [205] prepared the geopolymer in the dry state using fly ash (class F) and alkaline activators (NaOH and Na_2SiO_3). Two types of geopolymer were used; un-calcined (G) and calcined (AG) geopolymers. The solvent precipitation and chromatographic column test methods were used to investigate the effect of geopolymer on the SARA (saturates, aromatics, resins, and asphaltenes) components of asphalt binders, as shown in Figure 2.20. The results revealed that the addition of geopolymer to asphalt binder had no significant impact on the SARA components and properties of the asphalt binder. As a result, geopolymers have a lot of potential for use as modifiers for asphalt

binder.

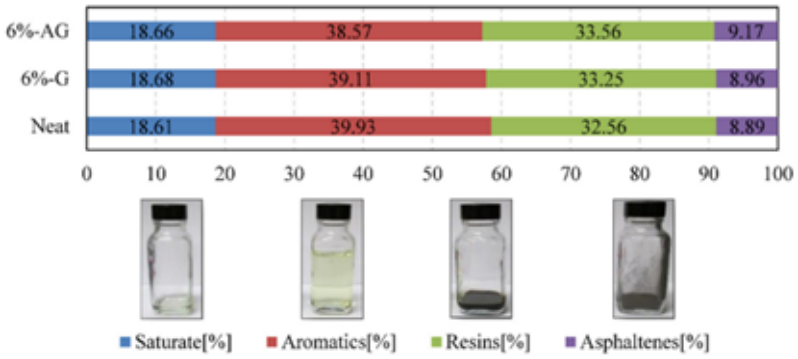

Figure 2.20: Geopolymer effect on the SARA components of asphalt binder [205]

2.6 Summary and Research Gaps

Geopolymer has environment benefits by reducing the waste and by-product materials, there are minimal CO_2 emissions during its production, and it can adsorb harmful chemical contaminants. Therefore, geopolymer has many applications in the field of construction materials, such as concrete construction and soil stabilization, whereby, it can also develop mechanical properties rapidly. Recently, there have been attempts to employ geopolymer to improve the quality of the pavement base and subbase layers or incorporate the geopolymer with the RAP to enhance its properties. There are promising and encouraging results, whereby it was noted that utilizing geopolymer with RAP in pavement construction has no environmental hazard, as the geopolymer binder reduces heavy metal leaching. On the other hand, the effect of geopolymer on the chemical and SARA component properties of asphalt binder has been investigated, which indicated that there is no significant effect on the FTIR spectra and SARA components. Thus, the geopolymer has a lot of potential for use as a modifier for asphalt binder.

The literature review showed that the use of geopolymer materials as a modifier for asphalt binder and mixture has received little attention, which may be because there has been no investigation to link the effect of temperature and curing time on the performance of geopolymer and the rheological behavior of asphalt binder. While the effect of temperature and frequencies on the rheological behavior of geopolymer modified asphalt binder hasn't been extensively investigated, considering the effect of geopolymer type and amount.

Thus, developing a geopolymer by considering the effect of temperature and cuing time on the performance of a geopolymer could encourage scientists to use different types of geopolymers with different by-products and waste materials, which will have essentially financial and environmental benefits.

Moreover, the geopolymer exhibits more resistance to high temperatures, which could be used to enhance the rutting performance of asphalt binder at high temperatures. Besides, the MSCR test has been widely utilized to predict the influence of polymer-modified asphalt binders on creep recovery and link that effect to rutting in the asphalt mixture. Unfortunately, the influence of geopolymer additives on the creep recovery behavior at high temperatures has not been investigated yet.

Furthermore, the literature review revealed that the geopolymer additive increased the asphalt binder's bonding and the high work cohesion value, which indicates that the cracking resistance of the asphalt binder is enhanced. In addition, the adhesion between asphalt binder modified using geopolymer and aggregate is improved. While the effect of geopolymer content on the fatigue and low temperature crack resistance of asphalt binder has not been investigated yet. The influence of aging and climate change conditions on the geopolymer modified asphalt binder and mixture should also be evaluated.

Globally, SBS was widely employed in many nations, and it had a considerable impact on the rheological and performance of asphalt binder. As a result, comparing the promised effects of employing the geopolymer as a modifier with the results of another modifier, such as SBS, could motivate the use of the geopolymer during pavement construction. Many studies have also noticed the effects of additives, temperatures, and frequencies on viscoelastic characteristics. On the other hand, the ANNs model is an effective tool for accurately predicting the rheological and performance of asphalt binder as discussed in the literature review (see Table 2.3). Predicting the creep recovery behavior of the asphalt binder using these effects and their changes in viscoelastic characteristics as inputs to the ANNs model could be effective for developing an accurate model that could have a significant effect on saving time and money during laboratory work.

Chapter 3

Research Methodology

3.1 Introduction

The main purpose of this study is to investigate the effects of geopolymer on the rheological and performance properties of asphalt binder and mixture, and to evaluate the impact of temperatures, stresses, and modifier content on the recovery and non-recovery properties of asphalt binder. According to the findings of the literature, there is a need to develop a new type of geopolymer that has a significant influence on the rheological and performance of asphalt binder, taking into account the effects of temperatures and curing time. Besides developing new models, considering the effects of geopolymer content, temperatures, and frequencies. The following methodology was conducted through several laboratory tests for prepared asphalt binders and mixtures with different percentages of modifiers. The research plan includes five tasks designed to achieve the general objectives of the project. The overall research methodology is presented in Figure 3.1.

3.2 Materials Preparation

3.2.1 Geopolymer Preparation

Geopolymer is made up of an alkali activator and fly ash mixture. Alkali activators included sodium silicate solution (Na_2SiO_3) and sodium hydroxide (NaOH) at an 8-molar concentration. Before making the geopolymer, the sodium hydroxide (NaOH) solution is prepared in a fume cabinet for at least one day. The low calcium fly ash (Class F) employed

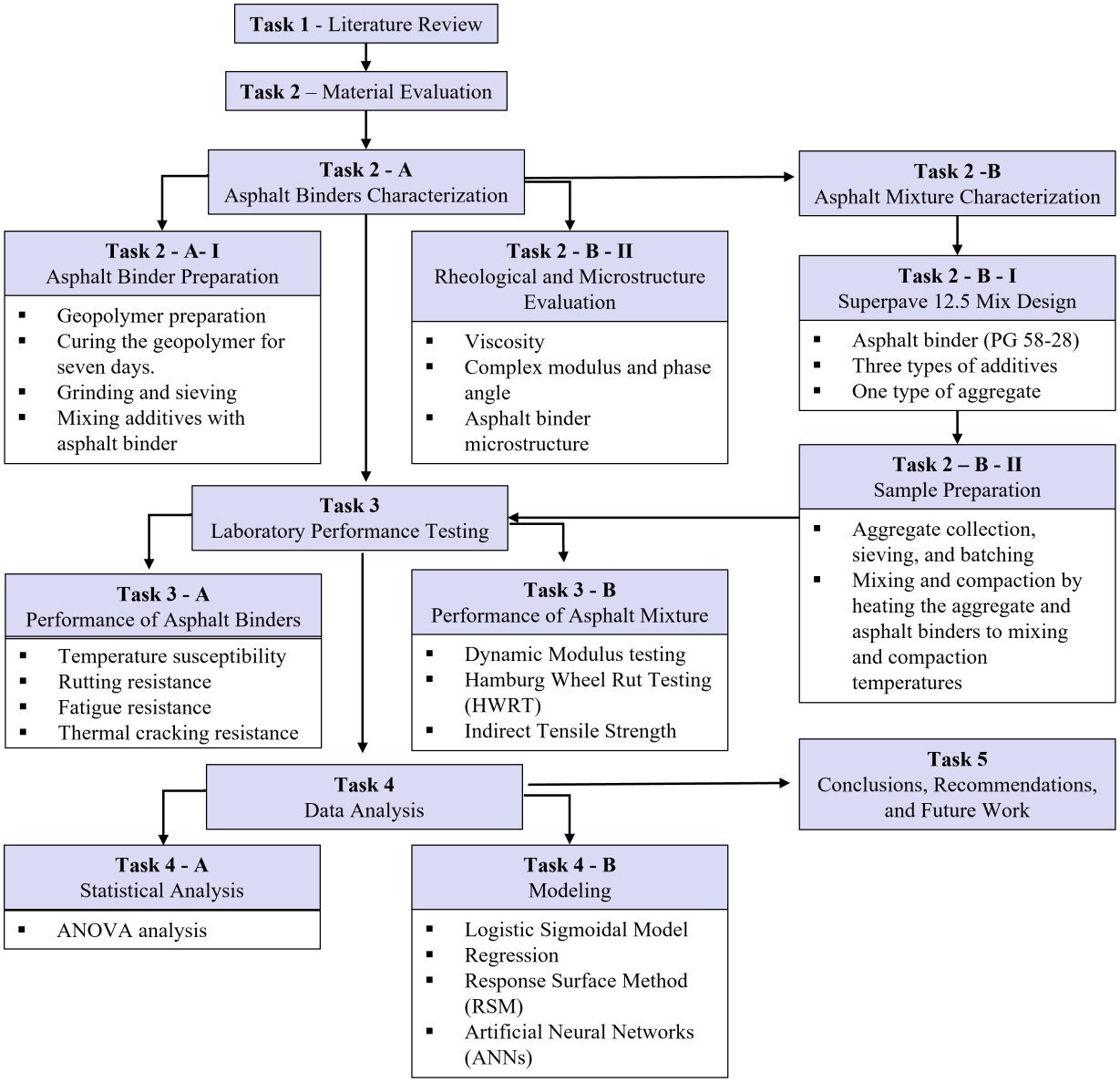

Figure 3.1: Research methodology

in this study has more silica and alumina, which is preferable than high calcium fly ash (Class C) as recommended by many researchers [110, 76, 92].

It was shown that curing time and type of activator have significant effects on chemical

reactions during preparation of geopolymer [59]. Also, it is noted that the sodium hydroxide and sodium silicate combination provide geopolymer with high mechanical performance [166]. The highest yield stress and storage modulus values are obtained when 8 molar of NaOH is used as an activator during the preparation of the fly ash-based geopolymer [177].

The geopolymers used in this investigation were fly ash-based geopolymer (GF) and glass powder and fly ash-based geopolymer (GFG). To activate the alumino-silicate precursors in fly ash and glass powder, a mixture of sodium silicate and sodium hydroxide solution in a 1:2 mass ratio was utilized. More information on the preparation of the two types of geopolymers can be found in Chapters 4 and 6. Figure 3.2 shows the different types of additives that were used in this research and the steps of geopolymer preparation.

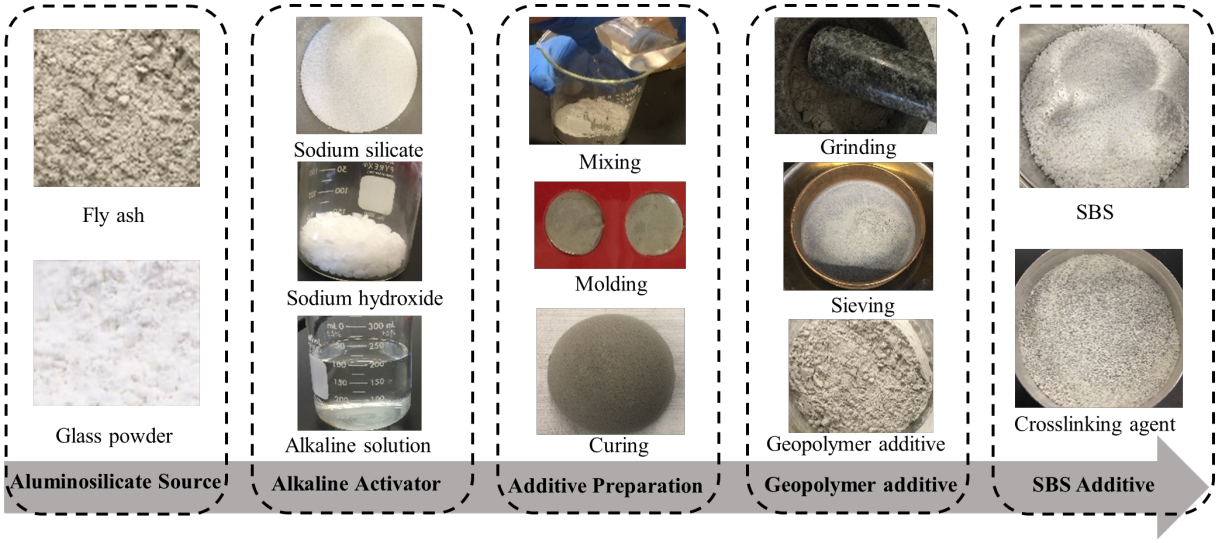

Figure 3.2: Additives preparation

3.2.2 Asphalt Binder Preparation

Modified asphalt binders were prepared using two scenarios. In the first one, the geopolymer-modified asphalt binder was prepared by heating 300 g of asphalt binder (PG 58-28) at 140 °C. Then the geopolymer was added into the neat asphalt blend in different amounts. A mechanical shear mixer, as depicted in Figure 3.3(a), was used at a speed of 2000 r/min for 60 minutes, controlling the temperature at 140 °C ± 5 to prepare a homogenous blend. In the second scenario, the SBS-modified asphalt binder was prepared by heating the asphalt binder (PG 58-28) at 170 °C. The SBS polymer has a linear microstructure with a styrene

content of 31.6%. The SBS was added and mixed, using the high shear mixer and heating mantle for 60 minutes at a temperature of 170 °C, as shown in Figure 3.3(b). At the end of the hour, 10% of the crosslinking agent was added and mixed for 30 minutes. Finally, a curing time of another 60 minutes was conducted by controlling the temperature at 180 °C ± 5 and reducing the high shear mixer speed.

(a) (b)

Figure 3.3: Asphalt binder mixing using (a) mechanical shear mixer and (b) high shear mixer

3.2.3 Aging Procedures

Short-Term Aging

The short-term aging simulates the aging during asphalt mixing when exposed to elevated temperatures. The Rolling Thin-Film Oven (RTFO), as depicted in Figure 3.4, was used to prepare the short-term aging of neat and modified asphalt binders according to the AASHTO T 240 [2]. The asphalt binders were filled into cylindrical glass bottles with 35 ± 0.5 g following the asphalt binders mixing method. All bottles were placed horizontally in a vertically revolving frame, rotating at a speed of 15 revolutions per minute, after cooling for 60 to 180 minutes. Because of the heat and motion, the samples flow along the walls of the glass bottles. During each cycle, which took a few seconds, air was blasted into each glass container once, whereby this procedure took 85 minutes at 163 °C.

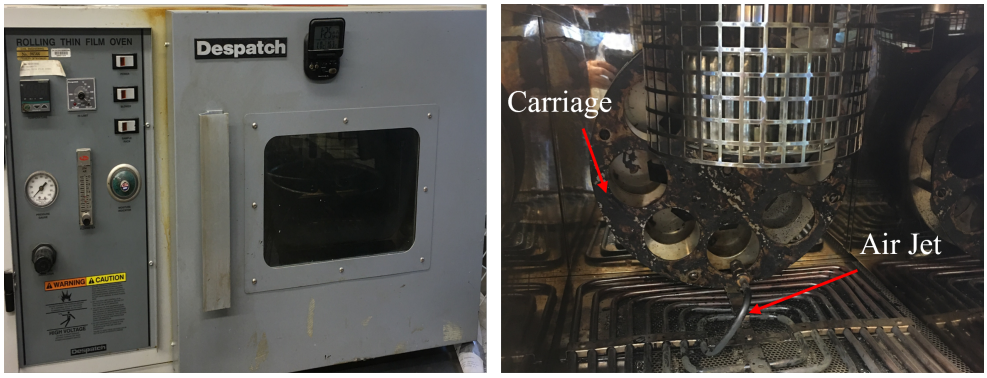

(a) (b)

Figure 3.4: Short-Term Aging, (a) Rolling Thin-Film Oven and (b) Inside the oven

Long-Term Aging

The long-term aging is designed to simulate the oxidative aging that occurs in asphalt binders during pavement use. The physical and chemical properties of asphalt binders after 5 to 10 years of in-service aging in the field can be estimated using the residue from this procedure [3]. The Pressure Aging Vessel (PAV), as shown in Figure 3.5, was used to prepare the long-term aging of neat and modified asphalt binders according to the AASHTO R 28 [3]. The RTFO asphalt binder was poured into stainless steel pans with 50 $\pm$ 0.5 g and aged in a vessel pressured with air to 2.10 MPa for 20 hours at the appropriate aging temperature of 100 °C. After that, the asphalt binder residue is vacuum degassed when the PAV process is completed.

3.3 Asphalt Binders Characterization

This section described the tests that were used to investigate the rheological and performance of neat and modified asphalt binders, as depicted in Figure 3.6.

3.3.1 Rotational Viscometer Test

The viscosity of neat and modified asphalt binders was measured using the Rotational Viscometer with 10 g of asphalt binder, as shown in Figure 3.7. For each test temperature, three readings were taken, and the average was used to calculate the test result.

(a) (b)

Figure 3.5: Long-Term Aging, (a) Pressure Aging Vessel and (b) Aged binders

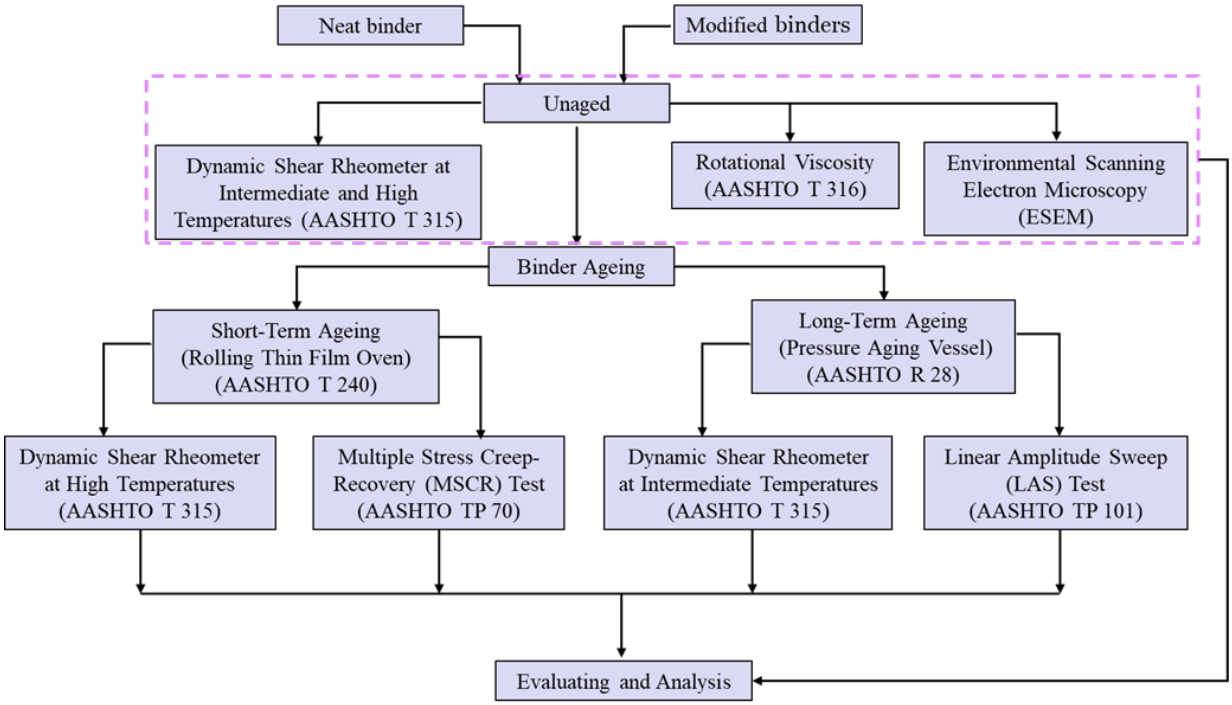

Figure 3.6: Asphalt binders characterization

The viscosity of asphalt binder at various temperatures is used to determine mixing and compaction temperatures.

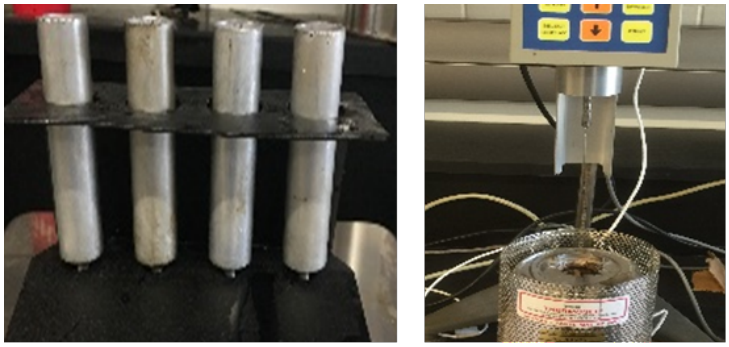

(a) (b)

Figure 3.7: Viscosity determination

3.3.2 Dynamic Shear Rheometer (DSR) Test

The Dynamic Shear Rheometer (DSR), as shown in Figure 3.8, is used to investigate the rheological behavior of asphalt binder at intermediate and high temperatures. Furthermore, DSR determines the complex shear modulus (G^*) and phase angle (δ) of asphalt binder at various temperatures and loading frequencies, as per AASHTO T315 [6]. In this study, DSR tests such as frequency sweeps, Linear Amplitude Sweep (LAS), and Multiple Stress Creep Recovery (MSCR) were performed for the neat and modified asphalt binders. The master curves, isochronal plots, and rutting and fatigue figures were all created using the DSR data. The DSR-grading test was also used to evaluate the failure temperatures. The construction of the master curve helps in the comparison of asphalt binder stiffness over various temperature and frequency ranges. A shift factor should be applied to the experimental complex modulus (G^*) and phase angle (δ) values to normalise them to a reference temperature in order to get the master curve.

Linear Amplitude Sweep (LAS)

The DSR-Linear Amplitude Sweep (LAS) test was conducted, according to AASHTO TP101 [1], using an 8 mm diameter plate with a 2 mm gap at three different temperatures: 10 °C, 20 °C, and 30 °C. Before the strain sweep test, a frequency sweep test was used to determine how the undamaged material responded. As a result, the strain sweep test was performed at a constant frequency (10 H_z) to accelerate fatigue damage. The VECD model was applied to analyse the test results and estimate asphalt binder fatigue life (N_f).

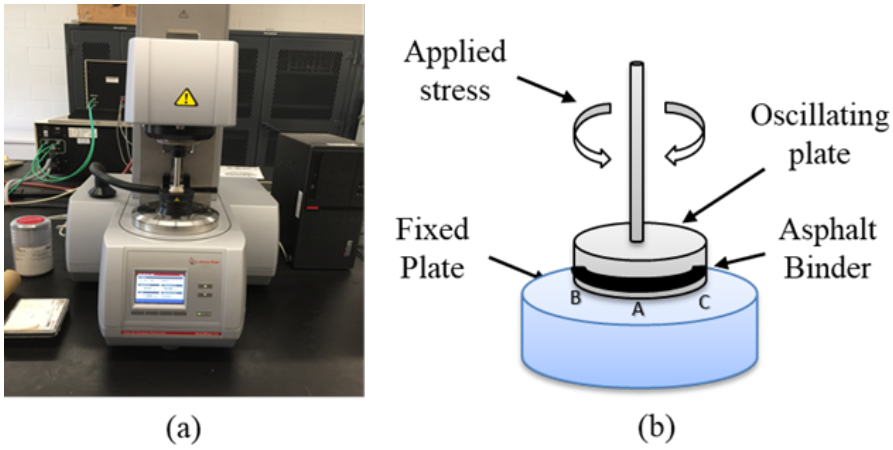

Figure 3.8: Dynamic Shear Rheometer (DSR) Test

The main benefit of this test is that it takes approximately 30 minutes to complete [112]. The VECD model was used to predict asphalt binder fatigue life (N_f) as the following [158]:

$$N_f = A(\gamma_{max})^{-B} \tag{3.1}$$

Where $B = 2\alpha$, $\alpha = 1/m$, and γ_{max} = the maximum strain, (%).

$$A = \frac{f(D_f)^k}{K(\pi C_1 C_2)^\alpha} \tag{3.2}$$

where f is the loading frequency (10 H_z), K is calculated using Equation 3.3.

$$K = 1 + (1 - C_2)\alpha \tag{3.3}$$

$$D_f = (\frac{C_0 - C}{C_1})^{1/C_2} \tag{3.4}$$

where D_f is the value of $D(t)$ at failure, which can be calculated using Equation 3.5.

The curve-fit coefficients C_1 and C_2 were computed from the relationship between C(t) and D (t) as represented in Equations 3.5 and 3.6 respectively.

$$D(t) = \sum_{i=1}^{N} [\pi \gamma_0^2 (C_{i-1} - C_i)]^{\frac{\alpha}{1+\alpha}} (t_i - t_{i-1})^{\frac{1}{1+\alpha}} \tag{3.5}$$

$$C(t) = \frac{|G^*|(t)}{|G^*|_{initial}} \tag{3.6}$$

where $|G^*|$ is the complex shear modulus, and t is the testing time, second.

The VECD model was validated in this work using the pseudo strain energy (PSE). The damage evolution is explained using Schapery's (1984) work potential theory [188]. According to Wang et al. (2015) [224], stored PSE is a useful parameter for describing the failure of the asphalt binder in LAS experiments. Furthermore, they found a strong link between fatigue life and the rate of PSE release. The pseudo strain energy can be divided into two types: stored (W_s^R) (Equation 3.7) and released (W_r^R) (Equation 3.8). After each cycle of loading, (W_s^R) represented the energy stored. An increase in W_s^R shows that the material can store more energy for greater loads. A drop in the W_s^R indicates that the material has failed since it is losing its ability to store energy as the load increases.

$$W_s^R = \frac{1}{2} C(S) (\gamma_P^R)^2 \tag{3.7}$$

$$W_r^R = \frac{1}{2} [1 - C(S)] (\gamma_P^R)^2 \tag{3.8}$$

where γ_P^R is the peak pseudo-strain for a cycle, $C(S)$ is pseudo-stiffness, which can be measured using Equation 3.9.

$$C(S) = \frac{\tau_p}{(DMR) \times (\gamma_P^R)} \tag{3.9}$$

where τ_p is the peak shear stress, DMR is the dynamic modulus ratio between $|G^*|_{initial}$ and $|G^*|(t)$

$$\gamma_{Pi}^R = \gamma_{Pi} \times |G^*|(t) \tag{3.10}$$

Multiple Stress Creep and Recovery (MSCR)

In this study, MSCR test was conducted to investigate the percent recovery (R) and non-recoverable creep compliance (J_{nr}) of asphalt binders. All asphalt binder samples were aged using Rolling Thin Film Oven (RTFO) according to standard AASHTO T 240 procedures [2]. Then, the 25 mm diameter samples were tested in creep and recovery at low and high stress levels of 0.1 kPa and 3.2 kPa. Two samples were tested, and the average was identified as the test result for each temperature. The test consisted of a one-second constant stress for creep, followed by a nine-second rest period with no creep stress. Each of the two stress levels has ten cycles, for a total of 20 cycles. The stress and strain must be recorded on an accumulating basis at least once every 0.1 second for the creep cycle and once every 0.45 second for the recovery cycle, with data points at 1.0 and 10.0 seconds for each cycle, as shown in Figure 3.9. The whole process of creep and recovery during this test takes a total of 200 seconds to complete. The average percent recovery (R), non-recoverable creep compliance (J_{nr}), and non-recoverable creep compliance difference (J_{nrdiff}) were calculated using Equations 3.11, 3.12, and 3.13, respectively.

$$R = (\frac{\varepsilon_1 - \varepsilon_{10}}{\varepsilon_1}) \times 100 \tag{3.11}$$

where ε_1 is accumulated strain after 1 s., ε_{10} is residual strain after 10 s.

$$J_{nr} = \frac{\varepsilon_{10}}{\sigma} \tag{3.12}$$

where σ is applied stress.

$$J_{nrdiff} = (\frac{J_{nr3.2} - J_{nr0.1}}{J_{nr0.1}}) \times 100 \tag{3.13}$$

$J_{nr0.1}$ is non-recoverable creep compliance at creep stress of 0.1 kPa, $J_{nr3.2}$ is non-recoverable creep compliance at creep stress of 3.2 kPa.

3.3.3 Bending Beam Rheometer (BBR)

Figure 3.10 shows the BBR test which performed on PAV-aged binders, according to ASTM D D6648 [27] to determine the flexural-creep stiffness (S) and m-value by means of a bending beam rheometer. Different temperatures (-12 °C, -18 °C, and -24 °C) were

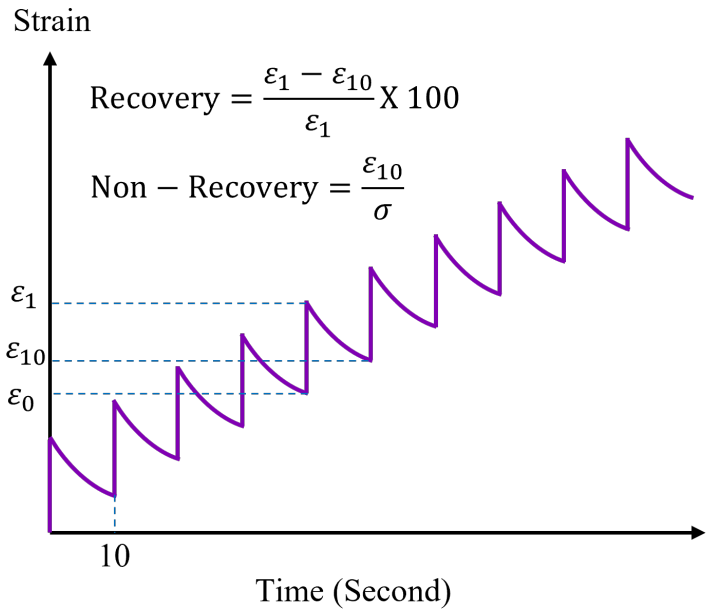

Figure 3.9: Typical MSCR test results

performed to replicate the minimum pavement temperatures of -22 °C, -28 °C, and -34 °C, respectively. These values were obtained by applying a steady creep load of 100 g for 240 seconds to an asphalt binder beam with dimensions of 125 mm long, 6.35 mm wide, and 12.7 mm high. Equation 3.14 was then used to compute the creep response. The slope of the logarithmic stiffness versus logarithmic time curve at time is known as the m-value.

$$S(t) = \frac{PL^3}{4bh^3\delta(t)} \tag{3.14}$$

where S(t) is Creep stiffness, P is the load, $\delta(t)$ is the Deflection, and b, h, and L are the beam dimensions.

To connect creep stiffness to thermal cracking resistance of the asphalt binder, ASTM D D6648 establishes an upper limit of 300 MPa for creep stiffness evaluated at 60 seconds and a lower limit of 0.300 for creep rate (m-value). It's worth mentioning that increasing the m-value reduces the creep stiffness of the binder, making it less stiff.

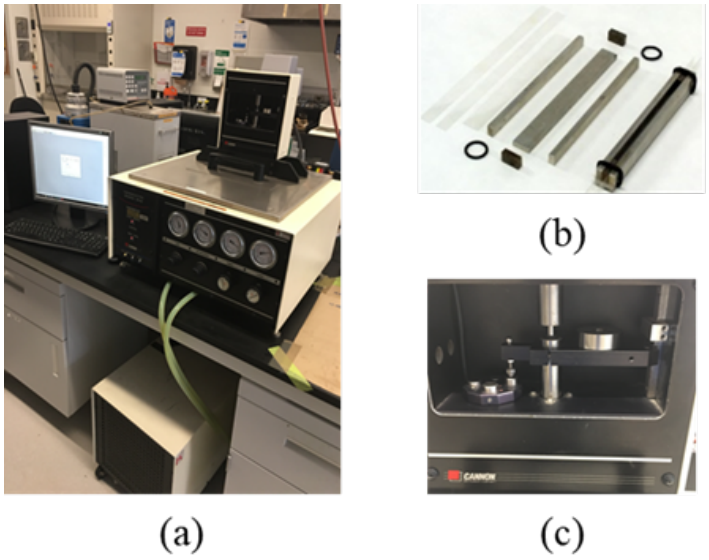

Figure 3.10: Bending Beam Rheometer (BBR) setup in the CPATT Lab

3.4 Asphalt Mixture Characterization

This section details the test procedures used to characterise mixes including various types of additives, as well as the methods for producing specimens for these tests.

3.4.1 Dynamic/Complex Modulus Test

The dynamic modulus is the stress-strain relationship under a continuous sinusoidal loading and is defined by its complex modulus (E^*), which determines the stiffness properties of the HMA as a function of temperature and loading rate [77]. The dynamic modulus was considered as a significant parameter input in the MEPDG design method of asphalt pavement, which used for characterizing asphalt mixtures [160]. Undoubtedly, the determination of the dynamic modulus of the asphalt mixture has become an important priority [57]. The dynamic modulus of an asphalt mixture can be measured by conducting laboratory tests in either a stress-controlled or a strain-controlled mode at different temperatures and frequencies.

In this study, the dynamic modulus tests were conducted according to the AASHTO T 342 [10]. Asphalt binders and aggregates were heated in an oven to get to their mixing

temperatures. The viscosities of the asphalt binders, using rotational viscometer according to AASHTO T 316 [7], were used to obtain the mixing and compaction temperatures. To simulate short-term aging of asphalt mixtures, the asphalt mixture was immediately conditioned at 135 °C for four hours after mixing, according to AASHTO R 30 [5]. The dynamic modulus tests were performed using specimens with 100 mm in diameter and 150 mm in height at 7% ± 0.5 of air void. These specimens were cored and cut from the middle of SGC compacted specimens with dimensions of 150 mm in diameter and 170 mm in height. The Material Testing System (MTS) at the CPATT labs were conducted using six loading frequencies (0.1, 0.5, 1, 5, 10 and 25 H_z) and five different temperatures (-10, 4, 21, 37, and 54 °C). Three extensometers were mounted at 120 ° intervals at mid-height of the specimens. Figure 3.11 demonstrates the dynamic modulus samples preparation and testing at the CPATT labs.

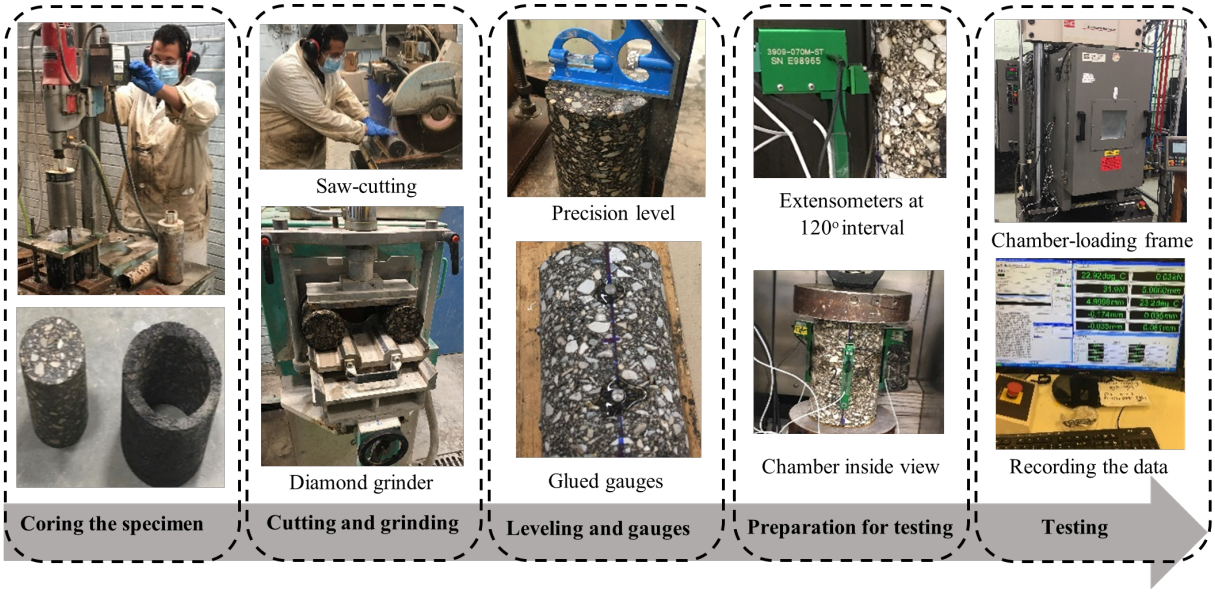

Figure 3.11: CPATT dynamic modulus test setup

3.4.2 Hamburg Wheel Rut Test

Rutting is a common sign of distress that affects the road network's serviceability and quality. Rutting is a permanent deformation that appears in the traffic direction because of unrecoverable strain accumulated by repetitive loads applied to the asphalt pavement [109]. The Hamburg Wheel Rut Test (HWRT) was used to evaluate the rutting resistance

of HMA using Hamburg Wheel Tracking Device (HWTD), as shown in Figure 3.12. The test was performed in accordance with AASHTO T 324 [8]. Four samples, with a 150 mm diameter and 63 mm height at 7% ± 0.5 of air void, were prepared using the Superpave Gyratory Compactor (SGC). The asphalt mixture samples were submerged and conditioned for 30 minutes at 44 °C in the water bath. The samples were tested using solid steel wheels and the average rutting depth was measured using Linear Variable Differential Transformers (LVDTs), whereby the data acquisition system was used to measure the amount of permanent deformation.

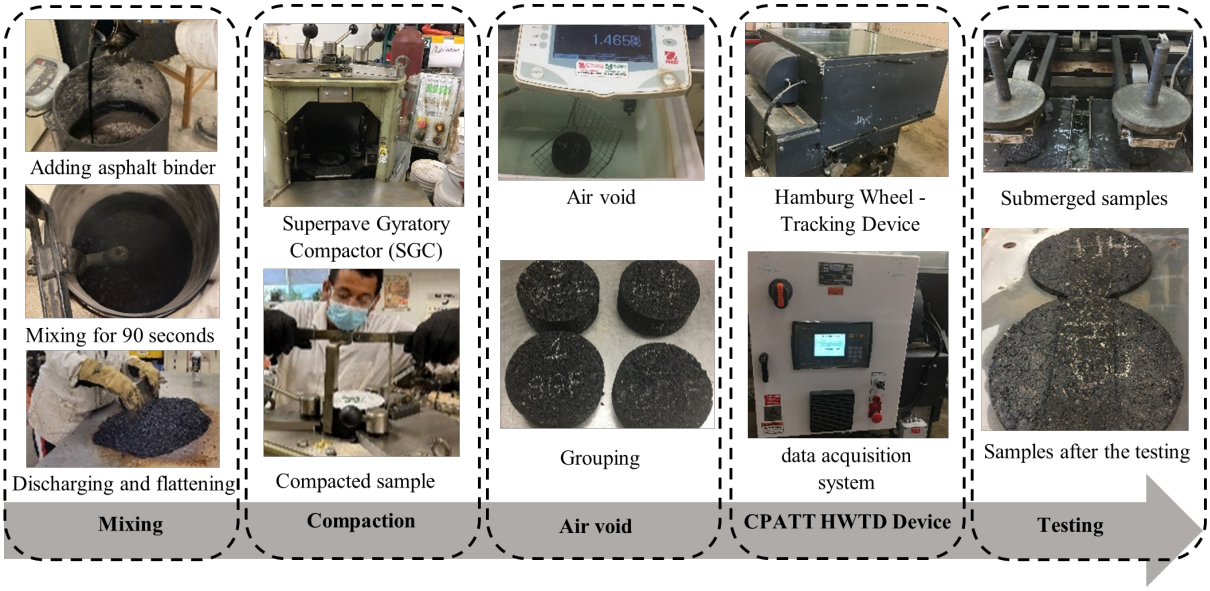

Figure 3.12: Hamburg Wheel Rut Test (HWRT) setup in the CPATT Lab

3.4.3 Moisture Sensitivity Testing

Moisture damage in pavement materials is the most important issue that affects the durability of asphalt pavement. Moisture damage in asphalt causes stripping, which is defined as the loss of adhesive bonding force between the binder and the aggregate particles. Moisture damage in asphalt mixtures occurs due to loss of adhesion and/or cohesion (the bond between asphalt binder molecules), whereby the mixture's strength and stiffness gradually deteriorate because of this process [109]. The test is conducted according to the AASHTO T283 using the MTS at the CPATT labs. Six SGC compacted specimens with dimensions of 150 mm in diameter and 95 mm thick at 7% ± 0.5 of air void were used. After that, these

specimens were divided into two groups: conditioned and unconditioned. The conditioned subset was vacuumed to a saturation range between 70% and 80% before being frozen for 16 hours at -18 °C and then thawed in a water bath for 24 hours at 60 °C.

The moisture susceptibility of asphalt mixtures was calculated using the Tensile Strength Ratio (TSR), which is the percentage of tensile strength retained after conditioning. For conditioned samples, the volume of air voids using Equation 3.15 and the volume of absorbed water using Equation 3.16 should be calculated to determine the degree of saturation using Equation 3.17. Figure 3.13 shows the preparation of samples in the CPATT labs, whereby the indirect tensile strength test with rate of 50 mm/minute was used to investigate the moisture damage resistance of asphalt mixtures.

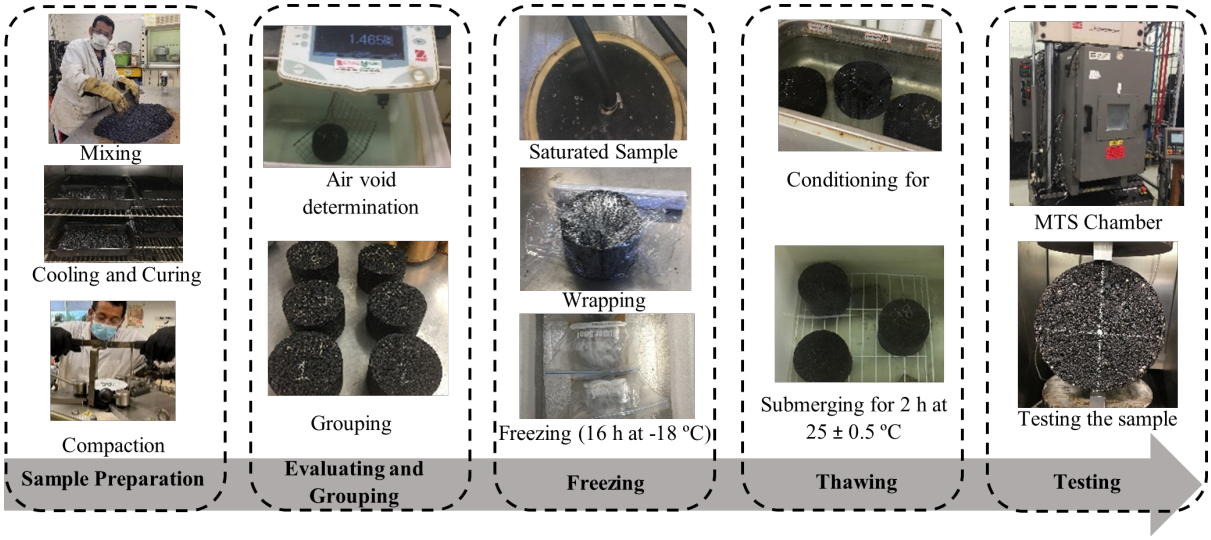

Figure 3.13: Moisture sensitivity testing setup in the CPATT labs

$$V_a = \frac{P_a E}{100} \tag{3.15}$$

V_a is the volume of air voids (cm^3), P_a is the percentage of air void, and E is the volume of the sample (cm^3).

$$J^{'} = B^{'} - A \tag{3.16}$$

$J^{'}$ is the volume of absorbed water (cm^3), $B^{'}$ is the mass of the saturated, surface-dry sample after partial vacuum saturation (g), and A is the mass of the dry sample in air (g).

$$S^{'} = \frac{100J^{'}}{V_a} \tag{3.17}$$

$S^{'}$ is the percentage of the saturation.

Chapter 4

Evaluating Fly Ash-Based Geopolymers as a Modifier for Asphalt Binders

This chapter is based on the following article, which was published in Advances in Materials Science and Engineering Journal. "Evaluating Fly Ash-Based Geopolymers as a Modifier for Asphalt Binders," by A. Hamid, H. Alfaidi, H. Baaj, and M. El-Hakim (2020). **DOI: 10.1155/2020/2398693**

Abstract

The severe Canadian winter conditions and growing traffic volumes are vital factors resulting in a reduction of the service life of flexible pavements. Researchers and engineers strived to develop several additives to develop balanced asphalt mixers capable of resisting distresses that caused deterioration of flexible pavements in Canada. In this study, a critical literature review regarding the use of geopolymers and their application in construction materials is provided. Moreover, an experimental matrix of laboratory testing was conducted to study the rheological and microstructural properties of the PG 58-28 asphalt binder; with different percentages of geopolymer; 0%, 3%, 6%, and 9%. The effect of geopolymer curing time on rheological properties was investigated. Rotational Viscometer, Dynamic Shear Rheometer (DSR), and Environmental Scanning Electron Microscopy (ESEM) imaging devices were utilized to compare the performance of control binder to a binder with different percentages of geopolymers. Results indicated that the increase in

the geopolymer content and the curing time affect the rheological behavior of the asphalt binder by increasing its viscosity, complex shear modulus and failure temperature. Samples with higher geopolymer percentage exhibited better performance in terms of rutting resistance. Moreover, an increase in the failure temperature of modified asphalt binder with 9% geopolymer is recorded as 8.58%, 14.2%, and 15.2% for 2, 7, and 14 days curing times respectively, compared with virgin asphalt. Furthermore, the nanoparticles appear to be well dispersed in the binder and increasing the percentage of the geopolymer does not seem to affect the microstructure of the binder. Overall research conclusion is that geopolymer application resulted in a potential enhancement of some of the properties of the asphalt binder.

4.1 Introduction

Modified asphalt binder could be utilized to reduce pavement distresses such as rutting and cracking. Polymer modification of asphalt binder could be a cost-effective solution to reduce the annual budget for maintenance and rehabilitation of flexible pavements. In the past two decades, growth in the utilization of polymer-modified asphalt binders in pavement-engineering applications was noticed. Significant improvement of the mechanical and rheological properties of the asphalt binder at different temperatures was reported in the literature [19, 33, 29]. Polymers can be defined as large molecules with numerous compositions of small molecules bonded together. These small molecules are called monomers [186]. The binder modification using polymers increases the sustainability of asphalt binders and asphalt mix designs. In addition, performance enhancement and cost reductions are achieved through polymer modification of asphalt binders [141]. Application of modifiers in asphalt binders would result in a reduction of optimum binder content, increasing stability, increasing the bond between asphalt binder and aggregates, and improving density [50]. In addition, modifiers would minimize the environmental impact on roads, such as traffic noise, the total expenditure for repair and maintenance of road structures.

Scholars investigated the utilization of waste materials to improve the performance of asphalt binders. Numerous studies have been conducted to evaluate the benefits of using crumb rubber [153, 55], cylinder oil [48], Palm Oil Fuel Ash (POFA) [47] as binder modifiers. Geopolymer Modified binder is a new method to capitalize on the use of waste materials in paved roads. Geopolymer concept was first introduced by Davidovits in 1978 [66]. The geopolymers are inorganic polymers with aluminosilicates base. The geopolymers are produced from the interaction between pozzolanic materials with an alkaline solution

such as sodium hydroxide (NaOH) and sodium silicate (Na_2SiO_3) or potassium hydroxide (KOH) and potassium silicate (K_2SiO_3) [97]. Materials stemming from solid wastes and by-products endowed with silica and/or aluminas such as fly ash, red mud, mine waste and blast furnace slag qualify as a pozzolanic component of geo-polymerization [189].

Geopolymer has also proven its ability to develop mechanical properties rapidly, to improve the high fire resistance property, and to reduce energy consumption and greenhouse emissions [67, 99, 223]. Geopolymer has many applications in the field of manufacturing such as in the aerospace and automobile, metallurgy and nonferrous foundries, civil engineering, and plastic industries [68]. Geopolymeric materials are utilized in toxic waste management due to their ability to absorb toxic chemical wastes [68].

During the past two decades, geopolymers were widely used as an environment friendly additive to cementous construction materials. Geopolymers were noted to reduce the CO_2 emissions associated with the production of cementous materials [79]. Geopolymer can also be used in fire-resistant wall panels [189], masonry units, protective coatings and repairs materials, shotcrete and high-performance fiber reinforced laminates [99]. Sumajouw et al. (2007) [199] investigated the structural behavior of geopolymer concrete columns and noted that the possibility of using the current concrete design standers for fly ash-based geopolymer concrete columns. Twelve columns were tested under axial load and uniaxial bending in the mode of single curvature during this investigation. Six columns were characterized by 40 MPa compressive strength, while the rest had 60 MPa compressive strength. Different reinforcement ratios and load eccentricities were considered. Load carrying capacity, deflection characteristic, and mode of the failure were determined. Results showed that the current concrete design standards could be used for designing fly ash-based geopolymer concrete columns.

Geopolymers have many applications in the field of soil stabilization. Recent studies investigated the effectiveness of using geopolymer to improve the physical and mechanical properties of soils. Cristelo et al. (2012) [61] experimentally studied the effectiveness of geopolymer on the improvement of rammed-earth construction soils. The ratio of liquid to solid, the ratio of Na_2O to ash, and the alkali concentration were investigated through this study. Furthermore, the influence of concrete superplasticizer, sodium chloride, and calcium hydroxide is also discussed. The results showed that there are only slight effects of sodium chloride or superplasticizer and there is a significant increase in compressive strength as an optimum value for the ratio of activator: solids and the concentration of alkali. Sukmak et al. (2013) [198] investigated the important factors such as sample sizes, heating conditions, and different percentages of silty clay and fly ash that affect the strength development in clay–fly ash geopolymer brick. In this study, sodium hydroxide and sodium silicate were used as an alkaline activator and fly ash was used as a pozzolanic

material. The results showed that the samples with optimum heat Energy per Weight (E/W) is 8.5 °C h/g for fly ash/clay ratios of 0.3 and 0.5 whereas the E/W is 7.57 °C h/g for fly ash/clay ratio of 0.7. Moreover, they recommended that a substantial relationship between weight and heat energy should be considered in the bricks production industry.

Recently, geopolymer was used as an additive during the preparation of warm mix asphalt. Tang et al. (2018) [204] studied the applications of geopolymer in warm mix asphalt. Sodium hydroxide and sodium silicate were used with different concentration as an activator for aluminosilicate in metakaolin, slag, and silica fume. The results showed that geopolymer could decrease the mixing temperature. Consequently, geopolymers could be utilized to reduce Warm Mix asphalt mixing cost. The need for new additive with high properties is in continuous growth to enhance the asphalt binder properties. The use of by-product materials such as fly ash enhances the sustainability of pavement mixtures and reduces the emission of CO_2. Fly ash can be divided into three classes, N, F, and C, based on its composition and source of origin [98]. Xu and van Deventer (2000) [229] noted that the addition of sodium hydroxide solution to the sodium silicate solution as the alkaline liquid improved the reaction with fly ash.

The main objective of this project is to study the rheological behavior and performance grading of geopolymer modified binder with the concentrations of 3%, 6%, and 9% at different temperatures using several laboratory experiments. The impact of curing time variation on the performance of geopolymer was also evaluated in this project. Finally, the microstructure of base and modified asphalt binder was investigated using the environmental scanning electron microscope (ESEM).

4.2 Experimental Methods

4.2.1 Materials

Geopolymer Preparation

Geopolymer was the combination of fly ash and the alkali activator. The alkali activator was sodium silicate solution (Na_2SiO_3) and sodium hydroxide (NaOH) pallet diluted in water to produce 8 Molar (8M) NaOH solution. A mixture of sodium silicate solution and sodium hydroxide solution was prepared to activate the alumino-silicate precursors in fly ash. In this study, fly ash with Class F is used which satisfies this chemical composition $SiO_2 + Al_2O_3 + Fe_2O_3 \geq 70\%$ according to the ASTM C618-17a [196]. The chemical

Table 4.1: Fly ash chemical composition

Constituent	SiO_2	Al_2O_3	Fe_2O_3	CaO	MgO	SO_3	Na_2O
Fly ash	57.2%	23.5%	3.8%	9.3%	1.0%	0.2%	2.43%

compositions of fly ash are listed in Table 4.1. Geopolymer additives were prepared using the alkaline medium as the chemical activator and fly ash as the aluminosilicate source.

Figure 4.1 shows the adopted mixing procedure to prepare the geopolymer. The following steps summarize the preparation of geopolymer:

1. Prepared alkaline solution using sodium hydroxide (8M) and sodium silicate solution with percentages of 100:50% by mass respectively.
2. 200 grams of fly ash powder were mixed with 80 grams of the alkaline medium for 6 minutes.
3. The formed slurry was transferred to silicon molds, as shown in Figure 4.1.
4. Geopolymers were cured at room temperature (23-25 °C) and in the oven (40 °C). Curing was performed in three different curing plans which will be explained in the following section.

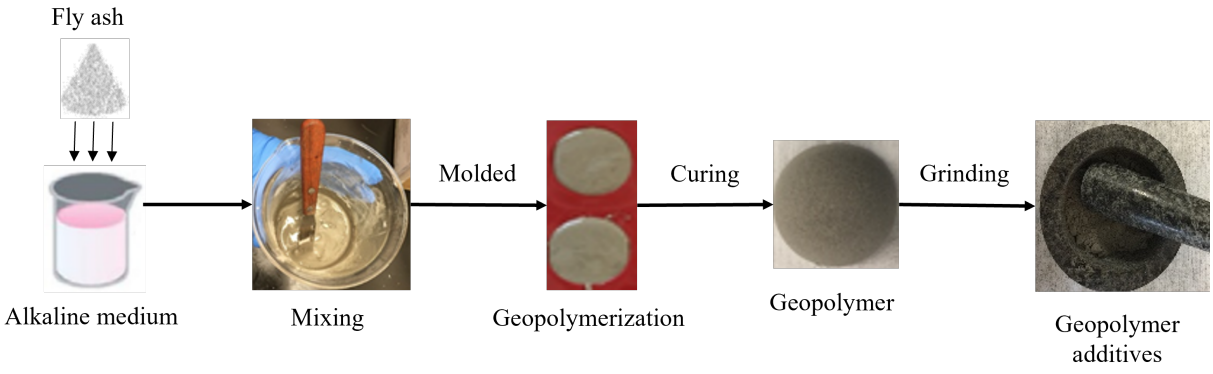

Figure 4.1: Preparation of geopolymer additives

Table 4.2: Properties of original asphalt binder

Index	Conditions	Unit	Results	Requirements
Specific Gravity	At 15 °C	....	1.03	....
Brookfield Viscosity	At 135 °C	Pa.s	0.275	3.0 max
Flash Point	....	°C	230+	230 min
$G^*/\sin\delta$	At 58 °C	kPa	1.195	1.0 min

In this study, there are three sets of geopolymer are prepared based on the curing time as the following: (i) first set was cured for 24 hours at room temperature, and then cured in the oven at 40 °C for 24 hours, (ii) second set was cured for 6 days at room temperature, and then cured in the oven at 40 °C for 24 hours, and (iii) third set was cured for 13 days at room temperature, and then cured in the oven at 40 °C for 24 hours. The particles size greater than 0.25 mm may impact the consistency of results obtained from tests such as DSR. Therefore, geopolymer samples were grinded into powder, as shown in Figure 4.1, and then were sieved using sieve No. 100 to avoid particles with a diameter of more than 0.15 mm.

Modified Binder Preparation

The base asphalt binder used was PG 58-28, the properties of the virgin asphalt binder are shown in Table 4.2. The base asphalt binder of 300 g was heated until it becomes fluid, then the geopolymer was added into the base asphalt blend with doses of 3%, 6%, and 9% by mass of the asphalt binder. Subsequently, the blends were mixed using a mechanical shear mixer for 120 minutes under a speed of 2000 r/min with a temperature of 150 °C ±5 to produce a homogenous blend, as depicted in Figure 4.2.

4.2.2 Experimental test Procedures

Rotational Viscometer Test

The viscosity of virgin and modified asphalt binder was measured using the Rotational Viscometer with 10 g of asphalt binder. Three readings were determined for each test temperature, and the average was recognized as the test result. Also, the test temperatures were ranged from 90 °C to 165 °C and using 15 °C as an interval.

Figure 4.2: Preparation of geopolymer additives

Dynamic Shear Rheometer (DSR) Test

The Dynamic Shear Rheometer (DSR) is used to study the rheological behavior of asphalt binder at intermediate and high temperatures. Moreover, DSR measures the complex shear modulus (G^*) and the phase angle (δ) of asphalt binder at different temperatures and frequencies of loading, as per AASHTO T315 [6]. In this study, DSR-frequency sweeps test was performed for the virgin and modified binders using a 25 mm and 8 mm diameter plate and a 1 mm and 2 mm gap, respectively. The tests were performed at sixteen frequencies ranging from 0.159 H_z to 15 H_z while the test temperatures ranged from 11 to 35 °C (intermediate temperature) and from 40 to 64 °C (high temperature). In this study, sinusoidal shear strains were conducted on asphalt binder samples by placing the samples between two parallel plates, one plate is fixed, and another one is moving freely. Then, the various frequencies are applied under several temperatures. Sinusoidally changing shear strain is expressed as [142, 21]:

$$\gamma(t) = \gamma_0 \sin \omega t \tag{4.1}$$

With resulting stress

$$\tau(t) = \tau_0 \sin(\omega t + \delta) \tag{4.2}$$

Where γ_0 is the peak strain,τ_0 is the peak stress, ω is the radian frequency, δ is the phase angle, and t is the time (seconds).

After changing the phase by $\pi/2$

$$\gamma^* = \gamma_0 e^{i\omega t} \tag{4.3}$$

$$\tau^* = \tau_0 e^{i(\omega t+\delta)} \tag{4.4}$$

Then, the complex shear modulus is determined by the following equation:

$$G^* = G^{'} + iG^{''} = \frac{\tau^*}{\gamma^*} = \frac{\tau_0 e^{i(\omega t+\delta)}}{\gamma_0 e^{i\omega t}} = \frac{\tau_0}{\gamma_0} \times e^{i\delta} = (\frac{\tau_0}{\gamma_0})(\cos\delta + i\sin\delta) \tag{4.5}$$

Equation 4.5 shows that:

$$|G^*| = \frac{\tau_0}{\gamma_0} = \sqrt{G'^2 + G''^2} \tag{4.6}$$

$$G^{'} = |G^*|\cos\delta \tag{4.7}$$

where $G^{'}$ is called storage modulus

$$G^{''} = |G^*|\sin\delta \tag{4.8}$$

where $G^{''}$ is called loss modulus

$$\tan\delta = \frac{G^{''}}{G^{'}} \tag{4.9}$$

The DSR results were used to construct the Master curves, isochronal plots, and rutting figures. Also, the failure temperatures were also determined from DSR-grading test. The development of the master curve helps to make a comparison between the stiffness of asphalt binder over different ranges of temperatures and frequencies. In order to obtain the master curve, a shift factor should be applied to the experimental complex modulus (G^*) and phase angle (δ) values in order to normalize them to a reference temperature. The master curve can be developed using a specified reference temperature and applying a relationship between complex modulus and frequency [57].

Environmental Scanning Electron Microscopy (ESEM)

ESEM is a microscope that utilizes high-pressure gas in a chamber to examine a relatively natural state in which materials are scanned analogously to a standard SEM without routine preparation for compatibility [149]. The model of ESEM unit used to test the specimens was FEI Quanta 250 FEG, as shown in Figure 4.3. A stainless-steel sample mold design was developed recently in the Centre for Pavement and Transportation Technology (CPATT) with an 8 mm diameter [150], as depicted in Figure 4.3.

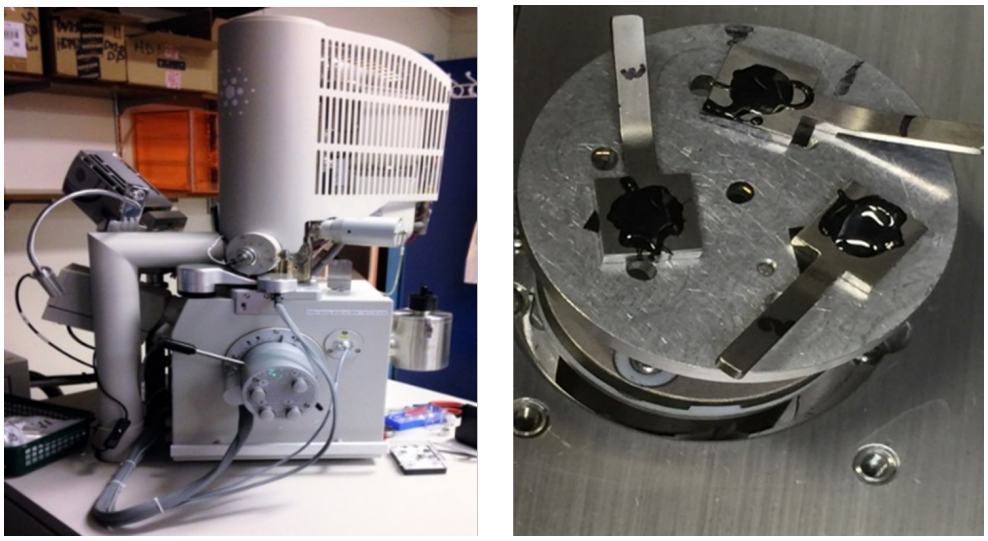

Figure 4.3: ESEM device (right) and sample mould with binder in ESEM stage (left)

4.3 Results and Discussion

4.3.1 Effects of Geopolymer on Viscosity

The rotational viscosity of asphalt binder is considered an important index to assess the workability for asphalt binder. Hence, determination of the adequate asphalt binder mixing temperature and compaction is significantly impacted by the geopolymer content. The percentage of geopolymers significantly affects the viscosity of the asphalt binder [204]. Figure 4.5 and 4.6 show the average viscosity of asphalt binder with different percentages of geopolymer (0, 3, 6, and 9%). The virgin binder was characterized by the lowest viscosity,

whereas the modified asphalt binder sample with 9% of geopolymer has the highest viscosity which indicates that 9% of geopolymer has better performance regarding rutting resistance. However, using statistical T-test to compare the viscosity of virgin binder and binder with 9% geopolymer at temperatures ranging from 90 °C to 165 °C resulted in the insignificant difference at 95% confidence level with a P_{value} of 0.126. It was noted that the viscosity of the 9% modified binder was higher than that of the virgin binder by 51% at 90 °C. The difference between the viscosity of the two binders vanishes at higher temperatures as shown in Figure 4.4.

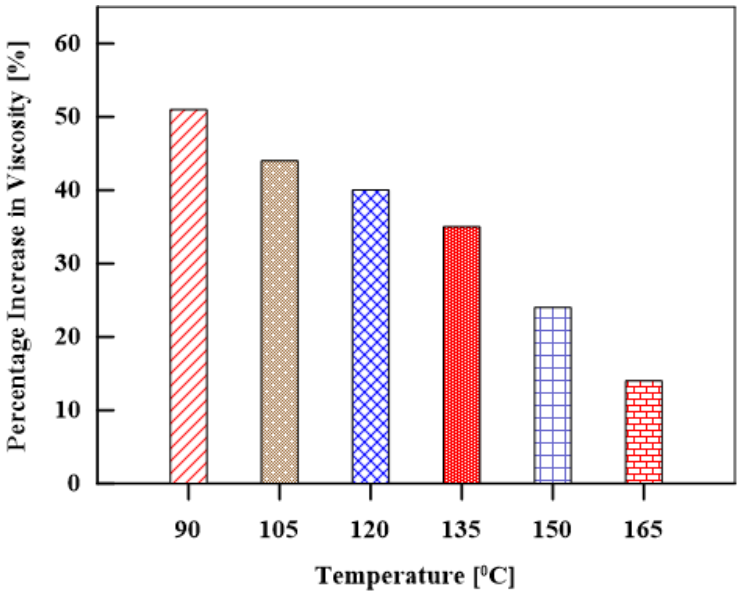

Figure 4.4: Percentage increase of viscosity comparing 9% polymer-modified binder to the virgin binder

The increase in binder viscosity due to adding geopolymer material was reported by previous scholars [19, 21, 200]. Asphalt binders with high viscosity achieve excellent weather resistance and provide strong binding forces between aggregates. In addition, asphalt binders with high viscosity have better resistance to displacement by water than those of low viscosity [209]. The viscosity results of asphalt binder with 3, 6 and 9% geopolymer content fell below the maximum limit of 3 Pa.s at the temperature of 135 °C according to the Superpave specifications.

Figure 4.5 shows the viscosity of asphalt binder samples with 9% geopolymer and conditioned at curing times of 2, 7, and 14 days. Figure 4.6 presents the viscosity data through two stages. In stage one, the viscosity of both virgin and modified binders with

various curing times was subjected to immediate reduction as the temperature increased from 90 to 120 °C. The highest viscosity was noted in the modified binder with 7 and 14 days curing time. Stage two witnessed a temperature change from 120 °C to 165 °C. The results of stage two show that the modified binders still were characterized by higher viscosity compared to the virgin binder.

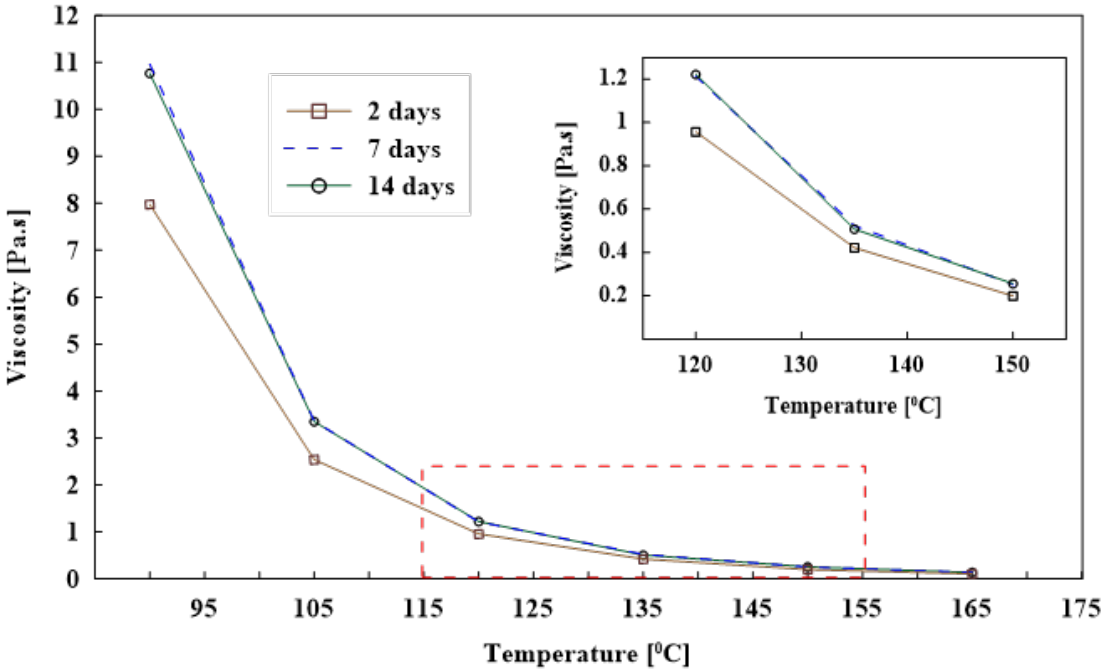

Figure 4.5: Effects of curing time on asphalt binder viscosity for 9% of geopolymer

The statistical analysis of the 9% geopolymer-modified binder confirmed that the curing time period does not have a significant impact on the viscosity. The 2-day curing period was considered the control curing period. The 7-day and 14-day curing period viscosity results were compared to the 2-day curing period to check the impact of curing period on viscosity. The statistical T-test resulted in P_{values} of 0.19 and 0.2 for the viscosity of 7-day and 14-day curing periods compared to the control curing period (2-days). Therefore, the additional curing time has an insignificant impact on viscosity. It should be noted that the percentage increase in viscosity was 30% by increasing the curing period from 2 to 7 days. The viscosity showed 0% change between 7 and 14 days curing period. Therefore, extending the curing period beyond the 7 days will not result in a significant change in the viscosity of geopolymer modified binders, which confirms the findings from [189, 238, 17].

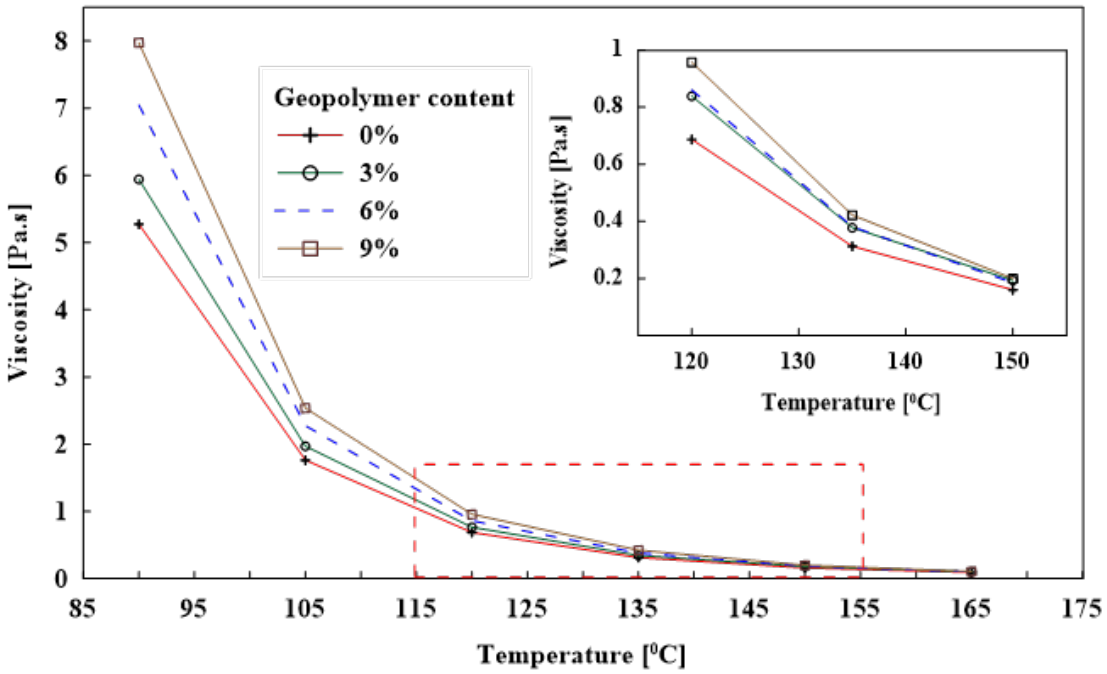

Figure 4.6: Asphalt binder viscosity changing with the temperature at different geopolymer additives

4.3.2 Effects of Geopolymer on Rheological Properties

Rheological Master Curve

Figures 4.7(a, and b) present the rheological Master curve at a reference temperature of 35 °C for complex shear modulus and phase angle. Figure 4.7(a) showed the insignificant difference between the complex shear modulus of modified asphalt binder with 6 and 9% of geopolymer. Airey (2003) [19] studied the rheological behavior of Styrene Butadiene Styrene (SBS) modified binder with 3%, 5%, and 7% of and reported an increase in complex shear modulus with increasing the modifier percentages. Based on results obtained from specimens tested in CPATT labs, an increase of geopolymer percentage above 6% did not have a significant impact on complex shear modulus. For example, the complex shear modulus at 10 H_z increased by 127%, 214%, and 224% through adding 3, 6 and 9% geopolymers respectively, compared to the virgin binder.

Figure 4.7(b) shows that the phase angle at 10 H_z decreased by 2.9%, 5.3%, and 6% due to increasing the geopolymer percentages 3, 6 and 9% respectively, compared with the

virgin binder. This indicates an increase in the elastic response of the modified binder. Therefore, the elasticity of the modified binder increased along with the increasing of geopolymer additives.

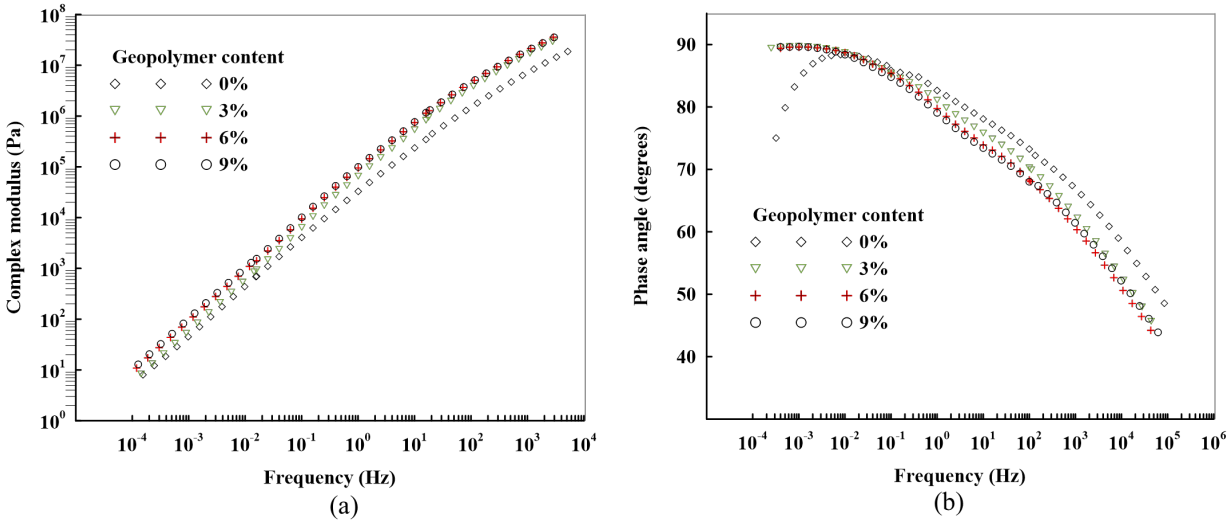

Figure 4.7: Rheological master curve at 35 °C for (a) complex modulus, and (b) phase angle

Isochronal Plot

Isochronal plots of complex shear modulus (G^*) and phase angle versus temperature at 1 H_z and 0.1 H_z of frequency are shown in Figures 4.8(a, and b). The results presented in Figures 4.8(a, and b) show that the complex shear modulus significantly increases at various temperatures (59% average increase) by adding 3% geopolymers compared to the virgin binder. The statistical t-test resulted in a P_{value} of 0.003. Therefore, the addition of 3% geopolymers results in a statistically significant increase in complex shear modulus with a confidence level of 95%. However, the insignificant difference is noticed by comparing the complex modulus at 6% and 9% geopolymer modified samples compared to the 3% geopolymer-modified. The P_{values} for the 6% and 9% geopolymer modified compared to the 3% are 0.098 and 0.104, respectively. This indicates the temperature susceptibility is improved. Previous research literature reported temperature susceptibility increase for elastomer modified binders such as epoxidized natural rubber [21] and styrene butadiene styrene (SBS) [19].

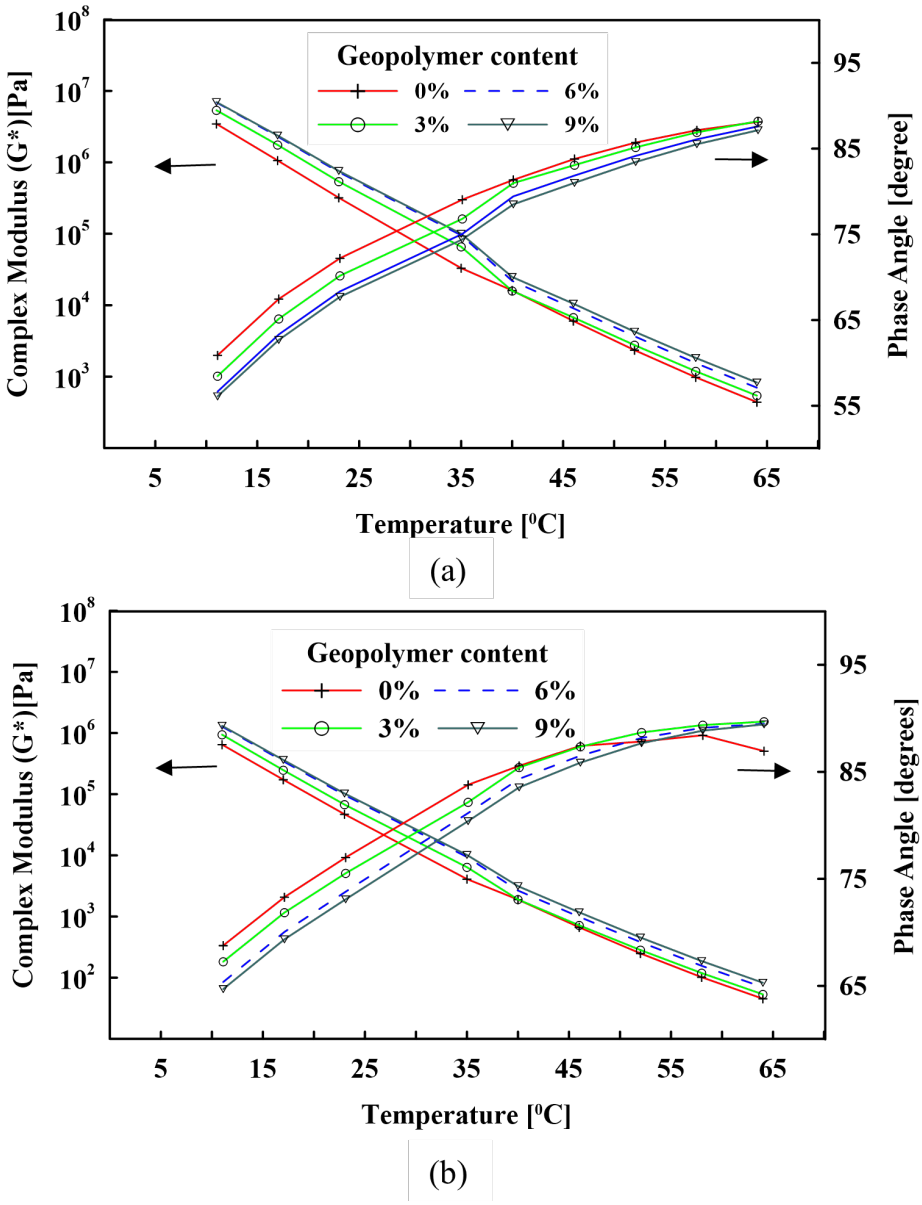

Figure 4.8: Isochronal plots of the complex modulus and phase angle at (a)1 H_z and (b) 0.1 H_z

Rutting Factor

Rutting is a permanent deformation which occurs at temperatures higher than 40 °C, leading to ruts in the direction of traffic and can be relevant to the viscosity of the asphalt binder

[16]. Figure 4.9 shows the effect of temperature on the rutting factor ($G^*/\sin\delta$), which represents a measure of the high-temperature stiffness of the asphalt binder's response to repeated load application at high temperatures. According to Superpave specification, the rutting factor must be a minimum 1.0 kPa for the unaged binder at 10 rad/sec. This specification is set to minimize the contribution of the asphalt binder to rutting. The results showed that the rutting factor increased by increasing the geopolymer additives which indicates that rutting resistance is improved. The same result for different binder modifiers is also recorded in previous studies [128, 21]. For example, the rutting factor at 58 °C increased by 22%, 58.2%, and 86.6% through adding 3, 6 and 9% of geopolymers by mass respectively, compared with the virgin binder.

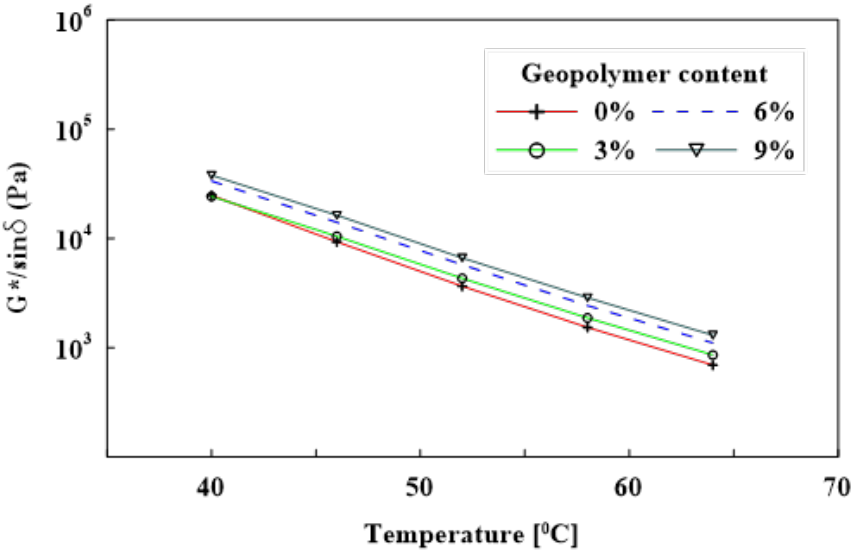

Figure 4.9: Temperature effect on rutting factor ($G^*/\sin\delta$)

4.3.3 Effects of Geopolymer on Performance Grading

Figures 4.10(a, and b) show the results of failure temperature obtained from DSR-grading test. Figure 4.10(a) shows that the virgin binder has the lowest failure temperature nearly 60.6 °C compared to geopolymer modified binder with various percentages. Addition of 3%, 6% and 9% of geopolymers resulted in an increase of 1.98%, 5.78%, and 8.58% in the failure temperature respectively. This indicates that the geopolymer could be utilized to increase the high-temperature grading of asphalt binder. Figure 4.10(b) shows the results of 9% modified binder with curing time 2, 7, and 14 days. The figure shows that failure

temperature for 2, 7, and 14-days curing time exceeded that of the virgin binder by 8.58%, 14.2%, and 15.2%, respectively.

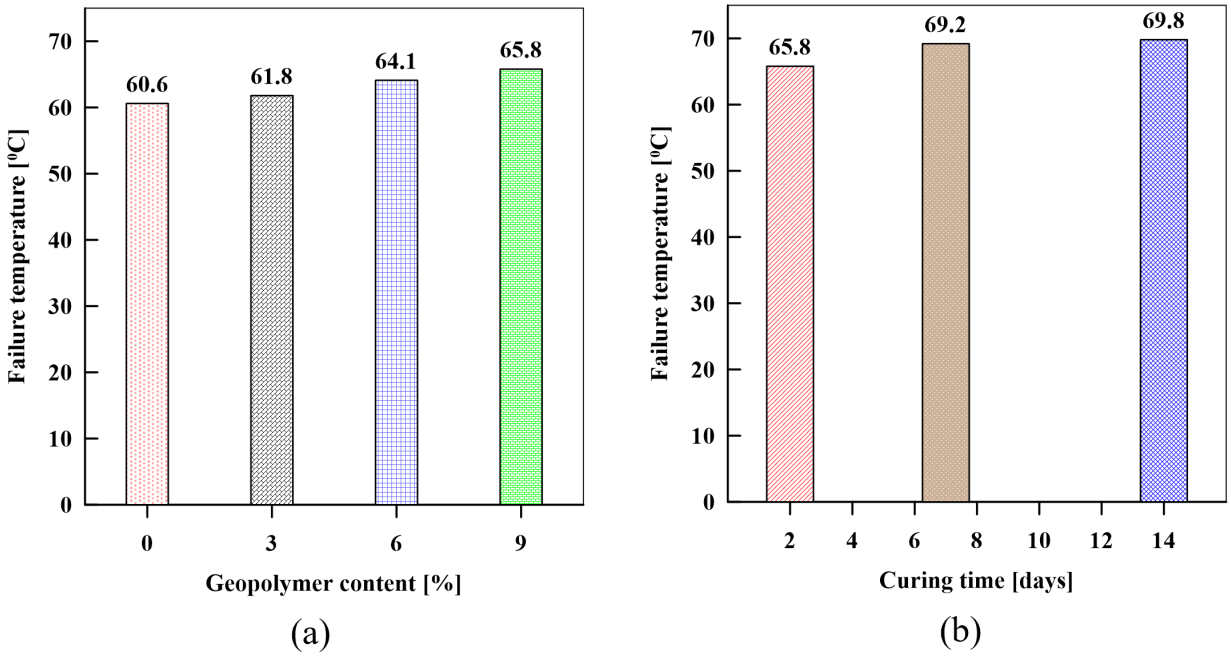

Figure 4.10: Effects of geopolymer on performance grading, (a) effects of geopolymer additives, (b) effects of curing time on 9% of geopolymer

4.3.4 Effects of Geopolymer on the Microstructure of the Binder

ESEM technology was used to observe polymer-modified asphalt binder microstructure [150, 197]. Stangl et al. (2006) [197] utilized ESEM to investigate the microstructure of asphalt binder with and without modifiers in aged and unaged conditions. The results indicated that aging has a significant effect on the microstructure of asphalt binder, whereby RTFOT-aging caused the network structures to become coarser. Meanwhile, Mikhailenko et al. (2019) [149] noted that the denser the structure of the fibrils in ESEM imaging, the stiffer the binder is. In this investigation, ESEM was utilized to study the microstructure of asphalt binder with different percentages of geopolymer, 3, 6 and 9%. It is noted that the microstructure of the asphalt binder with 0% of geopolymer matches the microstructure reported by Mikhailenko et al. (2018) [148]; whereas there is no significant effect of adding

3, 6 and 9% of geopolymer on the structure of the fibrils in ESEM imaging. Additionally, the nanoparticles of the geopolymer were observed under ESEM, as shown in Figure 4.11. The examination of the ESEM images indicates that the nanoparticles are well dispersed in the binder and that the microstructure of the binders with 3, 6 and 9% of geopolymer are quite homogeneous without any visible agglomerations of the geopolymers in the binder.

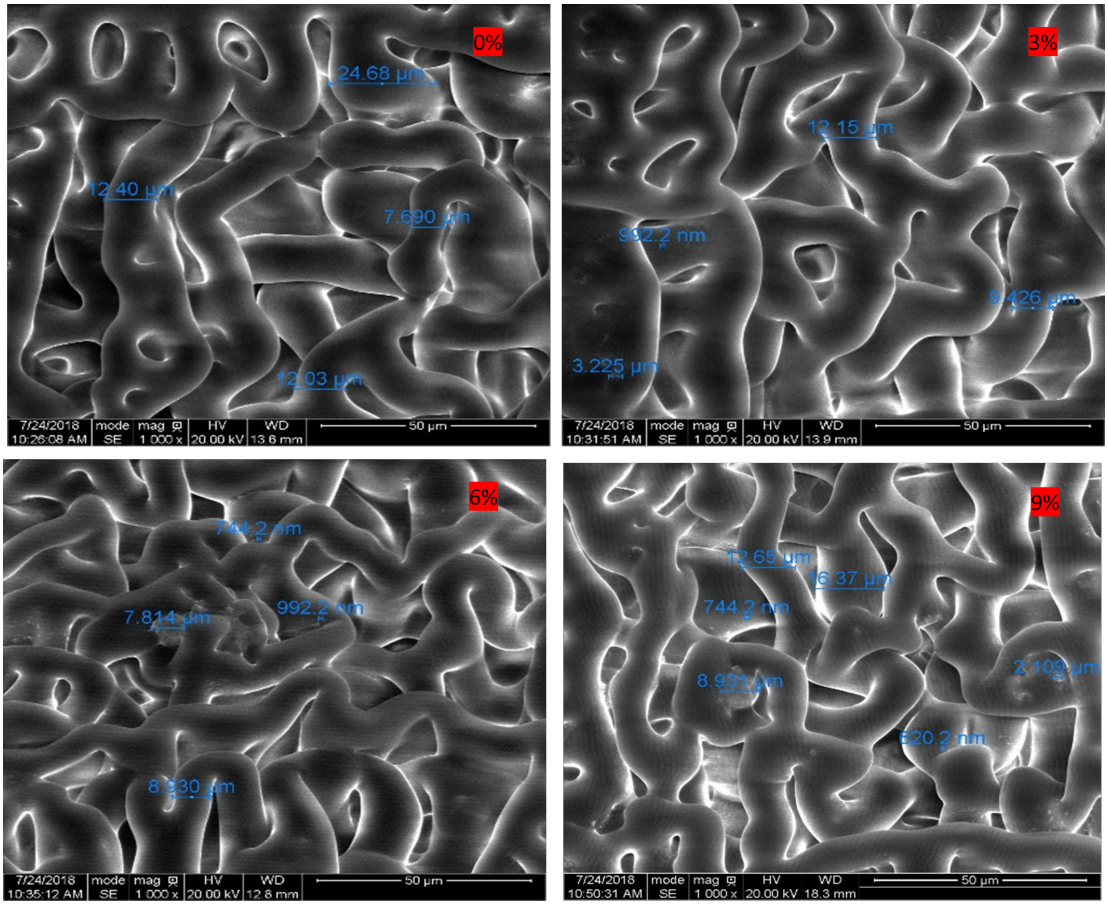

Figure 4.11: ESEM observation of different percentage of geopolymer

4.3.5 Economic and Environmental Effects of Geopolymer

Because of its critical impact on the growth of countries' economics, governments tend to facilitate considerable budgets to improve road-infrastructures. As a result of its severe

weather and high traffic load conditions, it is worth nothing that Canada spends millions annually for maintenance of deteriorated pavements for road-infrastructure. Asphalt binder is the world's most commonly used pavement materials, however, is facing several highly sensitive financial and environmental issues. The manufacture of asphalt binder consumes a lot of energy that involves the emission of CO_2 into the atmosphere. Greenhouse Gas (GHG) emissions must be decreased 50 to 80% by 2050 in order to limit the global temperature increase to 2 °C which is considered a challenge to achieve reductions of this magnitude [125]. Meanwhile, Ma et al. (2016) [144] noted that reducing (GHG) emission from the construction of asphalt pavement should be focused on the manufacturing stage of raw materials and the mixing process of asphalt concrete. Thus, reducing the usage of the high amount of asphalt binder and decreasing the energy amount during the preparation of hot mix asphalt would have potential financial and environmental effects.

Recently, there is a tendency to enhance the asphalt rheological properties using by-product and waste materials that have increased the world over in the last few decades.It is well known, however, that the potential development of geopolymer has a significant effect on reducing waste and by-product materials, such as fly ash, red mud, mine waste and blast furnace slag. Into the bargain, using geopolymer as an asphalt modifier has proven its efficiency to improve the rheological properties of asphalt binders thereby enhancing the rutting resistance that results in a reduction of pavement deterioration. Consequently, the reduction in the CO_2 emission increases, as a result of decreasing in the production amount of asphalt binder. Thus, the geopolymers have significant economical and environmental impacts on the construction of asphalt pavement. Table 4.3 summarizes the effect of the geopolymer contents on the viscosities; at 135 and 165 °C, and the compaction and mixing temperature ranges of asphalt mixture.

The results revealed a minor effect on the compaction and mixing temperature ranges for modified asphalt binder; in comparison with a virgin asphalt binder. However, a slight increase is observed in temperature of compaction and mixing processes for modified asphalt binder, for the curing times; for 9% of geopolymer at 7 and 14 days. In overall, we can draw the conclusion that the geopolymer application in asphalt binder has minor effects on the compaction and mixing temperatures which imply that there is a minor impact on the energy-consuming during compaction and mixing processes for asphalt mixtures.

4.4 Conclusions

Geopolymer was used in many disciplines such as soil and concrete to develop the mechanical properties rapidly and to improve the high fire resistance property. However, the

Table 4.3: Properties of original asphalt binder

Content (%)	**Curing Time (days)**	**Viscosity at 135 °C**	**Viscosity at 165 °C**	**Compaction Range (°C)**	**Mixing Range (°C)**
0	2	0.313	0.100	135-140	148-154
3	2	0.345	0.100	138-142	149-154
6	2	0.381	0.100	138-143	149-154
9	2	0.422	0.106	140-144	150-155
9	7	0.523	0.137	144-148	154-160
9	14	0.508	0.135	144-148	154-159

geopolymer is not widely utilized to enhance the rheological properties of asphalt binder or mixture. Geopolymer could be used as a sustainable and greener alternative to other asphalt modifiers due to its low carbon dioxide footprint and effective by-products/waste better recycling capacity. This paper presented a laboratory study to investigate the effects of geopolymer content on the rheological and microstructure properties of asphalt binder. The following conclusions have been drawn:

- Geopolymer additives had a notable impact on the rheological behavior of asphalt binder. It increased the temperature susceptibility by 1.98%, 5.78% and 8.58% through adding 3, 6 and 9% geopolymers respectively. The shear modulus of the modified asphalt binder was increased, and the phase angle was reduced through adding 3, 6 and 9% geopolymers.

- The rutting factor, at 10 rad/sec and at 58 °C, increased by 22%, 58.2%, and 86.6% through adding 3, 6 and 9% of geopolymers by mass of the binder respectively, compared with the virgin binder which indicates that rutting resistance is improved.

- Geopolymer gained its ultimate properties during the first 7 days and the curing time crucially impacts the geopolymerization process. The highest increase of failure temperature was for 7 and 14-days curing time with an improvement of 14.2 and 15.2%, respectively which indicates that the geopolymer could be utilized to increase the high-temperature grading of asphalt binder.

- The nanoparticles appear to be well dispersed in the binder. The use of geopolymer does not seem to affect the microstructure of the binder.

Chapter 5

Rutting Behaviour of Geopolymer and Styrene Butadiene Styrene-Modified Asphalt Binder

This chapter is based on the following article, which was published in Polymers Journal. "Rutting Behaviour of Geopolymer and Styrene Butadiene Styrene-Modified Asphalt Binder," by Hamid, A., Baaj, H., and El-Hakim, M. (2022). **DOI: 10.3390/polym14142780**

Abstract

Modifying asphalt binders is an effective method of improving the performance of asphalt pavement, such as its resistance to rutting. However, because modification changes the behaviour of binders, substantial laboratory testing is required before field application to determine the best mixtures. This research aimed to evaluate the impacts of temperature, stresses, polymer type, and modification rate on the rutting behaviour of the asphalt binder modified with fly ash-based geopolymer (GF), Styrene Butadiene Styrene (SBS), and a combination of SBS and GF. The rheological properties of asphalt binders were investigated using the frequency sweep test at various temperatures. Also, the Multiple Stress Creep Recovery test was conducted at various temperatures and stresses to calculate the non-recoverable creep compliance (J_{nr}) and the percent strain recovery (R). The rutting resistance of asphalt mixture was assessed using the Hamburg wheel rut test. The results revealed that the asphalt binder with 8% of geopolymer (8%GF) exhibited the best response in terms of complex shear modulus (G^*), rutting factor ($G^*/sin\delta$), R, and J_{nr} compared

to the 4%GF and 12%GF at different temperatures. Another interesting finding is that GF's use in the hybrid binder (2%SBS + 8%GF) has led to a significant increase in the shear complex modulus and a decrease in the phase angle compared to the binder modified with 2%SBS. The geopolymer decreases the binder's sensitivity to temperature for both unaged and RTFO asphalt binders. The hybrid binder would also improve strain recovery under high stress and temperatures as well as the ability to withstand severe traffic loads. Furthermore, there is a crucial relationship between temperature and J_{nr}, which could help asphalt pavement designers select suitable modifiers considering the local climate and traffic volume.

5.1 Introduction

Rutting is a widely noticeable mode of distress, impacting the serviceability and quality of the roadway network. Rutting is a permanent deformation that occurs in the direction of traffic due to the accumulation of unrecoverable strain from repeated loads applied to the asphalt pavement [109]. The existing SHRP binder specifications such as PG performance, fatigue parameter, and rutting parameter are determined based on the behavior of the asphalt binder in the linear viscoelastic range. In contrast, the asphalt binder in the mixture has a nonlinear response under high stress and strain conditions [64]. Therefore, these specifications cannot exactly capture or correlate the asphalt binder performance in the mixture.

Polymer modification of asphalt binder has been considered in recent decades as a significant method for improving rutting performance and pavement durability [236, 41, 121]. Asphalt binder modification is a valuable approach for improving the viscoelastic properties of asphalt binders. However, it introduces further complexity to the behavior of asphalt binders. The MSCR test was designed to obtain the nonlinear response of the asphalt binder and link that response to rutting in the asphalt mixture [64]. The Multiple Stress Creep-Recovery (MSCR) test has been widely utilized to predict the influence of polymer-modified asphalt binders on creep recovery [246, 226, 29, 62]. The MSCR test is also efficiently conducted and designed to be a sign of rutting performance in the field of modified and unmodified asphalt binders [111]. The MSCR test essentially uses a sequence of creep and recovery cycles at varying stress levels. The concept was that when shear stress is removed, the viscoelastic strain generated in the creep part can be recovered, allowing the permanent strain to be separated from the total strain, which could be used to predict field rutting [139].

There has been a lot of effort to establish a link between the MSCR test findings and the

rutting performance of asphalt mixtures as assessed by field studies [63, 64] or laboratory studies [64, 225, 132, 183, 42, 203, 173, 62]. It has been reported that the non-recoverable creep compliance (J_{nr}) has a better relationship with the asphalt mixture rutting depth using different asphalt mixture rutting tests, such as the Hamburg Wheel Tracking test (HWTT) [64, 225, 203], and the Wheel Tracking test [132, 183, 173]. Behnood et al. (2016) [42] conducted a laboratory investigation using the flow number test to correlate the flow number at 51 °C with the asphalt binder rutting parameter ($G^*/\sin\delta$) and J_{nr} at 64 °C and different stresses (0.1 kPa and 3.2 kPa). The results showed that there was the best correlation between flow number and J_{nr} at 3.2 kPa. Furthermore, the MSCR parameter (J_{nr}) correlates better with mixture rutting than the ($G^*/\sin\delta$) parameter [64, 111, 120]. Al-Adham et al. (2020) [20] concluded that J_{nr} and R have statistically significant relationships with mixture rutting.

Recently, there has been increasing awareness about decreasing the use of asphalt binders and reducing energy used during the preparation of asphalt concrete. Consequently, the need for new additives with high properties to enhance the asphalt binder properties is constantly growing. Moreover, reused waste materials would reduce the rehabilitation and storage costs of these materials and would provide a financial benefit to the producers. The term "geopolymer" was first formulated by Davidovits (1991) [66], which can be produced using pozzolanic materials, such as fly ash, metakaolin, and slag, with alkaline solutions, sodium hydroxide (NaOH) and sodium silicate (Na_2SiO_3) or potassium hydroxide (KOH) and potassium silicate (K_2SiO_3) [97]. The Geopolymer is an eco-friendly material that is produced using low energy and releases low greenhouse gas emissions during its manufacturing. Geopolymers can be made from materials that comprise reactive or amorphous silica and alumina [171].

Thus, using the geopolymer as a modifier can significantly impact the amount of the asphalt binder used, which will decrease the CO_2 emissions during the asphalt binder production. Hamid et al. (2019) [107] used fly ash and glass powder-based geopolymer as a modifier for asphalt binder with different percentages. The geopolymer modified asphalt binder performed better in terms of fatigue resistance, according to the findings. While Hamid et al. (2020) [106] noted that the fly ash-based geopolymer doesn't have an influence on the microstructure of the asphalt binder. Whereas, Tang et al. [204] used metakaolin, slag, and silica fume as alumino-silicate precursors and sodium hydroxide and sodium silicate as activators to make the geopolymer as a warm mix asphalt (WMA) additive. Using a geopolymer as an additive resulted in a 50% cost savings when compared to zeolite additives.

Moreover, geopolymers are used to improve the properties of recycled pavement materials. Hoy et al. (2016) [113] utilized fly ash (FA) and fly ash-based geopolymer with

Recycled Asphalt Pavement (RAP) and investigated the Unconfined Compressive Strength (UCS) for RAP-FA mix and RAP-FA geopolymer. The results showed that the UCS of RAP-FA geopolymer is greater than the UCS of RAP-FA mix, whereby the UCS of RAP-FA geopolymer is affected by the $NaOH/Na_2SiO_3$ ratio. Decreasing the $NaOH/Na_2SiO_3$ ratio showed a substantial increase in the UCS. Moreover, this investigation confirmed that RAP-FA blends and RAP-FA geopolymers could be utilized as stabilizers for pavement materials. Arulrajah et al. (2016) [25] used calcium carbide residue, fly ash, and slag as an aluminosilicate resource, with sodium silicate and sodium hydroxide as activators to produce the geopolymers. The study aimed to stabilize the Recycled Concrete Aggregates (RCA) and Crushed Brick (CB) using a geopolymer. The results indicated that modified RCA and CB could be used as base and subbase materials, while the resilient modulus of modified CB improved significantly.

There is a global movement toward lowering pollution through reducing by-products and waste materials. Therefore, governments set aside a significant budget to develop ways to incorporate these materials with the raw materials used in many fields. The amount of fly ash has increased worldwide because of increasing human activity, which has resulted in more landfill space being utilized to dispose of these materials. So, utilizing these materials as an aluminosilicate source during the geopolymer production to enhance the asphalt binder's properties and to decrease the use of asphalt binder during the construction of flexible pavement, would have significant economic and environmental benefits. Therefore, this study aimed to investigate the feasibility of using the geopolymer as a modifier to enhance the rutting resistance of asphalt binder by investigating the temperature and modification rate effects on the rheological behaviour of asphalt binder; the influence of geopolymer on the percent creep recovery (R) and non-recoverable creep compliance (J_{nr}) of asphalt binder; the effect of modifiers on traffic loading at different temperatures; and the rutting resistance of asphalt concrete with different additive types.

5.1.1 Chemical Interactions in Geopolymer

The geopolymer is formed when the aluminosilicate source, such as fly ash, reacts with the alkaline solution. This reaction was summarized into the following steps [76]: **(a)** hydroxyl ions (OH^-) in the highly concentrated alkaline solution cause the dissolution of fly ash minerals such as alumina and silica. **(b)** diffusion of the silica and alumina monomers, which interact to form dimers, trimers, tetramers, and so on. **(c)** condensation with sodium cations (Na^+) to form the N-A-S-H gel with time. This gel changes with time [59], whereby the initial gel 1 consists of high alumina ions in the early stages of the reaction because the Al-O bond is weaker than the Si-O bond. Consequently, gel 2 is

Table 5.1: Fly ash chemical composition(test results obtained from materials supplier)

Constituent	SiO_2	Al_2O_3	Fe_2O_3	CaO	MgO	SO_3	Na_2O	MC	LOI
Fly ash	57.2%	23.5%	3.8%	9.3%	1.0%	0.2%	2.43%	0.06%	0.77%

Note: MC is Moisture Content and LOI is Loss on Ignition

formed due to increasing the Si-O with time, which raises the silicon concentration in the N-A-S-H gel. **(d)** The last step is crystallization to hardening, whereby the tetrahedral silica (SiO_4) and alumina (AlO_4) are joined by oxygen (O_2) in the three-dimensional chain networks that are called geopolymers.

5.2 Research Methodology

5.2.1 Materials Preparation

Geopolymer Preparation

The geopolymer is made up of an alkali activator and a fly ash mixture. Alkali activators included Na_2SiO_3 and NaOH at a concentration of 8 molar. Before making the geopolymer, the NaOH solution was made in a fume cabinet by dissolving NaOH in deionized water for at least one day. Table 5.1 presents the chemical composition of fly ash (Class F). The low calcium fly ash (Class F) used in this study contains more silica and alumina than high calcium fly ash (Class C), as recommended by other researchers [110, 92]. It was shown that curing time and type of activator have substantial influences on chemical reactions during the preparation of geopolymer [59]. Also, it is noted that the sodium hydroxide and sodium silicate combination provide a geopolymer with high mechanical performance [166]. The maximum yield stress and storage modulus values are obtained when 8 molar of NaOH is used as an activator during the preparation of the fly ash-based geopolymer [177]. The alumino-silicate precursors in fly ash were activated using a 1:2 mass ratio of Na_2SiO_3 and NaOH solution, with 200 g of fly ash blended with 80 g of the alkaline medium for 5 minutes. The resulting slurry was poured into the silicon molds. The geopolymers were then cured for six days at room temperature (23 - 25 °C) before being cured for 24 hours at 65 °C. Finally, geopolymer samples were grinded into powder and sieved utilizing sieve No. 100 to remove particles larger than 0.15 mm diameter since the MSCR test does not apply to asphalt binder with particles larger than 0.25 mm [9].

Table 5.2: Geopolymer and SBS percentages in the modified asphalt binders

Parameter	**Neat** (%)	**4%GF** (%)	**8%GF** (%)	**12%GF** (%)	**2%SBS** (%)	**Hybrid** (%)
Asphalt	100	96	92	88	98	90
Geopolymer	0	4	8	12	0	8
SBS	0	0	0	0	2	2
Total	100	100	100	100	100	100

Asphalt Binder Preparation

The modified asphalt binders were made utilising two different ways in this investigation. In the first method, the geopolymer-modified asphalt binder was prepared by heating 300 g of asphalt binder (PG 58-28) at 140 °C. The geopolymer was then mixed into the neat asphalt binder in various proportions. To prepare a homogeneous blend, a mechanical shear mixer was employed at a speed of 2000 r/min for 60 minutes while maintaining a temperature of 140 °C ± 5. Hamid et al. (2019) [106] concluded that changing asphalt binder with varying percentages of geopolymer (3, 6, and 9%) has no effect on the microstructure of the asphalt binder.

In the second method, the SBS modified asphalt binder was prepared by heating the asphalt binder (PG 58-28) to 170 °C. The SBS polymer has a linear microstructure with 31.6% styrene content. The SBS was blended with asphalt binder using the high shear mixer and heating mantle at a speed of 2000 r/min and a temperature of 170 °C ± 5 for 60 minutes. At the end of the hour, 10% of the crosslinking agent was added and mixed for 30 minutes. Finally, a curing time of another 60 minutes was conducted by controlling the temperature at 180 °C ± 5 and reducing the high shear mixer speed to 1000 r/min . Following the mixing process, samples for short-term aging in a Rolling Thin Film Oven (RTFO) were prepared According to AASHTO T 240 [2]. Then, all RTFO specimens were subjected to the frequency sweep and MSCR tests using the Dynamic Shear Rheometer (DSR). Table 5.2 shows the asphalt binder modification process. Table 5.3 presents the sieve analysis of the aggregates used to produce HMA mixtures using the neat and modified asphalt binders.

Table 5.3: Aggregate size distribution

Sieve size (mm)	Passing (%)	Control point (maximum)	Control point (minimum)
19	100		
12.5	95	100	90
9.5	83	90	28
4.75	58		
2.36	40	58	28
1.18	19		
0.6	12		
0.3	8		
0.15	4.5		
0.075	3	10	2

5.2.2 Experimental Procedures

Rotational Viscosity

The neat and modified asphalt binders' viscosities were determined at 135 °C and 165 °C according to AASHTO T316 [7]. Each test result was calculated using the average of three readings for each temperature.

Dynamic Shear Rheometer (DSR)

The DSR was applied to evaluate neat and modified binders' rheological behavior, according to AASHTO T 315 [6]. A frequency sweep test was performed to study the influence of loading frequency, temperature, and additives on the asphalt binders' rheological properties. Two samples for each binder were tested, and the average was identified as the test result. Different frequencies ranging from 0.0159 H_z to 15 H_z were applied to different test temperatures (40, 46, 52, 58, 64, and 70 °C).

The MSCR test was performed on asphalt binders using 25 mm diameter samples in accordance with AASHTO T 350 [11] to determine percent recovery (R) and non-recoverable creep compliance (J_{nr}). All asphalt binder samples were tested in creep and recovery at low and high stress levels of 0.1 kPa and 3.2 kPa. The average of two repeated samples was used to calculate the test result for each temperature. The test was carried

out using a creep time of 1 second and a recovery time of 9 seconds. Figure 5.1 summarizes the research methodology.

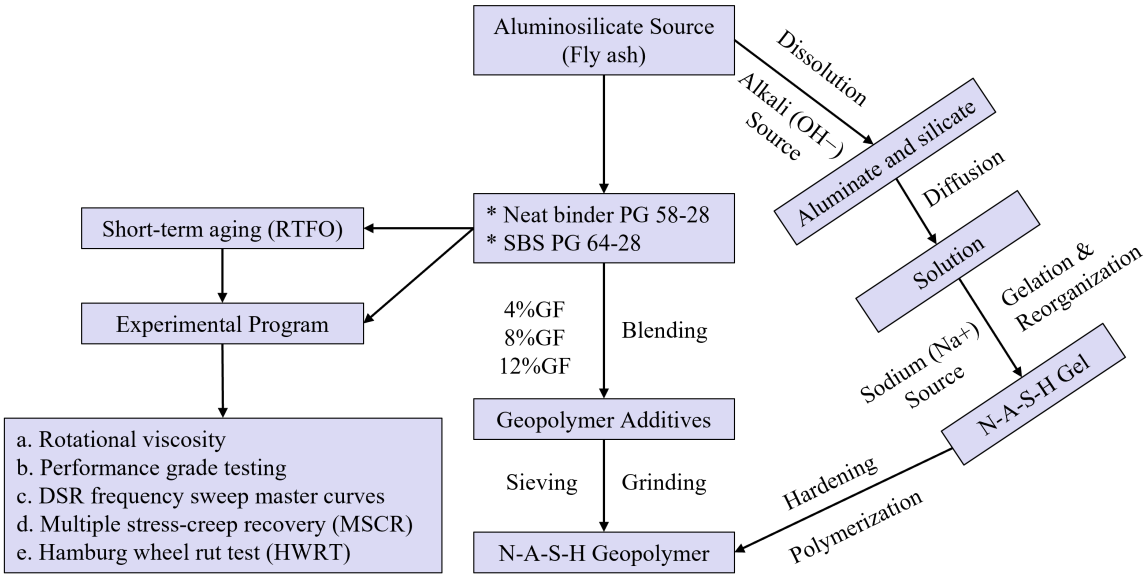

Figure 5.1: Research methodology

Hamburg Wheel Rut Test

Rutting is a common sign of distress that affects the road network's serviceability and quality. Rutting is a permanent deformation that appears in the traffic direction because of unrecoverable strain accumulated by repetitive loads applied to the asphalt pavement [109]. The Hamburg Wheel Rut Test (HWRT) was developed to investigate the resistance of asphalt mixtures to rutting and moisture damage . The test was conducted in accordance with AASHTO T 324 [8]. The Superpave Gyratory Compactor was used to prepare four samples with a 150 mm diameter and a 63 mm height at 7% $\pm$ 0.5 of air void. The asphalt mixture samples were submerged and conditioned for 30 minutes at 44 °C in the water bath. Solid steel wheels were used to test the samples, and Linear Variable Differential Transformers (LVDTs) were applied to determine the average rutting depth.

5.3 Results and Discussion

5.3.1 Effects of Additives on Rheological Properties

Viscosity Results

The viscosity of asphalt mixtures is a significant factor in establishing the temperature range for mixing and compaction. Therefore, the viscosities of neat and modified asphalt binders were measured at 135 °C and 165 °C to investigate the additives' influence on the viscosity change. Figure 5.2 shows that the viscosity of the asphalt binder increases as the modifier percentage increases. Increasing the viscosity is attributed to the larger particles present in the fluid [147], which could be induced by the formation of chain networks in the asphalt-geopolymer mixture. The viscosity of the SBS-modified asphalt binder is significantly greater than that of the asphalt binders modified with a geopolymer (4%, 8%, and 12%). A T-test was performed to examine the statistical significance between the viscosity of neat versus SBS-modified and geopolymer-modified binders. The P_{values} were 1.09×10^{-4} and 1.24×10^{-4}, respectively. The hybrid binder (2%SBS+8%GF) had the highest viscosity compared to neat and other modified asphalt binders.

A two-way Analysis of Variance (ANOVA) was performed to examine the significance of the variation in viscosity resulting from geopolymer and SBS modifications of the binders. The ANOVA test was performed using the data at 135 °C and 165 °C. The ANOVA test results indicated that binder modifications had a considerable strong impact on viscosity ($P_{value} = 1.9\times10^{-151}$), and the temperature had a strong influence on viscosity results as well ($P_{value} = 2.4\times10^{-154}$). Results obtained from the ANOVA test are presented in Table 5.4. A statistical t-test was performed to examine the significance of the variation in viscosity between the hybrid and neat binders at 135 °C and 165 °C. The viscosity of the hybrid binder was 116% ($P_{value} = 9.2\times10^{-24}$) and 97% ($P_{value} = 1.56\times10^{-15}$) higher than the neat at 135 °C and 165 °C respectively. Consequently, the hybrid asphalt binder demonstrated high viscosity compared to the other modified asphalt binders. The results also revealed a minor influence of geopolymer content on the viscosities between 4%GF and 12%GF binders at 135 °C.

Temperature Effect on the Complex Shear Modulus and Phase Angle

A variation of complex shear modulus and phase angle for neat and modified binders among different testing temperatures is shown in Figure 5.3. Throughout the test temperature range, the complex modulus of the geopolymer–modified asphalt binder was increased by

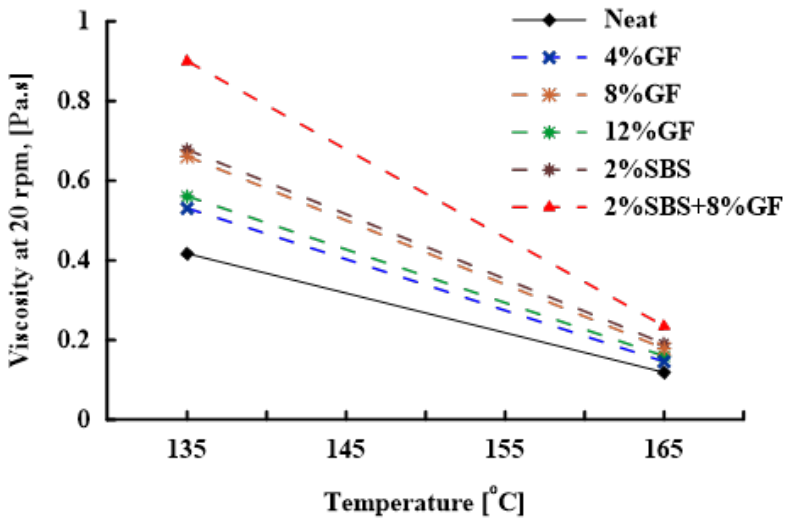

Figure 5.2: Rotational viscosity of neat and modified asphalt binders

Table 5.4: Two-way ANOVA testing of the viscosity of neat and modified asphalt binders

Source of variation	**SS**	**df**	**MS**	**F**	**P-value**	**F-crit**
Binder Modification	7859537	6	1309923	284324.4	1.9E-151	2.23
Temperature	7385222	1	7385222	1602994	2.4E-154	3.98
Interaction	2701719	6	450286.4	97736.59	3.3E-135	2.23
Within	322.5	70	4.607143			
Total	17946801	83				

adding up to 8% more geopolymer. However, beyond 8%GF, the shear complex modulus of the binder drops. The trend is quite similar to the one observed for viscosity. A closer look at the results of the shear complex modulus of geopolymer-modified binders with 4% and 12% revealed that the difference between the two binders is statistically insignificant ($P_{value} = 0.44$). Table 5.5 demonstrates the importance of the difference in shear modulus of several modified binders compared to the neat binder at 10 rad/s (1.59 H_z) using multiple F-tests. The SBS-modified asphalt binder showed a lower shear complex modulus and phase angle than the GF-modified asphalt binders throughout the test temperature range. The SBS is a thermoplastic elastomer material, which is composed of a

short chain of polystyrene, a long chain of polybutadiene, and finally another short chain of polystyrene. As a result, the polybutadiene blocks are crosslinked by the polystyrene clusters. The polystyrene clusters break and produce a short chain when SBS is heated. The modulus then starts to drop. On the other hand, the SBS utilized in this work includes approximately 70% butadiene, which gives the asphalt binder its elastic behaviour, and this explains the drop in phase angle value.

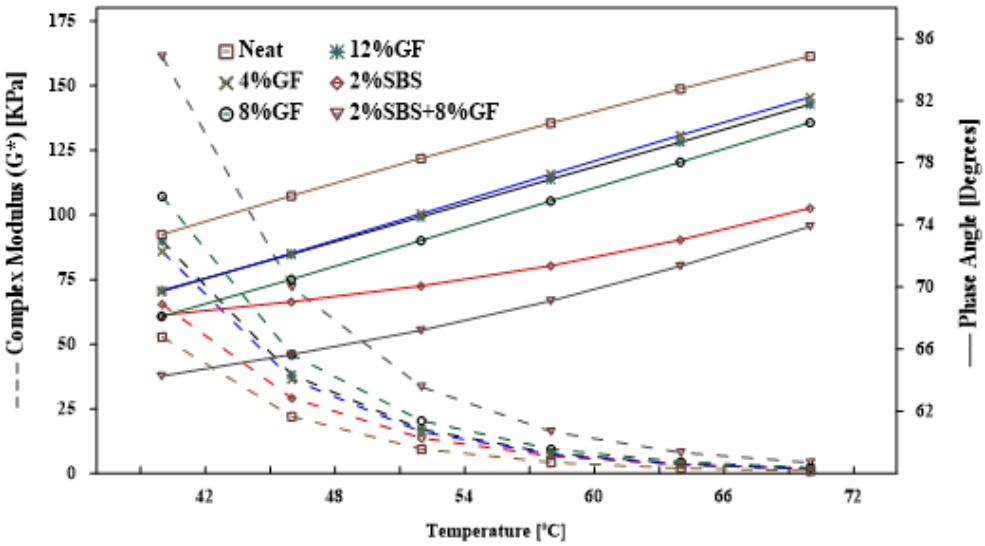

Figure 5.3: Rotational viscosity of neat and modified asphalt binders

In contrast, the hybrid binder exhibited complex shear modulus values almost double (up to 222% increase) those achieved by adding 2% of SBS to the asphalt binder, while it had the least phase angle compared to all the other binder modifications. The reduction in phase angle is 14% compared to the neat binder. The beneficial interaction between GF and SBS, as well as the effectiveness of the geopolymer modification rate, could explain this. This reduction in the phase angle indicates the change in the viscoelastic behaviour and a shift toward elastic behaviour. However, the results of phase angles cannot be used to figure out which asphalt binder type is more elastic. Therefore, the storage and loss modulus of the complex shear modulus should be separated.

Figures 5.4 and 5.5 show the logarithms of G' and G'' versus temperatures for unaged and RTFO binders, respectively. The equations for linear regression were created and are depicted in the figures. Table 5.6 displays the absolute values of the linear regression equations' slopes.The slopes depict the asphalt binders' temperature sensitivity; the steeper

Table 5.5: F-test comparing shear modulus of modified binders to the neat binder

Binder	**P-value**	**Significance**	**Percent increase in G***
4%GF	0.06	Insignificant	65%
8%GF	0.01	Significant	107%
12%GF	0.05	Insignificant	73%
2%SBS	0.26	Insignificant	31%
Hybrid	4.8×10^{-4}	Strongly significant	222%

the slope, the more sensitive the asphalt binder is to temperature changes.

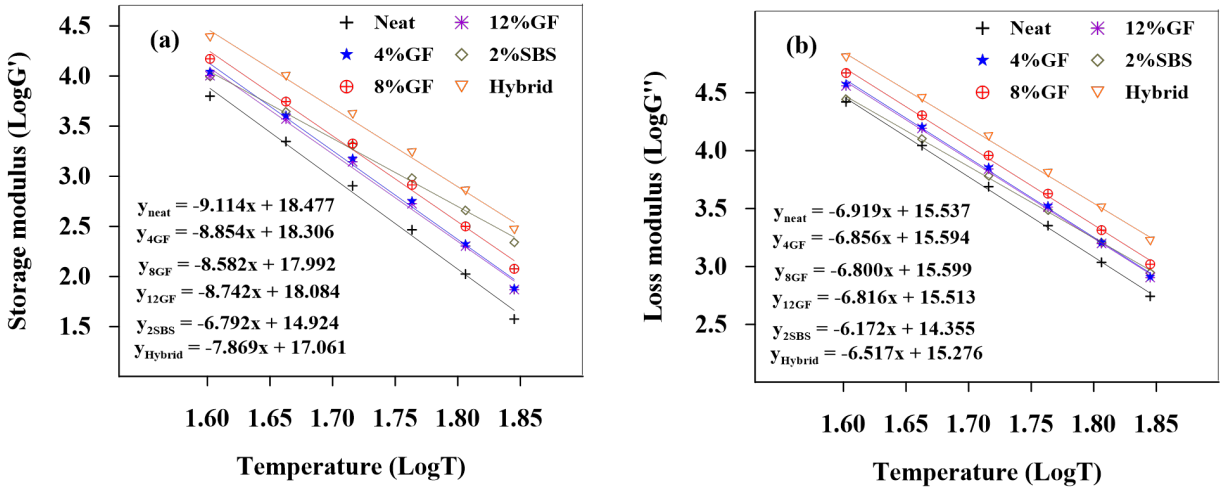

Figure 5.4: Geopolymer effect on the regression slope of (a) storage and (b) loss modulus

The results showed that the modifiers have a significant impact on the binder's sensitivity to temperature. The temperature sensitivity of G' and G'' for both unaged and RTFO modified asphalt binders decreases. The results indicted that the modifiers have a significant impact on the binder's sensitivity to temperature, whereby the temperature sensitivity of G' and G'' for both unaged and RTFO modified asphalt binders decreases.

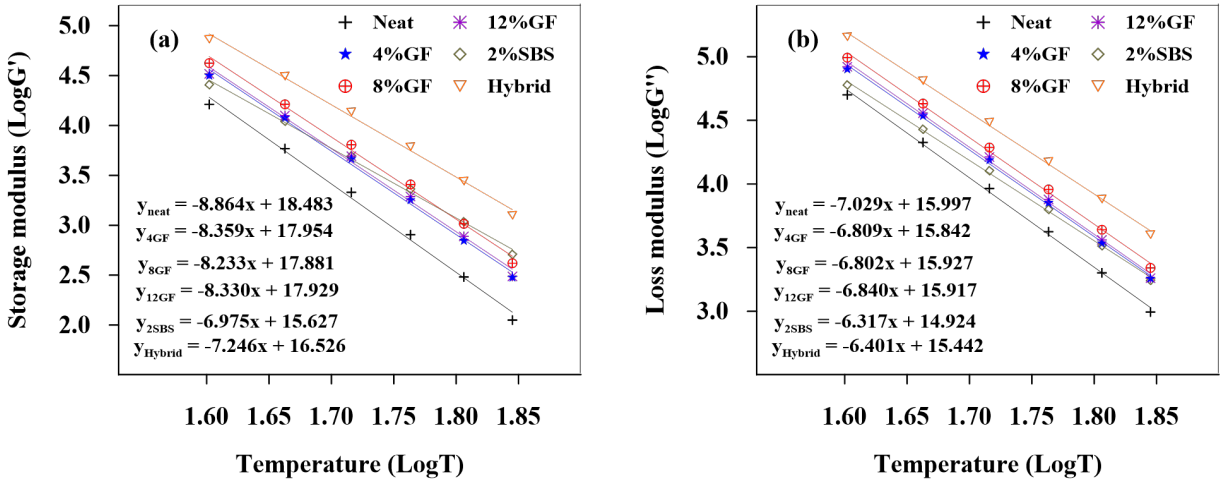

Figure 5.5: Temperature sensitivity on the (a) storage and (b) loss modulus of RTFO binders

Table 5.6: Geopolymer effect on the regression slope of storage and loss modulus

Binder	Slope $\|G'\|$	Slope $\|G'\|$RTFO	Slope $\|G''\|$	Slope $\|G''\|$ RTFO
Neat	9.114	8.864	6.919	7.029
4%GF	8.854	8.359	6.856	6.809
8%GF	8.582	8.233	6.800	6.802
12%GF	8.742	8.330	6.816	6.840
2%SBS	6.792	6.975	6.172	6.317
Hybrid	7.869	7.246	6.517	6.401

Temperature Effect on the Rutting Factor

The impact of the temperature on the rutting factor ($G^*/\sin\delta$) of neat and modified asphalt binders is presented in Figure 5.6 and Table 5.7. To achieve rutting standards, the rutting factor for unaged binder must be at least 1 kPa and 2.2 kPa for aged binder at 10 rad/s, according to the Superpave specifications [109]. The data was analyzed using the ANOVA statistical test to examine the effects of temperature and binder modification on the $G^*/\sin\delta$. Table 5.8 presents the ANOVA test results of temperature and binder

modification. The results indicate a statistically considerable impact on $G^*/\sin\delta$ with P_{values} of 4.33×10^{-60} and 9.88×10^{-44}, respectively.

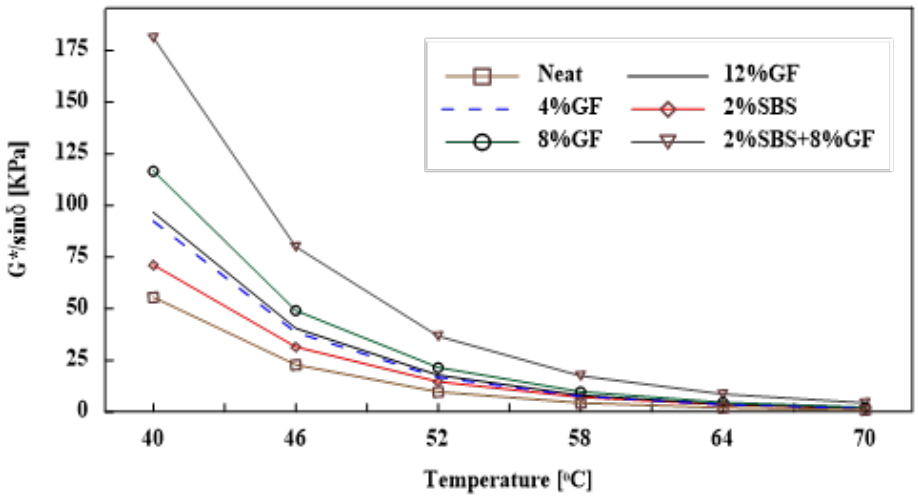

Figure 5.6: Temperature effect on rutting factor of neat and modified asphalt binders at 10 rad/s

The results showed that increasing the polymer additives increased the rutting factor, indicating an increase in rutting resistance. These results were also noted in previous research [128, 21, 62]. Multiple t-tests were conducted to specify the significance of asphalt binder modification on $G^*/\sin\delta$. For example, the rutting factor of 8%GF modified asphalt binder at 58 °C was 124% higher than the neat asphalt binder. However, the difference was statistically insignificant with a P-value = 0.19. While the rutting factor of 2%SBS increased only 64% more than the neat asphalt binder, the difference is statistically insignificant (P-value = 0.54).

The combination of SBS and geopolymer (2%SBS+8%GF)-modified asphalt binder produced an increase in the rutting factor that reached up to 300% more than the neat binder at 58 °C with a P_{value} = 0.059, as summarized in Table 5.7. Consequently, the hybrid asphalt binder remains superior in rutting resistance potential compared to other modified asphalt binders. This could be attributed to the geopolymer modification rate besides the positive interaction between SBS and geopolymer.

Table 5.7: Temperature effect on the rutting factor of asphalt binders at 10 rad/s

Binder	$\|G^*\|/\sin\delta$			Modified/Neat		
	52 °C	58 °C	64 °C	52 °C	58 °C	64 °C
Neat	9.73	4.38	2.05	1.00	1.00	1.00
4%GF	16.82	7.58	3.56	1.73	1.73	1.74
8%GF	21.52	9.81	4.63	2.21	2.24	2.26
12%GF	17.81	8.08	3.81	1.83	1.85	1.86
2%SBS	14.68	7.17	3.64	1.51	1.64	1.78
Hybrid	36.71	17.51	8.63	3.77	4.00	4.21

Table 5.8: Two-way ANOVA testing of the rutting parameters versus temperature

Source of variation	**SS**	**df**	**MS**	**F**	**P-value**	**F-crit**
Binder Modification	10897.36752	5	2179.474	2213.829	9.88E-44	2.477169
Temperature	88602.25547	5	17720.45	17999.78	4.33E-60	2.477169
Interaction	13562.98784	25	542.5195	551.0713	1.65E-39	1.814864
Within	35.44133564	36	0.984482			
Total	113098.0522	71				

Frequencies Effect on the Rutting Factor

The master curve of rutting factor was generated for the neat and various modified asphalt binders at 52 °C reference temperature, as shown in Figure 5.7. The frequency sweep test was carried out at high temperatures (46 °C, 52 °C, 58 °C, 64 °C, and 70 °C) with varied frequencies ranging from 0.0159 H_z to 15 H_z. At high temperatures, higher $|G^*|/\sin\delta$ values are preferred to reduce the energy dissipation due to repeated loading. The less energy is dissipated per cycle, the higher the rutting-resistance of the asphalt mixture [62]. The modified asphalt binders achieved the highest rutting resistance compared to the neat asphalt binder. It should be noted that the hybrid asphalt binder had the strongest potential for rutting resistance over a wide range of loading frequencies, whereby the combination of

SBS and geopolymer increasing the asphalt binder's stiffness. Meanwhile, the 8%GF had a slightly similar impact on the rutting resistance at low frequencies while having a higher rutting parameter than their 2%SBS part at high frequencies.

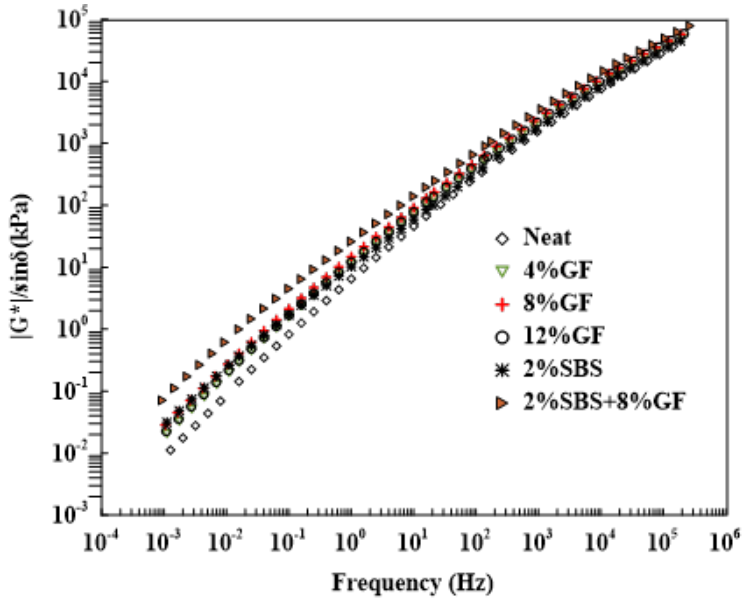

Figure 5.7: Master curve for rutting factor

The impact of various frequencies on the $|G^*|/\sin\delta$ of neat and modified asphalt binders at 52 °C is summarized in Table 5.9. At low modified frequency (10^{-2} H_z), the rutting factor of 4%GF, 8%GF, and 12%GF binders increased by 184%, 286%, and 214%, respectively, compared to the neat binder. While the 2%SBS binder showed a rutting factor almost the same as achieved by adding 8% of GF to the asphalt binder, whereas the combination of 2%SBS and 8%GF attained an increase of 786% compared to the rutting factor of the neat binder. The ANOVA was applied to test the significance of binder modification and loading frequency on the $|G^*|/\sin\delta$.

Table 5.10 presents the results of the ANOVA test. Loading frequency has a statistically significant impact on $|G^*|/\sin\delta$, with a P_{value} of 5.61×10^{-22}. The effect of binder modification on $|G^*|/\sin\delta$ is also statistically significant, but with a P_{value} of 5.45×10^{-15}. At a high modified frequency (10 H_z), the rutting factor of 2%SBS increased up to 30%, which showed the lowest rutting factor. While the hybrid asphalt binder also indicated the highest rutting factor with 207% more than the neat binder, as reported in Table 5.9. This confirms that the SBS and geopolymer combination has a considerable rutting performance improvement over the other modifiers.

Table 5.9: Frequencies effects on the rutting factor of neat and modified asphalt binders

Binder	$\|\mathbf{G}^*\|/\mathbf{sin}\delta$ $10^{-2}\mathrm{H}_z$	$\|\mathbf{G}^*\|/\mathbf{sin}\delta$ $10\mathrm{H}_z$	Modified/Neat $10^{-2}\mathrm{H}_z$	Modified/Neat $10\mathrm{H}_z$
Neat	0.07	45.71	1.00	1.00
4%GF	0.20	73.99	2.84	1.62
8%GF	0.27	91.67	3.86	2.01
12%GF	0.22	78.14	3.14	1.71
2%SBS	0.27	59.62	3.86	1.3
Hybrid	0.62	140.12	8.86	3.07

Table 5.10: Two-way ANOVA testing of the rutting parameters versus frequency

Source of variation	**SS**	**df**	**MS**	**F**	**P-value**	**F-crit**
Binder Modification	5423.876	5	1084.775	892.184	5.45E-15	3.106
Frequency	39625.466	1	39625.466	32590.36	5.61E-22	4.747
Interaction	5309.938	5	1061.988	873.442	6.19E-15	3.106
Within	14.590	12	1.216			
Total	50373.871	23				

5.3.2 MSCR Test Results Analysis

Effects of Additives on the Creep Recovery Behaviour

The MSCR test was carried out under two stress levels (0.1 kPa and 3.2 kPa) and a wide range of temperatures from 46 °C to 70 °C with an increment of 3 °C. The figures included in this paper present the average results obtained from three temperatures (52 °C, 58 °C, and 64 °C) due to page-space limitation. However, the statistical analysis of the data was performed on the data obtained from all testing temperatures. The influence of temperature, stresses, and polymer types on the recovery and non-recovery of asphalt binders was investigated. Percent-strain creep recovery, for neat and modified asphalt binders, at various temperatures (52 °C, 58 °C, and 64 °C) for low (0.1 kPa) and high (3.2

kPa) stress levels are shown in Figure 5.8 (a, b), respectively. The efficiency of geopolymer and SBS modification rates are reflected at all stress levels during all test temperatures. Also, the 8%GF binder showed the highest creep recovery compared to 4%GF (P_{value} = 2.5×10^{-3} and $P_{value} = 3.34\times10^{-6}$ for 0.1 kPa and 3.2 kPa, respectively) and 12%GF (P_{value} = 1.46×10^{-3} and $P_{value} = 4.38\times10^{-6}$ for 0.1 kPa and 3.2 kPa, respectively).

The recoverable strain increased by 23% and 32% by increasing the geopolymer percentage from 4% to 8% at 0.1 kPa and 3.2 kPa, respectively. The recoverable strain decreased by 15% and 20% by increasing the geopolymer percentage from 8% to 12% at 0.1 kPa and 3.2 kPa, respectively. However, the creep recovery of the 2% SBS binder was higher than that of the 8%GF binder at all temperatures and stress levels ($P_{value} = 9.77\times10^{-18}$) and 6.73×10^{-10} for 0.1 kPa and 3.2 kPa, respectively). Comparing 2%SBS and hybrid binders, it can be noted that 2%SBS binder showed a slight insignificant increase of 5% in creep recovery at 0.1 kPa of stress ($P_{value} = 0.64$) as shown in Figure 5.8 (a). While the hybrid asphalt binder performed at 6% insignificant higher creep recovery at 3.2 kPa (P_{value} = 0.77) as shown in Figure 5.8 (b). This is attributed to the various interaction mechanisms within the asphalt binder matrix for each modifier, which needs closer analyses of every modifier's physical and chemical interactions within the asphalt binder and their potential influences on the microstructure of the asphalt binder.

Figure 5.9 (a, b) presents the non-recoverable creep compliance of the neat and modified asphalt binders at 0.1 kPa and 3.2 kPa stresses, respectively. Generally, non-recoverable creep compliance with a low value is needed for acceptable rutting resistance. Simultaneously, asphalt binder with 0.5 kPa^{-1} or less of J_{nr} at 3.2 kPa is suitable for extremely heavy traffic ($\geq$ 30 million ESALs), according to the AASHTO standard [9]. The results revealed that the hybrid binder significantly outperformed all modifiers in terms of non-recoverable creep compliance at 0.1 kPa and 3.2 kPa.

Comparing the hybrid binder to the binder with the closest non-recoverable creep compliance strain, which is 2%SBS, the hybrid binder performed at 54% and 59% lower non-recoverable creep strain with P_{values} of 6.5×10^{-4} and 8.7×10^{-4} at 0.1 and 3.2 kPa, respectively. Besides, it can be observed that the 2%SBS binder showed a 17% reduction in non-recoverable strain values compared to the 8%GF at the 0.1 kPa stress level (P_{value} = 6.4×10^{-4}) and an insignificant difference of 2% in the non-recoverable strain at the 3.2 kPa stress level (P_{value} = 0.05). These observations are essential, considering that the 2%SBS binder showed close strain recovery as the hybrid binder at 3.2 kPa, for various temperatures, as shown in Figure 5.8. This reconfirms that the hybrid modification with GF and SBS has led to a superior strain recovery compared to the GF or SBS alone.

Figure 5.10 presents the difference in non-recoverable creep compliance strain (J_{nr}),

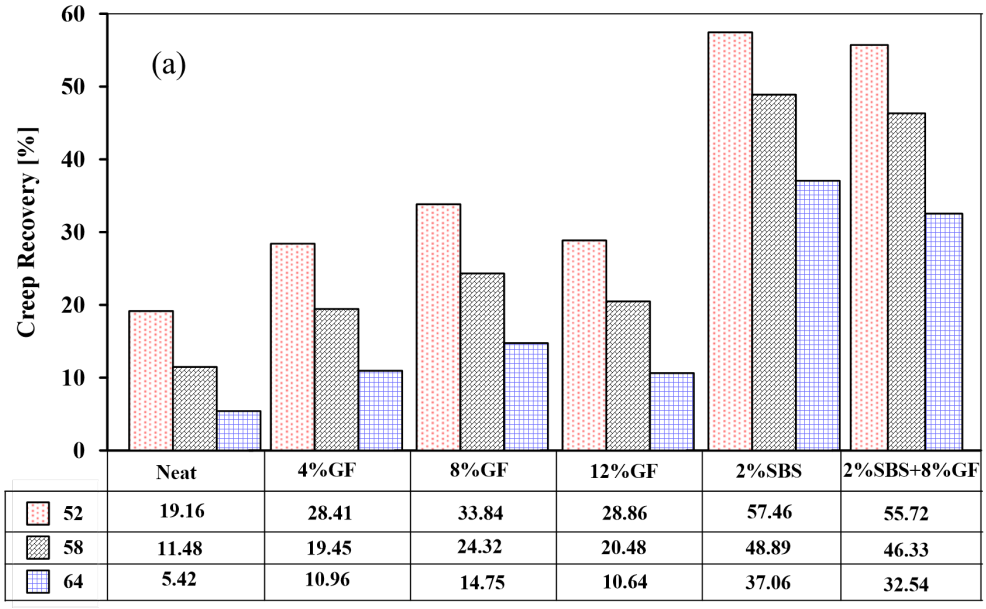

	Neat	4%GF	8%GF	12%GF	2%SBS	2%SBS+8%GF
52	19.16	28.41	33.84	28.86	57.46	55.72
58	11.48	19.45	24.32	20.48	48.89	46.33
64	5.42	10.96	14.75	10.64	37.06	32.54

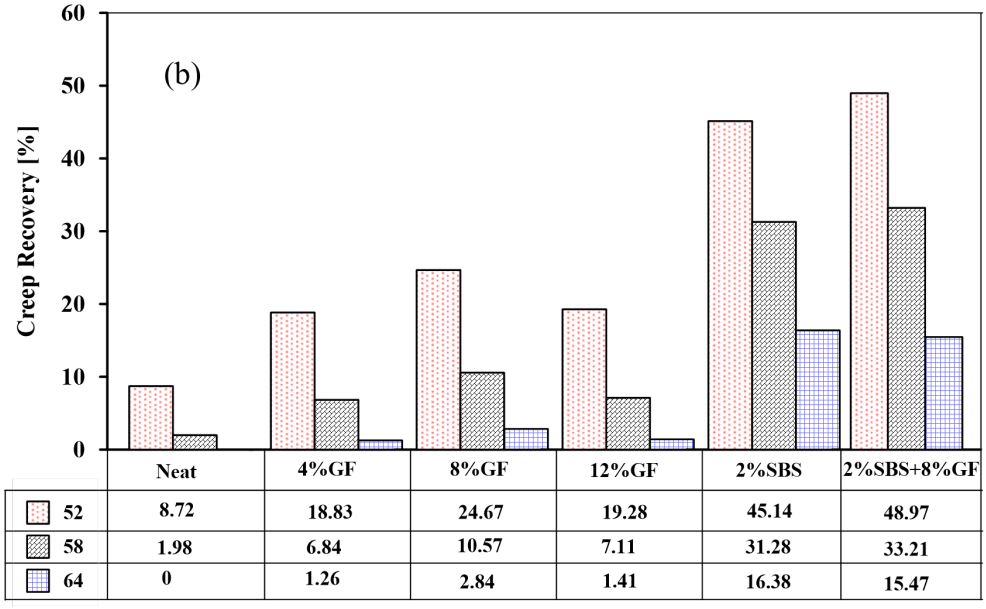

	Neat	4%GF	8%GF	12%GF	2%SBS	2%SBS+8%GF
52	8.72	18.83	24.67	19.28	45.14	48.97
58	1.98	6.84	10.57	7.11	31.28	33.21
64	0	1.26	2.84	1.41	16.38	15.47

Figure 5.8: Creep recovery of neat and modified asphalt binders at (a) 0.1 kPa and (b) 3.2 kPa

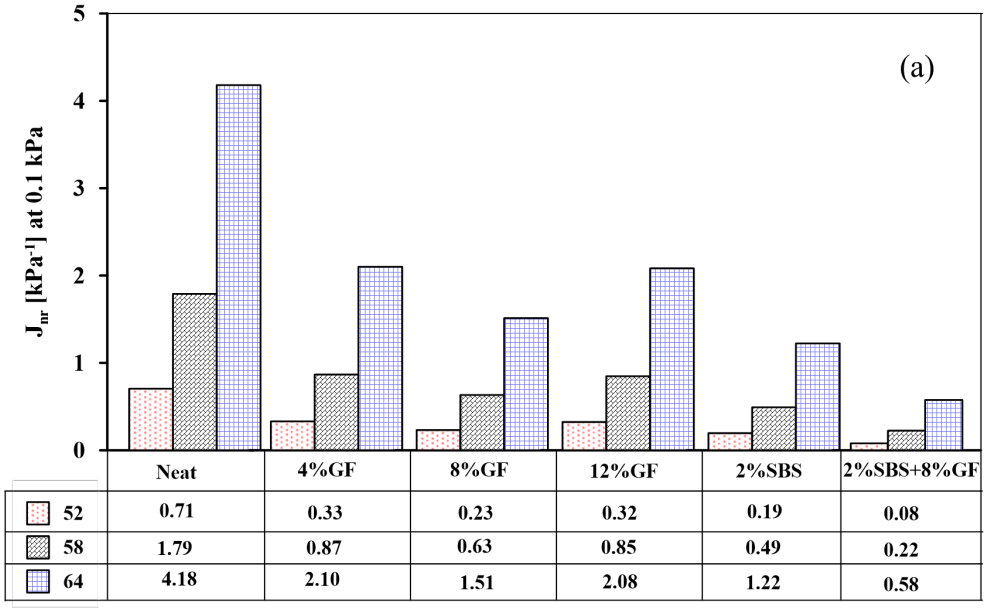

	Neat	4%GF	8%GF	12%GF	2%SBS	2%SBS+8%GF
52	0.71	0.33	0.23	0.32	0.19	0.08
58	1.79	0.87	0.63	0.85	0.49	0.22
64	4.18	2.10	1.51	2.08	1.22	0.58

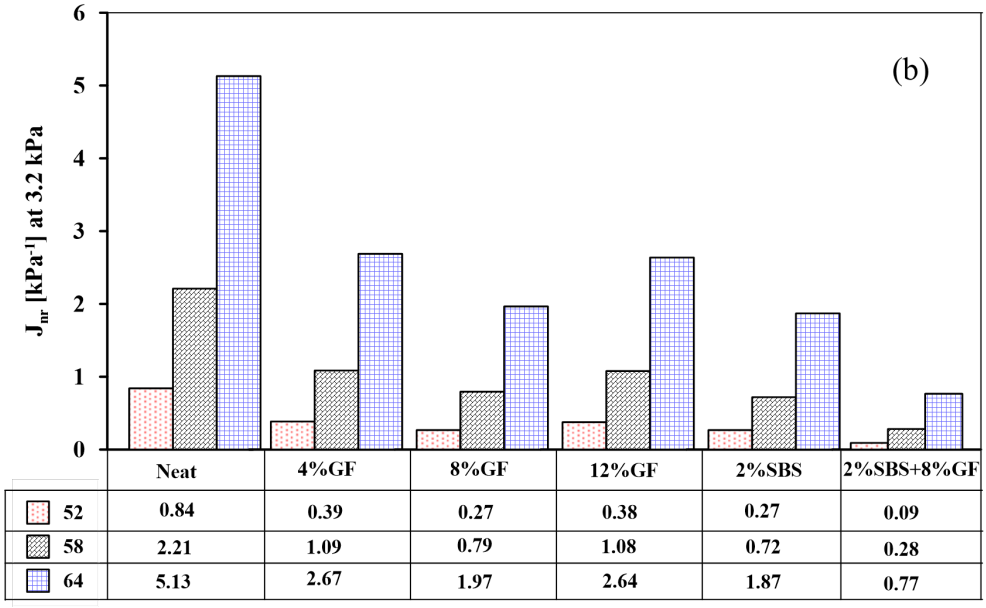

	Neat	4%GF	8%GF	12%GF	2%SBS	2%SBS+8%GF
52	0.84	0.39	0.27	0.38	0.27	0.09
58	2.21	1.09	0.79	1.08	0.72	0.28
64	5.13	2.67	1.97	2.64	1.87	0.77

Figure 5.9: Non-recoverable creep compliance of neat and modified asphalt binders at (a) 0.1 kPa and (b) 3.2 kPa

which was calculated as a percent increase in J_{nr} between 0.1 and 3.2 kPa stress levels. This (J_{nrdiff}) factor is an indicator of the stress sensitivity of modified asphalt binders. All modified asphalt binders showed J_{nrdiff} below the maximum limit (75%) that was recommended by the AASHTO standard [9]. However, it appears that the SBS-modified binder has a high sensitivity to stress levels compared with the hybrid and GF-modified binders at different temperatures.

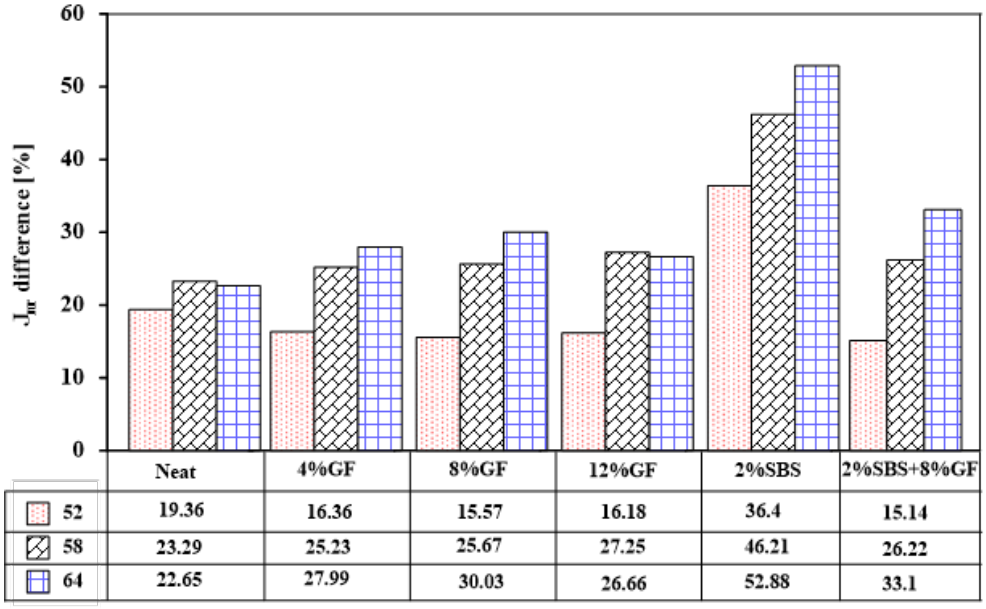

	Neat	4%GF	8%GF	12%GF	2%SBS	2%SBS+8%GF
52	19.36	16.36	15.57	16.18	36.4	15.14
58	23.29	25.23	25.67	27.25	46.21	26.22
64	22.65	27.99	30.03	26.66	52.88	33.1

Figure 5.10: Non-recoverable creep compliance difference of neat and modified asphalt binders

Influence of Temperature and Polymer Types on the Traffic Level

MSCR test results are influenced by temperature and polymer types and amounts. Figure 5.11 illustrates the impact of temperature and polymer types on the traffic level. AASHTO specification [9] classified the traffic loading into four classes (S is standard traffic ($\leq$ 10 million ESALs), H is heavy traffic (10-30 million ESALs), V is very heavy traffic ($\geq$ 30 million ESALs), and E is extremely heavy traffic ($\geq$ 30 million ESALs) with standing traffic), depending on the J_{nr} values at high stress (3.2 kPa).

The neat and modified binders were tested using the MSCR test at different temperatures and high stress (3.2 kPa). The research team prepared two samples for each

temperature (108 samples total) and the average value was used to determine the test result. Temperatures in the test varied from 46 °C to 70 °C, with a 3 °C increment. The influence of geopolymer and SBS on the asphalt binder grading, failing temperature, and traffic level is summarized in Table 5.11. The results obtained show that the geopolymer has a significant impact on the asphalt binder grading, which is consistent with the findings from [107, 106] .

The 8%GF binder had a high PG grading, failing temperature, and traffic level compared to the neat and modified binder with 4%GF, 12%GF. While it showed higher PG grading and failing temperatures than the 2%SBS binder did, and a similar traffic level. Modifying asphalt binder using the combination of SBS and geopolymer achieved the highest results compared to the other modifiers, which confirmed the earlier observations in $G^*/\sin\delta$, J_{nr}, and R. Table 5.11 offers a guidance to asphalt pavement designers to select suitable modifiers considering the local temperature and traffic volume.

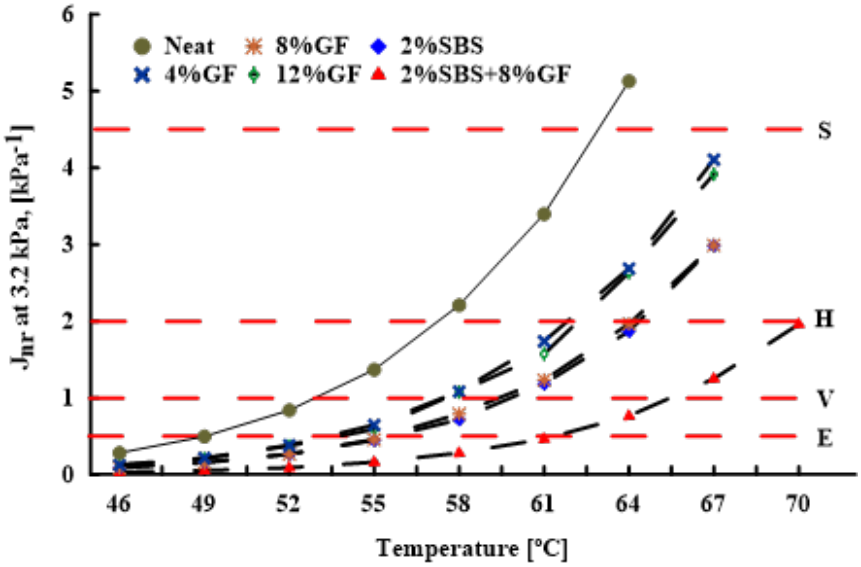

Figure 5.11: Temperature and additives effects on the traffic level

5.3.3 HWRT Results Analysis

Figure 5.12 shows the average rutting depth at different load passes for neat and modified asphalt binders. The findings of the HWRT tests describe the impact of rutting and moisture damage, whereby moisture damage begins after the creep-to-stripping inflection

Table 5.11: Grading and traffic level results of geopolymer, SBS, and hybrid asphalt binders

Binder	**PG**	**Temp. range for S (°C)**	**Temp. range for H (°C)**	**Temp. range for V (°C)**	**Temp. range for E (°C)**
Neat	58	$\geq$ 57.0	57.0-53.0	53.0-49.0	$\leq$ 49.0
4%GF	64	$\geq$ 62.0	62.0-57.0	57.0-53.0	$\leq$ 53.0
8%GF	70	$\geq$ 64.0	64.0-59.0	59.0-55.0	$\leq$ 55.0
12%GF	64	$\geq$ 62.5	62.5-57.0	57.0-53.0	$\leq$ 53.0
2%SBS	64	$\geq$ 64.5	64.5-59.5	59.5-55.0	$\leq$ 55.0
Hybrid	76	$\geq$ 70.0	66.0-70.0	61.0-66.0	$\leq$ 61.0

point. The results showed that there is no negative effect of additives on the moisture damage resistance. This finding indicated that geopolymer modified asphalt binder has a significant resistance to moisture damage as also concluded by Rosyidi, et al. [181]. As a result, the HMA with various additives had high moisture resistance. The hybrid binder achieved the highest resistance to rutting. While the 2%SBS binder achieved rut resistance larger than 8% GF. Compared with the neat binder, the permanent deformation decreases by 82%, 74%, and 55% by adding 2%SBS+8%GF, 2%SBS, and 8%GF, respectively. Therefore, the ability to resist permanent deformation is ranked as: 2%SBS+8% GF > 2%SBS > 8% GF > neat, which confirmed the earlier observation trends for MSCR test results in Figures 5.9, 5.10, and 5.11. These observations indicate that there is a good relationship between MSCR test results and asphalt mixture rutting as concluded by different studies [132, 237, 178].

5.4 Conclusions

Using geopolymers as a modifier for asphalt binder proved to be an efficient solution to enhance rutting performance. Moreover, the paper's findings offer guidance to asphalt pavement designers on selecting suitable modifiers considering the local temperature, stresses, and traffic volume. The following conclusions have been drawn:

- The shear complex modulus increases from 22 kPa to 72 kPa, and the phase angle decreases from 74.5° to 65° by adding 2%SBS+8%GF at 46 °C, showing that the viscoelastic behaviour becomes more elastic.
- $G^*/\sin\delta$ value of the hybrid binder was the highest among all the tested binders. This value reached 300% one of that of the neat binder. The combination of SBS

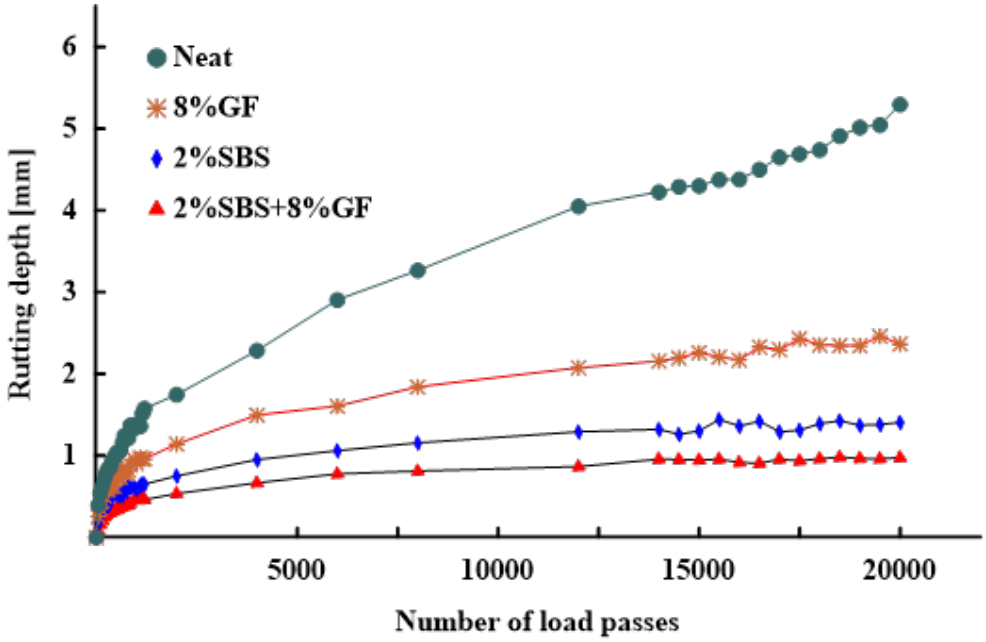

Figure 5.12: Additives effects on the rut depth of asphalt mixture

and geopolymer appears to have the highest rutting resistance.

- Geopolymer has a significant impact on the binder's sensitivity to temperature, whereby the temperature sensitivity of G' and G'' for both unaged and RTFO modified asphalt binders decreases.
- The 2%SBS binder exhibited the highest creep recovery at low-stress levels, while the hybrid binder exhibited the highest creep recovery at high-stress levels, during the test temperatures.
- It was noted that the stress levels, temperature, and polymer type had an important effect on the accumulated strain, whereby the modified asphalt binders maintained the lowest creep strains. The hybrid binder showed the lowest accumulated strain compared with other modified binders. This was another indicator that the hybrid binder had improved rutting resistance.
- Adding 8%GF to the neat binder enhances the rutting resistance of the asphalt mixture, which reduces the rut depth by 55%. While the combination of the SBS and GF (2%SBS+8%GF) reduced the rut depth to 82%.

- The MSCR test results could be used to develop preliminary indication of the permanent deformation of asphalt mixture as the results were aligned with the HWRT results.

In this study, the idea of using fly ash as an aluminosilicate source during the preparation of geopolymer and then utilizing it as a modifier for asphalt binder provides a practical explanation for improving asphalt pavement rut resistance, eliminating the threat of environmental landfilling of fly ash, and reducing CO_2 emissions and fuel consumption due to asphalt binder extraction and transportation. Since a few investigations have studied the rheological and mechanical performance of geopolymer-modified asphalt binder and mixtures, there remains a lack of evidence on the laboratory evaluation of geopolymer-modified asphalt binders and mixtures. Meanwhile, the effect of fly ash-based geopolymer content on the fatigue and low temperature crack resistance of asphalt binder and mixture has not been investigated yet. Also, the influence of aging and climate change conditions on the geopolymer modified asphalt binder and mixture should be evaluated. Therefore, it is recommended to investigate the fatigue and low temperature performances of geopolymer modified asphalt binder and mixtures using static and dynamic tests.

Globally, SBS was widely employed in many nations, and it had a considerable impact on the rheological and performance of asphalt binder. As a result, comparing the promised effects of employing the geopolymer as a modifier with the results of another modifier, such as SBS, could motivate the use of the geopolymer during pavement construction. Another interesting finding is that the combination of geopolymer and SBS has led to a promising change in the viscoelastic behaviour of the asphalt binder, increasing the storage modulus (elastic behaviour) and loss modulus (viscous behaviour). These changes indicate the need for using different combinations with different percentages of geopolymer and SBS and investigating the effects of various factors such as temperature, curing time, and mixing procedure on the behaviour of asphalt binder; and then the effect of these factors on the polymer structure should be discussed. Therefore, additional physical, chemical, and microstructural investigations are recommended.

Chapter 6

Temperature and Aging Effects on the Rheological Properties and Performance of Geopolymer-Modified Asphalt Binder and Mixture

This chapter is based on the following article, which will be submitted to the Road Material and Pavement Design Journal. "Temperature and Aging Effects on the Rheological Properties and Performance of Geopolymer-Modified Asphalt Binder and Mixture," by A. Hamid, H. Baaj, and M. El-Hakim (2022).

Abstract

Using geopolymer as a modifier for asphalt binder and mixture has received little attention in recent decades because there has been no investigation to link the effect of temperature and traffic loading on the rheological and performance of geopolymer modified asphalt binder. The primary objective of this study was to evaluate the effect of fly ash-based geopolymer (GF), Styrene-Butadiene-Styrene (SBS), and the combination of GF with SBS on the rheological properties and performance of asphalt binder at low and intermediate temperatures. The rheological properties and performance of neat and modified asphalt binders, 4%GF, 8%GF,12%GF, 2%SBS, and 2%SBS+8%GF, were investigated using Dynamic Shear Rheometer (DSR) and Bending Beam Rheometer (BBR) devices. Moreover, the Viscoelastic Continuum Damage (VECD) model with the Linear Amplitude Sweep

(LAS) was utilized to evaluate the fatigue behavior of asphalt binders. Dynamic/complex modulus and moisture damage evaluation tests were conducted to evaluate the effect of additives on the performance of asphalt mixes. The findings demonstrated that for both unaged and RTFO asphalt binders, additives reduce the temperature sensitivity of both G' and G''. When the binders are exposed to long-term aging using Pressure Aging Vessel (PAV), it was noticed that the 8%GF binder became more susceptible to temperature changes. The 2%SBS binder has the lowest creep stiffness compared with the neat and other modifiers. While the combination of GF and SBS (2%SBS+8%GF) exhibited the highest resistance to fatigue distress at different temperatures compared to other asphalt binders. The modified asphalt mixes, 8%GF, 2%SBS, and (2%SBS+8%GF) achieved the highest tensile strength compared to the neat binder, and the tensile strength ratio was more than 80%. The tensile strength has increased from 580.4 kPa to 740.4 kPa, 884.8 kPa, and 917.4 kPa by utilizing 8%GF, 2%SBS, and (2%SBS+8%GF) binders, respectively. Furthermore, the modified asphalt mixture exhibited more ability to resist cracking, which attained the highest fracture energy at dry and freezing-thawing conditions.

6.1 Introduction

The performance of asphalt mixtures depends on the rheological properties of the asphalt binder, volumetric properties of the asphalt mixture, and external influences such as traffic volume and weather. While subjected to extreme weather conditions, asphalt binders have the properties of both viscous liquids and elastic solids. Asphalt binder is a great adhesive material for use in paving, but it is a difficult material to analyze and describe due to its wide range of behavior. The behavior of the asphalt binder is characterized with viscoelastic properties; depending on the temperature and rate of loading, it has both elastic and viscous properties. Asphalt binder is subjected to a wide range of loading spectrum and temperatures; it's behavior leans towards soft-viscous material in hot weather and brittle behavior in cold conditions. One of the main causes of pavement distress is the overload traffic spectrum, which causes significant stresses inside the pavement layer. These distresses decrease the pavement's serviceability and increase the maintenance cost. There are a variety of ways of reducing pavement distress, including new mix design or the use of modifiers [129].

Cracking is one of the crucial problems in asphalt concrete pavement which occurs due to heavy traffic, harsh environmental conditions, and construction deficiencies. It leads to pavement failure in its later stages. Cracking appears at the top of the pavement layer in different shapes such as longitudinal, alligator, transverse, and reflective cracks.

Fatigue cracking is considered the main mode of pavement failure, which occurs when the pavement has been stressed for a long time by repeated load applications [109]. The fatigue life measures the resistance of the asphalt to fatigue cracking and is defined as the number cycles to which the material can be subjected before failing. Tensile stresses occur as repeated traffic loading acts on the pavement surface after the pavement has been in service [109]. There are two types of fatigue cracking, alligator or bottom-up cracking and longitudinal or top-down cracking. Alligator cracking occurs when cracks initiate at the bottom of the asphalt layer and then propagate to the surface of the pavement under repeated load applications. Whereas longitudinal cracking occurs when cracks initiate at the pavement surface and propagate downwards under repeated load applications. Fatigue cracks in asphalt pavement are influenced by different external factors such as compaction level and method, time of asphalt placement, and poor subgrade drainage [109]. Also, temperature, air voids, and amount and type of asphalt binder are affected the fatigue life [179].

Thermal cracking is one of the most common problems with asphalt pavement during the winter months. The main cause of thermal cracking is the contraction of the asphalt layer due to cold weather, which causes tensile stress to build up. Thermal cracking occurs when the tensile stress equals or exceeds the tensile strength of the asphalt layer. These cracks can expand to 20 mm (0.01in) in width over time, affecting the ride quality of the pavement or, in advanced stages, causing secondary cracking and structural concern [23].

The major motivations for modifying asphalt binder with various types of additives are to achieve softer mixtures at low temperatures and prevent cracking, or to improve mixture stability and strength, or to enhance the rutting and fatigue performance, or to decrease the pavement structural thickness. Bahia et al. (1997) [37] classified asphalt modifiers into various groups such as polymers (elastomeric and plastomeric), fillers, fibers, hydrocarbons, antistripping agents, and crumb rubber, according to their composition and effects. These additives have a wide range of physical and chemical properties, and they would impact the performance of asphalt mixtures in various aspects. The most often used asphalt binder modifiers are polymers. The performance of modified asphalt binders has been studied in several research. The polymer's nature and content have strongly enhanced the rheological properties by increasing the stiffness and decreasing the phase angle [51], and the temperature susceptibility [18] of the asphalt binder.

The utilization of geopolymers as asphalt binder modifiers is rapidly increasing because the manufacturing process of geopolymer does not require high temperatures, it can help to reduce CO_2 emissions, and it has ability to enhance the viscoelastic behavior of asphalt binder[118, 204, 205, 181, 106]. Geopolymers are like zeolites and feldspathoids in that they can both adsorb harmful chemical waste and function as a binder to turn semi-solid

waste into an adhesive solid [66]. Zain et al. (2017) [235] concluded that fly ash-based geopolymer material performed best in terms of aluminosilicate content and is currently the best practise in environmental protection applications. Ibrahim et al. (2016) [118] investigated the influence of geopolymer on the physical properties and storage stability of the 80/100 asphalt binder. The geopolymer additives were prepared in the dry state using fly ash (class F) and alkaline activators (NaOH and Na_2SiO_3). Different tests, including softening point, ductility, and viscosity, were conducted to investigate the physical properties of neat and modified asphalt binders. The results showed that as the geopolymer concentration was increased from 3% to 9%, the ductility of the asphalt binder decreased approximately from 150 cm to 70 cm, indicating that the stiffness of the modified asphalt binder increased. In addition, the modified asphalt binders were stable at high storage temperatures. Hamid et al (2020) [106] investigated the possibility of using fly ash-based geopolymer as a modifier for asphalt binder by using a new technique to produce the geopolymer. The geopolymer is used as a dry substance with a particle size of less than 0.15 mm. The results showed that geopolymer has a significant effect on the rheological properties of asphalt binder. Also, they found that there are no promising effects on the microstructure of asphalt binder. Rosyidi et al. (2020) [181] used fly ash based-geopolymer gel as a modifier for asphalt binder. The addition of geopolymer to the asphalt binder resulted in higher impact values by achieving the highest work adhesion value. Also, it was observed that there is no significant difference in the FTIR spectrum due modified asphalt binder using geopolymer.

6.1.1 Research Significance and Objectives

According to the literature review, the geopolymer additive increased the asphalt binder's workability and the work cohesion value, which reveals that the cracking resistance of the asphalt binder has been increased. In addition, the adhesion between asphalt binder modified using geopolymer and aggregate is enhanced. While the effect of geopolymer content on the fatigue and low temperature crack resistance of asphalt binder has not been investigated yet. Also, the influence of aging and climate change conditions on the geopolymer modified asphalt binder and mixture should be evaluated. On the other hand, SBS was broadly used in many countries, and it had a considerable impact on the rheological and performance of asphalt binder. As a result, comparing the promised effects of using the geopolymer as a modifier with the results of another modifier, such as SBS, could motivate the use of the geopolymer during pavement construction. Therefore, this study aimed to assess the impact of the fly ash-based geopolymer and its combination with the SBS polymer on the crack resistance of the asphalt binder by looking into the following:

- Investigating the effect of additives and temperature on the rheological and low and intermediate performance of asphalt binder.
- Investigating the additive, temperature, and frequency impacts on the dynamic modulus of asphalt mixture.
- Evaluating the additives effects moisture damage resistance of asphalt mixture.
- Evaluating the cracking resistance of unmodified and modified asphalt mixture.

6.2 Experiment and Methods

6.2.1 Materials

Geopolymer Preparation

Geopolymer is made up of an alkali activator and fly ash mixture. Alkali activators included sodium silicate solution (Na_2SiO_3) and sodium hydroxide (NaOH) at an 8-molar concentration. During the preparation of geopolymer, it was discovered that curing time and activator type have substantial effects on chemical reactions [59]. It's also worth noting that the combination of sodium hydroxide and sodium silicate gives geopolymer a good mechanical performance [166]. Rifaai et al. (2019) [177] concluded that the highest yield stress and storage modulus values are obtained when 8 molar of NaOH is used as an activator during the preparation of the fly ash-based geopolymer. Before making the geopolymer, the sodium hydroxide (NaOH) solution was made in a fume cabinet by dissolving sodium hydroxide in deionized water.

This study utilized low calcium fly ash (Class F), which includes more silica and alumina and is therefore preferable to high calcium fly ash (Class C), as many studies recommend [110, 76, 92]. To activate the alumino-silicate precursors in fly ash, a 1:2 mass ratio of sodium silicate and sodium hydroxide solution was utilized, with 200 g of fly ash being mixed with 80 g of the alkaline medium for 5 minutes. The resulting slurry was then transferred to the silicon moulds and cured for six days at room temperature (23-25 °C) and one day at 65 °C. Finally, geopolymer samples were grinded into powder and sieved with sieve No. 100 to remove particles larger than 0.15 mm in diameter. The procedure for producing the geopolymer additives is shown in Figure 6.1.

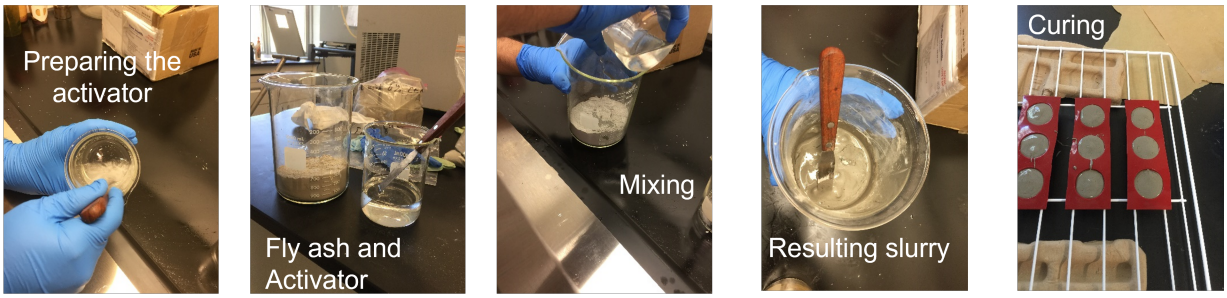

Figure 6.1: Geopolymer Preparation

Asphalt Binders Preparation

In this study, the modified asphalt binders were prepared using two methods. In the first method, the geopolymer-modified asphalt binder was prepared by heating 300 g of asphalt binder (PG 58-28) at 140 °C. Then the geopolymer was added into the neat asphalt blend in different amounts. A mechanical shear mixer was used at a speed of 2000 r/min for 60 minutes, controlling the temperature at 140 °C ± 5 to prepare a homogenous blend. Hamid et al. (2020) [106] noted that modifying asphalt binder using a geopolymer with different percentages (3, 6 and 9%) does not affect the asphalt binder's microstructure. In the second method, high shear mixer and heating mantle under a speed of 2000 r/min for 60 minutes with a temperature of 170 °C ± 5 were utilized to prepare the modified asphalt binder with 2% of SBS. After that 10% of the crosslinking agent was added and mixed for 30 minutes. Finally, a curing time was performed by reducing the high shear mixer speed to 1000 r/min for 60 minutes with a temperature of 180 °C ± 5. Table 6.1 presents the aggregate size distribution of asphalt mixture.

Aging Procedure

Following the mixing process of asphalt binders, samples for short-term aging in a Rolling Thin-Film Oven (RTFO) and long-term aging (20 hours) in a Pressure Aging Vessel (PAV) were prepared directly. All PAV specimens were subjected to the frequency sweep and LAS tests using the Dynamic Shear Rheometer (DSR). In addition, the low temperature performance of neat and modified asphalt binders was investigated using BBR test by measuring creep stiffness (S) and relaxation rate (m) parameters.

Table 6.1: Aggregate size distribution

Sieve size (mm)	**Passing (%)**	**Control point (maximum)**	**Control point (minimum)**
19	100		
12.5	95	100	90
9.5	83	90	28
4.75	58		
2.36	40	58	28
1.18	19		
0.6	12		
0.3	8		
0.15	4.5		
0.075	3	10	2

6.2.2 Experimental Work

Dynamic Shear Rheometer

The Dynamic Shear Rheometer (DSR) was applied to investigate neat and modified binders' rheological behavior, according to AASHTO T 315 [6]. A frequency sweep test was performed to investigate the impact of loading frequency, temperature and modification rate on asphalt binders' rheological properties. Two samples for each binder were tested and the average was identified as the test result. Different frequencies ranging from 0.0159 H_z to 15 H_z were applied for different test temperatures (5, 10, 15, 20, 25, and 30 °C). A frequency sweep test was conducted to investigate the effect of temperatures and additives content on the complex shear modulus and phase angle using a 8 mm diameter plate and a 2 mm gap. The DSR-Linear Amplitude Sweep (LAS) test was conducted, according to AASHTO TP 101 [1], for the neat and modified asphalt binders using an 8 mm diameter plate and a 2 mm gap at different intermediate temperatures (10 °C, 20 °C, and 30 °C). Prior to the strain sweep test, a frequency sweep test is carried out to determine how the undamaged material responds. Subsequently, the strain sweep test is performed at a constant frequency (10 H_z) to accelerate fatigue damage. In this study, the VECD model was used to analyze the test result and predict fatigue life (N_f) of asphalt binder.

Bending Beam Rheometer

The Bending Beam Rheometer (BBR) test was performed according to ASTM D6648 [27] to determine the flexural-creep stiffness (S) and m-value by means of a bending beam rheometer. Different temperatures (-12 °C, -18 °C, and -24 °C) were performed to investigate the effect of additives on the S and m-value parameters of the asphalt binder.

Dynamic / Complex Modulus Test

The dynamic modulus test, as depicted in Figure 6.2, was used to estimate dynamic modulus (E^*) and phase angle (δ), and to evaluate the effects of different additives on the performance of asphalt mixture. Firstly, the specimens were prepared, whereby asphalt binders and aggregates were heated in an oven to get to their mixing temperatures. The viscosities of the asphalt binders, using a rotational viscometer, were used to determine the mixing and compaction temperatures. Prior to compaction, the asphalt mixture was conditioned at 135°C for four hours after mixing to simulate short-term aging of asphalt mixes according to AASHTO R 30 [5]. After compaction, the specimens were cored to standard specimen with dimensions 100 mm diameter and 150 mm height. The cored specimens were tested using MTS machine in the CPATT lab by using different frequencies (0.1, 0.5, 1, 5, 10 and 25 H_z) and various temperatures (-10, 4, 21, 37 and 54 °C).

Moisture Sensitivity Testing

The moisture damage evaluation was conducted according to AASHTO T 283 [4]. The Superpave gyratory compactor was used to prepare six specimens with dimensions of 150 mm diameter and 95 mm height, with an air void content of 7% ± 0.5 percent. These specimens were divided into conditioned and unconditioned subsets (each with three specimens) with almost the same average air void percentage. The conditioned subset was vacuumed to a saturation level between 70% and 80% before being frozen for 16 hours at -18 °C and then thawed in a water bath for 24 hours at 60 °C. Before testing, the two subsets were conditioned for 2 hours at 25 °C. The strength testing was carried out by applying a 50 mm/min axial force until the maximum load was obtained. Equation 6.1 was then used to compute the indirect tensile strength.

$$S_t = \frac{2000 \times P}{\pi \times D \times t} \tag{6.1}$$

Where S_t is the tensile strength (kPa), P is the maximum load (N) that the specimen can resist, t is the specimen thickness (mm), and D is the specimen diameter (mm).

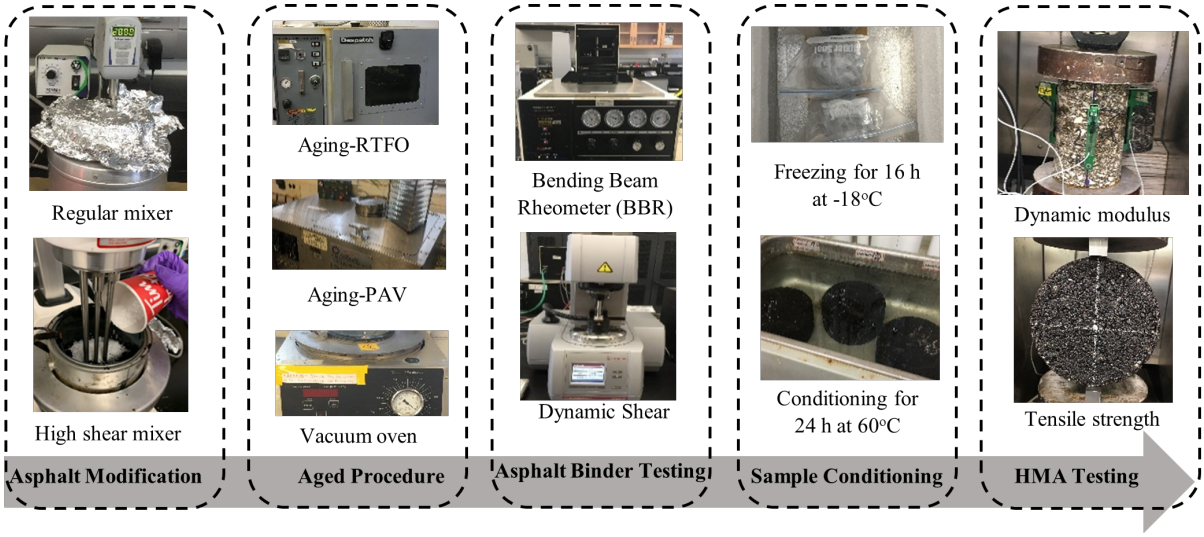

Figure 6.2: Experiment and methods

6.3 Results and Discussion

6.3.1 Rheological and Performance of Asphalt Binder

Master Curve

The master curve for complex shear modulus and phase angle at a reference temperature of 20 °C is presented in Figure 6.3. The results showed that there is a significant effect of additives on the viscoelastic behavior of asphalt binder, whereby the additives increase the complex shear modulus and decrease the phase angle. The results of phase angles, on the other hand, cannot be used to determine which asphalt binder type is more elastic or viscous. As a result, the complex shear modulus' storage and loss modulus should be separated. Table 6.2 shows the properties of unaged and aged (RTFO and PAV) asphalt binders.

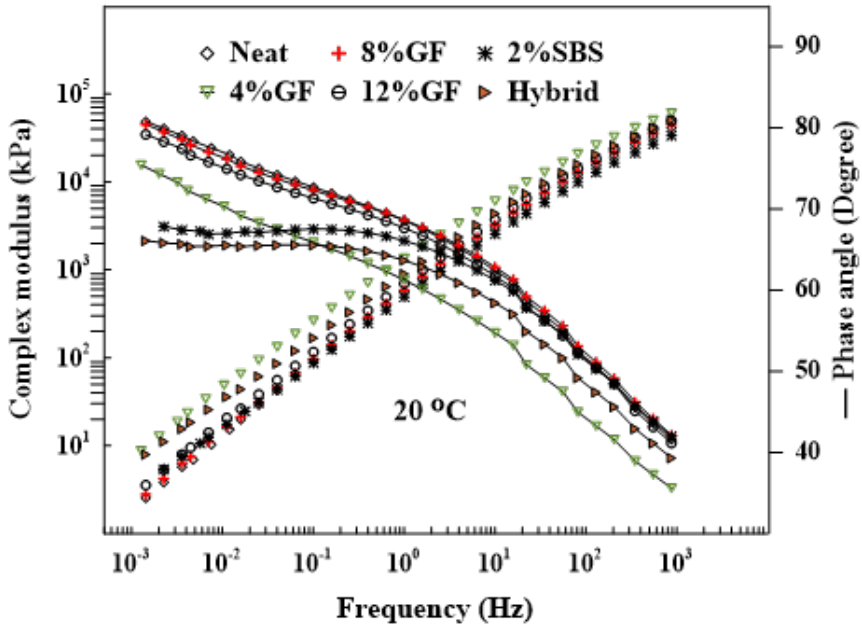

Figure 6.3: Master curve of the neat and modified asphalt binder

Temperature Susceptibility on the Loss and Storage Modulus

Figures 6.4, 6.5, and 6.6 show the logarithms of G' and G'' versus temperatures for unaged, RTFO, and PAV binders, respectively. The equations for linear regression were developed and are depicted in the figures. Table 6.3 shows the absolute values of the slopes of the linear regression equations. The slopes show the temperature sensitivities of the binders: the steeper the slope, the more sensitive a binder is to temperature variations. The results show that the temperature sensitivity of both G' and G'' decreases for unaged and RTFO modified asphalt binders. Low magnitudes for the G'' slope indicate lower susceptible to the temperature. When the binders are exposed to long-term aging (PAV), the 8%GF binder becomes more susceptible to temperature changes.

Fatigue Performance

Figure 6.7 shows the effect of additives on the fatigue life of asphalt binder at different temperatures (10 °C, 20 °C, and 30 °C). In this study, the fatigue life was calculated as the load repetitions at which the complex shear modulus is decreased to the 50% of its initial value. It is clear that the additives had better fatigue life than the neat binder at different

Table 6.2: Asphalt binder Properties

Parameter	**Neat**	**4%GF**	**8%GF**	**12%GF**	**2%SBS**	**Hybrid**
Orginal Asphalt Binder						
Rotational Viscosity @ 135 °C	0.417	0.531	0.661	0.561	0.678	0.900
Rotational Viscosity @ 165 °C	0.119	0.146	0.179	0.160	0.191	0.235
$G^*/\sin$ (kPa) @ 52 °C, at 1.6 H_z	5.036	7.517	9.606	7.244	6.756	14.532
RTFO-Asphalt Binder						
$G^*/\sin$ (kPa) @ 52 °C, at 1.6 H_z	9.73	16.82	21.52	17.81	14.68	36.71
% Recovery @ 52 °C, at 3.2 kPa	8.72	18.83	24.67	19.28	45.14	48.97
J_{nr} @ 52 °C at 3.2 kPa	0.84	0.39	0.27	0.38	0.27	0.09
PAV-Asphalt Binder						
Stiffness Critical Temperature (T_s)	-32.7	-32.7	-32.0	-32.7	-35.7	-33.4
Slope Critical Temperature (T_m)	-33.2	-33.1	-32.8	-32.9	-31.5	-33.3
$G^*.\sin$ (kPa) @ 20 °C, at 1.6 H_z	2817	2829	3360	3069	3006	3304

Table 6.3: Regression slope of unaged, RTFO, and PAV binders

Binders	The slope $\lvert G' \rvert$			The slope $\lvert G'' \rvert$		
	Unaged	RTFO	PAV	Unaged	RTFO	PAV
Neat	3.817	3.426	2.820	3.167	2.851	2.323
4%GF	3.486	3.198	2.915	2.878	2.674	2.381
8%GF	3.780	3.154	2.921	3.168	2.635	2.393
12%GF	3.681	3.204	2.873	3.089	2.688	2.355
2%SBS	3.529	3.209	2.773	3.044	2.725	2.306
Hybrid	3.409	2.998	2.781	2.941	2.514	2.306

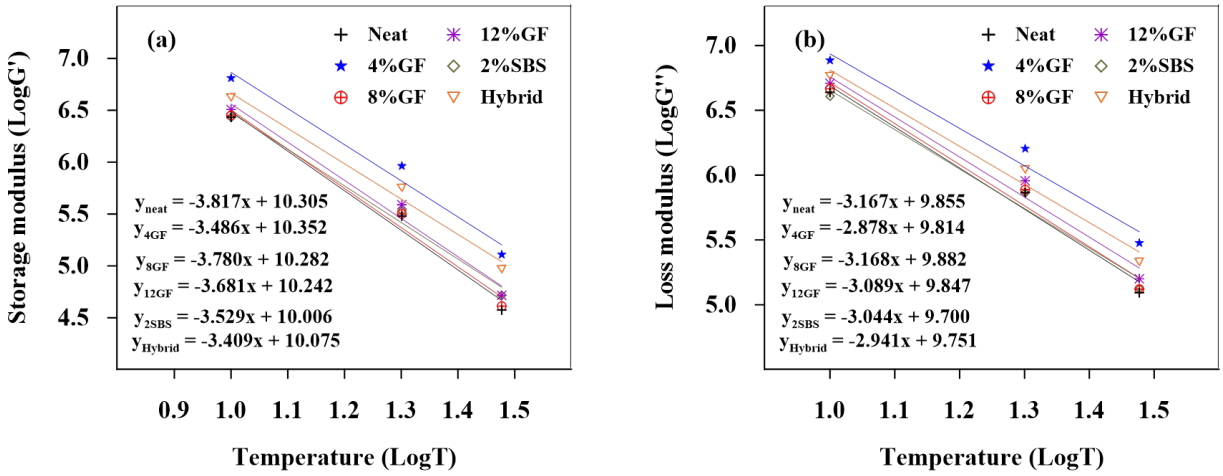

Figure 6.4: Temperature sensitivity on the (a) storage and (b) loss modulus of unaged binders

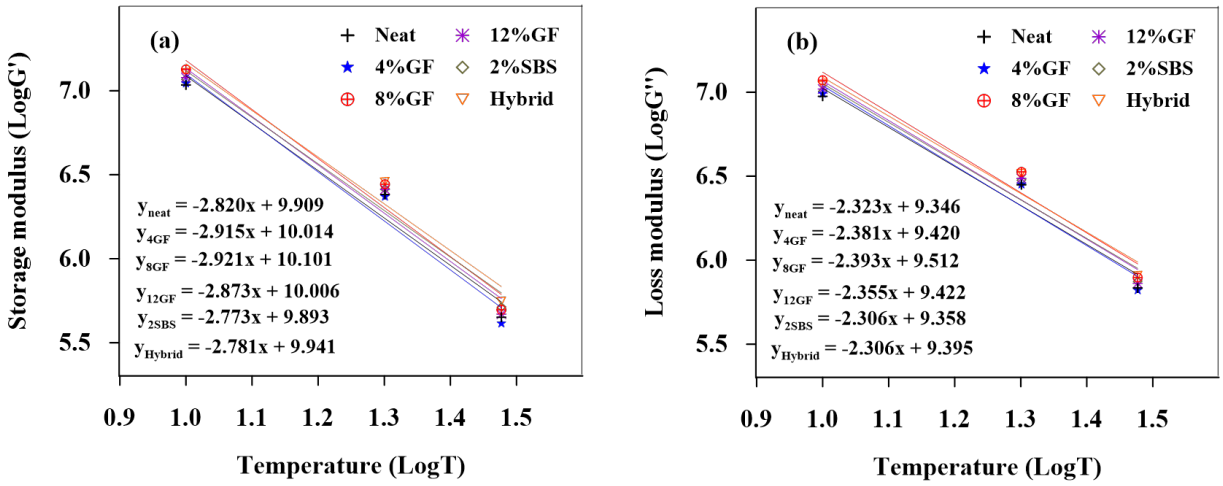

Figure 6.5: Temperature sensitivity on the (a) storage and (b) loss modulus of PAV binders

temperatures. Compared to the other binders, the hybrid binder had the best fatigue life at different temperatures. The hybrid binder increased the fatigue life by 61%, 41%, and 50% at 10 °C, 20 °C, and 30 °C, respectively, compared to the neat asphalt binder. Also, the 12%GF binder achieved the highest fatigue life compared with the neat, 4%GF, 8%GF, and 2%SBS binders. For example, using 12%GF increased the fatigue life of asphalt binder by 33%, 21%, and 20% at 10 °C, 20 °C, and 30 °C, respectively, compared to the neat

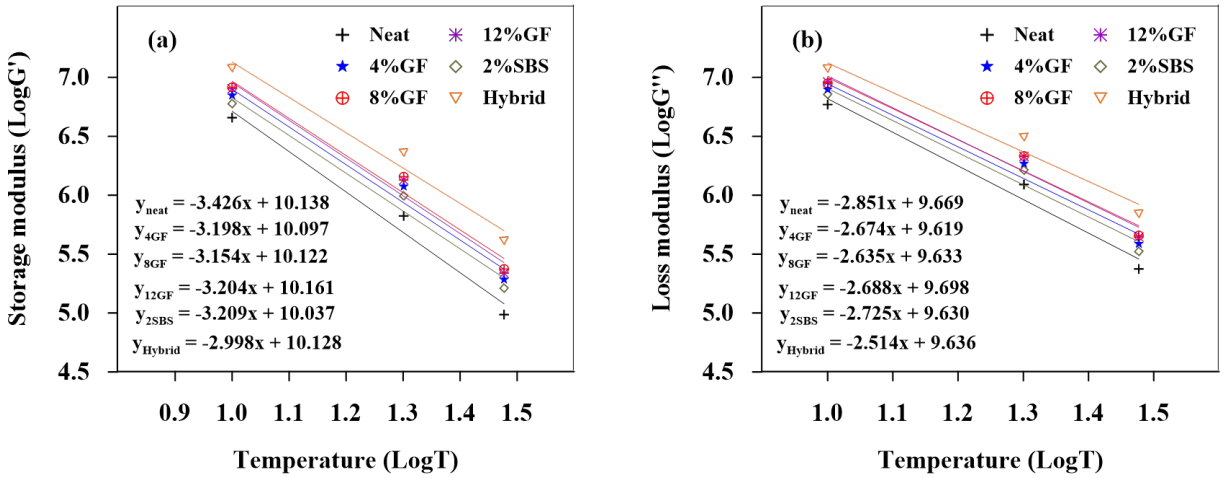

Figure 6.6: Temperature sensitivity on the (a) storage and (b) loss modulus of RTFO binders

asphalt binder. The findings indicated that the geopolymer modified asphalt binder has a significant impact on the fatigue performance of asphalt binder as also concluded by Hamid et al (2019) [107].

Low Temperature Performance

Flexural creep stiffness and the rate of stress relaxation (m-value) are parameters related to the low temperature cracking resistance of asphalt binder. A higher value (> 300 MPa) of creep stiffness causes a less resistance to the thermal cracking. Likewise, lower value (< 0.3) of m-value induces a lower ability to absorb stress when temperature drops and exhibit higher cracking tendency [109]. Figure 6.8 represents the effect of additives and different temperatures (-12 °C, -18 °C, and -24 °C) on the creep stiffness of neat and modified asphalt binders. When the temperature was -12 °C, the creep stiffness of the geopolymer–modified asphalt binder decreased with the addition of additional geopolymer by up to 8%, which indicated that the asphalt resistance to low temperature cracking increased. However, beyond 8% GF, the creep stiffness of the asphalt binder increased. While the 2%SBS achieved the lowest creep stiffness compared with the neat and other modifiers.

There was a critical change in the behavior of the modified asphalt binder when the temperature was -18 °C and -24 °C. When the temperature was -18 °C, the creep stiffness

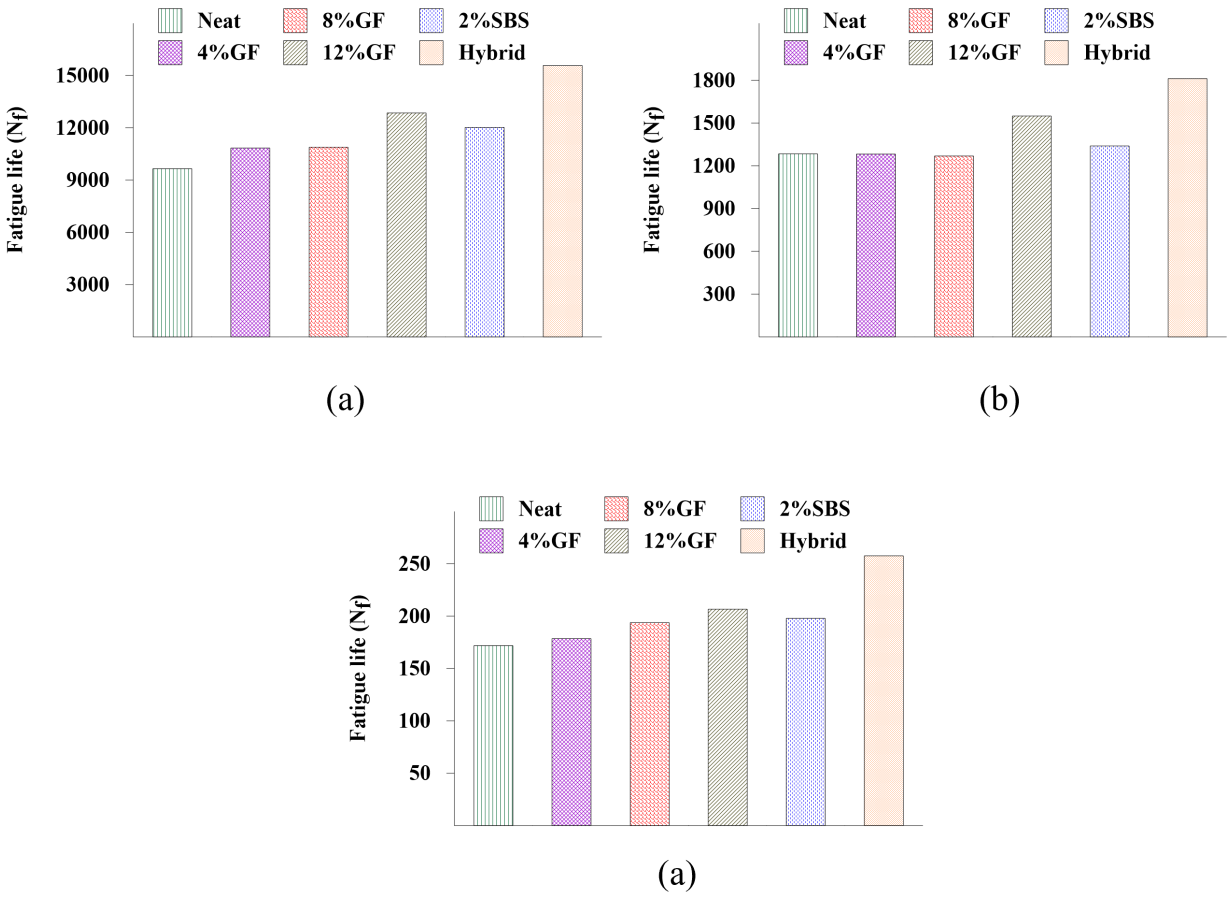

Figure 6.7: Additives effects on the fatigue life at (a) 10 °C, (b) 20 °C, and (c) 30 °C

of the 8%GF binder had increased, which indicated that the asphalt binder resistance to low temperature cracking decreased. However, it meets the condition of having a creep stiffness of less than 300 MPa. In comparison to the neat and other modifiers, the 2% SBS binder likewise had the lowest creep stiffness. When the temperature was -24 °C, the 2%SBS binder achieved a creep stiffness of less than 300 MPa, which meets the requirement that creep stiffness should be less than 300 MPa, whereas the other modifiers don't meet the requirement that creep stiffness be more than 300 MPa.

Figure 6.9 shows the influence of additives and temperature on the rate of stress relaxation (m-value). When the temperature was -12 °C, 8%GF and 2%SBS achieved the highest values of m-value compared with other modifiers, which indicates that the

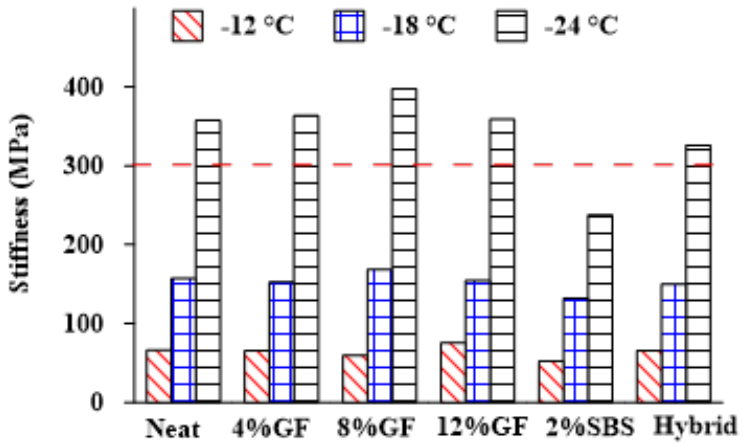

Figure 6.8: Effect of additives on the creep stiffness

stress relaxation performance increased. A higher m-value indicates the binder's ability to absorb stress in the case of a temperature drop and exhibits a lower cracking tendency [109]. While 4% GF and hybrid binders exhibit more improvement of stress relaxation performance at -18 °C. The results showed that the neat and modified asphalt binders meet the condition of having an m-value of more than 0.3 at -12 °C and -18 °C. While at temperature -24 °C, and 4% and 8% geopolymer content, the m-value change trend had a point of inflection, and the value was lower than the value of base asphalt. 12%GF and hybrid binders achieved approximately the same value of m-value as neat asphalt binder. The neat and modified asphalt binders don't meet the condition of having an m-value of more than 0.3 at -24 °C.

Aging Effect

In this study, the crossover modulus is used to assess the influence of aging on the asphalt binders, which has been used to evaluate the relaxation properties [122] and the oxygen uptake due to oxidation aging [83] in asphalt binder. Jing et al. (2020) [122] investigated the effects of aging time, temperature, and pressure on the crossover modulus and concluded that aging has a significant effect on the asphalt binder as the crossover modulus decreases. Also, there is a better relationship between inverse crossover modulus and the carbonyl changes in asphalt binders due to aging [83, 95, 243, 137].

The crossover modulus (G_c^*) was determined from the relationship between complex shear modulus and phase angle in the black diagram. The crossover modulus, shown in

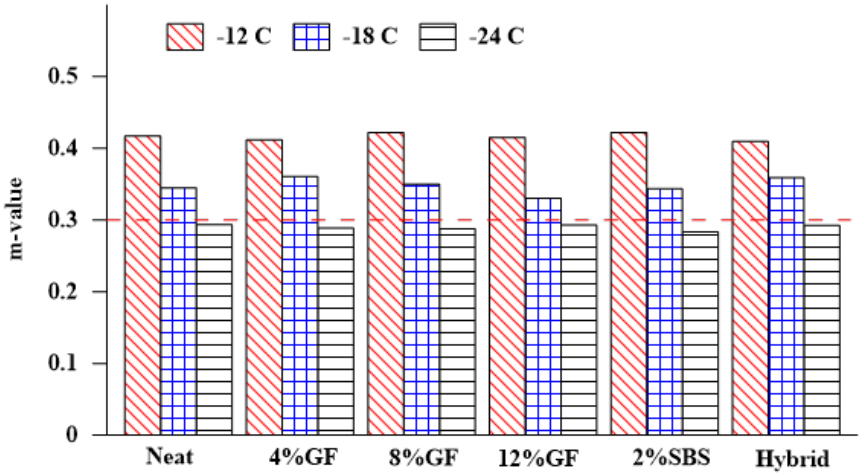

Figure 6.9: Effect of additives on the m-value

Figure 6.10, is related to a phase angle of 45°, whereby the storage and loss shear modulus have the same value. The material acts more solidly (elastic) when the phase angle is less than 45°. When it is greater than 45°, the material behaves more fluid (viscous). If there are more data points in the region with a phase angle greater than 45^o, this shows that the asphalt binder is becoming more fluid (viscous reaction) and less solid (elastic response) as it ages. An aging index was proposed to measure the aging effect on asphalt binder's crossover modulus [122], which is represented as the ratio of the ($G_c{}^*$) of unaged asphalt binder over the ($G_c{}^*$) of aged asphalt binder.

$$AI = \frac{G^*_{c-unaged}}{G^*_{c-aged}} \tag{6.2}$$

where AI is the aging index of crossover modulus, $G^*_{c-unaged}$ is the crossover modulus of unaged asphalt binder and G^*_{c-aged} is the crossover modulus of unaged asphalt binder.

Figure 6.11 shows the crossover modulus of long-term aged neat and modified asphalt binders at 20 °C. The results demonstrated that the modified asphalt binder achieved the highest crossover modulus compared with the neat binder. This is attributed to decreasing the effect of aging on the asphalt binder based on previous research [83, 122].

The results showed that there is a significant influence of modifiers on the crossover modulus, whereby the crossover modulus of the neat binder is enhanced by adding modifiers. For example, the crossover modulus increased by 36% when 8%GF was added to the neat asphalt binder, demonstrating that the geopolymer had a considerable impact on the

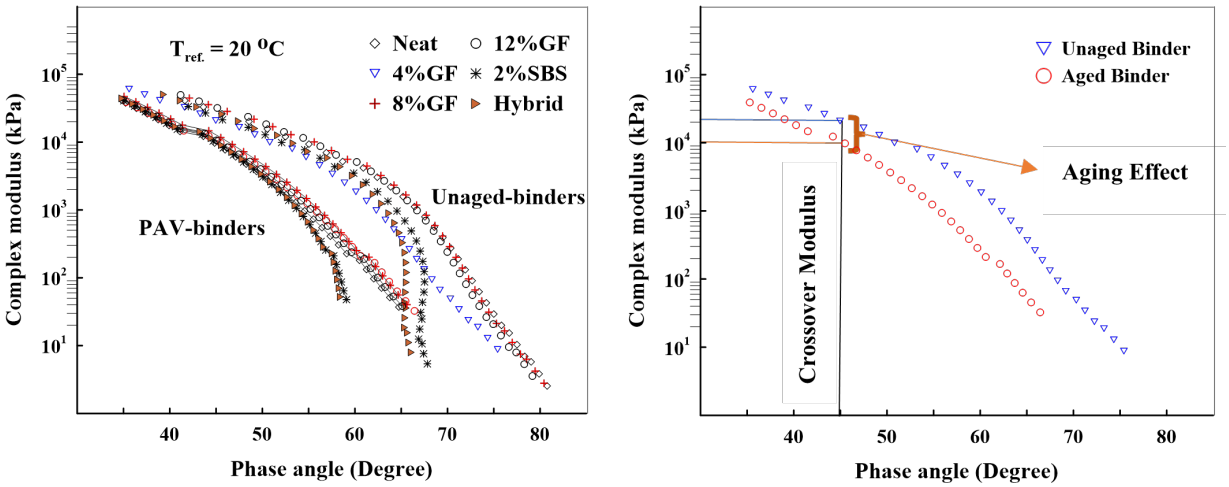

Figure 6.10: Evaluating the aging effect on the crossover modulus

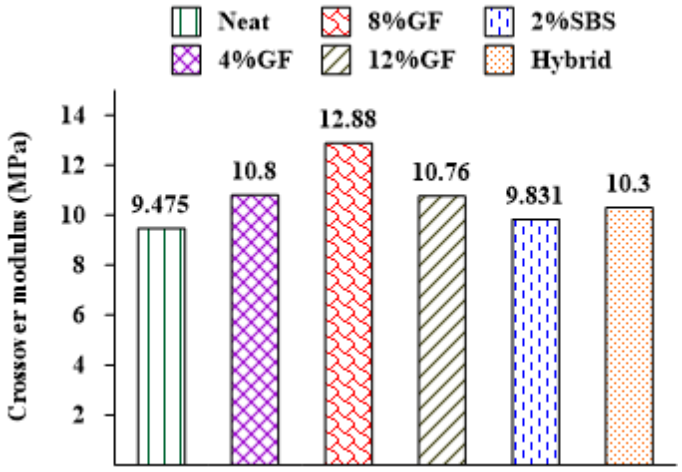

Figure 6.11: Crossover modulus of neat and modified asphalt binders

viscoelastic behavior. In contrast, the 2%SBS exhibited low resistance to oxidation aging, whereby it achieved the smallest value of crossover modulus. Figure 6.12 represents the change in the crossover modulus between unaged and aged asphalt binders. 8%GF and hybrid binders showed the same rate of change in the crossover modulus due to aging, while the smallest rate is obtained by adding 2% of SBS.

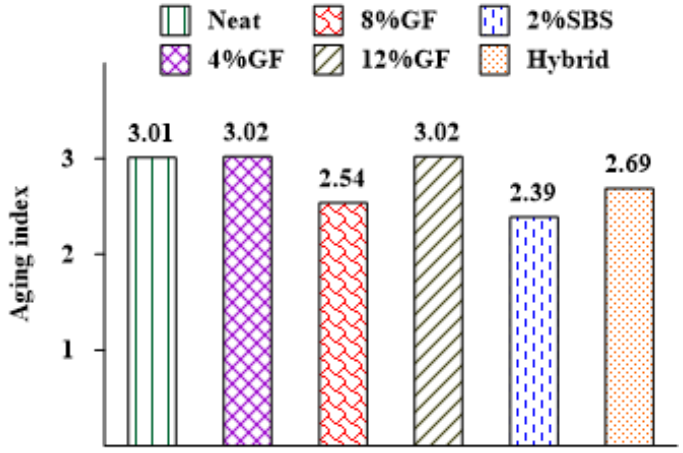

Figure 6.12: Aging index of neat and modified asphalt binder

6.3.2 Additives Effects on the Performance of Asphalt Mixture

Dynamic / Complex Modulus Test Analysis

The stress-strain relationship in HMA is characterised by its complex modulus (E^*), which determines the stiffness characteristics of the HMA as a function of temperature and loading rate under continuous sinusoidal loading [77]. The dynamic modulus was considered as a significant parameter input in the MEPDG design method of asphalt pavement, which used for characterizing asphalt mixtures [160]. The dynamic modulus of an asphalt mixture can be measured by performing stress-controlled or strain-controlled laboratory tests at various temperatures and frequencies. The analysis of dynamic/complex modulus test data includes the development of master curves, which assists in the comparison of the stiffness of asphalt mixtures over a variety of temperature and frequency ranges.

The linear viscoelastic properties of the asphalt binder and mixture at different temperatures and frequencies have been described by constructing the master curves using different models and shift factors. Rowe et al. (2009) [182] remarked that the generalised logistic sigmoidal model works well for the analysed samples and suggested that it be used to obtain a better master curve for non-symmetric curves. Pellinen et al. (2002) [162] concluded that the use of the sigmoidal fitting function to generate the master curve for the dynamic modulus test data appears to fit the data well because it matches the physical shape of the measured data throughout a wide range of temperatures. In this study, the shift factor (a_t) using the Williams, Landel and Ferry (WLF) equation (Equation 6.3) and

the generalised logistic sigmoidal model (Equation 6.4) were used to construct the master curve of asphalt mixture with different temperatures (-10 °C and 21 °C), as shown in Figure 6.13. The master curve was developed with the use of the Microsoft Excel spreadsheet and the solver function. Table 1 summarizes the coefficients of the shift factor and sigmoidal model equations for various additives at different temperatures. The results revealed that asphalt mixtures including various modified asphalt binders are stiffer than asphalt mixtures containing the neat asphalt binder, which has the maximum dynamic modulus at various frequencies.

$$Log\ a_t = \frac{-C_1(T - T_{ref})}{C_2 + (T - T_{ref})} \tag{6.3}$$

Where T_{ref} is the reference temperature, and C_1 and C_2 are constants to reduce the difference between actual and predicted data [234].

$$Log\ E^*(f,T) = \delta + \frac{\alpha}{(1 + \lambda \exp(\beta + \gamma(Log f_r)))^{\frac{1}{\lambda}}} \tag{6.4}$$

Where E*(f, T) is the dynamic modulus as a function of frequency and temperature, δ is the lower asymptote, α is the difference between the values of the upper and lower asymptotes, β and γ are the shape coefficients, and λ is used to allow the curve to have a non-symmetrical shape [234].

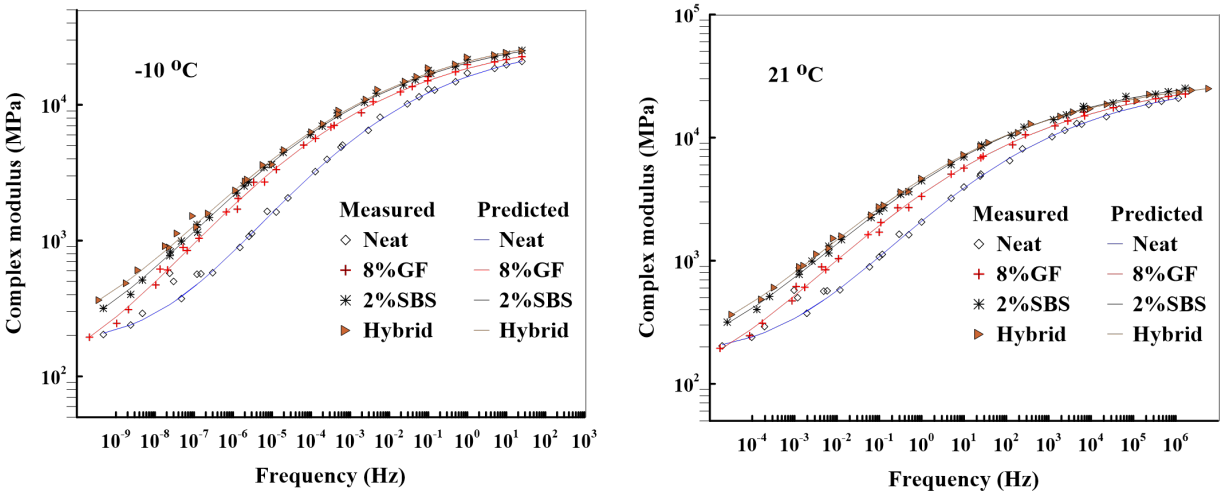

Figure 6.13: Master curve for dynamic/complex modulus at -10 °C and 21 °C

Table 6.4: Summary of the shift factor and sigmoidal model coefficients

Temp.	**Binder**	**Shifting**		**Model**					
		C_1	C_2	α	β	δ	γ	λ	R^2
-10 °C	Neat	35.029	205.401	2.244	-1.953	2.257	-0.372	0.125	0.999
	8%GF	31.837	170.798	2.569	- 2.225	1.960	-0.311	0.064	0.999
	2%SBS	29.515	163.013	2.389	- 2.181	2.173	-0.312	0.046	0.999
	Hybrid	33.829	192.746	2.299	- 2.096	2.284	-0.306	0.042	0.998
21 °C	Neat	28.484	220.324	2.234	-0.250	2.256	-0.377	0.131	0.999
	8%GF	27.124	205.103	2.589	- 0.717	1.939	-0.314	0.065	0.999
	2%SBS	23.141	179.736	2.355	- 0.725	2.184	-0.324	0.047	0.999
	Hybrid	17.179	129.899	2.256	- 0.742	2.253	-0.329	0.042	0.999

Figures 6.14 and 6.15 show E^* and δ values measured for mixtures with various types of additives at various frequencies (0.1, 0.5, 1, 5, 10, and 25 H_z) and temperatures (-10 and 21 °C) but normalised to those obtained for the asphalt mixture with neat binder. The results revealed that the modified asphalt mixtures have the highest values of E^* at low temperature (-10 °C) and intermediate (21 °C) temperatures compared with unmodified asphalt mixture. Whereas there is a reduction in the phase angle at different temperatures and frequencies, which indicates that the viscoelastic behavior of asphalt binder is changed to be more elastic.

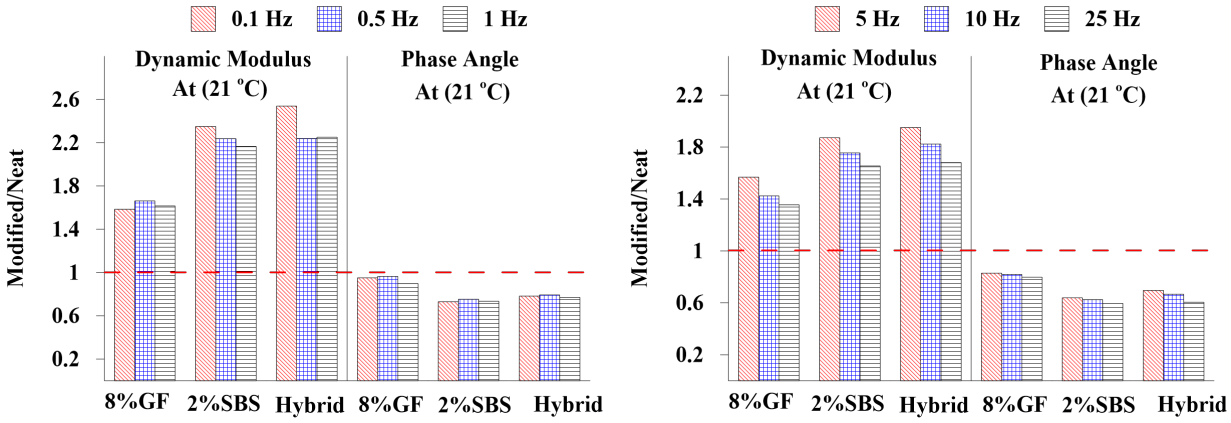

Figure 6.14: Frequencies effects on the E and δ of different asphalt mixtures at 21 °C

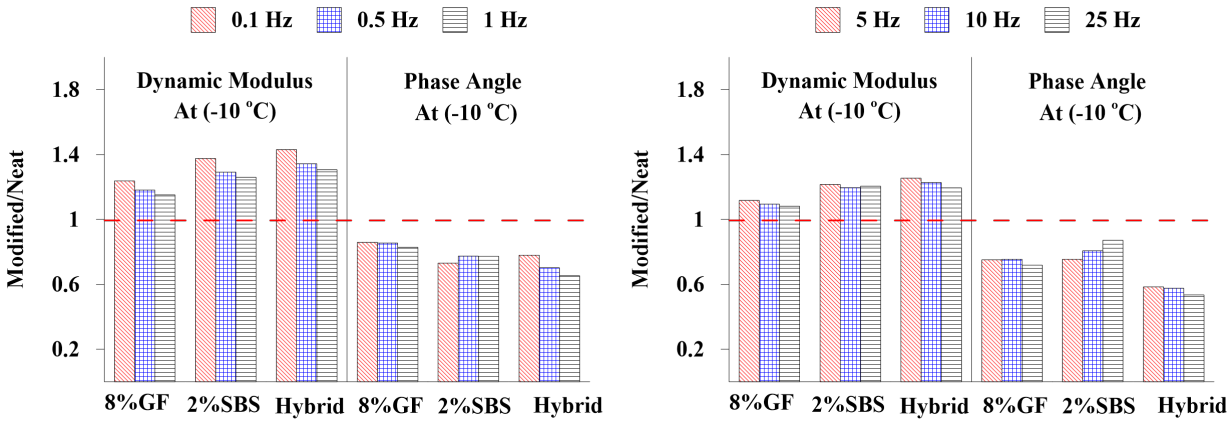

Figure 6.15: Frequencies effects on the E* and δ of different asphalt mixtures at -10 °C

Moisture Sensitivity Evaluation

Moisture damage in pavement materials is the most important issue that affects the durability of asphalt pavement. Moisture damage causes stripping, which is defined as the loss of adhesive bonding force between the binder and the aggregate particles. Moisture damage in asphalt mixes is caused by a loss of adhesion and/or cohesion, resulting in a progressive deterioration of the mixture's strength and stiffness [109]. The Tensile Strength Ratio (TSR), which is the ratio of tensile strength before and after conditioning, is used to determine the moisture sensitivity of asphalt mixtures.

Figure 6.16 shows the effects of different additives on the tensile strength of the asphalt mixture before and after conditioning. In the dry condition, the tensile strength has increased from 580.4 kPa to 740.4 kPa, 884.8 kPa, and 917.4 kPa by using 8%GF, 2%SBS, and hybrid binders, respectively. In the freezing-thawing condition, there is a high reduction in the tensile strength by using 8%GF, 2%SBS, and hybrid binders, but the tensile strength has still increased from 563.7 kPa to 618.9 kPa, 787.8 kPa, and 832.1 kPa, respectively.

The results revealed that the asphalt mixes for neat and modified asphalt binder are susceptible to moisture damage, whereby the asphalt mixtures achieved tensile strength ratio (TSR) values more than 80%. The asphalt mixes with different modifiers have a higher tensile strength compared with neat binder. It is observed that the hybrid mixed is the least susceptible to moisture damage with a TSR of 91% compared with other modifiers. This finding indicated that geopolymer-modified asphalt binder has a significant resistance to moisture damage as also concluded by Rosyidi et al. (2020) [181].

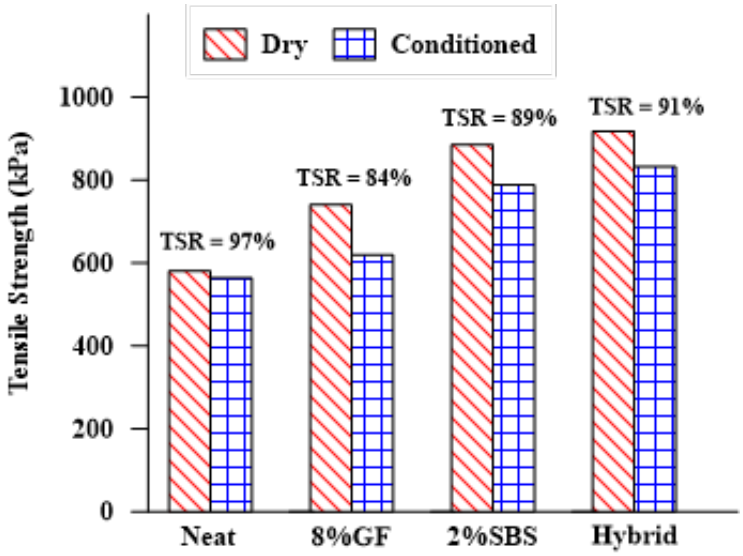

Figure 6.16: Moisture sensitivity evaluation

Fracture Energy of Asphalt Mixture

Additives effects on the macro cracking resistance of asphalt mixes and the effect of freezing and thawing on the cracking resistance of asphalt mixes were investigated in Figure 6.17. Fracture energy is one of the parameters that characterizes the asphalt mix's cracking resistance; asphalt mixes with higher fracture energy have enhanced cracking resistance [242]. After the peak stress, the load bearing capacity of asphalt mix will certainly decline as the macro-crack begins to form and grows. Therefore, to evaluate the effects of additives on the cracking resistance of asphalt mixes, the fracture energy was calculated at the maximum tensile strength and at the dropping of the tensile strength to 85% and 75% using Equations 6.5 and 6.6.

$$W_f = \sum_{i=1}^{n-1}((l_{i+1} - l_i) \times P_i + \frac{1}{2}(l_{i+1} - l_i) \times (P_{i+1} - P_i)) \tag{6.5}$$

$$G_f = \frac{W_f}{Dt} \times 10^6 \tag{6.6}$$

Where G_f is the failure energy (Joules/m^2), W_f is the work of failure (Joules), D specimen diameter (mm), and t is the thickness of specimen (mm). The results revealed that

the cracking resistance of the asphalt mixture is enhanced by using geopolymer, SBS, and the combination of geopolymer and SBS. The hybrid binder achieved the highest fracture energy at dry and freezing-thawing conditions which means the highest cracking resistance compared to the other modifiers. It was also noted that freezing-thawing condition has a negative influence on the fracture energy of modified asphalt mixtures due to the presence of water, which causes a reduction in the adhesion between the asphalt binder and aggregate. The fracture energy of modified asphalt mixes is still higher than the mixture with the neat asphalt binder despite this reduction.

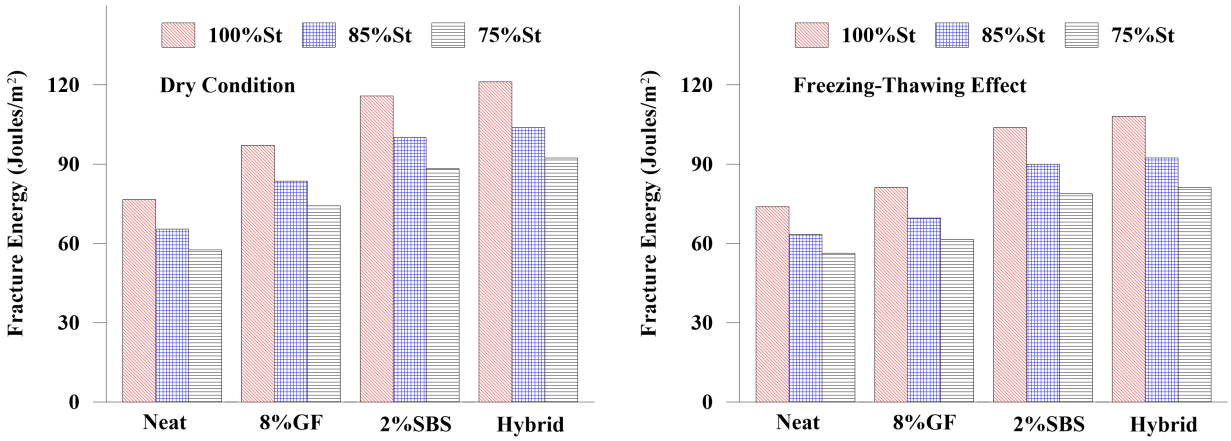

Figure 6.17: Additives effect on the fracture energy of asphalt mixture

6.4 Conclusions

In this research, the rheological and performance of asphalt binder modified using geopolymer and SBS polymer were investigated. Also, the effects of additives, temperatures, and aging on the asphalt binder performance were also evaluated. Meanwhile, the influence of additives on the moisture damage and cracking resistance were studied. Based on the findings, the following conclusions can be drawn:

- The 12%GF modified asphalt binder achieved the highest fatigue life compared to the neat, 4% GF, 8%GF, and 2%SBS binders. Compared to the neat asphalt binder, the fatigue life increased by 33%, 21%, and 20% at 10 °C, 20 °C, and 30 °C, respectively.

- Compared to the neat asphalt binder, the (2%SBS+8%GF) modified asphalt binder increased the fatigue life by 61%, 41%, and 50% at 10 °C, 20 °C, and 30 °C, respectively.

- The thermal cracking performance of the asphalt binder was enhanced when the 2%SBS and hybrid modifier were used as modifiers, which achieved the lowest creep stiffness.

- The crossover modulus of the neat binder is enhanced by adding 8% of geopolymer. Compared to the neat asphalt binder, adding 8%GF increased the crossover modulus by 36%, indicating a significant effect of geopolymer on the viscoelastic behavior. Whereas adding 2%SBS and (2%SBS+8%GF) to the asphalt binder increased the crossover modulus by 4% and 9%, respectively.

- Asphalt mixes with different modifiers had a higher tensile strength compared to neat binder. By using 8% GF, 2% SBS, and hybrid binders, the tensile strength increased from 580.4 kPa to 740.4 kPa, 884.8 kPa, and 917.4 kPa, respectively.

- The asphalt mixture with hybrid binder had the least susceptible to moisture damage, with a TSR of 91% compared to other modified asphalt binders. This finding indicates that using the combination of SBS and GF as a modifier for asphalt binder had a significant resistance to moisture damage.

- Due to the presence of water, which reduces the adhesion between the asphalt binder and aggregate, freezing-thawing conditions have a negative impact on the fracture energy of modified asphalt mixtures. Despite this reduction, modified asphalt mixes still have higher fracture energies than mixtures prepared with neat asphalt binder.

Chapter 7

Evaluating the Effect of Glass Powder/Fly Ash-Based Geopolymer on the Rheological and Performance of Asphalt Binder

This chapter is based on the following article, which was submitted to the International Journal of Pavement Engineering. "Evaluating the Effect of Glass Powder/Fly Ash-Based Geopolymer on the Rheological and Performance of Asphalt Binder," by A. Hamid, H. Baaj, and M. El-Hakim (2022).

Abstract

This study was performed to evaluate the impact of temperature and additive content on the rheological behavior of asphalt binders modified with glass powder and fly ash-based geopolymer (GFG). Four different percentages GFG, 0%, 4%, 8%, and 12%, have been used. The rheological properties and performance of asphalt binders were evaluated using the rotational viscometer and dynamic shear rheometer (DSR). The Multiple Stress Creep Recovery (MSCR) test was conducted to study the rutting potential of asphalt binders, which were tested at temperatures ranging from 46 °C to 70 °C with a 3 °C gap. The interactive effects of geopolymer content and temperature on non-recoverable creep compliance (J_{nr}) and creep recovery percentage (R) of geopolymer modified asphalt binders were investigated and predictive mathematical models were developed using the response

surface method (RSM) and regression method. The Linear Amplitude Sweep (LAS) was carried out to investigate the potential effect of geopolymer on the fatigue performance of asphalt binders using the VECD model and Schapery's work potential theory. The results showed that the GFG additives change the viscoelastic behavior, increasing the shear complex modulus and decreasing the phase angle. Adding 8%GFG increases the modulus from 9.48 kPa to 22.32 kPa and drops the phase angle from 76.9° to 71.6°, indicating that the material becomes more elastic at 52 °C. In addition, at low and high stress levels, modified asphalt binders outperformed the neat binder in terms of rutting resistance. The findings confirmed that temperature is statistically more significant than the geopolymer content, and the RSM is an effective method to predict the recovery and non-recovery performance of geopolymer modified asphalt binder. The 8%GFG exhibited the highest potential to fatigue resistance followed by 12%GFG then 4%GFG. The neat asphalt binder exhibited the lowest potential to fatigue resistance. This research confirms that the use of glass powder/fly ash-based geopolymer would improve rutting and fatigue resistance of the asphalt binders.

7.1 Introduction

The asphalt binder is a viscoelastic material that exhibits both viscous and elastic properties when deformed. The asphalt binder is suitable for most environmental conditions that lie between the extremes of hot and cold climates. Because of this variety of behavior, asphalt binder is an appropriate adhesive substance for paving. However, due to its complexity, it is a difficult material to understand and describe [109]. While the production of asphalt binder requires a substantial quantity of energy, resulting in the emission of CO_2. Therefore, lowering the amount of asphalt binder and energy utilized in the production of hot mix asphalt could be beneficial.

Governments provide significant budgets to improve their road infrastructure, as this is critical for the growth of the country's economy. In this regard, it is worth noting that countries spend a significant amount of money each year on road infrastructure maintenance due to severe weather and high traffic loads that cause pavement deterioration. Modifiers that have a significant effect on the performance of asphalt binders could be used to reduce pavement distress such as rutting and cracking [19, 106]. Consequently, the potential development of modifier materials could reduce maintenance and rehabilitation costs.

Glass, a non-degradable waste item, accounts for 2% of total waste materials in Canada, according to Environment and Climate Change Canada [80]. This includes beverage con-

tainers, windows, and dishware. In the meantime, 0.44 million tonnes have been disposed of in landfills during 2016. While the European Union accumulates 15.2 million tonnes of glass waste each year [82]. Worldwide, there is a trend toward improving asphalt performance by utilising waste materials such as waste glass that have rapidly accumulated over the last few decades. In the developed world, waste glass collection and treatment are becoming more regular parts of environmental policy [212]. Because the collected waste glass has different properties, it has been regarded as a critical problem all over the world. Consequently, recycling and reusing waste glass is a difficult procedure for glass producers [169, 190, 217].

Glass powder was used as a construction material, and it was noted that it is an appropriate alternative to natural fine sand in concrete [202, 15, 104, 105]. Tan and Du (2013) [202] replaced the fine aggregate in the binder mortar with different percentages of waste glass (0%, 25%, 50%, 75%, and 100%) of four different types (brown, green, clear, and mixed colour glass). As a result of the irregular form and lower density of waste glass particles, there is a drop in density and flowability, as well as more air content. In addition, there is a reduction in the mechanical properties due to the weakened bond between the binder paste and glass particles. Adaway and Wang (2015) [15] explored the effective amount of waste glass required to replace the fine aggregate in concrete, which achieved the optimal compressive strength. Five percentages (15, 20, 25, 30, and 40%) of waste glass were used, whereby three samples were prepared for every percentage and then tested at 7 and 28 days. According to the findings, the optimal compressive strength was attained by utilising 30% waste glass at 7 and 28 days.

Moreover, the glass powder was used as a filler to enhance the asphalt binder and mixture performance [191, 56, 123]. Simone et al. (2019) [191] concluded that galss powder could be reused as a filler with both neat and modified asphalt binder and has a potential enhancement to the bearing capacity and rutting performance of the asphalt mixture. Choudhary et al. (2021) [56] used glass powder as a filler in the asphalt mixture and noted that there was a substantial impact on rutting, fatigue, and low-temperature cracking at low asphalt content. On the other hand, the significant amount of silica in the glass powder reduced adhesion and moisture resistance. While Jony et al. (2011) [123] investigated the possibility of using glass powder as a filler in asphalt mixtures compared with ordinary Portlant cement and lime stone. The results revealed that using 7% of galss powder produced an asphalt mixture with a lower density, high stability, and lower flow.

Recently, glass powder has been used as an alkaline activator [213, 210] or as a precursor blended with fly ash [175, 211] for geopolymer applications. Torres-Carrasco and Puertas (2015) [213] explored the possibility of using waste glass as an alkaline activator in the preparation of fly ash-based geopolymer. Three solutions (8 molars of sodium hydroxide, 10

molars of sodium hydroxide with 15% waterglass, and 10 molar of sodium hydroxide with 15 g of waste glass) were used as activators for fly ash, and the mechanical and microstructural properties were determined. It was concluded that waste glass is an effective alkaline activator in the preparation of geopolymer. Tchakouté et al. (2016) [210] studied the possibility of using waste glass and rice hush as a source of sodium waterglass, which is used as an activator for pozzolanic material during the preparation of geopolymers based on metakaolin. It was noted that sodium water glass made from rice hush ash is less reactive than waste glass, and the highest compressive strength is achieved in the metakaolin-based geopolymer from waste glass.

Moreover, replacing fly ash with waste glass in geopolymer has been investigated by many researchers [175, 211]. It was shown that there are significant effects on the mechanical properties of geopolymers. Redden and Neithalath (2014) [175] noted that the compressive strength was higher for glass powder than for fly ash when activated using NaOH at low curing temperatures. Meanwhile, Tho-In et al. (2018) [211] studied the potential usage of waste glass powder as a replacement for fly ash during the geopolymer's preparation. Nine mixtures were prepared to investigate glass powder's effect on the compressive strength and microstructure of geopolymer. Sodium hydroxide (NaOH) and sodium silicate were used as alkali activators. The results revealed that waste glass could be utilized as a replacement for fly ash during the preparation of geopolymers. Bobirica et al. (2015) [43] investigated the effect of waste glass on the strength and microstructure of geopolymer-based on fly ash or fly ash with slag. Sodium hydroxide (NaOH) and sodium silicate were utilized as activators for four different compositions using waste glass to replace fly ash with different percentages. The results indicated that the compressive strength was decreased due to increasing the waste glass proportions, whereby increasing the SiO_2/Al_2O_3 molar ratio caused a change in the microstructure of geopolymers.

Nowadays, application of statistical modelling approaches such as response surface method (RSM) is significant since it has a great deal of potential for analysing the impact of many factors on a given response. RSM has been widely utilized to predict the influence of different factors on the rheological and performance of modified asphalt binders [38, 54]. RSM has been used to improve the performance of various asphalt binder modifiers by modifying the asphalt binder and optimising the modification mixing parameters using a variety of dependent and independent variables related to the asphalt binder, the modification process, and the asphalt binder's performance [138]. Badri et al. (2020) [35] investigated the effects of crumb rubber content (5%, 7%, 10%, 12%, and 15%) and temperatures (ranging from 46 °C to 82 °C) on the rheological properties of asphalt binder using a dynamic shear rheometer (DSR). RSM was performed using temperature and crumb content as independent variables and rheological parameters (complex modulus (G^*) and

phase angle) as responses. It was concluded that crumb content has more influence on the response than temperature, and the RSM approach is an effective method to investigate the rheological properties of asphalt binder.

7.1.1 Objectives

This study aimed to investigate the feasibility of using glass powder as an aluminosilicate source during the preparation of geopolymer as a modifier for asphalt binder. Also, the potential of using the GFG to enhance the rutting and fatigue performances of asphalt binder by investigating the following:

1. Investigating the influence of GFG on the viscoelastic behavior of asphalt binder.
2. Evaluating the effect of various parameters (Temperature and geopolymer content) on the non-recoverable creep compliance (J_{nr}) and creep recovery percentage (R) of modified asphalt binders using statistical analysis.
3. Using the response surface method (RSM) and the regression method to predict J_{nr} and R at different stresses, considering the effect of temperature and geopolymer content.
4. Assessing the effect of GFG on the fatigue performance of asphalt binder

7.2 Experiment and methods

7.2.1 Materials

Preparation of Geopolymer

Fly ash (180 g) and glass powder (20 g) were used as alumino-silicate precursors during geopolymer preparation. The alumino-silicate precursors were activated using 80 g of sodium hydroxide and sodium silicate at a ratio of 2:1 by mass. The mixture was stirred for 5 minutes before being transferred to silicone moulds and curing for 6 days at room temperature (23 - 25 °C) and 24 hours at 65 °C. After that, the geopolymer was grinded and sieved using sieve No. 100 to remove particles larger than 0.15 mm, which may affect the consistency of the result. The preparation steps of geopolymer additives are depicted

in Figure 7.1. The geopolymer is formed when the aluminosilicate source reacts with the alkaline solution, whereby the tetrahedral silica (SiO_4) and alumina (AlO_4) are joined by oxygen (O_2) in three-dimensional chain networks [76].

Preparation of Asphalt Binders

The PG 58-28 asphalt binder was heated until it became fluid. The temperature was kept constant at 140 °C ± 5, and the GFG was added to the neat asphalt binder blend at three different concentrations: 4%GFG, 8%GFG, and 12%GFG. The mixture was then mixed using a mechanical shear mixer at a speed of 2000 r/min for 60 minutes, as shown in Figure 7.1.

Aging Procedure

Following the mixing process of asphalt binders, samples for short-term aging in a rolling thin-film oven (RTFO) were filled in cylindrical glass bottles with 35 ± 0.5 grams. After cooling for 60 to 180 minutes, all bottles were put horizontally in a vertically revolving frame, rotating at a speed of 15 revolutions per minute. The sample flows along the glass bottle's wall due to the temperature and movement. Air was pumped into each glass bottle once throughout each cycle, which took a few seconds. This operation proceeded at 163 °C for 85 minutes.

7.2.2 Rheological Properties Tests

Rotational and Dynamic Shear Viscosities

The rotational viscosities of the neat and modified asphalt binders were measured at 135 °C and 165 °C using a rotational viscometer, as dipicted in Figure 7.1. At each temperature, three readings were obtained, and the average was used as the test result. The test was performed according to AASHTO T 316 [7]. The dynamic shear viscosities were determined using a dynamic shear rheometer at different temperatures ranging from 46 °C to 70 °C at a constant frequency (10 rad/s).

Performance Grade (PG) Test

The performance grades (PG) of neat and modified asphalt binder at high temperatures were determined according to AASHTO T315 [6]. Also, the failure temperature of aged

and unaged asphalt binders was evaluated. High-performance grading represents the high temperature in the summer that the binder can resist, which was determined using the superpave parameters $G^*/\sin\delta = 1$ kPa for unaged asphalt binder and $G^*/\sin\delta = 2.2$ kPa for aged asphalt binder.

Frequency Sweep (FS) Test

The frequency sweep test was used to determine the effects of frequencies, temperatures, and GFG content on asphalt binders' linear viscoelastic behavior. The testing used a 25 mm diameter plate with a 1-mm gap, and the frequencies varied from 0.159 H_z to 15 H_z.

Temperature Sweep (TS) Test

The test was applied using a 1.59 H_z frequency and different temperatures ranging from 46 °C to 70 °C with 6 °C increments. Two plates with a 25 mm diameter and a 1 mm gap between them were used in the test.

Multiple Stress Creep Recovery (MSCR) test

The MSCR test was used to evaluate the percent recovery (%R) and non-recoverable creep compliance (J_{nr}) of asphalt binders. The asphalt binders were aged (short-term aging) using the Rolling Thin Film Oven (RTFO). The MSCR test was carried out with a 25 mm diameter plate and a 1 mm gap at various temperatures (from 46 °C to 70 °C) and stresses (0.1 kPa and 3.2 kPa). The test was performed by applying creep for one second and recovering for nine seconds, whereby the %R and J_{nr} were calculated.

Linear Amplitude Sweep (LAS)

For the neat and modified asphalt binders, the LAS test was carried out according to AASHTO TP 101 [1], utilizing DSR with an 8 mm diameter plate and a 2 mm gap at a temperature of 20 °C. This test should take about 30 minutes in total, which is deemed a considerable advantage [112]. The LAS test is repeated at a steady frequency (10 H_z) to accelerate fatigue damage. The test findings were used to assess the fatigue life (N_f) of asphalt binders using the VECD model and Schapery's work potential theory (1984) [188].

Figure 7.1: Experiment and methods

7.3 Results and Discussion

7.3.1 Rheological Properties Tests Analysis

Additives and Temperature Effects on the Viscosity

Figure 2 (a, b) shows the influence of geopolymer on the rotational and dynamic shear viscosity of neat and modified asphalt binders. The viscosity is a key factor in determining the feasibility and ease of handling in pumping, as well as the required mixing and compaction temperatures. Figure 7.2 (a) demonstrated the rotational viscosity of all binders at 135 °C and 165 °C to determine the mixing and compaction temperatures of asphalt mixtures. The test was conducted according to AASHTO T 316 [7].

The results showed that the geopolymer modified asphalt binder achieved the highest viscosities compared to the neat binder, but less than 3 Pa.s at 135 °C and 20 rpm as recommended by the Superpave specification [109]. Increasing the viscosity is attributed to larger modules present in the fluid [147], which may be caused by the formation of the chain networks in the asphalt-geopolymer mixture. Also, Figure 7.2 (b) revealed a similar pattern, whereby the dynamic shear viscosity is increased for all modified asphalt binders at different temperatures (46 °C, 52 °C, 58 °C, 64 °C and 70 °C).

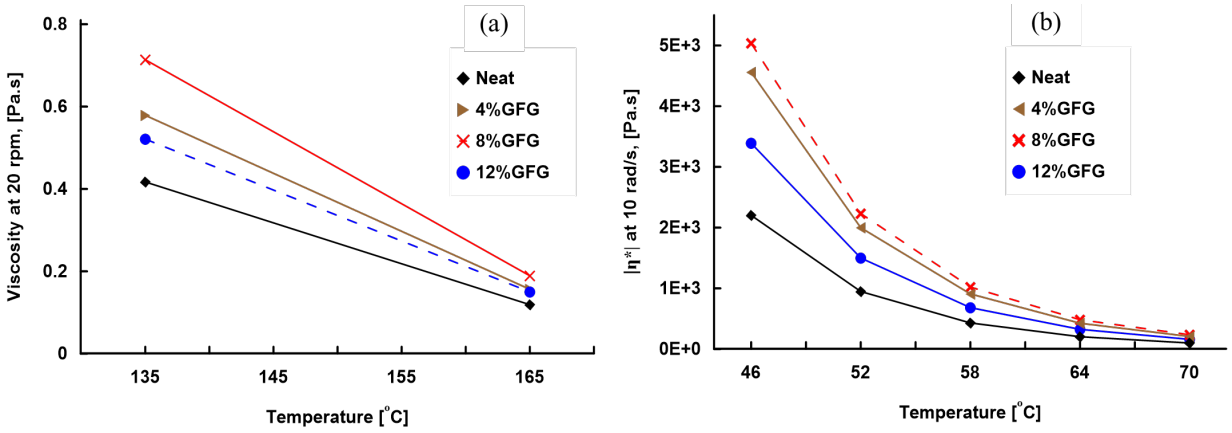

Figure 7.2: Effect of geopolymer on (a) rotational viscosity and (b) dynamic shear viscosity

Effect of Temperatures on the Complex Shear Modulus and Phase Angle

Figure 7.3 represents the complex shear modulus and phase angle variation for neat and modified binders at different testing temperatures. When compared to the neat binder, the geopolymer modified asphalt binder changes the asphalt binder's viscoelastic behavior at different temperatures by increasing the shear complex modulus and decreasing the phase angle. The geopolymer-modified asphalt binder's complex modulus was increased by adding additional geopolymer up to 8%GFG throughout the test temperature range. For example, The shear complex modulus has increased from 9.48 kPa to 22.32 MPa, and the phase angle dropped from 76.9° to 71.6°, indicating that the viscoelastic behavior becomes more elastic at 52 °C.

The shear complex modulus of the asphalt binder drops, and the phase angle increases as GFG increases above 8%. Thus, increasing the geopolymer content by more than 8% has caused a reduction in elastic behavior compared to 8%GFG. This reduction may be attributed to the particle-particle repulsion due to steric forces, which caused an inverse chemical reaction and prevented the formation of molecular networks. It was found that adding geopolymer to the neat asphalt binder reduces the phase angle, indicating the change in the viscoelastic behavior and a shift toward elastic behavior. However, the results of phase angles cannot be utilized to establish which asphalt binder type is more elastic. As a result, the storage and loss modulus of the complex shear modulus should be separated.

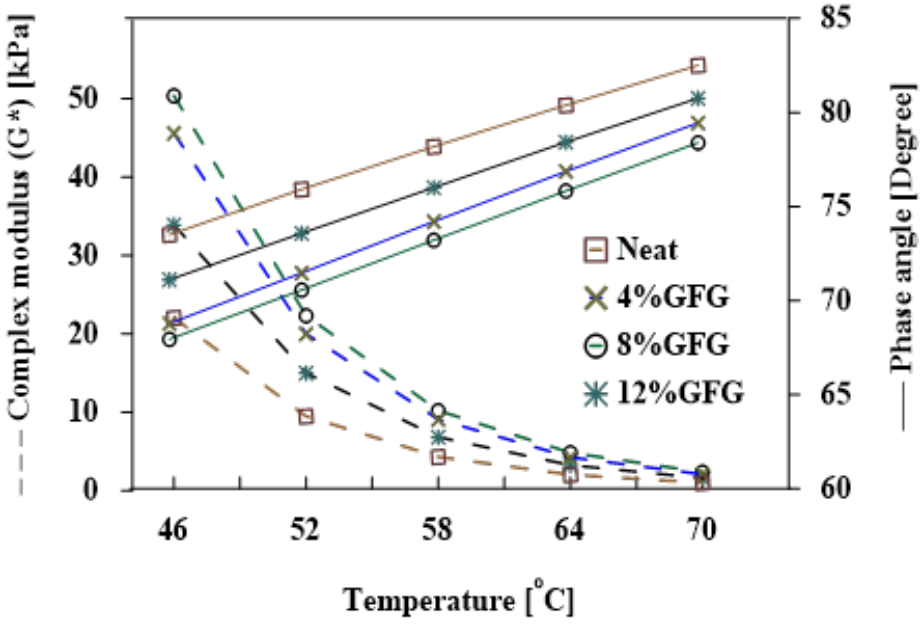

Figure 7.3: Temperature effect on the complex shear modulus and phase angle

Temperatures Effect on the Storage and Loss Modulus

Figure 7.4 shows the impact of frequencies and temperatures (46 °C and 58 °C) on the storage modulus (G') and loss modulus (G'') values, respectively. It was noted that the G' and G'' values increased geometrically as frequency increased from 0.1 to 10 H_z, while both G' and G'' decreased as temperature increased. When $G' > G''$, the asphalt binder has more ability to recover from deformation. When $G'' > G'$, the asphalt binder has more ability to resist the deformation. Tables 7.1 and 7.2 show that the neat binder has a loss modulus greater than a storage modulus because the individual molecules do not have such strong links [147]. Whereas, adding geopolymer causes a significant increase in both G' and G''. For example, the G' is increased 400% by adding 8% of geopolymer at 58 °C and 0.1 H_z compared with neat binder, while the G'' is increased 170% at the same geopolymer content, temperature, and frequency. This significant increase in the G' is attributed to the internal connections inside the material, such as chemical bonding or physical-chemical interactions [147].

Asphalt binders with 4%GFG, 8%GFG, and 12%GFG achieved more ability to resist and recover from deformation, whereby they have higher storage and loss modulus than neat asphalt binder. The 8%GFG binder achieves higher storage and loss modulus than

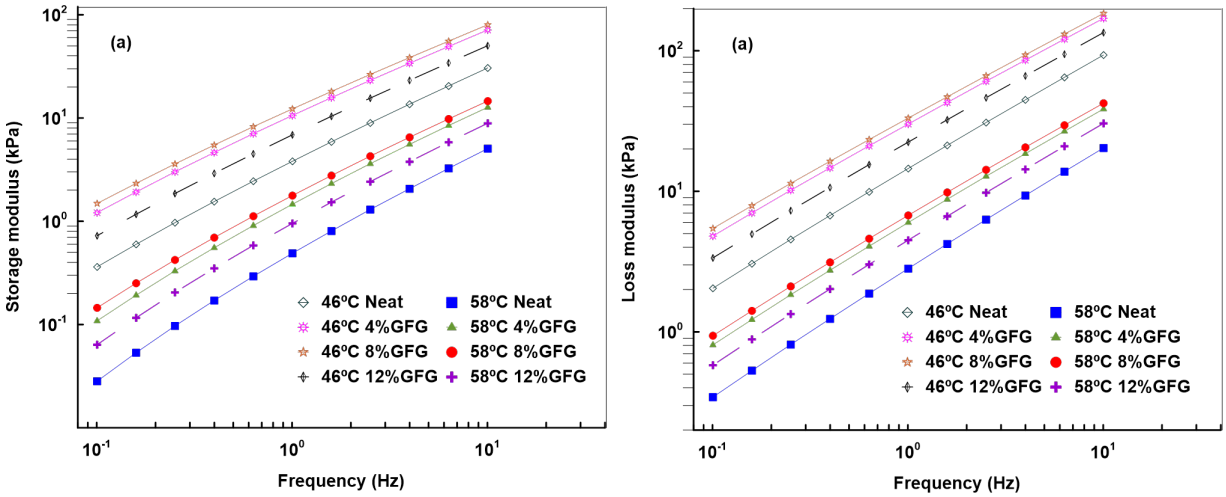

Figure 7.4: Temperature and frequency effects on the (a) storage modulus and (b) loss modulus

Table 7.1: Temperature and frequency effects on the storage modulus (kPa)

Binder	**G′ at 0.1 H_z**		**G′ at 10 H_z**	
	46 °C	58 °C	46 °C	58 °C
Neat	0.36	0.03	30.61	5.07
4%GFG	1.21	0.11	71.40	12.72
8%GFG	1.49	0.15	80.08	14.62
12%GFG	0.73	0.06	50.27	8.92

the 4% GFG and 12%GFG binder. Also, it has more ability to resist the deformation at various temperatures (46 °C and 58 °C) and frequencies (from 0.1 to 10 H_z), whereby G″ is greater than G′, as shown in Tables 7.1 and 7.2. Therefore, the ability to resist and recover the deformation is ranked as: 8% GFG > 4% GFG > 12% GFG > 0% GFG.

Effect of Geopolymer Content on the PG Grading and Rutting Factor

Table 7.3 shows the performance grades (PG) for asphalt binders at high temperatures. The results showed that the GFG modified asphalt binder with 4%, 8%, and 12% acheieved

Table 7.2: Temperature and frequency effects on the loss modulus (kPa)

Binder	**G″ at 0.1 H_z**		**G″ at 10 H_z**	
	46 °C	58 °C	46 °C	58 °C
Neat	2.04	0.34	93.28	20.35
4%GFG	4.81	0.81	170.01	38.54
8%GFG	5.44	0.94	184.21	42.37
12%GFG	3.36	0.58	134.80	30.45

Table 7.3: Additive type and amount effects on high temperature resistance

Binder	**HPG**	**$G^*/\sin\delta$ = 1 kPa**	**$G^*/\sin\delta$ = 2.2 kPa**
	°C	**°C**	**°C**
Neat	58	61.65	63.35
4%GFG	64	64.00	69.60
8%GFG	64	64.10	70.75
12%GFG	64	64.00	67.25

the highest resistance to the high temperatures compared with the neat binder. While 8%GFG exhibited more resistance to high temperatures for aged and unaged asphalt binders.

The influence of temperature and GFG content on the rutting factor ($G^*/\sin\delta$) of asphalt binder is shown in Figure 7.5. The results showed that increasing the geopolymer additives increased the rutting factor, indicating that the asphalt binder becomes stiffer and more elastic, and hence more resistant to rutting deformation. These findings were also noted in the prior study [106, 108]. When compared to other modified asphalt binders, the 8%GFG binder has a higher rutting factor. This might be due to the geopolymer modification rate and the positive interaction between asphalt binder and geopolymer molecules.

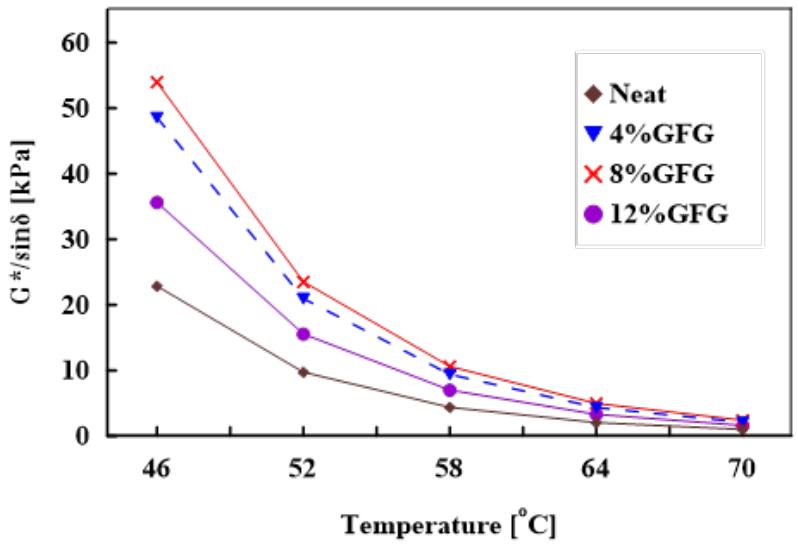

Figure 7.5: Additives and temperature effect on the rutting factor

7.3.2 MSCR results analysis

Temperature and Additives Effects on the Accumulated Strain

Figure 7.6 presents the average accumulated strain of ten creeps (1 s) for neat and modified asphalt binders at low and high stresses (0.1 kPa and 3.2 kPa), and different temperatures (46 °C and 58 °C). It was noted that the temperature and geopolymer content had crucial influences on the accumulated strain. The results showed that modified asphalt binders achieved the smallest accumulated creep strain at various temperatures and stresses. The accumulated strain of asphalt binder modified with geopolymer is lower than that of neat asphalt binder, indicating that the geopolymer enhanced the rutting performance of the asphalt binder; this supported the conclusions from previous studies [106, 108]. Also, the 8% GFG binder has the lowest accumulated strain compared with the 4%GFG and 12%GFG. Therefore, the accumulated strain is ranked as: 8%GFG < 4%GFG < 12%GFG < 0%GFG.

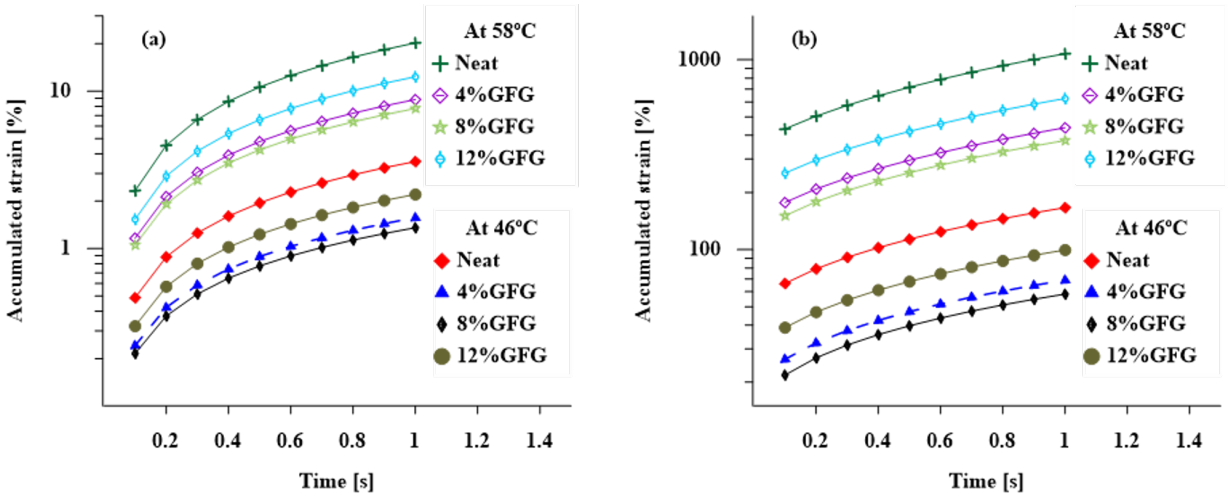

Figure 7.6: Temperature effect on the accumulated strain of GFG at (a) 0.1 kPa and (b) 3.2 kPa

Temperature and Additives Effects on the Recovery and Non-Recovery Behavior

The MSCR test was performed under low and high stresses (0.1 kPa and 3.2 kPa) and a wide temperature range of 46 °C to 70 °C with a 3 °C increment. Tables 7.4 and 7.5 represent the effect of geopolymer content and temperatures (46 °C, 52 °C, and 58 °C) on the creep recovery of asphalt binder. The results revealed that asphalt binder modified by 4%, 8%, and 12% of geopolymer enhanced the recovery properties at different temperatures and stresses. Also, the 8%GFG binder achieved the highest creep recovery compared to 4%GFG and 12%GFG binders at different stresses and temperatures. At low stress (0.1 kPa), the 8%GFG creep recovery increased by 57%, 74%, and 107% at 46 °C, 52 °C, and 58 °C, respectively, when compared to the neat binder. At 46 °C, 52 °C, and 58 °C, it increases by 88%, 188%, and 456%, respectively, under high stress (3.2 kPa). Therefore, the ability for creep recovery is ranked as: 8%GFG > 4%GFG > 12%GFG > 0%GFG.

Tables 7.6 and 7.7 represent the effects of geopolymer content and temperatures on the non-recoverable creep compliance (J_{nr}) of asphalt binder at 0.1 kPa and 3.2 kPa, respectively. The results showed that asphalt binder modified by 4%, 8%, and 12% of geopolymer induced the lowest J_{nr} compared to the neat binder, which confirmed the potential effect of geopolymer on the rutting resistance. Besides, the 8%GFG binder achieved the smallest J_{nr} compared with 4% and 12%GFG at different stresses and temperatures. For example, under low stress (0.1 kPa), the J_{nr} value of 8%GFG decreased by 72%, 69%, and 67% at 46

Table 7.4: Temperature impact on the (%R) of asphalt binders at 0.1 kPa

Binder	**(%R)**			$R_{modified}/R_{neat}$		
	46 °C	52 °C	58 °C	46 °C	52 °C	58 °C
Neat	28.39	19.16	11.48	1.00	1.00	1.00
4%GFG	40.16	28.97	20.16	1.42	1.51	1.76
8%GFG	44.67	33.28	23.80	1.57	1.74	2.07
12%GFG	34.96	24.47	16.14	1.23	1.28	1.41

Table 7.5: Temperature impact on the (%R) of asphalt binders at 3.2 kPa

Binder	**(%R)**			$\mathbf{R}_{modified}/\mathbf{R}_{neat}$		
	46 °C	52 °C	58 °C	46 °C	52 °C	58 °C
Neat	21.17	8.72	1.99	1.00	1.00	1.00
4%GFG	35.24	20.55	8.19	1.66	2.36	4.12
8%GFG	39.75	25.12	11.07	1.88	2.88	5.56
12%GFG	28.92	15.21	5.09	1.37	1.74	2.56

Table 7.6: Temperature impact on the (J_{nr}) of asphalt binders at 0.1 kPa

Binder	**($\mathbf{J}_{nr}$)**			$\mathbf{J}_{nr-modified}/\mathbf{J}_{nr-neat}$		
	46 °C	52 °C	58 °C	46 °C	52 °C	58 °C
Neat	0.25	0.71	1.79	1.00	1.00	1.00
4%GFG	0.09	0.27	0.70	0.36	0.38	0.39
8%GFG	0.07	0.22	0.59	0.28	0.31	0.33
12%GFG	0.14	0.39	1.02	0.56	0.55	0.57

°C, 52 °C, and 58 °C, respectively, when compared to the neat binder. While it decreases by 72%, 71%, and 67%, respectively, under high stress (3.2 kPa).

Table 7.7: Temperature impact on the (J_{nr}) of asphalt binders at 3.2 kPa

Binder	**(J_{nr})**			**$J_{nr-modified}/J_{nr-neat}$**		
	46 °C	52 °C	58 °C	46 °C	52 °C	58 °C
Neat	0.29	0.84	2.21	1.00	1.00	1.00
4%GFG	0.10	0.30	0.86	0.35	0.36	0.39
8%GFG	0.08	0.24	0.72	0.28	0.29	0.33
12%GFG	0.16	0.46	1.26	0.55	0.55	0.57

The impact of geopolymer on the asphalt binder traffic level is depicted in Figure 7.7. The traffic loading was classified at a high PG temperature (58 °C) for the neat binder to explain the significant effect of geopolymer. These results depend on the J_{nr} values at high stress (3.2 kPa), whereby the traffic loading was classified into four class (S is standard traffic ($\leq$ 10 million ESALs), H is heavy traffic (10-30 million ESALs), V is very heavy traffic ($\leq$ 30 million ESALs), and E is extremely heavy traffic ($\geq$ 30 million ESALs) with standing traffic) [9]. The results showed that 4%GFG, 8%GFG, and 12%GFG binders have greater load traffic resistance than the neat binder. The results showed that temperature and geopolymer content have significant influences on MSCR results.

7.3.3 Statistical Analysis

A detailed statistical analysis can be used to develop a better understanding of the temperature and geopolymer content influences on the non-recoverable creep compliance (J_{nr}) and creep recovery (R) of modified asphalt binders. As a result, the response surface method (RSM), regression method, and analysis of variance (ANOVA) were used. J_{nr} and R responses data at different stresses (0.1 kPa and 3.2 kPa) were used in the analysis, and statistical models were developed. The factors and levels that were used in the statistical models are shown in Table 7.8. Minitab-17 was used to conduct all statistical analyses.

Response Surfaces Method (RSM) Analysis

RSM has been successfully used in the pavement field for a variety of purposes. RSM can be used to increase the sustainability and performance of various asphalt modifiers by modifying the asphalt binder and optimizing the modification mixing parameters [215].

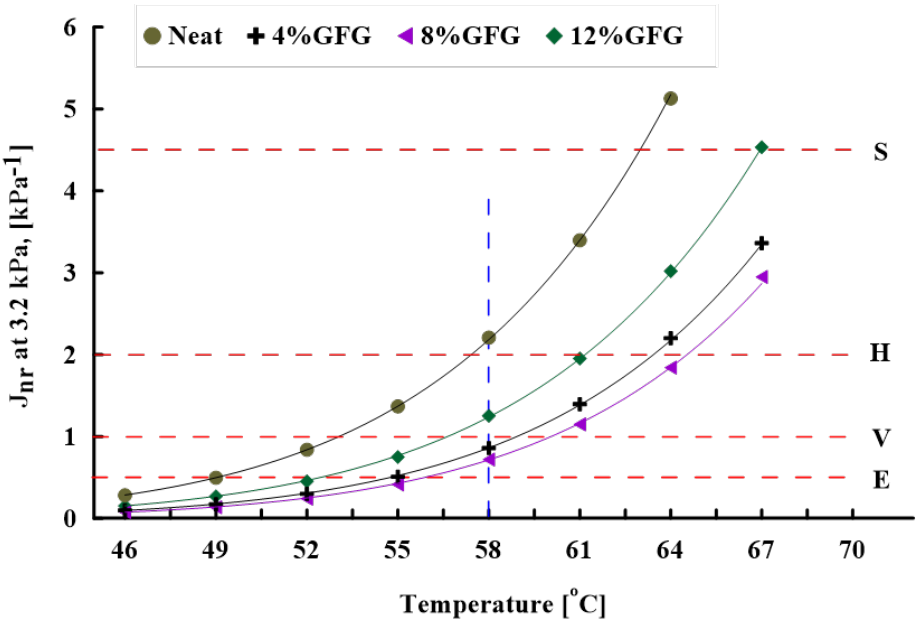

Figure 7.7: Effect of temperature and additives on the $J_{nr3.2}$

Table 7.8: The statistical models' factors and levels

Symbol	**Factor**	**Level**		
		Low	Center	High
T	Temperature (°C)	46	58	70
C	Geopolymer content (%)	4	8	12

RSM can be used to develop an empirical model for each response, such as a second-order model (Equation 7.1), and then take advantage of these models to evaluate the configuration of the design factors that provide optimal or at least acceptable response values [152].

$$y = \beta_0 + \beta_1 T + \beta_2 C + \beta_{12} TC + \beta_{11} T^2 + \beta_{22} C^2 \tag{7.1}$$

Where y is the response, T and C are the studied factors, β_0 is constant, and β^s are regression coefficients.

The RSM analysis was utilized in this work to analysis the effect of various parameters

(Temperature and geopolymer content) on the non-recoverable creep compliance (J_{nr}) and creep recovery percentage (R) of modified asphalt binders using response surfaces and contour plots, and to predict the $J_{nr0.1}$, $J_{nr3.2}$, $R_{0.1}$, and $R_{3.2}$ of asphalt binders. To study the effects of primary components and their interactions, a full-quadratic RSM analysis was used. Figures 7.8 and 7.9 describe the 3D response surface and contour plots for the non-recoverable creep compliance and creep recovery percentage of modified asphalt binders versus two factors (temperature and geopolymer content).

The 3D surface plots, as shown in Figures 7.8 and 7.9, revealed considerable change in the graph when the temperature increased, which indicated that temperature had a major impact on responses. Furthermore, the contour plots clearly demonstrated the significance of the investigated parameters. The influence of temperature was substantially greater than the geopolymer content, according to both the stepper surface and contour pattern. Table 7.9 presents the RMS models for predicting the J_{nr} and R of modified asphalt binder at different stresses (0.1 kPa and 3.2 kPa). A high R^2 was obtained with a range of 0.97-0.99. At varied geopolymer content and temperatures, these empirical equations can be used to predict $J_{nr0.1}$, $J_{nr3.2}$, $R_{0.1}$, and $R_{3.2}$.

Regression Model

The empirical models were developed using regression analysis to predict the $J_{nr0.1}$, $J_{nr3.2}$, $R_{0.1}$, and $R_{3.2}$ of asphalt binder modified using GFG with different percentages, 4%, 8%, and 12%. As a result, Equation 7.2 was provided as a basic linear model.

$$y = \beta_0 + \beta_1 T + \beta_2 C \tag{7.2}$$

Where y is the response, T and C are the factors that were independently investigated, β_0 is constant, and β_1 and β_2 are coefficients of regression.

Table 7.9 provides regression models for predicting the J_{nr} and R of the neat and modified asphalt binders under various stresses (0.1 kPa and 3.2 kPa), with an R^2 ranging from 0.8 to 0.94. At varied geopolymer content (4%GFG, 8%GFG, and 12%GFG) and temperatures (ranging from 46 °C to 70 °C with a 3 °C increment), these empirical equations can be used to predict $J_{nr0.1}$, $J_{nr3.2}$, $R_{0.1}$, and $R_{3.2}$.

Analysis of Variance (ANOVA)

ANOVA was applied in this study to investigate the significance influence of the two factors (geopolymer content and temperature) on the responses ($J_{nr0.1}$, $J_{nr3.2}$, $R_{0.1}$, and $R_{3.2}$) with

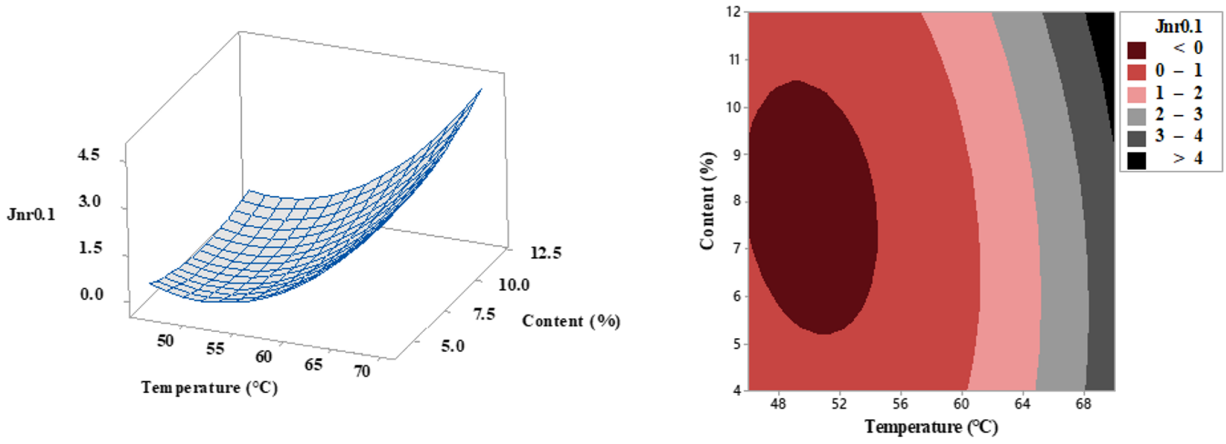

(a)

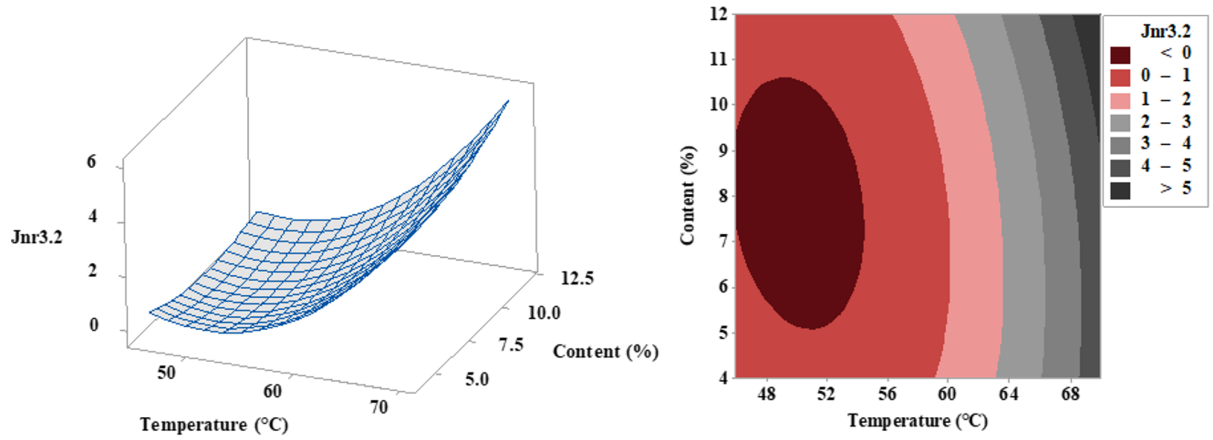

(b)

Figure 7.8: 3D response surface and contour plots for J_{nr} verses temperature and geopolymer content at different stresses (a) 0.1 kPa and (b) 3.2 kPa

a 95% level of confidence. Tables 7.10 and 7.11 summarize the results of the ANOVA analysis for the models.

The ANOVA results for RSM models in Table 7.10 indicated that all the studied factors are statistically significant except the interaction effect between temperature and geopolymer content (TC) for the $R_{3.2}$ model, which was insignificant with a P_{value} more than 0.05. While the ANOVA results for RM models in Table 7.11 indicated that the

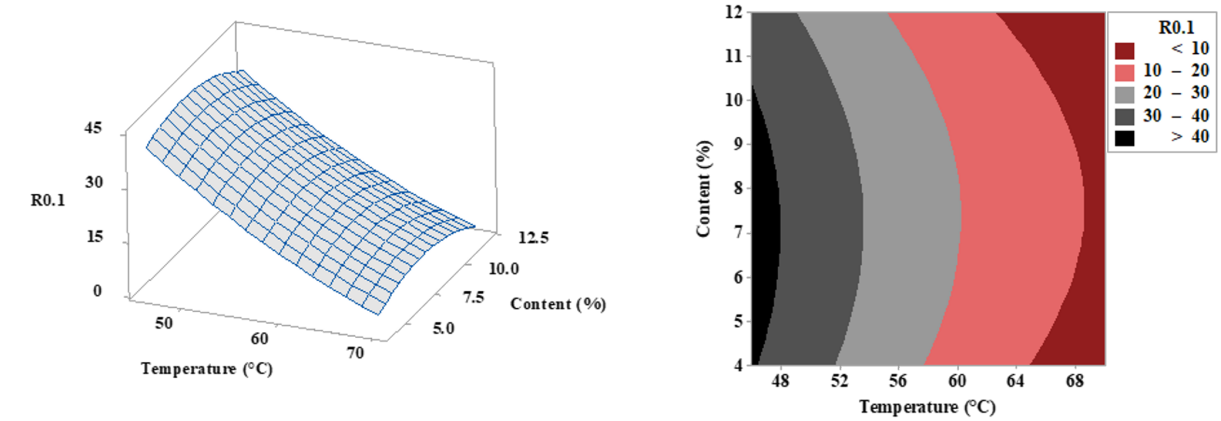

(a)

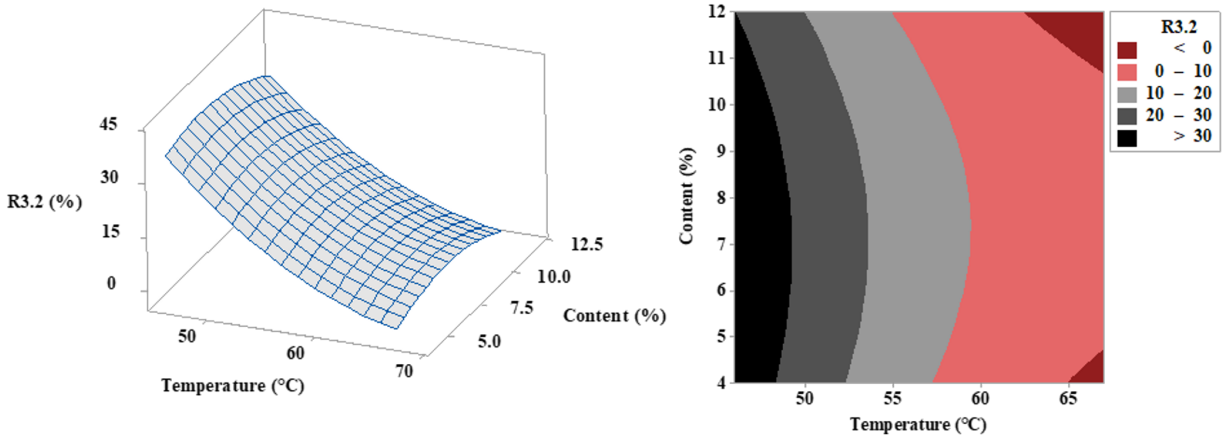

(b)

Figure 7.9: 3D response surface and contour plots for R verses temperature and geopolymer content at different stresses (a) 0.1 kPa and (b) 3.2 kPa

geopolymer content factor is insignificant for the $J_{nr0.1}$ and $J_{nr3.2}$ models, with P_{values} of 0.142 and 0.158, respectively. Besides, it can be observed from Tables 7.10 and 7.11 that temperature has a higher statistical significance than geopolymer content, because the P_{values} were substantially smaller. These results confirmed the observations of the 3D response surface and contour plots in Figures 7.8 and 7.9, whereby the impact of the temperature was much higher than the geopolymer content.

Table 7.9: Summary of the RM and RSM models

Model	**RM**				**RSM**						
	β_0	β_1	β_2	R^2	β_0	β_1	β_2	β_{12}	β_{11}	β_{22}	R^2
$\mathbf{J}_{nr3.2}$	-10.6	0.20	0.07	0.90	36.4	-1.33	- 0.89	0.01	0.01	0.03	0.99
$\mathbf{J}_{nr3.2}$	-8.39	0.16	0.06	0.80	29.08	- 1.05	- 0.76	0.01	0.01	0.03	0.97
$\mathbf{J}_{nr3.2}$	116.2	-1.74	-0.55	0.91	288.4	- 8.33	2.83	0.03	0.06	- 0.31	0.98
$\mathbf{J}_{nr3.2}$	108.7	-1.45	-0.45	0.94	168.8	- 4.04	3.85	0.02	0.02	- 0.33	0.99

Table 7.10: RSM-ANOVA analysis for $J_{nr0.1}$, $J_{nr3.2}$, $R_{0.1}$, and $R_{3.2}$

Response	**Factor**	**SS**	**DF**	**MS**	**F-value**	**P-value**	**Significance**
$J_{nr0.1}$	T	41.16	1	41.16	561.79	0.000	Yes
	C	1.05	1	1.05	14.29	0.001	Yes
	T^2	7.43	1	7.43	101.46	0.000	Yes
	C^2	1.13	1	1.13	15.40	0.001	Yes
	TC	0.77	1	0.77	10.54	0.004	Yes
$J_{nr3.2}$	T	65.96	1	65.96	680.01	0.000	Yes
	C	1.46	1	1.46	15.08	0.001	Yes
	T^2	11.93	1	11.93	122.99	0.000	Yes
	C^2	1.53	1	1.53	15.73	0.001	Yes
	TC	1.05	1	1.05	10.80	0.004	Yes
$R_{0.1}$	T	3425.70	1	3425.70	4421.16	0.000	Yes
	C	59.30	1	59.30	76.53	0.000	Yes
	T^2	33.36	1	33.36	43.05	0.000	Yes
	C^2	169.71	1	169.71	219.02	0.000	Yes
	TC	5.25	1	5.25	6.78	0.017	Yes
$R_{3.2}$	T	2780.70	1	2780.70	1233.56	0.000	Yes
	C	54.64	1	54.64	24.24	0.000	Yes
	T^2	110.37	1	110.37	48.96	0.000	Yes
	C^2	129.07	1	129.07	57.26	0.000	Yes
	TC	8.61	1	8.61	3.82	0.067	No

Table 7.11: RM-ANOVA analysis for $J_{nr0.1}$, $J_{nr3.2}$, $R_{0.1}$, and $R_{3.2}$

Response	Factor	SS	DF	MS	F-value	P-value	Significance
$J_{nr0.1}$	T	41.16	1	41.16	90.86	0.000	Yes
	C	1.05	1	1.05	2.31	0.142	No
$J_{nr3.2}$	T	65.96	1	65.96	95.71	0.000	Yes
	C	1.46	1	1.46	2.12	0.158	No
$R_{0.1}$	T	3425.70	1	3425.70	366.07	0.000	Yes
	C	59.30	1	59.30	6.34	0.019	Yes
$R_{3.2}$	T	3056.82	1	3056.82	202.87	0.000	Yes
	C	71.81	1	71.81	4.77	0.041	Yes

7.3.4 LAS Results Analysis

Figure 7.10 (a) represents the relationship between stress and strain for neat and modified asphalt binders. The results showed that the asphalt binder modified by 4%, 8%, and 12% of geopolymer achieved the highest shear stress compared with the neat binder. When compared to the modified asphalt binders, the neat binder exhibits a rapid decrease in C(t), as shown in Figure 7.11. Thus, it is observed that the damage intensity of a neat binder is lower than the binders 4%GFG, 8%GFG, and 12%GFG at the same reduction in C(t), which could be related to the decrease in the shear stress, as shown in Figure 7.10 (a). A similar pattern was noted in Figure 7.10 (b), whereby the stored PSE is increased for all modified asphalt binder at different strains. Also, the 4%GFG binder achieved the highest PSE than other binders at different strains.

Figure 7.12 (a, b) illustrated the impact of geopolymer content on the fatigue life (N_f) of neat and modified asphalt binders, whereby the N_f was calculated considering the strain at different percentages (50%, and 75%) of shear stress and stored PSE. The results showed that 4%GFG achieved the highest fatigue life compared with the neat, 8%GFG, and 12%GFG binders, as depicted in Figure 7.12 (a, b). This finding supports the usage of glass powder/fly ash and based-geopolymer modified asphalt binder to improve asphalt binder fatigue performance.

7.4 Conclusions

This research aimed to evaluate and predict the performance of asphalt binder modified with glass powder/fly ash-based geopolymer at high temperatures. The following are some

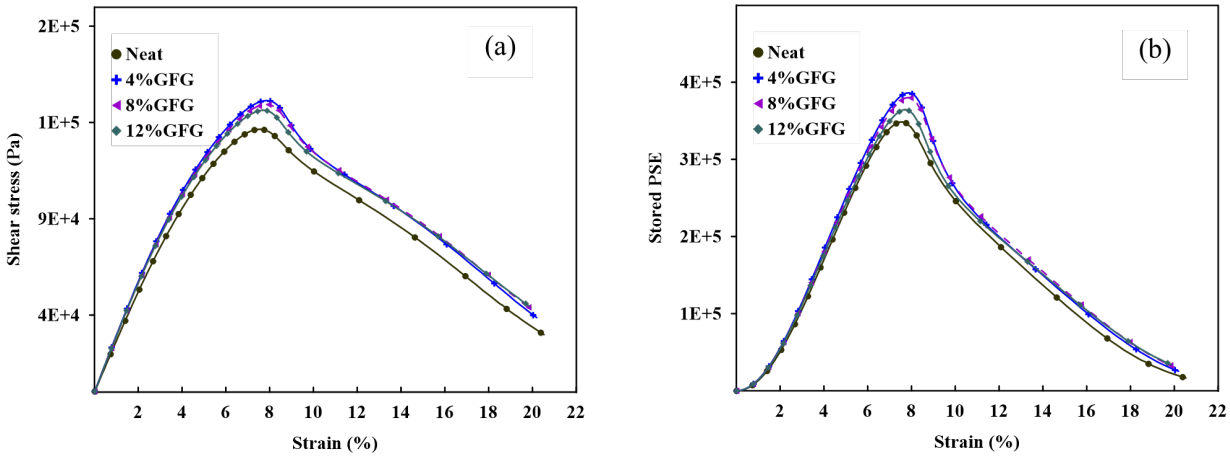

Figure 7.10: Geopolymer effects on (a) shear stress and (b) stored PSE

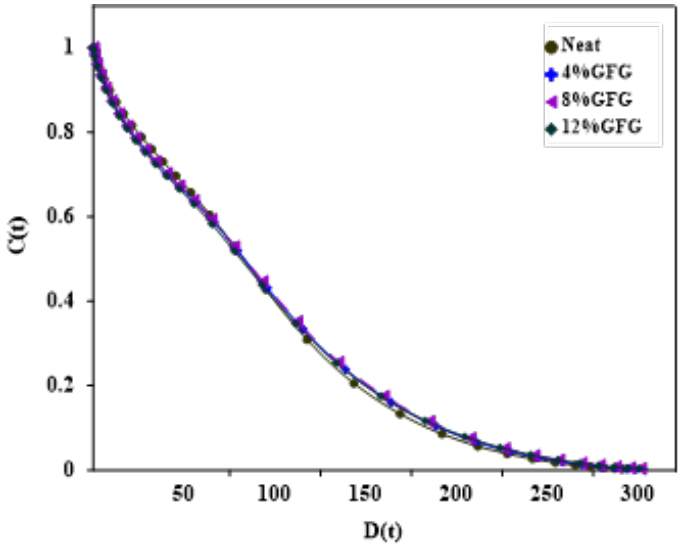

Figure 7.11: Geopolymer influence on the damage behavior of asphalt binder

possible conclusions:

- The shear complex modulus at 52 °C increased from 9.48 kPa to 22.32 kPa, and the phase angle decreased from 76.9° to 71.6° by adding 8%GFG. This indicates that the behavior becomes more elastic with the addition of the geopolymer.
- The addition of 8% GFG increased the creep recovery of asphalt binder at 52 °C by

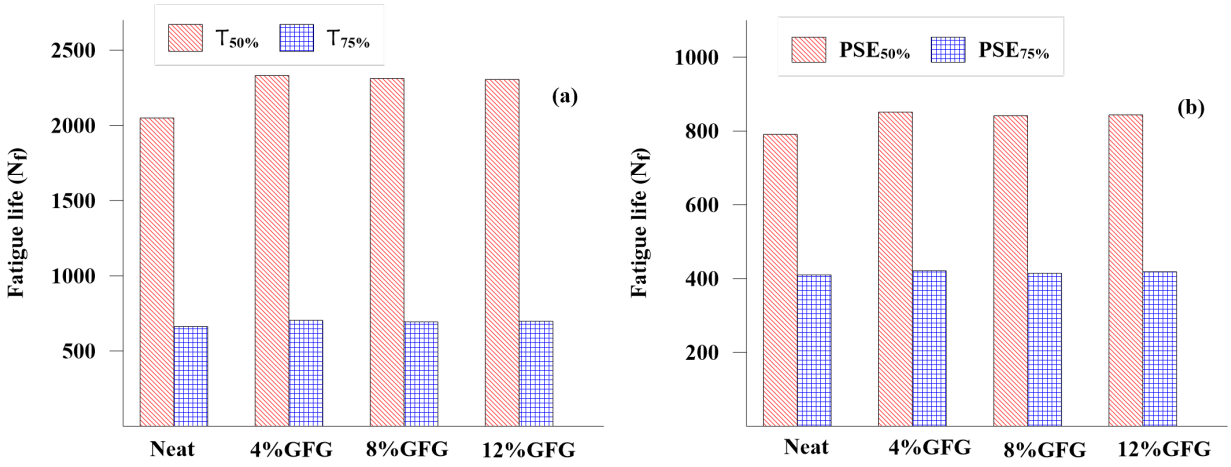

Figure 7.12: Influence of geopolymer on fatigue life at different percentages of (a) shear stress and (b) stored PSE

74% and 188% under 0.1 kPa and 3.2 kPa stresses, respectively, indicating that the elastic behavior is enhanced.

- The addition of 8% GFG decreased the non-recoverable creep compliance of asphalt binder at 52 °C by 69% and 71% under 0.1 kPa and 3.2 kPa stresses, respectively. This finding revealed that the geopolymer enhanced the rutting resistance. The analyse of the MSCR results using ANOVA test have shown that both the geopolymer content and the temperature have statistically significant impact on the responses ($J_{nr0.1}$, $J_{nr3.2}$, $R_{0.1}$, and $R_{3.2}$). The exceptions in the significance analysis were the interaction between temperature and geopolymer content in the $R_{3.2}$ model, as well as the geopolymer content factor for the $J_{nr0.1}$ and $J_{nr3.2}$ models. These two exceptions were statistically insignificant.

- The ANOVA analysis concluded that temperature has higher statistical influence on the MSCR results than the geopolymer content as the P-values associated with temperature were substantially lower than the ones associated with geopolymer content.

- The percent recovery and non-recoverable creep compliance of asphalt binder modified with geopolymer can be predicted using RSM with excellent R^2 values (95%) under different stresses and temperatures.

- The addition of GFG modifier to the asphalt binder could enhance the fatigue performance. The 4%GFG binder exhibited the highest fatigue life compared to the

8%GFG and 12%GFG binders.

- Overall, glass powder could be used as an aluminosilicate source during the preparation of geopolymer as an asphalt modifier, which has an essential influence on the rheological and performance of asphalt binder.

Chapter 8

Predicting the Recovery and Non-Recovery Performance of Asphalt Binders Using Artificial Neural Networks

This chapter is based on the following article, which will be submitted to the Canadian Journal of Civil Engineering. "Predicting the Recovery and Non-Recovery Performance of Asphalt Binders Using Artificial Neural Networks," by A. Hamid, H. Baaj, and M. El-Hakim (2022).

Abstract

The purpose of this research was to use artificial neural networks (ANNs) to predict the recovery and non-recovery performance of asphalt binders based on mechanical test parameters and asphalt binder properties. The study involved rheological testing of asphalt binders using a dynamic shear rheometer (DSR), which included the production of 11 laboratory-blended asphalt binders with a total of 880 data points. Also, Multiple Stress Creep Recovery (MSCR) was performed to evaluate the recovery and non-recovery properties of asphalt binders. The ANN model was developed using five input parameters (temperature, frequency, storage modulus, loss modulus, and viscosity) and one hidden layer with five neurons. The results pointed out that the hybrid and 4%SBS binders achieved the highest ability to resist extremely heavy traffic and to recover the deformation with 60.1%

and 85.5% at 46 °C, respectively, compared with the other modified asphalt binders. Excellent R-values for the total data set of 0.937, 0.997, 0.985, and 0.987 for $J_{nr3.2}$ of unaged binder, $J_{nr3.2}$ of aged binder, $R_{3.2}$ of unaged binder, and $R_{3.2}$ of aged binder, respectively. Therefore, the ANNs model is appropriate to predict the $R_{3.2}$ and $J_{nr3.2}$ using unaged or aged binders at different temperatures.

8.1 Introduction

Rutting is a common sign of distress that affects the road network's serviceability and quality. It is a permanent deformation that occurs in the traffic direction because of unrecoverable strain accumulated by repetitive loads applied to the asphalt pavement [109]. Due to the combined effects of viscoelastic characteristics and shear loads on the HMA layer, asphalt is highly susceptible to rutting. As the temperature increases, the asphalt binder decreases the ability to elastically recover from deformation, increasing the sensitivity to permanent deformation. In recent decades, there has been attention to modified asphalt binder using different modifiers to enhance the rutting performance. The viscoelastic properties of asphalt binders can be improved by modifying the asphalt binder using different modifiers. Modification, on the other hand, adds to the complexity of binders' behavior; thus, substantial laboratory testing is required before field application to establish the best solutions.

The Multiple Stress Creep-Recovery (MSCR) test was developed to measure the binder's nonlinear reaction and to link that response to rutting in asphalt mixtures [64]. The MSCR test has long been used to predict how polymer-modified asphalt binders may affect creep recovery [246, 226, 29, 62]. In the field of modified and unmodified asphalt binders, the MSCR test is also efficiently conducted and designed to be an indicator of rutting performance [111]. The MSCR test consists of a series of creep and recovery cycles performed at various stress levels. The idea was that by removing shear stress from the creep section, the viscoelastic strain created in the creep component could be recovered, allowing the permanent strain to be separated from the overall strain, which could be used to predict field rutting [139]. The MSCR test was used to determine non-recoverable creep compliance (J_{nr}) and percent recovery (R). The J_{nr} had a good correlation with the HMA performance test results and can thus be used to characterise asphalt binders to address HMA rutting characteristics [237]. Tabatabaee and Tabatabaee (2010) [201] reported that the J_{nr} was highly correlated to the compliance measured from unconfined dynamic creep, with R^2 values over 80%. While Dreessen Gallet (2012) [74] noted that the J_{nr} may be a better choice than $G^*/\sin\delta$ and/or the softening point, whereby it corresponds better to

mix rutting performance as measured by the French rutting test.

Several methods have been developed to predict asphalt pavement performance to eliminate laboratory tests for individual mixes, which are expensive and time-consuming. Using a reliable calibrated model to predict the effects of additives on the behavior of asphalt binder can significantly reduce operating and testing expenses. Recently, Artificial neural networks have been used in many disciplines of civil engineering, such as water supply engineering [58], pavement materials [81, 77] and pavement structure [168]. Plati et al. (2016)[168] summarized some advantages that make ANN a powerful problem-solving tool that could be used to develop complex models through data mining. The ANNs model was also used to predict the mechanical properties, creep compliance, fatigue and rutting performance of asphalt concrete. Baldo et al. (2018) [40] used artificial neural networks to predict Marshall stability, flow, quotient, and stiffness modulus of asphalt concrete. Seven input parameters with one hidden layer and ten artificial neurons were applied to predict one output. The results indicated that the ANNs model could be used to predict the mechanical properties of asphalt concrete, whereby the developed models were excellent with coefficients of correlation ranging from 0.910 to 0.988. Esfandiarpour and Shalaby (2017) [81] performed ANNs to calibrate the creep compliance for different asphalt mixtures at different test temperatures (0 °C, -10 °C, and -20 °C). It was noted that the ANNs model has the highest reliability and is considered as an alternative method to predict creep compliance values.

Meanwhile, the complex mechanism of fatigue behavior under various loading and climate conditions complicated the modelling of the fatigue life of asphalt mixtures using an empirical model [103]. Recently, using ANNs proved to be an effective tool to predict the fatigue life of asphalt binder mixtures [228, 206]. Xiao et al. (2009) [228] investigated the possibility of using ANNs to predict the fatigue life of rubberized asphalt binder mixtures containing Reclaimed Asphalt Pavement (RAP). The results indicated that the ANNs produced an accurate and precise prediction of the fatigue life compared to the traditional statistical methods. Tapkin (2014) [206] predicted the fatigue life of asphalt mixtures that contained fly ash as a filler using neural networks. It was noted that ANN resulted in accurate and precise modelling of fatigue life by utilizing changes in the physical properties of asphalt mixtures. Development of ANN models to accurately predict HMA fatigue life would result in substantial time and cost savings by reducing laboratory testing.

Moreover, the ANNs model was used to predict the rutting performance of asphalt concrete. Kamboozia et al. (2018) [124] studied the possibilty of using the viscoelastic parameters and ANNs model to predict the rutting depth of asphalt concrete using dynamic creep test. The viscoelastic properties were collected from creep diagrams, and an artificial neural network was used to train and develop a rut depth prediction model for asphalt

concrete. The developed ANNS used 560 specimens, whereby 70% of the data was used for training and the remaining 30% for validation and testing. The results showed that by utilizing the effective parameters, the ANNs model can be used to estimate the creep behavior and rut depth of asphalt concrete without the need for costly and time-consuming testing.

The ANNs model was also used to predict the rheological behavior, fatigue and rutting performance of asphalt binder [220, 244, 22, 216]. Venudharan and Biligiri (2017) [220] used the ANNs model to predict the rutting performance of asphalt binder using the gradation of crumb rubber, mechanical test parameters, and the properties of binder. A DSR test was used to characterise 18 different asphalt binders. The ANN architecture used a back-propagation learning algorithm with scaled conjugate gradient (SCG) as the training technique, with two hidden layers of seven and three neurons, respectively. The results indicated that the ANNs model is a significant method to predict the performance of asphalt binder with R vaule of 0.997, 0.994, and 0.977 for $G^*/\sin\delta$, η , and $\tan\delta$, respectively. Ziari et al. (2018) [244] used ANNs and regression models to predict the rutting performance of a carbon nanotube-modified asphalt binder. A multilayer feed-forward back-propagation method with 480 experimental data points was used to predict the rutting parameter, whereby 60% of the data was used for training, while 40% was used for validation and testing the model. The results showed that the ANN method outperformed multiple regression and linear regression in predicting rutting performance, with R^2 values of 0.997, 0.819, and 0.420, respectively.

Alas and Ali (2019) [22] utilized ANNs method to predict the shear complex modulus, phase angle, storage modulus, and loss modulus using temperature, frequency, and polymer contents as input parameters. A total of 252 data sets were randomly divided into two groups, with 70% of the empirically observed data being used to train the model and 30% of the data being used to test the model. The results showed that the developed model for the shear complex modulus is excellent with high R^2 values for training and testing data, 0.996 and 0.971, respectively. While the testing data for phase angle and storage modulus achieved the least R^2 with values less than 0.9. The model's poor prediction performance for the testing data suggested that it was unable to learn the complexity of the data. Uwanuakwa et al. (2020) [216] conducted the ANNs to predict the rutting and fatigue performance of unaged and aged asphalt binders. A frequency sweep test using the dynamic shear rheometer (DSR) was performed on the 8 mixes of asphalt binders to measure the complex shear modulus and phase angle at various temperatures. According to the results, the model performed better in estimating the rutting parameter than the fatigue parameter. Furthermore, unaged input variables have a higher level of predictability when it comes to the fatigue parameter.

Table 8.1: Fly ash chemical composition [106]

Constituent	SO_2	Al_2O_3	Fe_2O_3	CaO	MgO	SO_3	Na_2O
Fly ash	57.2%	23.5%	3.8%	9.3%	1.0%	0.2%	2.43%

The literature on the use of artificial neural networks (ANNs) in pavement engineering demonstrates that ANNs could be used to determine and understand the performance of asphalt binders and mixtures based on material characteristics and mechanical test data. This study aimed to predict the recovery (R) and non-recovery (J_{nr}) behavior of asphalt binder, considering the effects of temperatures, frequencies, and additives on the viscoelastic properties of the asphalt binder.

8.2 Methodology

8.2.1 Materials and Methods

In this investigation, 11 mixes of fly ash, Styrene-butadiene-styrene (SBS) polymer, fly ash-based geopolymer, fly ash and glass powder-based geopolymer modified asphalt binder (PG58-28) were utilized to build the database. Table 8.1 presents the chemical composition of fly ash (Class F) satisfies $SiO_2 + Al_2O_3 + Fe_2O_3 \geq 70\%$ according to ASTM C618-17a. Many scholars advocate that low calcium fly ash (Class F) be utilized because it includes more silica and alumina than high calcium fly ash (Class C) [110, 92].

Geopolymer is prepared using alkali activators and aluminosilicate source, such as fly ash and glass powder. Alkali activators included Na_2SiO_3 and NaOH at a concentration of 8 molar. The NaOH solution was prepared one day before mixing with the aluminosilicate source to make the geopolymer. Fly ash and geopolymer additives were blended with asphalt binder in various contents at 140 °C ± 5 for 60 minutes using a mechanical shear mixer at a speed of 2000 r/min. While the SBS was mixed with asphalt binder using the high shear mixer at a speed of 2000 r/min and a temperature of 170 °C ± 5 for 60 minutes. Figure 8.1 presents the preparation of modifiers, asphalt binder mixing, and testing. Following the mixing procedure, all asphalt binders were exposed to the short term aging using rolling thin-film oven (RTFO) for 85 minutes at 163 °C, as depicted in Figure 8.1.

The Dynamic Shear Rheometer (DSR) was used to investigate the rheological behavior and recovery and non-recovery properties of asphalt binder at high temperatures from 46

to 70 °C, with 6 °C increments. A frequency sweep test was conducted to investigate the effect of temperatures, frequencies, and additives on the viscosity and storage and loss modulus using a 25 mm diameter plate and a 1 mm gap. The tests were performed at sixteen frequencies ranging from 0.159 H_z to 15 H_z. Two samples were tested, and the average was identified as the test result for each temperature. While Multiple Stress Creep Recovery (MSCR) was performed to evaluate the influence of temperatures, stresses, and additives on the recovery and non-recovery properties of asphalt binders using a 25 mm diameter plate and a 1 mm gap. Two samples were tested, and the average was identified as the test result for each temperature. The test was conducted using (1 s) for creep and (9 s) for recovery. While the average percent recovery (R), and non-recoverable creep compliance (J_{nr}) were calculated using Equations 8.1 and 8.2, respectively.

$$R = (\frac{\varepsilon_1 - \varepsilon_{10}}{\varepsilon_1}) \times 100 \tag{8.1}$$

where ε_1 is accumulated strain after 1 s., ε_{10} is residual strain after 10 s.

$$J_{nr} = \frac{\varepsilon_{10}}{applied\ stress} \tag{8.2}$$

R is the recovery percentage and J_{nr} is non-recoverable creep compliance.

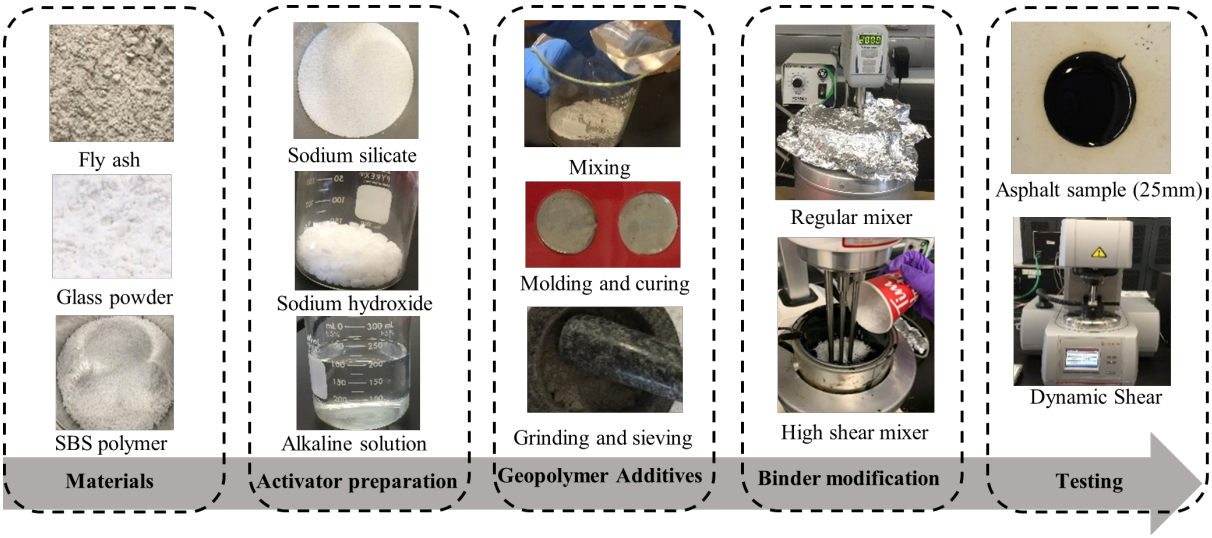

Figure 8.1: Additive's preparation and testing

8.2.2 Artificial Neural Networks Modelling

Artificial Neural Network (ANN) is a mathematical model that formed of elements called neurons. This model consists of three groups of rules: multiplication, summation, and activation. In the multiplication stage, the inputs are weighted by multiplying each input value with its individual weight. After that, all weights and bias are summed in the summation stage. Finally, the sum of previously weighted inputs and bias is passing through the transfer function, acting as the activation function. In this study the models developed for recovery and non-recovery behavior of asphalt binder, as shown in Figure 8.2, involved of three layers: an input layer, a hidden layer, and an output layer. The dataset for these layers was based on experimental observations from frequency sweep test and MSCR test. The developed ANNs used 880 experimental data points, whereby 70% of the data was used for training and the remaining 30% for validation and testing.

The feedforward neural networks were considered in this study. The learning of the network in this form of ANN is supervised, which means that the associated output (target) for each input vector is known. The learning phase entails adjusting the ANN's connections such that, for each input, the network returns a computed value that is as close to the target as possible. The developed ANNs model considered the effects of external factors (Temperature and frequency) on the rheological properties (storage modulus, loss modulus, and shear viscosity) of neat and modified asphalt binder. These factors and properties were considered as input parameters in the ANNs model to predict each target ($J_{nr3.2}$ and $R_{3.2}$). The developed model has one hidden layer with five neurons, whereby the input to each neuron is a summation of all weighted connections between the input and the neuron in the hidden layer [170]. The weighted sum is denoted as (a) and represented in Equation 8.3.

$$a = \sum_{i=1}^{N} w_i x_i + b \tag{8.3}$$

N represents the number of neurons in the input layer, w_i is the weight factor, x_i is the input vector, and b is the bias term.

Then, the transfer or activation function was used to transfer the neuron to the new output. In this study, the sigmoid function is used as activation function. The final output of the neuron is given in the Equation 8.4.

$$output = f(a) = f(\sum_{i=1}^{N} w_i x_i + b) = f(\sum_{i=1}^{N^0} w_i x_i^0 + w_0) \tag{8.4}$$

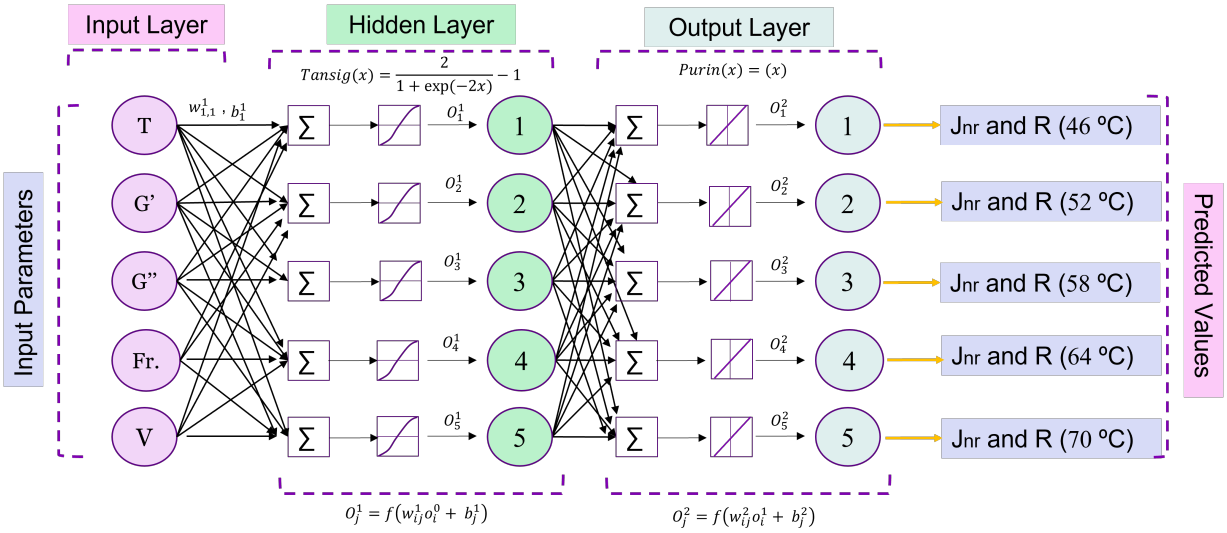

Figure 8.2: ANN model for predicting recovery and non-recovery performance of asphalt binder

In this study, the sigmoidal function is used as a transfer function which has the following expression, Equation 8.5:

$$f(a) = \frac{2}{1 + e^{-2a}} - 1 \tag{8.5}$$

For the multiple neurons, j^{th} in the layer l^{th} the output of the neuron is described in the Equations 8.6 and 8.7.

$$a_j^l = \sum_{i=1}^{N^{l-1}} w_{ij}^l o_i^{l-1} + w_{j0}^l \tag{8.6}$$

$$o_j^l = f_j(a_j^l) = f_j^l(\sum_{i=1}^{N^{l-1}} w_{ij}^l o_i^{l-1} + w_{j0}^l) \tag{8.7}$$

Equation 8.8 can be used to describe the output of the network at the last layer.

$$y_j = o_j^l \tag{8.8}$$

Back-Propagation Calculations

The most common approach for training a supervised neural network is backpropagation. The purpose of this method is to iteratively modify the weights in the network to minimise output error and provide the desired result [170]. Backpropagation is a gradient-descent method that finds an optimal solution by minimising first-order derivatives. The delta rule is used to adjust the weights in the network, whereby the output error can be computed using Equation 8.9.

$$E_p = \frac{1}{2}\sum_{j=1}^{N^L}(t_{pj} - y_{pj})^2 \tag{8.9}$$

Where E is the error, t is the target output, y is predicted output. The sum of the errors in the feedforward network is expressed in Equation 8.10.

$$E = \sum_{p=1}^{p} E_p = \frac{1}{2}\sum_{p=1}^{p}\sum_{j=1}^{N^L}(t_{pj} - y_{pj})^2 \tag{8.10}$$

The error is minimized by taking the partial derivative of the total error with respect to the weights in the network using Equation 8.11.

$$\frac{\partial E}{\partial w_{ij}^l} = \sum_{p=1}^{p}\frac{\partial E_p}{\partial w_{ij}^l} \tag{8.11}$$

Using the chain rule, the partial derivative is divided into two parts as expressed in Equation 8.12.

$$\frac{\partial E_p}{\partial w_{ij}^l} = \frac{\partial E_p}{\partial a_{pj}^l}\frac{\partial a_{pj}^l}{\partial w_{ij}^l} \tag{8.12}$$

$$\frac{\partial a_{ij}^l}{\partial w_{ij}^l} = \frac{\partial}{\partial w_{ij}^l}\sum_{k=1}^{N^l} w_{jk}^l o_{pk}^{l-1} + w_{j0}^l = o_{pk}^{l-1} \tag{8.13}$$

$$\frac{\partial E_p}{\partial w_{ij}^l} = \frac{\partial E_p}{\partial a_{pj}^l} o_{pi}^{l-1} \tag{8.14}$$

$$\frac{\partial E_p}{\partial a_{pj}^l} = \frac{\partial E_p}{\partial o_{pj}^l} \frac{\partial o_{pj}^l}{\partial a_{pj}^l} \tag{8.15}$$

$$\frac{\partial E_p}{\partial a_{pj}^l} = (y_{pj} - t_{pj}).\nabla f(a_{pj}^l) \tag{8.16}$$

Then,

$$\frac{\partial E_p}{\partial w_{ij}^l} = (y_{pj} - t_{pj}).\nabla f(a_{pj}^l).o_{pi}^{l-1} \tag{8.17}$$

At each iteration, the gradient can be evaluated, and the weight values can be optimised in this manner. In this study, the Levenberg-Marquardt (LM) algorithm was used to train the ANNs model. The LM algorithm approximates the Hessian matrix (H) using Jacobian matrix (J) which contains the first derivative of error (E_p) with respect to the weight, as expressed in Equation 8.18. The weight update is given in Equation 8.19.

$$H \approx J^T J \tag{8.18}$$

$$\triangle w = w - J^T (J^T J + uI)^{-1} \tag{8.19}$$

Where I is the identity matrix. At each iteration, the weight is changed using the following equation:

$$w_t = w_{t-1} + \triangle w \tag{8.20}$$

8.2.3 Data Analysis

The data from the DSR and MSCR tests on the eleven asphalt binders were modelled using MATLAB, whereby the data divided into three main parts, training, validation, and test. The training set often contains the majority of the data, while the validation and test sets typically contain smaller quantities of data. 70% of the total data was used to train the neural network, 15% was used to validate the neural network, and 15% was utilized for testing the capability of the network to predict the output. To train neural networks, Scaled Conjugate Gradient (SCG), Levenberg-Marquardt (LM), and Bayesian

Regularization (BR) were performed to implement a backpropagation learning process in a feed-forward neural network with one hidden layer and five neurons. After selecting the parameters and calculating the magnitudes of the weights and biases, the neural network was trained using the software's training data. The weights and biases of the training phase were evaluated after the training session based on the difference between measured and predicted values. Consistently, the test data set was used by the software to understand the neural network's performance once it had been validated.

8.3 Results and Discussion

8.3.1 Temperatures and Frequencies Effects on the Viscosity

Figure 8.3 demonstrate the effects of different temperatures (46 °C, 52 °C, 58 °C, 64 °C, and 70 °C) and frequencies (0.1 H_z and 10 H_z) on the shear viscosity of neat and modified asphalt binder. When comparing the modified asphalt binders to the neat asphalt binder, the results showed that the modified asphalt binders had the highest viscosities. Larger molecules present in a fluid can induce increased viscosity, which can be produced by the formation of chain networks in the asphalt binder mixture [147]. At high frequency (10 rad/sec), the hybrid binders achieved the highest viscosity at 46 °C, 52 °C, and 58 °C, while 4%SBS binder has the highest viscosity at 64 °C, and 70 °C. At low frequency (0.1 rad/sec), the 4%SBS binder has the highest viscosity compared with the other modifiers at different temperatures. In conclusion, it was observed that the viscosity of asphalt binder is significantly dependent on the effect of additives on asphalt binder characteristics, temperature, and frequency.

8.3.2 Temperatures and Frequencies Effects on the Storage and Loss Modulus

The 3D plot in Figure 8.4 presents the effect of external factor (temperature and frequency) on the storage and loss modules of the unaged neat and GF-modified asphalt binders. G' and G'' values increased geometrically when frequency increased, however both G' and G'' values dropped as temperature increases. The 8%GF binder achieved the highest values of G' and G'' compared to the neat and other modifiers. It is evident that adding geopolymer increases both G' and G'' significantly, enhancing the asphalt binder's ability to recover and resist the deformation. Figure 8.5 shows the impact of temperatures, and frequencies on

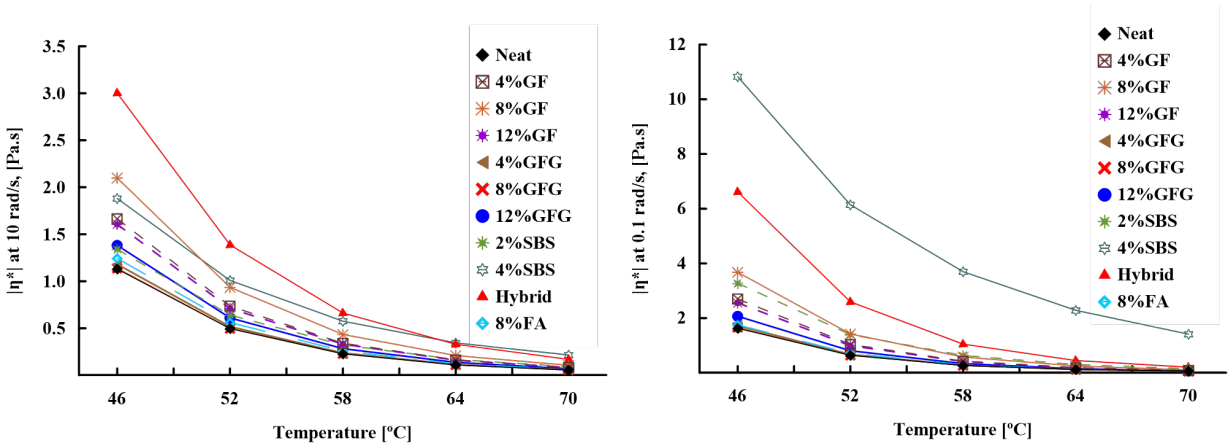

Figure 8.3: Effects of temperatures and frequencies on the shear viscosity

the G′ and G″ of glass powder/fly ash-based geopolymer (GFG) modified asphalt binder. The results indicated that the GFG modifier with different percentages (4%, 8%, and 12%) has a slightly effect on the G′ and G″ of the neat binder compared with GF modifier, as demonstrated in Figure 8.4.

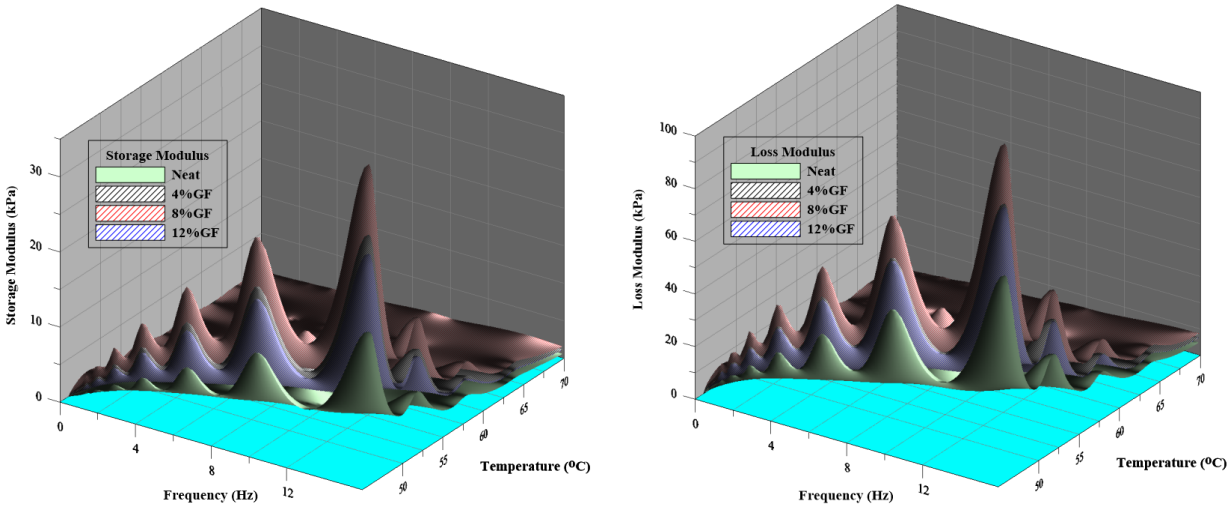

Figure 8.4: Temperatures and frequencies effects on the G′ and G″ of GF

Figure 8.6 demonstrates the influence of temperatures and frequencies on the G′ and G″ of the 8%FA, 2%SBS, 4%SBS, and hybrid asphalt binders. The hybrid binder achieved the highest values of G′ and G″ compared with the other modifiers at different temperatures

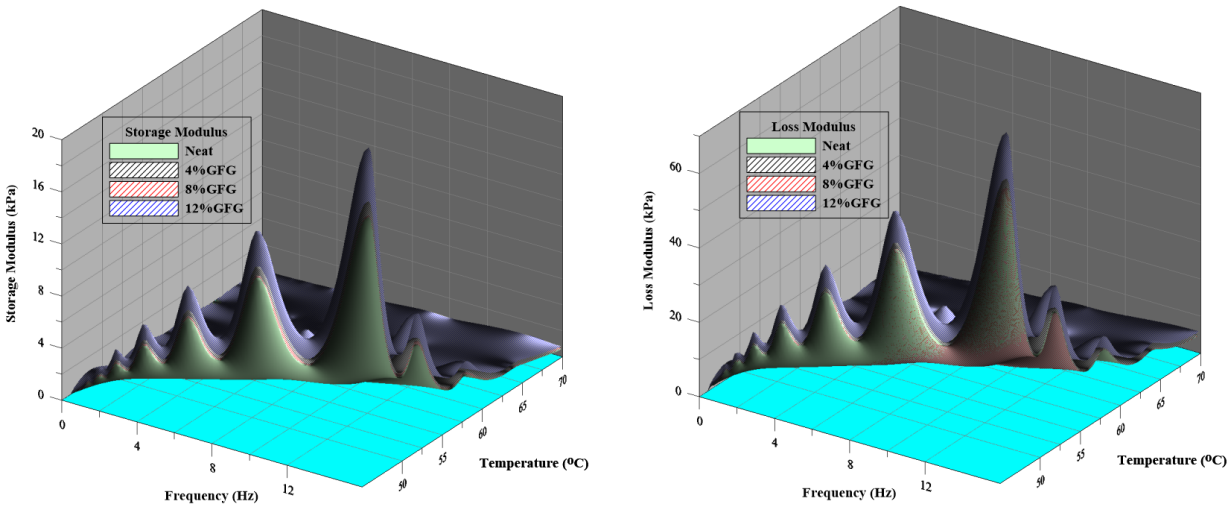

Figure 8.5: Temperatures and frequencies effects on the G′ and G″ of GFG

and frequencies. This indicated that the hybrid binder has the highest recovery resistance for deformations. While the 4%SBS binder exhibited more elastic than neat, 8%FA, 2%SBS binders at low and high frequencies, with the highest value of G′. Besides, the 8%FA binders more viscous than the neat and 2%SBS, with the highest value of the G″. Figures 8.4, 8.5, and 8.6 show that the neat and modified asphalt binders have a higher G″ than G′. It's possible that this is due to the lack of strong interactions between individual molecules [147].

8.3.3 MSCR Test Results

Table 8.2 presents the MSCR test result of neat and modified asphalt binders at different temperatures. The influence of additives and temperatures on the non-recovery and recovery properties of asphalt binder was investigated. Also, the effect of additives on the traffic level was also evaluated. According to the J_{nr} values under high stress (3.2 kPa), the traffic loading was classified into four groups: S is standard traffic ($\leq$ 10 million ESALs), H is heavy traffic (10-30 million ESALs), V is very heavy traffic ($\leq$ 30 million ESALs), and E is extremely heavy traffic ($\geq$ 30 million ESALs) with standing traffic [9]. Apart from the neat asphalt binder properties, the modifiers enhance the asphalt binder's resistance to traffic loading. It was observed that the hybrid and 4%SBS binders achieved the highest ability to resist extremely heavy traffic compared with the other modified asphalt binders. Furthermore, among the other geopolymer modifier percentages, the geopolymer

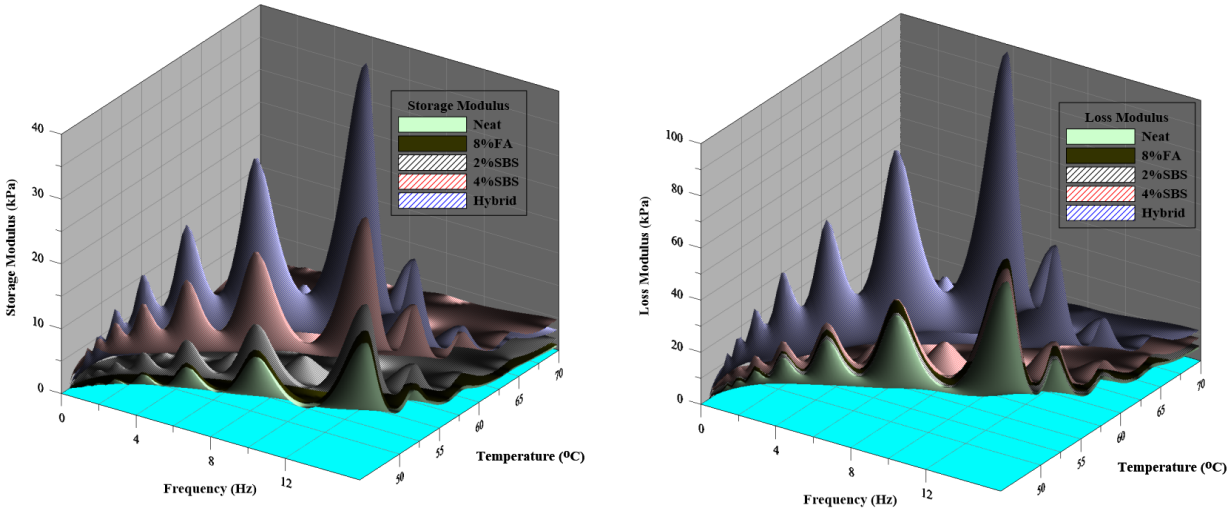

Figure 8.6: Temperatures and frequencies effects on the G′ and G″ of SBS and FA binders

modified asphalt binders with 8%GF and 8%GFG have the highest creep recovery at 46 °C, with 39.5% and 39.8%, respectively. While the hybrid and 4%SBS binders have the highest ability to recover the deformation with 60.1% and 85.5% at 46 °C, respectively. In summary, additives and temperatures have significant effects on the non-recovery and recovery properties of asphalt binder.

8.3.4 ANNs Model Results

The results of frequency sweep and MSCR test indicated that various parameters have significant effects on the neat and modified asphalt binders. So, five input parameters were considered, temperature (T), frequency (f), storage modulus (G′), loss modulus (G″), and viscosity (V). A total of 880 data points were used for ANNs models to predict the two outputs, percent recovery at 3.2 kPa ($R_{3.2}$) and non-recovery at 3.2 kPa ($J_{nr3.2}$) of unaged and RTFO asphalt binders at different temperatures. To establish the optimal backpropagation learning algorithm for the study, the LM, BR, and SCG training algorithms were used in a feed-forward, single-hidden-layer neural network of 5 neurons. The best neural network was built using the training techniques. Figure 8.7 shows the statistical fit the model measurements R-value for the outputs using three different training procedures. The LM and BR training methods, with R values more than 0.90, did higher R values than the SCG algorithm. The LM training technique is the better ANN for the study data, according to the results.

Table 8.2: Temperature effect on the $J_{nr3.2}$ and $R_{3.2}$ of asphalt binders

Asphalt Binders	**MSCR**	**46 °C**		**52 °C**		**58 °C**		**64 °C**		**70 °C**	
	(grade)	$\mathbf{J_{nr3.2}}$	$\mathbf{R_{3.2}}$	$\mathbf{J_{nr3.2}}$	$\mathbf{R_{3.2}}$	$\mathbf{J_{nr3.2}}$	$\mathbf{R_{3.2}}$	$\mathbf{J_{nr3.2}}$	$\mathbf{R_{3.2}}$	$\mathbf{J_{nr3.2}}$	$\mathbf{R_{3.2}}$
Neat (PG58-28)	S58	0.29	21.2	0.84	8.72	2.21	1.98	5.13	0.00	10.7	0.00
4%GF(PG64-28)	H58	0.13	33.4	0.39	18.8	1.09	6.84	2.69	1.26	6.04	0.00
8%GF(PG70-28)	V58	0.09	39.5	0.27	24.7	0.79	10.6	1.97	2.84	4.56	0.00
12%GF(PG64-28)	H58	0.12	34.6	0.38	19.3	1.08	7.11	2.64	1.41	5.83	0.00
4%GFG (PG64-28)	V58	0.10	35.2	0.30	20.6	0.86	8.19	2.20	1.69	5.04	0.00
8%GFG (PG64-28)	V58	0.08	39.8	0.24	25.1	0.72	11.1	1.84	2.89	4.43	0.00
12%GFG (PG64-28)	H58	0.16	28.9	0.46	15.2	1.26	5.09	3.02	0.75	6.68	0.00
8%FA (PG64-28)	H58	0.19	25.1	0.61	11.4	1.58	3.39	3.82	0.03	8.25	0.00
2%SBS (PG64-28)	V58	0.09	55.7	0.27	45.1	0.72	31.3	1.87	16.4	4.59	4.83
4%SBS (PG76-28)	E58	0.02	85.5	0.04	85.0	0.07	84.2	0.16	81.4	0.43	70.4
Hybrid (PG76-28)	E58	0.03	60.1	0.09	48.9	0.28	33.2	0.77	15.5	1.96	4.56

Note: S is standard traffic, H is heavy traffic, V is very heavy traffic, and E is extremely heavy traffic

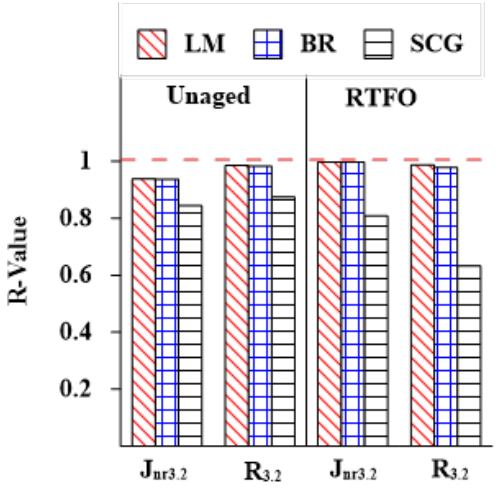

Figure 8.7: R-values for different training algorithms

Figures 8.8 and 8.9 describe the relationships between mean squared errors (MSEs)

and the number of epochs [1] for $J_{nr3.2}$ and $R_{3.2}$, respectively, of unaged and aged asphalt binders. As the number of epochs increased, the MSE value declined. In addition, for unaged and aged $J_{nr3.2}$ and $R_{3.2}$, every phase of training, validation, and testing results in a simultaneous MSE magnitude reduction. This reduction approach validates that the training operation was correctly completed with no overfitting in the training, validation, and test sections.

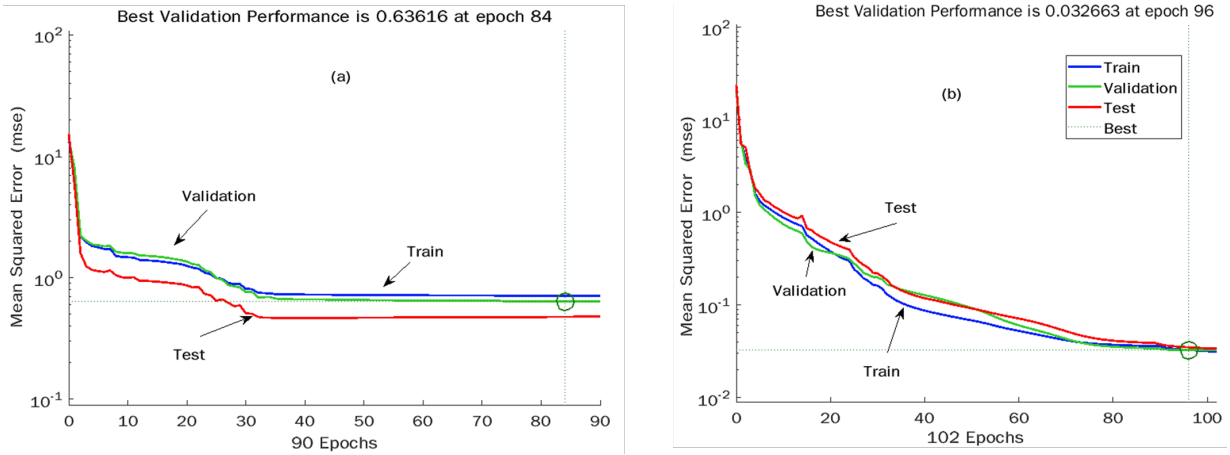

Figure 8.8: MSE versus Epoch plot for $J_{nr3.2}$ of (a) Unaged and (b) RTFO binders

Figures 8.10, 8.11, 8.12, and 8.13 present the relationship between the measured and predicted values for $J_{nr3.2}$ of unaged binder, $J_{nr3.2}$ of aged binder, $R_{3.2}$ of unaged binder, and $R_{3.2}$ of aged binder, respectively. The figures include graphs for training, validation, test, and total data, which indicate excellent R-values for the total data set of 0.997, 0.985, and 0.987 for $J_{nr3.2}$ of aged binder, $R_{3.2}$ of unaged binder, and $R_{3.2}$ of aged binder, respectively. While $J_{nr3.2}$ of unaged binder achieved an R-value of 0.937. R-values for $J_{nr3.2}$ and $R_{3.2}$ of aged binder and unaged binder demonstrated a very good correlation between measured and predicted output values with high accuracy.

Tables 8.3 8.4 8.5 8.6 show the weights and biases for $J_{nr3.2}$ and $R_{3.2}$ of unaged binders, as well as $J_{nr3.2}$ and $R_{3.2}$ of RTFO binders, respectively. Once the values of the five-input data are available, the ANNs model's weights and biases can be used to predict a certain output. The weight and bias matrix of the hidden layer in the optimal network design, which estimates the magnitudes of $J_{nr3.2}$ and $R_{3.2}$ of unaged binders and $J_{nr3.2}$ and $R_{3.2}$ of RTFO binders, were 5 by 5 and 5 by 1, respectively. The output layer was 1 by

[1] Epoch is the number of times all the training data are applied to update the weights at the same time [170]

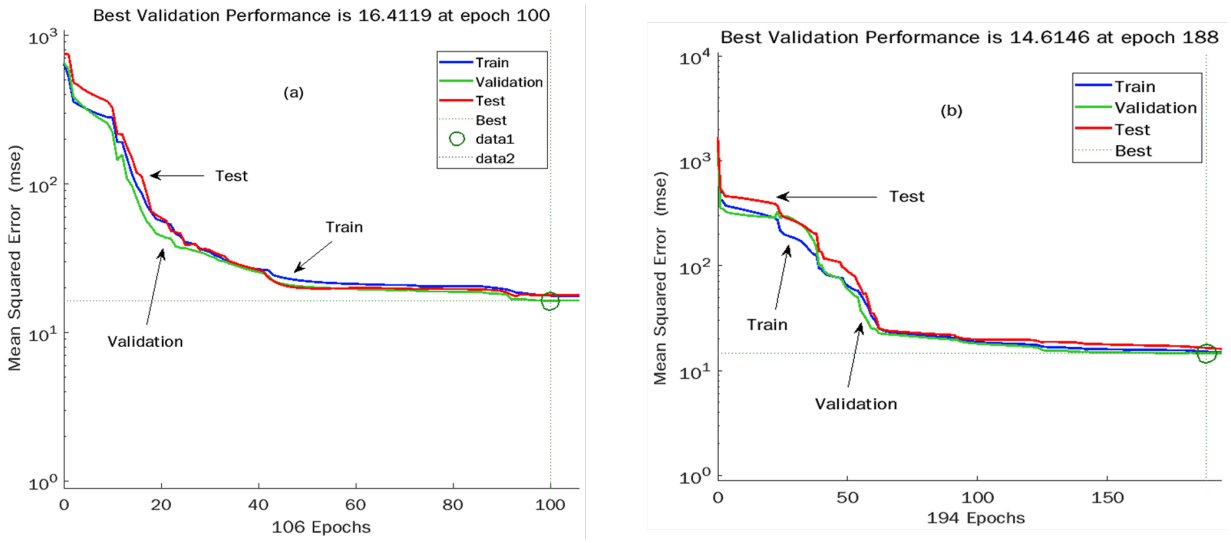

Figure 8.9: MSE versus Epoch plot for $R_{3.2}$ of (a) Unaged and (b) RTFO binders

Table 8.3: Weights and Biases for $J_{nr3.2}$ model of unaged binders

Layer	**Weights**						**Bias**
	w_{ij}	1	2	3	4	5	B_j
Hidden	1	3.0687	1.4113	-1.9778	-0.5590	-3.1384	-7.4256
	2	-2.2073	0.2155	-1.8096	0.4862	3.7408	5.2631
	3	0.2415	0.1634	0.8874	-0.8957	-0.7172	0.2491
	4	0.8178	-5.2766	4.1197	-0.1631	-14.6446	-17.7319
	5	-0.0726	-0.0056	-0.3132	0.2839	0.2459	0.1831
Output	1	2.5500	5.8313	-1.0532	9.0893	-3.2397	5.5766

5. Overall, the non-recovery and recovery properties of asphalt binder are influenced by test temperature and frequency, storage modulus, loss modulus, and viscosity, according to ANN modelling.

8.4 Conclusions

This research aimed to investigate the possibility of using ANNs model to predict the non-recovery and recovery properties of modified asphalt binders using mechanical test parameters and asphalt binder properties. Over 880 data points were covered using eleven

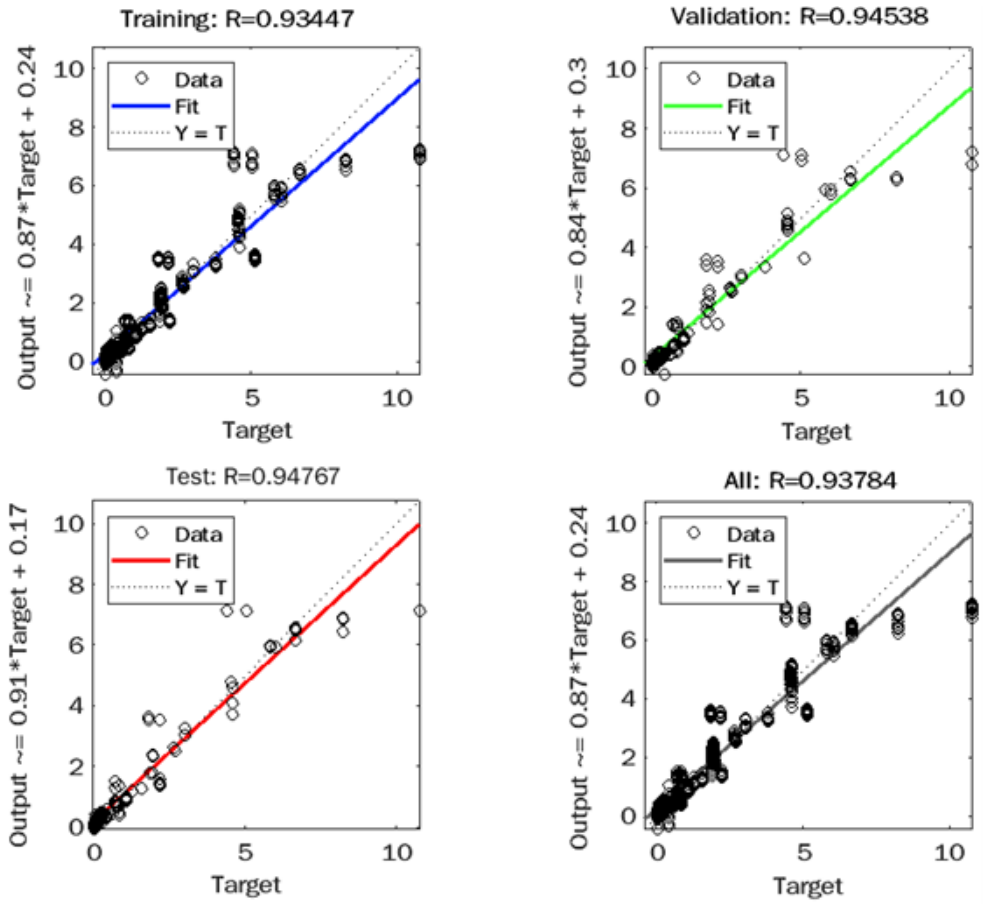

Figure 8.10: Observed versus predicted plot for $J_{nr3.2}$ of unaged binders

Table 8.4: Weights and biases for $R_{3.2}$ model of unaged binders

Layer	**Weights**						**Bias**
	w_{ij}	1	2	3	4	5	B_j
Hidden	1	0.2898	7.2419	-8.4904	-3.0088	0.1703	-5.6115
	2	0.4935	-1.1931	1.1313	-0.2653	-1.8445	-3.0253
	3	-0.5490	-1.6869	1.4974	0.3046	1.4068	2.3104
	4	0.0126	21.8102	-4.7578	2.1766	0.1879	20.1986
	5	-0.0792	-23.5214	2.6726	-2.5512	-0.2272	-23.6901
Output	1	7.9974	-14.8164	-11.8496	22.3949	6.6711	-10.5029

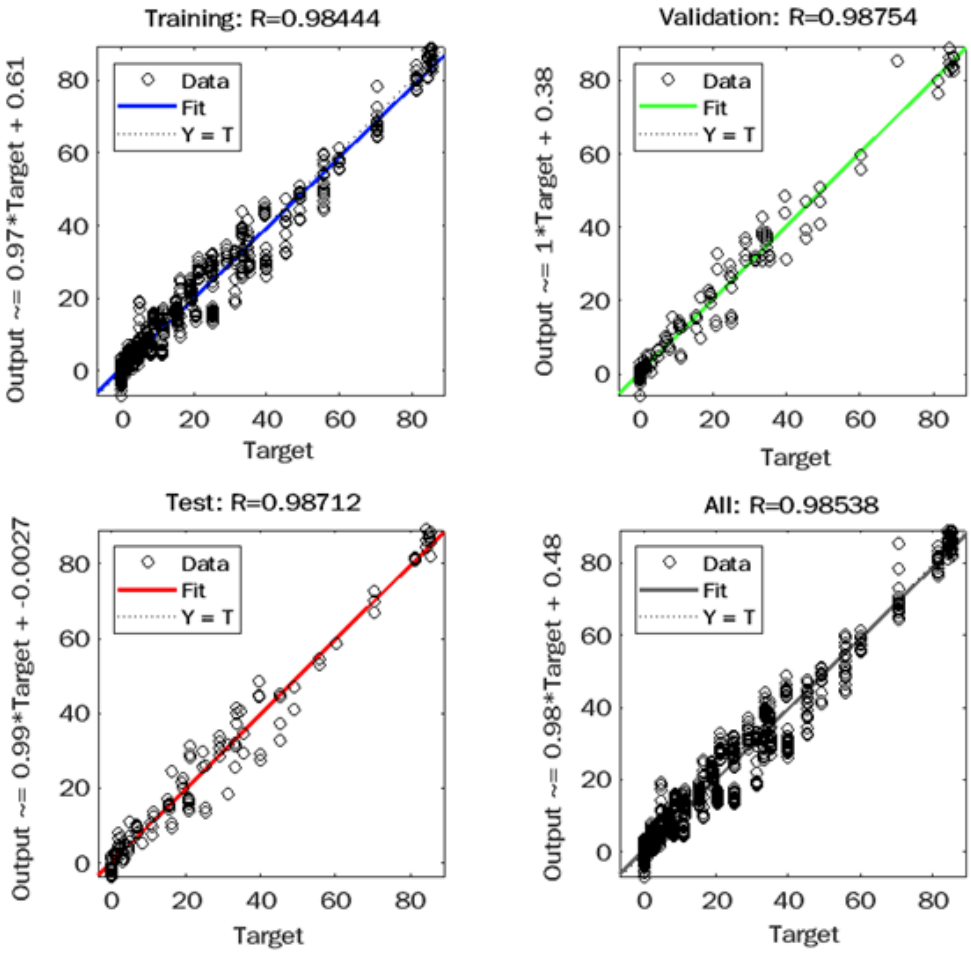

Figure 8.11: Observed versus predicted plot for $R_{3.2}$ of unaged binders

mixed asphalt binders, one neat asphalt binder, and four modifiers at various percentages. Frequency sweep and MSCR tests were conducted on all eleven binders at different temperatures. J_{nr} and R of unaged and aged asphalt binders were predicted using an ANNs model which was developed using five inputs: test temperature and frequency, storage modulus, loss modulus, and viscosity.

The optimal ANN architecture was chosen, and the LM algorithm was used to train the ANN model, one-hidden-layer neural network with five neurons. For $J_{nr3.2}$ and $R_{3.2}$ of unaged asphalt binders and $J_{nr3.2}$ and $R_{3.2}$ of aged asphalt binders, respectively. The statistical goodness of fit values (R) between measured and predicted values were 0.938,

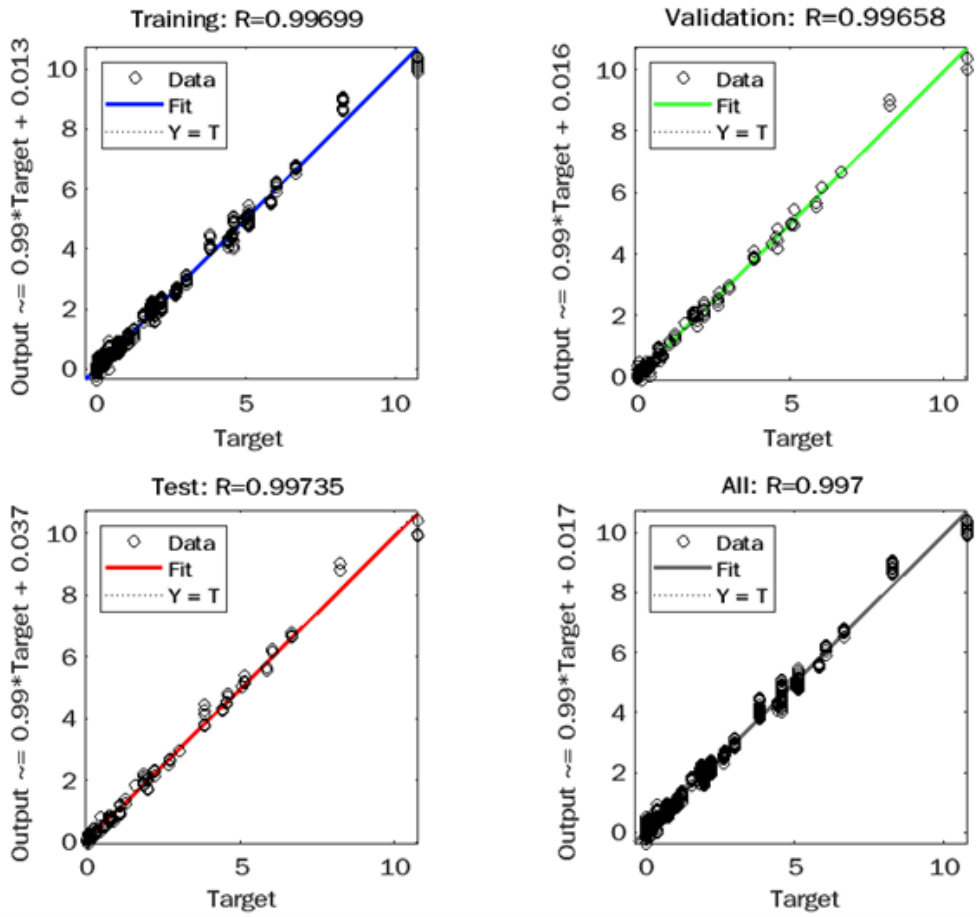

Figure 8.12: Observed versus predicted plot for $J_{nr3.2}$ of RTFO binders

Table 8.5: Weights and biases for $R_{3.2}$ model of RTFO binders

Layer	**Weights**						**Bias**
	w_{ij}	1	2	3	4	5	B_j
Hidden	1	0.3531	-3.2255	2.6827	-0.1436	-0.6694	-3.2348
	2	0.2972	110.0916	-153.517	-4.6041	-0.1512	-48.9735
	3	0.1343	-264.734	-8.2407	-6.7266	-0.6619	-282.7398
	4	0.0943	-37.4940	17.8878	-1.2657	-0.1527	-23.0206
	5	0.3477	10.6872	-10.7883	-0.1537	-0.1725	-2.5832
Output	1	-33.8622	3.3053	-81.5495	-24.3071	54.3905	-81.7113

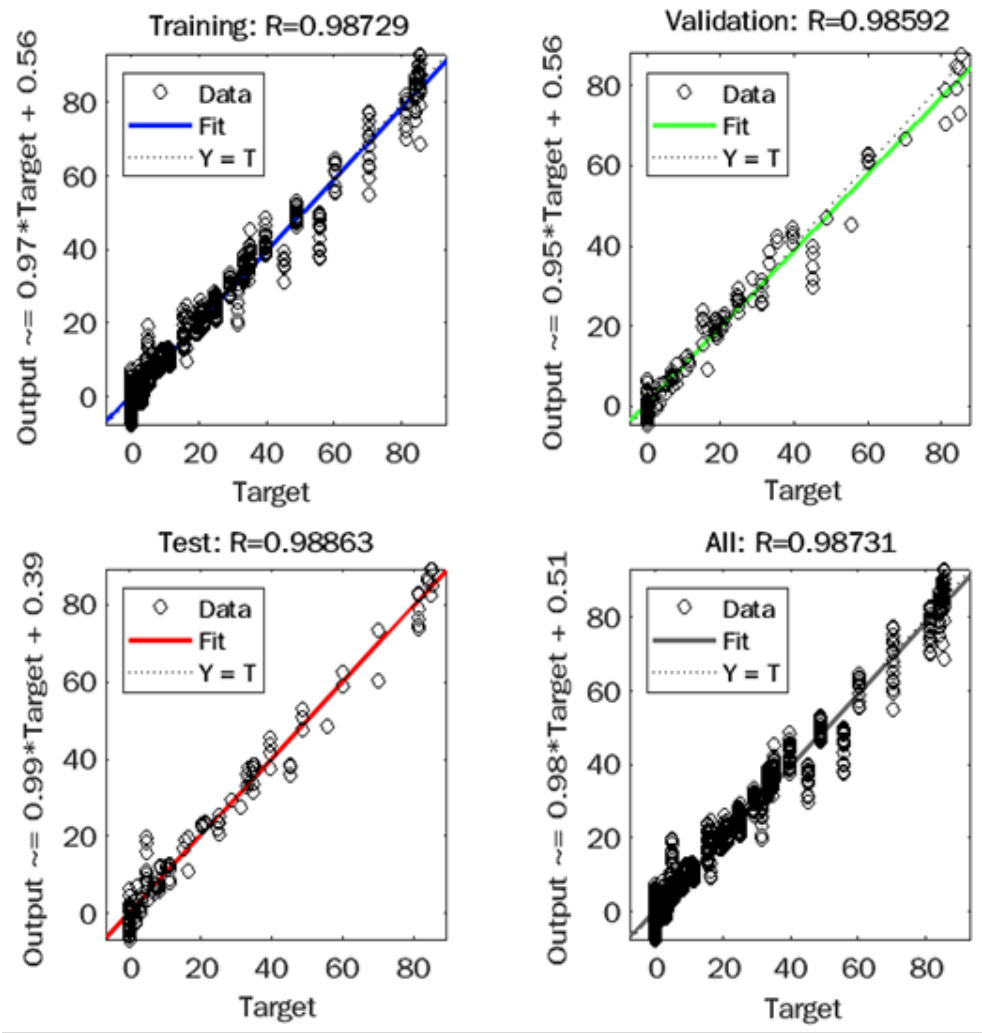

Figure 8.13: Observed versus predicted plot for $R_{3.2}$ of RTFO binders

0.985, 0.997, and 0.987, respectively. Thus, the magnitudes of biases and weights specified in this study could be useful in predicting the non-recovery and recovery properties of asphalt binders at various temperatures.

The use of the ANN algorithm to determine mathematical weights and biases of the input parameters and examine the influence of different types of modifiers on the rheological, non-recovery and recovery properties of asphalt binder was a noteworthy contribution of this study.

Table 8.6: Weights and biases for $J_{nr3.2}$ model of RTFO binders

Layer	**Weights**						**Bias**
	w_{ij}	1	2	3	4	5	B_j
Hidden	1	0.8441	5.4098	-3.2639	-4.8063	-1.0246	-5.1963
	2	-0.0645	9.1026	4.5755	0.0736	41.4092	56.4210
	3	0.1424	-1.7009	-0.7260	-0.1259	-19.6814	-22.5069
	4	-0.1090	-0.9572	2.8982	0.1693	21.3224	24.2650
	5	0.7024	-10.9267	5.5517	-4.8844	-1.4464	-13.4161
Output	1	-5.1251	-24.3633	6.2432	19.5944	10.1596	15.0747

Chapter 9

Conclusions and Recommendations

9.1 Conclusions

Based on the asphalt binder characteristics findings, the following main conclusions can be drawn:

- Curing the geopolymer for seven days has significant effects on its properties, which has an important impact on the rheological and performance of asphalt binder when it is used as a modifier.
- The ESEM results indicated that the geopolymer particles appear to be effectively dispersed in the asphalt binder and have no effect on the microstructure of the asphalt binder.
- The geopolymer (GF and GFG) modifier considerably enhances the performance of asphalt binder at different temperatures and frequencies by increasing shear complex modulus and reducing phase angle.
- The geopolymer (GF and GFG) modified asphalt binder achieved the highest resistance for fatigue and rutting distresses compared to the neat binder.
- Temperature, stress, and geopolymer content have significant effects on MSCR results.
- Modifying the asphalt binder using the combination of SBS and geopolymer modifiers achieved the highest fatigue and rutting resistance at different temperatures, compared to the other modifiers.

- The low-temperature performance of the asphalt binder was enhanced by using 2%SBS and hybrid modifiers, which achieve the lowest creep stiffness.
- Geopolymer has a significant impact on the binder's sensitivity to temperature, whereby the temperature sensitivity of G' and G'' for both unaged and RTFO modified asphalt binders decreases.
- The 2%SBS binder exhibited the highest creep recovery at low-stress levels, while the hybrid binder exhibited the highest creep recovery at high-stress levels, during the test temperatures.
- Using SBS with a geopolymer as a modifier enhances the ability of the asphalt binder to withstand extreme (E) and very heavy (V) traffic under high stress and temperature. In hot climate countries, this combination could be implemented to enhance asphalt binders' rutting resistance.
- Modifying asphalt binder with 8% geopolymer resulted in the smallest rate of change in crossover modulus due to aging, indicating that the asphalt binder's aging resistance has improved.
- Fly ash and glass powder could be used as an aluminosilicate source during the preparation of geopolymer as an asphalt modifier, which has an essential influence on the performance of asphalt binder.

Based on the asphalt mixture characteristics findings, the following conclusions can be drawn:

- Modifying asphalt mixture using modified asphalt binder with geopolymer, SBS, and hybrid modifiers enhances the resistance to rutting, whereby the permanent deformation decreases by 82%, 74%, and 55% by adding hybrid, 2%SBS, and 8%GF modifiers, respectively.
- Modified asphalt mixtures achieved the highest values of E^* at low temperature (-10 °C) and intermediate (21 °C) temperatures under low and high frequencies, compared to unmodified asphalt mixture.
- The asphalt mixture with different modifiers has a higher tensile strength compared to the neat binder.

- When compared to other modified asphalt binders, the asphalt mixture with hybrid asphalt binder is the least susceptible to moisture damage, with a TSR of 91%.
- The findings indicated that geopolymer modified asphalt binder has a significant resistance to moisture damage.
- The hybrid binder achieved the highest fracture energy under dry and freezing-thawing conditions, implying that the asphalt mix's crack resistance has improved.

Based on the findings of predicted models, the following conclusions can be drawn:

- Using a reliable calibrated model to predict the effects of additives on the behavior of asphalt binder can significantly reduce operating and testing time and expenses.
- The Response Surface Method (RSM) is an effective method to predict the recovery and non-recovery performance of geopolymer modified asphalt binder with excellent R^2 values, considering the effects of temperatures and additives content.
- The statistical goodness of fit values, using ANNs model, for the total data set for $J_{nr3.2}$ of unaged binder, $J_{nr3.2}$ of aged binder, $R_{3.2}$ of unaged binder, and $R_{3.2}$ of aged binder are 0.937, 0.997, 0.985, and 0.987, respectively.
- The ANNs model is appropriate to predict the percent recovery and non-recovery compliance of modified asphalt binder using unaged or aged binders at different temperatures.

9.2 Contribution and Motivation

The investigation in this thesis into the effect of geopolymer on the rheological, microstructure, and performance of asphalt binder will be utilized to gain better knowledge and understanding about the possibility of using the geopolymer to enhance the asphalt binder properties. This study may encourage researchers to develop new geopolymers with potential effects on rutting, fatigue, and thermal crack resistance. Environmentally, reducing the amount of asphalt binder used during the construction of asphalt pavement by using geopolymer as an additive, where there are minimal CO_2 emissions during its production, will have environmental benefits by reducing emissions and fuel consumption due to the extraction and transport of asphalt binder. Also, using different models to predict the performance of asphalt binder considering the material characteristics and mechanical test

data can have a significant effect on reducing the time and cost for laboratory testing. This thesis will provide the scientists with eight manuscripts, whereby each manuscript contains an introduction, objectives, experiments and methods, analysis, and discussion. Four manuscripts have been published, and four more have been submitted to valuable journals.

Journal Papers

- **Abdulrahman Hamid**, Hamed Alfaidi, Hassan Baaj, and Mohab El-Hakim. Evaluating fly ash-based geopolymers as a modifier for asphalt binders. Advances in Materials Science and Engineering, 2020, **DOI: 10.1155/2020/2398693**.
- **Abdulrahman Hamid**, Hassan Baaj, and Mohab El-Hakim. Rutting Behaviour of Geopolymer and Styrene Butadiene Styrene-Modified Asphalt Binder. Polymers Journal, 2022, **DOI: 10.3390/polym14142780**.
- **Abdulrahman Hamid**, Hassan Baaj, and Mohab El-Hakim. Temperature and Aging Effects on the Rheological Properties and Performance of Geopolymer-Modified Asphalt Binder and Mixture.
- **Abdulrahman Hamid**, Hassan Baaj, and Mohab El-Hakim. Evaluating the Effect of Glass Powder/Fly Ash-Based Geopolymer on the Rheological and Performance of Asphalt Binder.
- **Abdulrahman Hamid**, Hassan Baaj, and Mohab El-Hakim. Predicting the Recovery and Non-Recovery Performance of Asphalt Binders Using Artificial Neural Networks.

Conference Papers

- **Abdulrahman Hamid**, Hassan Baaj, and Mohab El-Hakim. Enhancing asphalt cement properties using geopoltmer-based on fly ash and glass powder. In Laval, Canada, 7th CSCE International Specialty Conference on Engineering Mechanics and Materials, 2019.
- **Abdulrahman Hamid**, Hassan Baaj, and Mohab El-Hakim. Predicting the potential impact of geopolymers on the creep recovery properties of asphalt binder. In RILEM International Symposium on Bituminous Materials, pages 1481–1487. Springer, 2020.

- **Abdulrahman Hamid**, Hassan Baaj, and Mohab El-Hakim. Effect of High Temperature on the Behavior of Geopolymer Modified Asphalt Binders. Transportation Association of Canada (TAC) Conference, Edmonton, AB, Canada, 2022.

9.3 Recommendations for Future Work

In Chapter 4, the viability of employing geopolymer as an asphalt binder modifier was discussed, as well as the effects of temperature and curing time on the performance of geopolymer materials. The results showed that there was a promising effect in enhancing the performance of the asphalt binder. Despite this, the influence of different types of alkaline solutions with varied concentrations on the performance of geopolymer will be interesting to observe.

In Chapter 5, the effects of temperatures, stresses, polymer types (fly ash-based geopolymer (GF), Styrene Butadiene Styrene (SBS), and a combination of SBS and GF), and modification rate on the rutting behavior of the asphalt binder and mixture were evaluated. The results showed that additive content has a significant influence on increasing resistance to heavy traffic loads and improving strain recovery under high stress and temperatures. Also, it was noted that there is a good relationship between MSCR test results and asphalt mixture rutting as concluded by different studies. Therefore, it would be more interesting if there is a model to predict the asphalt concrete rutting depth using the MSCR test results as well as the effect of temperatures and additive type and amount on the performance of the asphalt binder and mixture.

In Chapter 7, glass powder was used to replace 10% of the fly ash during the preparation of the geopolymer. It was noted that the glass powder/fly ash-based geopolymer has significant effects on rutting and fatigue performance of asphalt binder. Therefore, it would be useful to evaluate the rheological properties and performance of modified asphalt binders using different percentages of glass powder and investigate the effect of modified binders on the asphalt concrete performance.

References

[1] AASHTO TP 101. Standard method of test for estimating fatigue resistance of asphalt binders using the linear amplitude sweep. *AASHTO: Washington, DC, USA*, 2012.

[2] AASHTO T 240. Standard method of test for effect of heat and air on a moving film of asphalt binder (rolling thin-film oven test). *American Association of State Highway and Transportation Officials*, 2013.

[3] AASHTO R 28. Standard practice for accelerated aging of asphalt binder using a pressurized aging vessel (pav). *American Association of State Highway and Transportation Officials*, 2016.

[4] AASHTO T 283. Standard method of test for resistance of compacted asphalt mixtures to moisture-induced damage. *AASHTO Provisional Standards: Washington, DC, USA*, 2018.

[5] AASHTO R 30. Standard practice for mixture conditioning of hot-mix asphalt (hma). standard specifications for transportation materials and methods of sampling and testing, part 1b: specifications, 2015.

[6] AASHTO T 315. Standard method of test for determining the rheological properties of asphalt binder using a dynamic shear rheometer (dsr). *American Association of State Highway and Transportation Officials*, 2018.

[7] AASHTO T 316. Standard method of test for viscosity determination of asphalt binder using rotational viscometer, 2017.

[8] AASHTO T 324. Standard method of test for hamburg wheel-track testing of compacted hot mix asphalt (hma). *Standard Specificaitons for Transportation Materials and Methods of Sampling and Testing*, 2017.

[9] AASHTO M 332. Standard specification for performance-graded asphalt binder using multiple stress creep recovery (mscr) test. *American Association of State and Highway Transportation Officials: Washington, DC, USA*, 2010.

[10] AASHTO T 342. Standard method of test for determining dynamic modulus of hot mix asphalt (hma), 2011.

[11] AASHTO T 350. Standard method of test for multiple stress creep recovery (mscr) test of asphalt binder using a dynamic shear rheometer (dsr). *American Association of State and Highway Transportation Officials: Washington, DC, USA*, 2019.

[12] Hayder H Abdullah, Mohamed A Shahin, and Prabir Sarker. Stabilisation of clay with fly-ash geopolymer incorporating GGBFS. In *Proceedings of the second Proceedings of the Second World Congress on Civil, Structural and Environmental Engineering (CSEE'17)*, pages 1–8. Citeseer, 2017.

[13] Saad Abo-Qudais and Ibrahem Shatnawi. Prediction of bituminous mixture fatigue life based on accumulated strain. *Construction and Building Materials*, 21(6):1370–1376, 2007.

[14] Saad Abo-Qudais and Akram Suleiman. Monitoring fatigue famage and crack healing by ultrasound wave velocity. *Nondestructive Testing and Evaluation*, 20(2):125–145, 2005.

[15] M Adaway and Y Wang. Recycled glass as a partial replacement for fine aggregate in structural concrete–effects on compressive strength. *Electronic Journal of Structural Engineering*, 14(1):116–122, 2015.

[16] A Adedeji, T Grünfelder, FS Bates, CW Macosko, M Stroup-Gardiner, and DE Newcomb. Asphalt modified by sbs triblock copolymer: structures and properties. *Polymer Engineering & Science*, 36(12):1707–1723, 1996.

[17] Saeed Ahmari, Lianyang Zhang, and Jinhong Zhang. Effects of activator type/concentration and curing temperature on alkali-activated binder based on copper mine tailings. *Journal of Materials Science*, 47(16):5933–5945, 2012.

[18] Gordon D Airey. Rheological evaluation of ethylene vinyl acetate polymer modified bitumens. *Construction and Building Materials*, 16(8):473–487, 2002.

[19] Gordon D Airey. Rheological properties of styrene butadiene styrene polymer modified road bitumens. *Fuel*, 82(14):1709–1719, 2003.

[20] Khaleel Al-Adham, MA Dalhat, and HI Al-Abdul Wahhab. Strain recovery rate and absolute per cent recovery of polymer-modified asphalt binders. *International Journal of Pavement Engineering*, 21(7):919–929, 2020.

[21] Ramez A Al-Mansob, Amiruddin Ismail, Aows N Alduri, Che Husna Azhari, Mohamed Rehan Karim, and Nur Izzi Md Yusoff. Physical and rheological properties of epoxidized natural rubber modified bitumens. *Construction and Building Materials*, 63:242–248, 2014.

[22] Mustafa Alas and Shaban Ismael Albrka Ali. Prediction of the high-temperature performance of a geopolymer modified asphalt binder using artificial neural networks. *Int. J. Technol*, 10(2):417–427, 2019.

[23] David A Anderson, Laurence Lapalu, Mihai O Marasteanu, Yann M Le Hir, Jean-Pascal Planche, and Didier Martin. Low-temperature thermal cracking of asphalt binders as ranked by strength and fracture properties. *Transportation Research Record*, 1766(1):1–6, 2001.

[24] Edith Arambula and M Emin Kutay. Tension-compression fatigue test evaluation using fracture mechanics and field data. *Road materials and pavement design*, 10(1):83–108, 2009.

[25] Arul Arulrajah, Alireza Mohammadinia, Itthikorn Phummiphan, Suksun Horpibulsuk, and Wisanukorn Samingthong. Stabilization of recycled demolition aggregates by geopolymers comprising calcium carbide residue, fly ash and slag precursors. *Construction and Building Materials*, 114:864–873, 2016.

[26] Alireza Askari, Pouria Hajikarimi, Mehrdad Ehsani, and Fereidoon Moghadas Nejad. Prediction of rutting deterioration in flexible pavements using artificial neural network and genetic algorithm. *Amirkabir Journal of Civil Engineering*, (Articles in Press), 2022.

[27] ASTM. Standard test method for determining the flexural creep stiffness of asphalt binder using the bending beam rheometer (bbr). ASTM West Conshohocken, PA, USA, 2016.

[28] D4402 ASTM et al. Standard test method for viscosity determination of asphalt at elevated temperatures using a rotational viscometer. In *American Society for Testing and Materials*, 2015.

[29] Mike Aurilio, Peter Mikhailenko, Hassan Baaj, and Lily D Poulikakos. Properties of asphalt binders with increasing sbs polymer modification. In *International Symposium on Asphalt Pavement & Environment*, pages 55–66. Springer, 2019.

[30] SS Awanti, MS Amarnath, and A Veeraragavan. Influence of rest periods on fatigue characteristics of sbs polymer modified bituminous concrete mixtures. *International Journal of Pavement Engineering*, 8(3):177–186, 2007.

[31] H Baaj, H Di Benedetto, and P Chaverot. Different experimental approaches and criteria for fatigue of asphalt mixes. In *Proceedings of the Forty-Ninth Annual Conference of the Canadian Technical Asphalt Association (CTAA)-Montreal, Quebec*, 2004.

[32] Hassan Baaj, Herve Di Benedetto, and Pierre Chaverot. Fatigue of mixes: an intrinsic damage approach. In *6th RILEM Symposium PTEBM, Zurich*, pages 394–400, 2003.

[33] Hassan Baaj, Hervé Di Benedetto, and Pierre Chaverot. Effect of binder characteristics on fatigue of asphalt pavement using an intrinsic damage approach. *Road Materials and Pavement Design*, 6(2):147–174, 2005.

[34] Hassan Baaj, Peter Mikhailenko, Haya Almutairi, and Herve Di Benedetto. Recovery of asphalt mixture stiffness during fatigue loading rest periods. *Construction and Building Materials*, 158:591–600, 2018.

[35] Rawand M Badri, Muslich Sutanto, Maan k Alobaidi, et al. Investigating the rheological properties of asphalt binder incorporating different crumb rubber contents based on a response surface methodology. *Journal of King Saud University-Engineering Sciences*, 2020.

[36] Abraham Bae, Shelley Stoffels, Timothy Clyne, Benjamin Worel, and Ghassan Chehab. Direct effects of thermal cracks on pavement roughness. In *Asphalt Paving Technology: Association of Asphalt Paving Technologists-Proceedings of the Technical Sessions*, volume 76, pages 59–83. Association of Asphalt Paving Technologist, 2007.

[37] Hussain U Bahia, Dario Perdomo, and Pamela Turner. Applicability of superpave binder testing protocols to modified binders. *Transportation Research Record*, 1586(1):16–23, 1997.

[38] N Bala, I Kamaruddin, M Napiah, and N Danlami. Polyethylene polymer modified bitumen: Process optimization and modeling of linear viscoelastic rheological

properties using response surface methodology. *Journal of Engineering and Applied Sciences*, 13(9):2818–2827, 2018.

[39] Nicola Baldo, Evangelos Manthos, and Matteo Miani. Stiffness modulus and marshall parameters of hot mix asphalts: Laboratory data modeling by artificial neural networks characterized by cross-validation. *Applied Sciences*, 9(17):3502, 2019.

[40] Nicola Baldo, Evangelos Manthos, and Marco Pasetto. Analysis of the mechanical behaviour of asphalt concretes using artificial neural networks. *Advances in Civil Engineering*, 2018, 2018.

[41] Ali Behnood and Mahsa Modiri Gharehveran. Morphology, rheology, and physical properties of polymer-modified asphalt binders. *European Polymer Journal*, 112:766–791, 2019.

[42] Ali Behnood, Ayesha Shah, Rebecca S McDaniel, Matthew Beeson, and Jan Olek. High-temperature properties of asphalt binders: comparison of multiple stress creep recovery and performance grading systems. *Transportation Research Record*, 2574(1):131–143, 2016.

[43] Constantin Bobirică, Jae-Ho Shim, Jun-Hyeon Pyeon, and Joo-Yang Park. Influence of waste glass on the microstructure and strength of inorganic polymers. *Ceramics International*, 41(10):13638–13649, 2015.

[44] Thomas Bodley, Adrian Andriescu, Simon Hesp, and Kai Tam. Comparison between binder and hot mix asphalt properties and early top-down wheel path cracking in a northern ontario pavement trial. *Asphalt Paving Technology-Proceedings*, 76:345, 2007.

[45] Adhesive Bond, Arno Hefer, and Dallas Little. Adhesion in bitumen-aggregate systems and quantification of the effects of water on the adhesive bond. 2005.

[46] FP Bonnaure, AHJJ Huibers, and A Boonders. A laboratory investigation of the influence of rest periods on the fatigue characteristics of bituminous mixes (with discussion). In *Association of Asphalt Paving Technologists Proceedings*, volume 51, 1982.

[47] Muhamad Nazri Borhan, Amiruddin Ismail, and Riza Atiq Rahmat. Evaluation of palm oil fuel ash (pofa) on asphalt mixtures. *Australian Journal of Basic and Applied Sciences*, 4(10):5456–5463, 2010.

[48] Muhamad Nazri Borhan, Fatihah Suja, Amiruddin Ismail, and RA Rahmat. Used cylinder oil modified cold-mix asphalt concrete. *Journal of Applied Sciences*, 7(22):3485–3491, 2007.

[49] SF Brown. Discussion: mechanical properties of bituminos materials for pavement design. *Journal of International Asphalt Technology*, 35:11–13, 1989.

[50] SF Brown, KE Cooper, and GR Pooley. Mechanical properties of bituminous materials for pavement design. *Asphalt Technology*, (36), 1985.

[51] F Cardone, G Ferrotti, F Frigio, and F Canestrari. Influence of polymer modification on asphalt binder dynamic and steady flow viscosities. *Construction and Building Materials*, 71:435–443, 2014.

[52] Halil Ceylan et al. Modeling of concrete airfield pavements using artificial neural networks. 1999.

[53] Halil Ceylan, Erol Tutumluer, and Ernest J Barenberg. Artificial neural networks as design tools in concrete airfield pavement design. In *Airport Facilities: Innovations for the Next Century. Proceedings of the 25th International Air Transportation Conference. American Society of Civil Engineers*, 1998.

[54] Conglin Chen, Joseph H Podolsky, R Christopher Williams, and Eric W Cochran. Determination of the optimum polystyrene parameters using asphalt binder modified with poly (styrene-acrylated epoxidised soybean oil) through response surface modelling. *Road Materials and Pavement Design*, 20(3):572–591, 2019.

[55] Fayssal Cheriet, Khedoudja Soudani, and Smail Haddadi. Influence of natural rubber on creep behavior of bituminous concrete. *Procedia-Social and Behavioral Sciences*, 195:2769–2776, 2015.

[56] Jayvant Choudhary, Brind Kumar, and Ankit Gupta. Utilization of waste glass powder and glass composite fillers in asphalt pavements. *Advances in Civil Engineering*, 2021, 2021.

[57] Timothy R Clyne, Xiaopeng Li, Mihai O Marasteanu, and Eugene L Skok. Dynamic and resilient modulus of mn/dot asphalt mixtures. Technical report, 2003.

[58] GA Cuesta Cordoba, L Tuhovčák, and M Tauš. Using artificial neural network models to assess water quality in water distribution networks. *Procedia Engineering*, 70:399–408, 2014.

[59] María Criado, A Palomo, and Ana Fernández-Jiménez. Alkali activation of fly ashes. part 1: Effect of curing conditions on the carbonation of the reaction products. *Fuel*, 84(16):2048–2054, 2005.

[60] Nuno Cristelo, Stephanie Glendinning, Lisete Fernandes, and Amândio Teixeira Pinto. Effects of alkaline-activated fly ash and portland cement on soft soil stabilisation. *Acta Geotechnica*, 8(4):395–405, 2013.

[61] Nuno Cristelo, Stephanie Glendinning, Tiago Miranda, Daniel Oliveira, and Rui Silva. Soil stabilisation using alkaline activation of fly ash for self compacting rammed earth construction. *Construction and building materials*, 36:727–735, 2012.

[62] MA Dalhat, Khaleel Al-Adham, and HI Al-Abdul Wahhab. Multiple stress–creep–recovery behavior and high-temperature performance of styrene butadiene styrene and polyacrylonitrile fiber–modified asphalt binders. *Journal of Materials in Civil Engineering*, 31(6):04019087, 2019.

[63] John D'Angelo, Robert Kluttz, Raj N Dongre, Keith Stephens, and Ludo Zanzotto. Revision of the superpave high temperature binder specification: the multiple stress creep recovery test (with discussion). *Journal of the Association of Asphalt Paving Technologists*, 76, 2007.

[64] John A D'Angelo. The relationship of the mscr test to rutting. *Road Materials and Pavement Design*, 10(sup1):61–80, 2009.

[65] Joseph Davidovits. Geopolymers and geopolymeric materials. *Journal of thermal analysis*, 35(2):429–441, 1989.

[66] Joseph Davidovits. Geopolymers: inorganic polymeric new materials. *Journal of Thermal Analysis and calorimetry*, 37(8):1633–1656, 1991.

[67] Joseph Davidovits. Global warming impact on the cement and aggregates industries. *World resource review*, 6(2):263–278, 1994.

[68] Joseph Davidovits. Geopolymer chemistry and applications book. *Geopolymer Institute, St Quentin, France*, 2015.

[69] Srividya Dayal and Nagan Soundarapandian. Effect of fly-ash based geopolymer coated aggregate on bituminous mixtures. *Graevinar*, 70(03.):187–199, 2018.

[70] Guy Demortier. Pixe, pige and nmr study of the masonry of the pyramid of cheops at giza. *Nuclear Instruments and Methods in Physics Research Section B: Beam Interactions with Materials and Atoms*, 226(1-2):98–109, 2004.

[71] Yong Deng and Xianming Shi. An accurate, reproducible and robust model to predict the rutting of asphalt pavement: neural networks coupled with particle swarm optimization. *IEEE Transactions on Intelligent Transportation Systems*, 2022.

[72] Hervé Di Benedetto, A Ashayer Soltani, and Pierre Chaverot. Fatigue damage for bituminous mixtures: a pertinent approach. *Journal of the Association of Asphalt Paving Technologists*, 65, 1996.

[73] Hervé Di Benedetto, C De La Roche, H Baaj, A Pronk, and Robert Lundström. Fatigue of bituminous mixtures. *Materials and structures*, 37(3):202–216, 2004.

[74] S Dreessen and T Gallet. Mscrt: Performance related test method for rutting prediction of asphalt mixtures from binder rheological characteristics. In *Proc. of the 5th Eurasphalt & Eurobitume Congress (Istanbul)*, 2012.

[75] Yan-Jun Du, Bo-Wei Yu, Kai Liu, Ning-Jun Jiang, and Martin D Liu. Physical, hydraulic, and mechanical properties of clayey soil stabilized by lightweight alkali-activated slag geopolymer. *Journal of Materials in Civil Engineering*, 29(2):04016217, 2017.

[76] Peter Duxson, Ana Fernández-Jiménez, John L Provis, Grant C Lukey, Angel Palomo, and Jannie SJ van Deventer. Geopolymer technology: the current state of the art. *Journal of materials science*, 42(9):2917–2933, 2007.

[77] Sherif El-Badawy, Ragaa Abd El-Hakim, and Ahmed Awed. Comparing artificial neural networks with regression models for hot-mix asphalt dynamic modulus prediction. *Journal of Materials in Civil Engineering*, 30(7):04018128, 2018.

[78] Mohab El-Hakim. Instrumentation and overall evaluation of perpetual and conventional flexible pavement designs. Master's thesis, University of Waterloo, 2009.

[79] Hafez E Elyamany, M Abd Elmoaty, and Ahmed M Elshaboury. Magnesium sulfate resistance of geopolymer mortar. *Construction and Building Materials*, 184:111–127, 2018.

[80] Environment and Climate Change Canada. National waste characterization report: the composition of canadian residual municipal solid waste. 2020.

[81] Saman Esfandiarpour and Ahmed Shalaby. Local calibration of creep compliance models of asphalt concrete. *Construction and Building Materials*, 132:313–322, 2017.

[82] Eurostat. Packaging waste statistics-statistics explained. 2019.

[83] Michael J Farrar, Thomas F Turner, Jean-Pascal Planche, John F Schabron, and P Michael Harnsberger. Evolution of the crossover modulus with oxidative aging: Method to estimate change in viscoelastic properties of asphalt binder with time and depth on the road. *Transportation research record*, 2370(1):76–83, 2013.

[84] Ana Fernández-Jiménez, A Palomo, and M Criado. Microstructure development of alkali-activated fly ash cement: a descriptive model. *Cement and concrete research*, 35(6):1204–1209, 2005.

[85] Ana Fernández-Jiménez, Angel Palomo, Isabel Sobrados, and Jesús Sanz. The role played by the reactive alumina content in the alkaline activation of fly ashes. *Microporous and Mesoporous materials*, 91(1-3):111–119, 2006.

[86] Berhanu Abesha Feyissa. *Analysis and modeling of rutting for long life asphalt concrete pavement*. PhD thesis, Technische Universität, 2009.

[87] M Firouzinia and Gh Shafabakhsh. Investigation of the effect of nano-silica on thermal sensitivity of hma using artificial neural network. *Construction and Building Materials*, 170:527–536, 2018.

[88] Thomas J Freeman, Jacob Uzan, Dan G Zollinger, and Eun Sug Park. Sensitivity analysis of and strategic plan development for the implementation of the me design guide in txdot operations-volume 1 and volume 2. Technical report, 2006.

[89] Superpave Fundamentals. Superpave fundamentals reference manual. *Federal Highway Administration-FHWA, National Highway Institute: NHI (National Highway Institute)*, 2000.

[90] Gabriel Garcia and Marshall Thompson. Hma dynamic modulus predictive models (a review). Technical report, 2007.

[91] Jose Garcia and Kent Hansen. *HMA pavement mix type selection guide*. National Asphalt Pavement Association, 2001.

[92] I Garcia-Lodeiro, A Palomo, and A Fernández-Jiménez. An overview of the chemistry of alkali-activated cement-based binders. *Handbook of alkali-activated cements, mortars and concretes*, pages 19–47, 2015.

[93] Pooria Ghadir and Navid Ranjbar. Clayey soil stabilization using geopolymer and portland cement. *Construction and Building Materials*, 188:361–371, 2018.

[94] Mojtaba Ghasemi and Seyed Morteza Marandi. Performance improvement of a crumb rubber modified bitumen using recycled glass powder. *Journal of Zhejiang University SCIENCE A*, 14(11):805–814, 2013.

[95] Ronald R Glaser, John F Schabron, Thomas F Turner, Jean-Pascal Planche, Stephen L Salmans, and Jenny L Loveridge. Low-temperature oxidation kinetics of asphalt binders. *Transportation research record*, 2370(1):63–68, 2013.

[96] M Glavind. Sustainability of cement, concrete and cement replacement materials in construction. In *Sustainability of construction materials*, pages 120–147. Elsevier, 2009.

[97] Gökhan Görhan and Gökhan Kürklü. The influence of the naoh solution on the properties of the fly ash-based geopolymer mortar cured at different temperatures. *Composites part b: engineering*, 58:371–377, 2014.

[98] JT Gourley. Geopolymers; opportunities for environmentally friendly construction materials. In *Materials 2003 Conference: Adaptive Materials for a Modern Society, Sydney, Institute of Materials Engineering Australia*, 2003.

[99] JT Gourley and GB Johnson. Developments in geopolymer precast concrete. In *World congress geopolymer*, pages 139–143. Geopolymer Institute Saint-Quentin, France, 2005.

[100] J Groenendijk, CH Vogelzang, A Miradi, AAA Molenaar, and LJM Dohmen. Linear tracking performance tests on full-depth asphalt pavement. *Transportation research record*, 1570(1):39–47, 1997.

[101] Jacob Groenendijk. Accelerated testing and surface cracking of asphaltic concrete pavements. 2000.

[102] Muhammad NS Hadi, Nabeel A Farhan, and M Neaz Sheikh. Design of geopolymer concrete with ggbfs at ambient curing condition using taguchi method. *Construction and Building Materials*, 140:424–431, 2017.

[103] I Hafeez, MA Kamal, MW Mirza, S Bilal, et al. Laboratory fatigue performance evaluation of different field laid asphalt mixtures. *Construction and Building Materials*, 44:792–797, 2013.

[104] Ailar Hajimohammadi, Tuan Ngo, and Alireza Kashani. Glass waste versus sand as aggregates: The characteristics of the evolving geopolymer binders. *Journal of Cleaner Production*, 193:593–603, 2018.

[105] Ailar Hajimohammadi, Tuan Ngo, and Jitraporn Vongsvivut. Interfacial chemistry of a fly ash geopolymer and aggregates. *Journal of cleaner production*, 231:980–989, 2019.

[106] Abdulrahman Hamid, Hamed Alfaidi, Hassan Baaj, and Mohab El-Hakim. Evaluating fly ash-based geopolymers as a modifier for asphalt binders. *Advances in Materials Science and Engineering*, 2020, 2020.

[107] Abdulrahman Hamid, Hassan Baaj, and Mohab El-Hakim. Enhancing asphalt cement properties using geopoltmer-based on fly ash and glass powder. In *Laval, Canada, 7th CSCE International Specialty Conference on Engineering Mechanics and Materials*, 2019.

[108] Abdulrahman Hamid, Hassan Baaj, and Mohab El-Hakim. Predicting the potential impact of geopolymers on the creep recovery properties of asphalt binder. In *RILEM International Symposium on Bituminous Materials*, pages 1481–1487. Springer, 2020.

[109] Asphalt Handbook. Asphalt handbook, 2007.

[110] Djwantoro Hardjito. *Studies of fly ash-based geopolymer concrete*. PhD thesis, Curtin University, 2005.

[111] Tom Harman, Jack Youtcheff, John Bukowski, et al. The multiple stress creep recovery (mscr) procedure. Technical report, United States. Federal Highway Administration, 2011.

[112] Md Amanul Hasan, Md Mehedi Hasan, Biswajit Kumar Bairgi, Umme Amina Mannan, and Rafiqul A Tarefder. Utilizing simplified viscoelastic continuum damage model to characterize the fatigue behavior of styrene-butadiene-styrene (sbs) modified binders. *Construction and Building Materials*, 200:159–169, 2019.

[113] Menglim Hoy, Suksun Horpibulsuk, and Arul Arulrajah. Strength development of recycled asphalt pavement–fly ash geopolymer as a road construction material. *Construction and Building Materials*, 117:209–219, 2016.

[114] Menglim Hoy, Suksun Horpibulsuk, Runglawan Rachan, Avirut Chinkulkijniwat, and Arul Arulrajah. Recycled asphalt pavement–fly ash geopolymers as a sustainable

pavement base material: Strength and toxic leaching investigations. *Science of the Total Environment*, 573:19–26, 2016.

[115] Tung-Wen Hsu and Kuo-Hung Tseng. Effect of rest periods on fatigue response of asphalt concrete mixtures. *Journal of Transportation Engineering*, 122(4):316–322, 1996.

[116] Yang Hsien Huang. *Pavement analysis and design*. 2004.

[117] Sabahat Hussan, Mumtaz Ahmed Kamal, Imran Hafeez, Danish Farooq, Naveed Ahmad, and Shahab Khanzada. Statistical evaluation of factors affecting the laboratory rutting susceptibility of asphalt mixtures. *International Journal of Pavement Engineering*, 20(4):402–416, 2019.

[118] Ahmad Nazrul Hakimi Ibrahim, Nur Izzi Md Yusoff, Norliza Mohd Akhir, and Muhamad Nazri Borhan. Physical properties and storage stability of geopolymer modified asphalt binder. *Jurnal Teknologi*, 78(7-2), 2016.

[119] Asphalt Institute. *Thickness Design–asphalt Pavements for Highways and Streets*, volume 1. Asphalt Inst, 1981.

[120] Muhammad Aakif Ishaq, Loretta Venturini, and Filippo Giustozzi. Correlation between rheological rutting tests on bitumen and asphalt mix flow number. *International Journal of Pavement Research and Technology*, pages 1–20, 2021.

[121] Muhammad Jamal and Filippo Giustozzi. Chemo-rheological investigation on waste rubber-modified bitumen response to various blending factors. *International Journal of Pavement Research and Technology*, pages 1–20, 2021.

[122] Ruxin Jing, Aikaterini Varveri, Xueyan Liu, Athanasios Scarpas, and Sandra Erkens. Rheological, fatigue and relaxation properties of aged bitumen. *International journal of pavement engineering*, 21(8):1024–1033, 2020.

[123] Hassan H Jony, M Al-Rubaie, and I Jahad. The effect of using glass powder filler on hot asphalt concrete mixtures properties. *Engineering and Technology Journal*, 29(1):44–57, 2011.

[124] N Kamboozia, H Ziari, and H Behbahani. Artificial neural networks approach to predicting rut depth of asphalt concrete by using of visco-elastic parameters. *Construction and Building Materials*, 158:873–882, 2018.

[125] Andrew I Kay, Robert B Noland, and Caroline J Rodier. Achieving reductions in greenhouse gases in the us road transportation sector. *Energy Policy*, 69:536–545, 2014.

[126] Orhan Kaya, Adel Rezaei-Tarahomi, Halil Ceylan, Kasthurirangan Gopalakrishnan, Sunghwan Kim, and David R Brill. Neural network-based multiple-slab response models for top-down cracking mode in airfield pavement design. *Journal of Transportation Engineering, Part B: Pavements*, 144(2):04018009, 2018.

[127] Mustafa Keskin and Murat Karacasu. Artificial neural network modelling for asphalt concrete samples with boron waste modification. *Journal of Engineering Research*, 2021.

[128] Alireza Khadivar and Amir Kavussi. Rheological characteristics of sbr and nr polymer modified bitumen emulsions at average pavement temperatures. *Construction and Building Materials*, 47:1099–1105, 2013.

[129] Farag Khodary Moalla Hamed. *Evaluation of fatigue resistance for modified asphalt concrete mixtures based on dissipated energy concept*. PhD thesis, Technische Universität, 2010.

[130] Dong-Hyuk Kim, Sang-Jik Lee, Ki-Hoon Moon, and Jin-Hoon Jeong. Prediction of indirect tensile strength of intermediate layer of asphalt pavements using artificial neural network model. *Arabian Journal for Science and Engineering*, 46(5):4911–4922, 2021.

[131] Baha Vural Kok, Mehmet Yilmaz, Burak Sengoz, Abdulkadir Sengur, and Engin Avci. Investigation of complex modulus of base and sbs modified bitumen with artificial neural networks. *Expert Systems with Applications*, 37(12):7775–7780, 2010.

[132] Olli-Ville Laukkanen, Hilde Soenen, Terhi Pellinen, Serge Heyrman, and Geert Lemoine. Creep-recovery behavior of bituminous binders and its relation to asphalt mixture rutting. *Materials and Structures*, 48(12):4039–4053, 2015.

[133] Hyun-Jong Lee, Jo S Daniel, and Y Richard Kim. Laboratory performance evaluation of modified asphalt mixtures for inchon airport pavements. *International Journal of Pavement Engineering*, 1(2):151–169, 2000.

[134] Hsiao Yun Leong, Dominic Ek Leong Ong, Jay G Sanjayan, and Ali Nazari. Strength development of soil–fly ash geopolymer: assessment of soil, fly ash, alkali activators, and water. *Journal of Materials in Civil Engineering*, 30(8):04018171, 2018.

[135] Eyal Levenberg and Ayesha Shah. Interpretation of complex modulus test results for asphalt-aggregate mixes. *Journal of Testing and Evaluation*, 36(4):326–334, 2008.

[136] Chaves Lima, Lindiane Bieseki, Paloma Vinaches Melguizo, and Sibele Berenice Castellã Pergher. *Environmentally Friendly Zeolites*. Springer, 2019.

[137] Fang Liu, Zhidong Zhou, and Yu Wang. Predict the rheological properties of aged asphalt binders using a universal kinetic model. *Construction and Building Materials*, 195:283–291, 2019.

[138] Hanbing Liu, Mengsu Zhang, Yubo Jiao, and Liuxu Fu. Preparation parameter analysis and optimization of sustainable asphalt binder modified by waste rubber and diatomite. *Advances in Materials Science and Engineering*, 2018, 2018.

[139] Hanqi Liu, Waleed Zeiada, Ghazi G Al-Khateeb, Abdallah Shanableh, and Mufid Samarai. Use of the multiple stress creep recovery (mscr) test to characterize the rutting potential of asphalt binders: A literature review. *Construction and Building Materials*, 269:121320, 2021.

[140] Jun Liu, Kezhen Yan, Jenny Liu, and Xiaowen Zhao. Using artificial neural networks to predict the dynamic modulus of asphalt mixtures containing recycled asphalt shingles. *Journal of Materials in Civil Engineering*, 30(4):04018051, 2018.

[141] Shutang Liu, Weidong Cao, Jianguo Fang, and Shujie Shang. Variance analysis and performance evaluation of different crumb rubber modified (crm) asphalt. *Construction and Building Materials*, 23(7):2701–2708, 2009.

[142] Xiaohu Lu and Ulf Isacsson. Rheological characterization of styrene-butadiene-styrene copolymer modified bitumens. *Construction and building materials*, 11(1):23–32, 1997.

[143] Robert Lundstrom, Hervé Di Benedetto, and Ulf Isacsson. Influence of asphalt mixture stiffness on fatigue failure. *Journal of materials in civil engineering*, 16(6):516–525, 2004.

[144] Feng Ma, Aimin Sha, Ruiyu Lin, Yue Huang, and Chao Wang. Greenhouse gas emissions from asphalt pavement construction: A case study in china. *International journal of environmental research and public health*, 13(3):351, 2016.

[145] RB McGennis, RM Anderson, TW Kennedy, and M Solaimanian. Background of superpave asphalt mixture design & analysis. final report. Technical report, 1994.

[146] A Mehrara and A Khodaii. Evaluation of moisture conditioning effect on damage recovery of asphalt mixtures during rest time application. *Construction and Building Materials*, 98:294–304, 2015.

[147] Thomas G Mezger. *Applied rheology: with Joe flow on rheology road*. Anton Paar, 2021.

[148] Peter Mikhailenko, Hassan Baaj, Changjiang Kou, Lily D Poulikakos, Augusto Cannone Falchetto, Jeroen Besamusca, and Bernhard Hofko. Esem microstructural and physical properties of virgin and laboratory aged bitumen. In *RILEM 252-CMB-Symposium on Chemo Mechanical Characterization of Bituminous Materials*, pages 150–155. Springer, 2018.

[149] Peter Mikhailenko, Changjiang Kou, Hassan Baaj, Lily Poulikakos, Augusto Cannone-Falchetto, Jeroen Besamusca, and Bernhard Hofko. Comparison of esem and physical properties of virgin and laboratory aged asphalt binders. *Fuel*, 235:627–638, 2019.

[150] Peter Mikhailenko, Changjiang Kou, Hassan Baaj, and Susan Tighe. Observation of polymer modified asphalt microstructure by esem. In *Proceedings of the 6th International Conference on Engineering Mechanics and Materials*, 2017.

[151] Alireza Mohammadinia, Arul Arulrajah, Jay Sanjayan, Mahdi M Disfani, Myint Win Bo, and Stephen Darmawan. Stabilization of demolition materials for pavement base/subbase applications using fly ash and slag geopolymers. *Journal of Materials in Civil Engineering*, 28(7):04016033, 2016.

[152] Douglas C Montgomery. *Design and analysis of experiments*. John wiley & sons, 2017.

[153] F Moreno Navarro, María del Carmen Rubio Gámez, E Tomás Fortún, F Valor Hernández, and A Ramírez Rodriguez. Evaluation of the fatigue macro-cracking behavior of crumb rubber modified bituminous mixes. *Materiales de construcción*, (315):6, 2014.

[154] F Moghadas Nejad, E Aflaki, and MA Mohammadi. Fatigue behavior of sma and hma mixtures. *Construction and Building Materials*, 24(7):1158–1165, 2010.

[155] Quang Tuan Nguyen, Hervé Di Benedetto, and Cédric Sauzéat. Determination of thermal properties of asphalt mixtures as another output from cyclic tension-compression test. *Road Materials and Pavement Design*, 13(1):85–103, 2012.

[156] Tatsuo Nishizawa, S Shimeno, and M Sekiguchi. Fatigue analysis of asphalt pavements with thick asphalt mixture layer. In *Eighth International Conference on Asphalt PavementsFederal Highway Administration*, number Volume II, 1997.

[157] A Nmiri, N Hamdi, O Yazoghli-Marzouk, M Duc, and E Srasra. Synthesis and characterization of kaolinite-based geopolymer: Alkaline activation effect on calcined kaolinitic clay at different temperatures. *Journal of materials and Environmental Sciences*, 8(2):276–290, 2017.

[158] American Association of State Highway and Transportation Officials. Standard method of test for estimating damage tolerance of asphalt binders using the linear amplitude sweep, 2014.

[159] Transportation Officials. Mechanistic-empirical pavement design guide: A manual of practice. *AASHTO: Washington, DC, USA*, 2008.

[160] Chris Olidis and D Hein. Guide for the mechanistic-empirical design of new and rehabilitated pavement structures materials characterization: Is your agency ready. In *2004 annual conference of the transportation association of Canada*. Citeseer, 2004.

[161] Hratch Sebouh Papazian. The response of linear viscoelastic materials in the frequency domain with emphasis on asphaltic concrete. In *International Conference on the Structural Design of Asphalt PavementsUniversity of Michigan, Ann Arbor*, volume 203, 1962.

[162] Terhi K Pellinen, Matthew W Witczak, and Ramon F Bonaquist. Asphalt mix master curve construction using sigmoidal fitting function with non-linear least squares optimization. In *Recent advances in materials characterization and modeling of pavement systems*, pages 83–101. 2004.

[163] Daniel Perraton, Hassan Baaj, and Alan Carter. Comparison of some pavement design methods from a fatigue point of view: effect of fatigue properties of asphalt materials. *Road materials and pavement design*, 11(4):833–861, 2010.

[164] Chayakrit Phetchuay, Suksun Horpibulsuk, Arul Arulrajah, Cherdsak Suksiripattanapong, and Artit Udomchai. Strength development in soft marine clay stabilized by fly ash and calcium carbide residue based geopolymer. *Applied clay science*, 127:134–142, 2016.

[165] Chayakrit Phetchuay, Suksun Horpibulsuk, Cherdsak Suksiripattanapong, Avirut Chinkulkijniwat, Arul Arulrajah, and Mahdi M Disfani. Calcium carbide residue: Alkaline activator for clay–fly ash geopolymer. *Construction and Building Materials*, 69:285–294, 2014.

[166] Tanakorn Phoo-ngernkham, Akihiro Maegawa, Naoki Mishima, Shigemitsu Hatanaka, and Prinya Chindaprasirt. Effects of sodium hydroxide and sodium silicate solutions on compressive and shear bond strengths of fa–gbfs geopolymer. *Construction and Building Materials*, 91:1–8, 2015.

[167] Itthikorn Phummiphan, Suksun Horpibulsuk, Runglawan Rachan, Arul Arulrajah, Shui-Long Shen, and Prinya Chindaprasirt. High calcium fly ash geopolymer stabilized lateritic soil and granulated blast furnace slag blends as a pavement base material. *Journal of hazardous materials*, 341:257–267, 2018.

[168] Christina Plati, Panos Georgiou, and Vasilis Papavasiliou. Simulating pavement structural condition using artificial neural networks. *Structure and Infrastructure Engineering*, 12(9):1127–1136, 2016.

[169] Craig Polley, Steven M Cramer, and Rodolfo V de la Cruz. Potential for using waste glass in portland cement concrete. *Journal of materials in Civil Engineering*, 10(4):210–219, 1998.

[170] Kevin L Priddy and Paul E Keller. *Artificial neural networks: an introduction*, volume 68. SPIE press, 2005.

[171] John L Provis and Jan Stephanus Jakob Van Deventer. *Geopolymers: structures, processing, properties and industrial applications*. Elsevier, 2009.

[172] John L Provis and Jannie SJ Van Deventer. *Alkali activated materials: state-of-the-art report, RILEM TC 224-AAM*, volume 13. Springer Science & Business Media, 2013.

[173] Vishnu Radhakrishnan, M Ramya Sri, and K Sudhakar Reddy. Evaluation of asphalt binder rutting parameters. *Construction and Building Materials*, 173:298–307, 2018.

[174] KD Raithby and AB Sterling. The effect of rest periods on the fatigue performance of a hot-rolled asphalt under reversed axial loading and discussion. In *Association of Asphalt Paving Technologists Proc*, 1970.

[175] Rachel Redden and Narayanan Neithalath. Microstructure, strength, and moisture stability of alkali activated glass powder-based binders. *Cement and Concrete Composites*, 45:46–56, 2014.

[176] Adel Rezaei-Tarahomi, Orhan Kaya, Halil Ceylan, K Gopalakrishnan, S Kim, and DR Brill. Neural networks based prediction of critical responses related to top-down and bottom-up cracking in airfield concrete pavements. In *Tenth International Conference on the Bearing Capacity of Roads, Railways and Airfields*, 2017.

[177] Yasser Rifaai, Ammar Yahia, Ahmed Mostafa, Salima Aggoun, and El-Hadj Kadri. Rheology of fly ash-based geopolymer: Effect of naoh concentration. *Construction and Building Materials*, 223:583–594, 2019.

[178] C Roberts, R van Rooijen, and L Thimm. A comparison of binder tess that relate to asphalt mixture deformation. In *Proc. 5th Eurasphalt & Eurobitume Congress (Istanbul)*, 2012.

[179] Stefan A Romanoschi, Nicoleta Ileana Dumitru, Octavian Dumitru, and Glenn Fager. Dynamic resilient modulus and fatigue properties of superpave hma mixes used in the base layer of kansas flexible pavements. Technical report, 2006.

[180] Reynaldo Roque, B Birgisson, Zh Zhang, B Sangpetngam, and Th Grant. Implementation of shrp indirect tension tester to mitigate cracking in asphalt pavements and overlays. Technical report, 2002.

[181] Sri Atmaja P Rosyidi, Suzielah Rahmad, Nur Izzi Md Yusoff, Aini Hazwani Shahrir, Ahmad Nazrul Hakimi Ibrahim, Nor Farah Nadia Ismail, and Khairiah Haji Badri. Investigation of the chemical, strength, adhesion and morphological properties of fly ash based geopolymer-modified bitumen. *Construction and Building Materials*, 255:119364, 2020.

[182] G Rowe, G Baumgardner, and M Sharrock. Functional forms for master curve analysis of bituminous materials. In *Proceedings of the 7th international RILEM symposium ATCBM09 on advanced testing and characterization of bituminous materials*, volume 1, pages 81–91, 2016.

[183] Nikhil Saboo and Praveen Kumar. Analysis of different test methods for quantifying rutting susceptibility of asphalt binders. *Journal of Materials in Civil Engineering*, 28(7):04016024, 2016.

[184] Mohammadreza Sabouri, Danial Mirzaiyan, and Ali Moniri. Effectiveness of linear amplitude sweep (las) asphalt binder test in predicting asphalt mixtures fatigue performance. *Construction and Building Materials*, 171:281–290, 2018.

[185] SF Said. Variable in roadbase layer properties conducting indirect tensile test. In *Eight International Conference on The Structural Design of Asphalt Pavements*, volume 2.

[186] S Saoula, Ait K Mokhtar, H Haddadi, and E Ghorbel. Improvement of the stability of a modified bituminous binders within eva. *International Journal of Applied Engineering Research*, 3(4):575–585, 2008.

[187] Paul Sargent, Paul N Hughes, Mohamed Rouainia, and Maggie L White. The use of alkali activated waste binders in enhancing the mechanical properties and durability of soft alluvial soils. *Engineering geology*, 152(1):96–108, 2013.

[188] Richard A Schapery. Correspondence principles and a generalizedj integral for large deformation and fracture analysis of viscoelastic media. *International journal of fracture*, 25(3):195–223, 1984.

[189] Rasoul Shadnia, Lianyang Zhang, and Peiwen Li. Experimental study of geopolymer mortar with incorporated pcm. *Construction and building materials*, 84:95–102, 2015.

[190] Caijun Shi and Keren Zheng. A review on the use of waste glasses in the production of cement and concrete. *Resources, conservation and recycling*, 52(2):234–247, 2007.

[191] Andrea Simone, Francesco Mazzotta, Shahin Eskandarsefat, Cesare Sangiorgi, Valeria Vignali, Claudio Lantieri, and Giulio Dondi. Experimental application of waste glass powder filler in recycled dense-graded asphalt mixtures. *Road Materials and Pavement Design*, 20(3):592–607, 2019.

[192] Avinash Kumar Singh and Jagdish Prasad Sahoo. Rutting prediction models for flexible pavement structures: A review of historical and recent developments. *Journal of Traffic and Transportation Engineering (English Edition)*, 8(3):315–338, 2021.

[193] Ali Soltani and David A Anderson. New test protocol to measure fatigue damage in asphalt mixtures. *Road materials and pavement design*, 6(4):485–514, 2005.

[194] Injun Song, Dallas N Little, Eyad A Masad, and Robert Lytton. Comprehensive evaluation of damage in asphalt mastics using x-ray ct, continuum mechanics, and micromechanics (with discussion). *Journal of the association of asphalt paving technologists*, 74, 2005.

[195] Seick Omar Sore, Adamah Messan, Elodie Prud'Homme, Gilles Escadeillas, and François Tsobnang. Stabilization of compressed earth blocks (cebs) by geopolymer binder based on local materials from burkina faso. *Construction and Building Materials*, 165:333–345, 2018.

[196] ASTM Standard et al. Standard specification for coal fly ash and raw or calcined natural pozzolan for use in concrete. *ASTM Standard C*, 618, 2018.

[197] Klaus Stangl, Andreas Jäger, and Roman Lackner. Microstructure-based identification of bitumen performance. *Road Materials and Pavement Design*, 7(sup1):111–142, 2006.

[198] Patimapon Sukmak, Suksun Horpibulsuk, Shui-Long Shen, Prinya Chindaprasirt, and Cherdsak Suksiripattanapong. Factors influencing strength development in clay–fly ash geopolymer. *Construction and Building Materials*, 47:1125–1136, 2013.

[199] DMJ Sumajouw, D Hardjito, SE Wallah, and BV Rangan. Fly ash-based geopolymer concrete: study of slender reinforced columns. *Journal of materials science*, 42(9):3124–3130, 2007.

[200] Aravind Krishna Swamy, Uma Devi Rongali, and Pramod Kumar Jain. Effect of hdpeh polymer on viscoelastic properties of sbs modified asphalt. *Construction and Building Materials*, 136:230–236, 2017.

[201] Nader Tabatabaee and Hassan Ali Tabatabaee. Multiple stress creep and recovery and time sweep fatigue tests: Crumb rubber modified binder and mixture performance. *Transportation Research Record*, 2180(1):67–74, 2010.

[202] Kiang Hwee Tan and Hongjian Du. Use of waste glass as sand in mortar: Part i–fresh, mechanical and durability properties. *Cement and Concrete Composites*, 35(1):109–117, 2013.

[203] Naipeng Tang, Weidong Huang, Mao Zheng, and Jianying Hu. Investigation of gilsonite-, polyphosphoric acid-and styrene–butadiene–styrene-modified asphalt binder using the multiple stress creep and recovery test. *Road Materials and Pavement Design*, 18(5):1084–1097, 2017.

[204] Ning Tang, Zhaoxue Deng, Jian-Guo Dai, Kaikai Yang, Chongyang Chen, and Qing Wang. Geopolymer as an additive of warm mix asphalt: Preparation and properties. *Journal of cleaner production*, 192:906–915, 2018.

[205] Ning Tang, Kai-kai Yang, Yazan Alrefaei, Jian-Guo Dai, Li-Mei Wu, and Qing Wang. Reduce vocs and pm emissions of warm-mix asphalt using geopolymer additives. *Construction and Building Materials*, 244:118338, 2020.

[206] Serkan Tapkin. Estimation of fatigue lives of fly ash modified dense bituminous mixtures based on artificial neural networks. *Materials Research*, 17(2):316–325, 2014.

[207] RA Tarefder, Musharraf Zaman, and K Hobson. A laboratory and statistical evaluation of factors affecting rutting. *International Journal of Pavement Engineering*, 4(1):59–68, 2003.

[208] Yuksel Tasdemir. Artificial neural networks for predicting low temperature performances of modified asphalt mixtures. 2009.

[209] Mark A Taylor and N Paul Khosla. *Stripping of asphalt pavements: State of the art (discussion, closure)*. Number 911. 1983.

[210] Hervé K Tchakouté, Claus H Rüscher, Sakeo Kong, Elie Kamseu, and Cristina Leonelli. Geopolymer binders from metakaolin using sodium waterglass from waste glass and rice husk ash as alternative activators: A comparative study. *Construction and Building Materials*, 114:276–289, 2016.

[211] Tawatchai Tho-In, Vanchai Sata, Kornkanok Boonserm, and Prinya Chindaprasirt. Compressive strength and microstructure analysis of geopolymer paste using waste glass powder and fly ash. *Journal of cleaner production*, 172:2892–2898, 2018.

[212] Manuel Torres-Carrasco and F Puertas. Waste glass as a precursor in alkaline activation: Chemical process and hydration products. *Construction and Building Materials*, 139:342–354, 2017.

[213] Manuel Torres-Carrasco and FJJOCP Puertas. Waste glass in the geopolymer preparation. mechanical and microstructural characterisation. *Journal of cleaner production*, 90:397–408, 2015.

[214] Ankita Upadhya, MS Thakur, Nitisha Sharma, and Parveen Sihag. Assessment of soft computing-based techniques for the prediction of marshall stability of asphalt concrete reinforced with glass fiber. *International Journal of Pavement Research and Technology*, pages 1–20, 2021.

[215] Aliyu Usman, Muslich Hartadi Sutanto, Madzlan Bin Napiah, and Nura Shehu Aliyu Yaro. Response surface methodology optimization in asphalt mixtures: A review. 2021.

[216] Ikenna D Uwanuakwa, Shaban Ismael Albrka Ali, Mohd Rosli Mohd Hasan, Pinar Akpinar, Ashiru Sani, and Khairul Anuar Shariff. Artificial intelligence prediction of rutting and fatigue parameters in modified asphalt binders. *Applied Sciences*, 10(21):7764, 2020.

[217] Mostafa Vafaei and Ali Allahverdi. High strength geopolymer binder based on waste-glass powder. *Advanced Powder Technology*, 28(1):215–222, 2017.

[218] W Van Dijk, H Moreaud, A Quedeville, and P Uge. The fatigue of bitumen and bituminous mixes. In *Presented at the Third International Conference on the Structural Design of Asphalt Pavements, Grosvenor House, Park Lane, London, England, Sept. 11-15, 1972.*, volume 1, 1972.

[219] G Van Gooswilligen, E De Hilster, and C Robertus. Changing needs and requirements for bitumen and asphalts. In *Proceedings of the 6th Conference on Asphalt Pavements for Southern Africa, CAPSA'94, Held Cape Town October 1994. Vol. 2*, 1994.

[220] Veena Venudharan and Krishna Prapoorna Biligiri. Heuristic principles to predict the effect of crumb rubber gradation on asphalt binder rutting performance. *Journal of Materials in Civil Engineering*, 29(8):04017050, 2017.

[221] Les Vickers, Arie Van Riessen, and William DA Rickard. *Fire-resistant geopolymers: role of fibres and fillers to enhance thermal properties.* Springer, 2015.

[222] Harold L Von Quintus, James S Moulthrop, et al. Mechanistic-empirical pavement design guide flexible pavement performance prediction models: Volume iii field guide–calibration and user's guide for the mechanistic-empirical pavement design guide. Technical report, Montana. Dept. of Transportation. Research Programs, 2007.

[223] Steenie Wallah and B Vijaya Rangan. Low-calcium fly ash-based geopolymer concrete: long-term properties. 2006.

[224] Chao Wang, Cassie Castorena, Jinxi Zhang, and Y Richard Kim. Unified failure criterion for asphalt binder under cyclic fatigue loading. *Road Materials and Pavement Design*, 16(sup2):125–148, 2015.

[225] TLJ Wasage, Jiri Stastna, and Ludo Zanzotto. Rheological analysis of multi-stress creep recovery (mscr) test. *International Journal of Pavement Engineering*, 12(6):561–568, 2011.

[226] Greg White. Grading highly modified binders by multiple stress creep recovery. *Road Materials and Pavement Design*, 18(6):1322–1337, 2017.

[227] Malcolm L Williams, Robert F Landel, and John D Ferry. The temperature dependence of relaxation mechanisms in amorphous polymers and other glass-forming liquids. *Journal of the American Chemical society*, 77(14):3701–3707, 1955.

[228] Feipeng Xiao, Serji Amirkhanian, and C Hsein Juang. Prediction of fatigue life of rubberized asphalt concrete mixtures containing reclaimed asphalt pavement using artificial neural networks. *Journal of Materials in Civil Engineering*, 21(6):253–261, 2009.

[229] Hua Xu and JSJ Van Deventer. The geopolymerisation of alumino-silicate minerals. *International journal of mineral processing*, 59(3):247–266, 2000.

[230] Erkut YALÇIN, Ahmet Munir Ozdemir, and Mehmet Yilmaz. Prediction of rheological parameters of asphalt binders with artificial neural networks. *The Eurasia Proceedings of Science Technology Engineering and Mathematics*, 12:7–16, 2000.

[231] Kezhen Yan and Lingyun You. Investigation of complex modulus of asphalt mastic by artificial neural networks. 2014.

[232] Hao Yin, Ghassan R Chehab, Shelley M Stoffels, Tanmay Kumar, and Laxmikanth Premkumar. Use of creep compliance interconverted from complex modulus for thermal cracking prediction using the m–e pavement design guide. *International Journal of Pavement Engineering*, 11(2):95–105, 2010.

[233] Xian-Xun Yuan, Warren Lee, and Ningyuan Li. Ontario's local calibration of the mepdg distress and performance models for flexible roads: A summary. *Proceedings of the TAC*, 2017.

[234] Nur Izzi Md Yusoff, Emmanuel Chailleux, and Gordon D Airey. A comparative study of the influence of shift factor equations on master curve construction. *International Journal of Pavement Research and Technology*, 4(6):324, 2011.

[235] Hariz Zain, Mohd Mustafa Al Bakri Abdullah, Kamarudin Hussin, Nurliyana Ariffin, and Ridho Bayuaji. Review on various types of geopolymer materials with the

environmental impact assessment. In *MATEC Web of Conferences*, volume 97, page 01021. EDP Sciences, 2017.

[236] L Zani, Filippo Giustozzi, and John Harvey. Effect of storage stability on chemical and rheological properties of polymer-modified asphalt binders for road pavement construction. *Construction and building materials*, 145:326–335, 2017.

[237] Jun Zhang, Lubinda F Walubita, Abu NM Faruk, Pravat Karki, and Geoffrey S Simate. Use of the mscr test to characterize the asphalt binder properties relative to hma rutting performance–a laboratory study. *Construction and Building Materials*, 94:218–227, 2015.

[238] Lianyang Zhang, Saeed Ahmari, and Jinhong Zhang. Synthesis and characterization of fly ash modified mine tailings-based geopolymers. *Construction and Building Materials*, 25(9):3773–3781, 2011.

[239] Mo Zhang, Hong Guo, Tahar El-Korchi, Guoping Zhang, and Mingjiang Tao. Experimental feasibility study of geopolymer as the next-generation soil stabilizer. *Construction and building materials*, 47:1468–1478, 2013.

[240] Zhanmin Zhang, Reynaldo Roque, Bjorn Birgisson, and Boonchai Sangpetngam. Identification and verification of a suitable crack growth law (with discussion). *Journal of the Association of Asphalt Paving Technologists*, 70, 2001.

[241] Zifeng Zhao, Jiayu Wang, Xiangdao Hou, Qian Xiang, and Feipeng Xiao. Viscosity prediction of rubberized asphalt–rejuvenated recycled asphalt pavement binders using artificial neural network approach. *Journal of Materials in Civil Engineering*, 33(5):04021071, 2021.

[242] Fujie Zhou, Soohyok Im, Lijun Sun, and Tom Scullion. Development of an ideal cracking test for asphalt mix design and qc/qa. *Road Materials and Pavement Design*, 18(sup4):405–427, 2017.

[243] Cheng Zhu. *Evaluation of thermal oxidative aging effect on the rheological performance of modified asphalt binders*. University of Nevada, Reno, 2015.

[244] Hasan Ziari, Amir Amini, Ahmad Goli, and Danial Mirzaiyan. Predicting rutting performance of carbon nano tube (cnt) asphalt binders using regression models and neural networks. *Construction and Building Materials*, 160:415–426, 2018.

[245] Corey James Zollinger. *Application of surface energy measurements to evaluate moisture susceptibility of asphalt and aggregates.* PhD thesis, Texas A&M University, 2005.

[246] SE Zoorob, JP Castro-Gomes, LA Pereira Oliveira, and J O'connell. Investigating the multiple stress creep recovery bitumen characterisation test. *Construction and Building Materials*, 30:734–745, 2012.

[247] Gui-lian Zou and Jiang-miao Yu. Effects of interface modifier on asphalt concrete mixture performance and analysis of its mechanism. *International Journal of Pavement Research and Technology*, 5(6):419, 2012.